ESTIMATION OF TIME PARAMETER PROPORTIONALITY RATIOS IN LARGE CATCHMENTS: CASE STUDY OF THE MODDER-RIET RIVER CATCHMENT, SOUTH AFRICA

by

CHRISTOPHER EARL ALLNUTT

A dissertation submitted in fulfilment of the requirements for the degree

Master of Engineering in Civil Engineering

in the

Department of Civil Engineering

of the

Faculty of Engineering, Built Environment and Information Technology

of the

Central University of Technology, Free State, South Africa

Supervisor: Dr OJ Gericke

Co-supervisor: Mr JPJ Pietersen

June 2019

DECLARATION

I, the undersigned, declare that the dissertation hereby submitted by me for the degree *Master of Engineering in Civil Engineering* at the Central University of Technology, Free State, is my own independent work and has not been submitted by me to another University and/or Faculty in order to obtain a degree. I further cede copyright of this dissertation in favour of the Central University of Technology, Free State.

Christopher Earl Allnutt

Signature: 

Date: 12 June 2019

Bloemfontein, South Africa

ABSTRACT

Catchment response time parameters such as the time of concentration (T_C), lag time (T_L) and time to peak (T_P) are fundamental to design flood estimation in ungauged catchments; hence, errors in time parameter estimates directly impact on design flood estimates. As much as 75% of the total error in design peak discharge estimates in ungauged catchments could be ascribed to errors in the estimation of catchment response time. The seven different time parameter definitions available in hydrological literature are interchangeably used when time parameters are obtained from observed rainfall and streamflow data, respectively. As a result, time intervals from various points during a storm extracted from a hyetograph (*e.g.* effective rainfall centroid, end of effective rainfall, and/or maximum rainfall intensity) to various points on the resultant hydrograph (*e.g.* peak discharge, inflection point on recession limb, and centroid of direct runoff) are often misinterpreted as T_C, T_L and/or T_P.

Due to the difficulty in estimating the centroid values from above-mentioned hyetographs and hydrographs, other T_L estimation techniques have been proposed in literature. Instead of using T_L as an input for design flood estimation methods, it is rather used as input to the computation of T_C. In using T_L defined as the time from the centroid of effective rainfall to the centroid of direct runoff, T_C and T_L are normally related by $T_C = 1.417T_L$. In T_L defined as the time from the centroid of effective rainfall to the time of the peak discharge, the proportionality ratio increases to 1.667. However, in contradiction, Schultz (1964) established that for small catchments in Lesotho and South Africa, $T_L \approx T_C$. In addition, Gericke and Smithers (2016; 2017) also showed that $T_P \approx T_C$ at medium to large catchment scales in South Africa, but the relevance of the T_L proportionality ratio ($x = 1.667$), *i.e.* $T_L = 0.6T_C$, was not established.

The overall purpose of this study is thus to investigate and establish the suitability of the currently recommended time parameter definitions and proportionality ratios for small catchments in larger sub-catchment areas (exceeding 50 km²) of the Modder-Riet River Catchment in South Africa. The focus is on the estimation of time parameter proportionality ratios from observed rainfall and streamflow data using a

simplified convolution process and the seven different time parameter definitions currently recognised in hydrological literature.

The time parameters T_C, T_L and T_P were individually estimated using the various time variables obtained from observed hyetographs and hydrographs to establish average time parameter proportionality ratios at a catchment level. The time parameter estimates proved to be highly variable due to the spatial and temporal distribution of rainfall events, variation in peak discharges and the distance of the rainfall events from the catchment outlet. However, the variability in the average estimated time parameter proportionality ratios proved to be less significant. In this study, where T_L is defined as the time from the centroid of effective rainfall to the peak discharge, T_C and T_L proved to be related by $T_C = 1.003T_L$ and where T_L is defined as the time from the centroid of effective rainfall to the centroid of direct runoff, the proportionality ratio reduced to 0.992. In all the sub-catchments under consideration, the preliminary findings of Gericke and Smithers (2014; 2016; 2017), *i.e.* $T_P \approx T_C \approx T_L$, were confirmed. In other words, it highlighted that the proportionality ratios currently proposed for small catchments, *i.e.* $T_C = 1.417T_L$ and $T_C = 1.667T_L$, are not applicable at larger catchment levels.

Building upon the critical assessment of the available time parameter definitions and proportionality ratios, it is envisaged that the implementation and expansion of both the identified research values and adopted methodology to other catchments in South Africa and internationally, will ultimately contribute towards improved time parameter estimations at a catchment level. Consequently, the improved time parameter estimations will also result in improved design flood estimations.

ACKNOWLEDGEMENTS

A number of special acknowledgements deserve specific mention:

(a) The Rectorate and relevant functionaries from the Central University of Technology, Free State, for the opportunity of completing this research;
(b) The various agencies for funding and in particular the Central University of Technology, Free State and the National Research Foundation;
(c) Dr OJ Gericke, my supervisor, who is an incredible mentor, for all the guidance, support and patience. His knowledge, hardworking, high efficiency attitude, deeply impressed me, and I have learned a lot from him. I am very pleased to have worked with him;
(d) Mr JPJ Pietersen, my co-supervisor, for the motivation, encouragement and technical assistance;
(e) Department of Water and Sanitation for providing the observed streamflow data;
(f) The Agricultural Research Council and the South African Weather Services for providing the observed rainfall data;
(g) The anonymous external examiners for their constructive review comments, which have helped to significantly improve the dissertation;
(h) My family and colleagues, for their love and support that they gave me throughout my research; and
(i) My mother, Petro, for her unfailing love and for always believing in me.

Acknowledgement above all to my Heavenly Father for helping me to reach this point in my studies. Through many tribulations, He has humbled me and made me a better person.

TABLE OF CONTENTS

Page

Page

Page

LIST OF TABLES

Page

Page

LIST OF FIGURES

Page

Page

LIST OF APPENDICES

Page

Page

Page

Page

Page

LIST OF ABBREVIATIONS

A	Catchment area
ARC	Agricultural Research Council
ARC-ISCW	Agricultural Research Council - Institute for Soil, Climate and Water
AWS	Automatic weather station
CCTV	Closed Circuit Television
CN	Curve Number
CSIR	Council for Scientific and Industrial Research
DREU	Daily Rainfall Extraction Utility
DWAF	Department of Water Affairs and Forestry
DWS	Department of Water and Sanitation
EX-HYD	Flood Hydrograph Extraction Software
GIS	Geographical Information Systems
GOF	Goodness-of-Fit
HAT	Hydrograph Analysis Tool
HRU	Hydrological Research Unit
L	Distance from catchment outlet
MAE	Mean Annual Evaporation
MAP	Mean Annual Precipitation
MRC	Modder River Catchment
NRCS	Natural Resources Conservation Service
N_X	Number of rainfall stations
PDS	Partial duration series
P_T	Total rainfall
P_E	Effective rainfall
Q_D	Direct runoff
Q_B	Baseflow
Q_P	Peak discharge
Q_T	Total streamflow
R_L	Average record length
RRC	Riet River Catchment
RSA	Republic of South Africa
SANRAL	South African National Roads Agency

LIST OF ABBREVIATIONS (continued)

SAWS	South African Weather Services
SCS	Soil Conservation Service
SDF	Standard Design Flood
S_d	Daily spatial distribution
S_e	Event spatial distribution
SUH	Synthetic Unit Hydrograph
T_B	Hydrograph time base
T_C	Time of concentration
t_{er0}	Start of effective rainfall
t_{erc}	Centroid of effective rainfall
t_{ere}	End of effective rainfall
t_{ip}	Time of inflection point on recession limb
T_L	Lag time
T_P	Time to peak
TP	Time Parameter
TPPR	Time Parameter Proportionality Ratio
t_{q0}	Start of total runoff
t_{qc}	Centroid of direct runoff
t_{qpk}	Time of peak discharge
t_{rmax}	Time of maximum rainfall
TW	Thiessen Weight
USA	United States of America
USACE	United States Army Corps of Engineers
USBR	United States Bureau of Reclamation
USDA	United States Department of Agriculture
USGS	United States Geological Survey
WMO	World Meteorological Organisation
WRC	Water Research Commission

CHAPTER 1: INTRODUCTION

This chapter provides some background on the estimation of catchment response time parameters and proportionality ratios generally applicable to small catchments in order to establish how these definitions and/or proportionality ratios should or could be applied in catchment areas exceeding 50 km^2. The problem statement, and purpose and limitations of the study are discussed thereafter. The outline of the dissertation structure is provided at the end.

1.1 Background

In event-based deterministic design flood estimation methods, estimates of the peak discharge (Q_P) depend on a single catchment response time parameter, while the catchment is at an 'average condition' and the risk or hazard associated with a specific return period (T) is reflected by the joint-probability of the 1: T-year rainfall and 1: T-year flood event (SANRAL, 2013). Catchment response time parameters, *e.g.* time of concentration (T_C), lag time (T_L) and time to peak (T_P) serve as fundamental input to design flood estimation in ungauged catchments; hence, errors in catchment response time estimates have a direct impact on design flood estimates (McCuen, 2009; Gericke and Smithers, 2014). Bondelid *et al.* (1982) demonstrated that as much as 75% of the all the errors in design peak discharge estimates in ungauged catchments could be attributed to errors in the estimation of catchment response time parameters, while Gericke and Smithers (2014) also demonstrated that the underestimation of time parameters by 80% or more could result in the overestimation of design peak discharges of up to 200%.

1.2 Problem Statement

Time variables describe the individual events defined on either a rainfall hyetograph or streamflow hydrograph, while time parameters, *e.g.* T_C, T_L and/or T_P, are defined by the difference between two interrelated observed time variables (McCuen, 2009). In small catchments, time parameters are estimated using a simplified convolution process between a single rainfall hyetograph and the resulting single-peaked hydrograph. Therefore, rainfall and streamflow data are required when a simplified convolution process is applied, and a synthetic transfer function is used to convert

the effective runoff producing rainfall into direct runoff based on the principle of linear super-positioning, *i.e.* multiplication, translation and addition (Chow *et al.*, 1988). The estimation of catchment response time parameters from observed rainfall and streamflow data in large heterogeneous catchments also requires a similar convolution process to establish the temporal relationship between a catchment rainfall hyetograph, which may be derived from numerous rainfall stations, and the resulting outflow hydrograph (Gericke and Smithers, 2017).

Unfortunately, hydrological literature, frequently fails to recognise all the distinct time parameters, or poorly describes the relationship between the time variables utilised to estimate these time parameters. This creates perplexity and results in numerous definitions being utilised to characterise the same time parameter. McCuen (2009) featured seven unique definitions that are conversely used to characterise time parameters as obtained from observed rainfall and streamflow data. Therefore, time intervals from different points during a storm extracted from a hyetograph (*e.g.* effective rainfall centroid, end of effective rainfall, and/or maximum rainfall intensity) to different points on the resultant hydrograph (*e.g.* peak discharge, inflection point on recession limb, and centroid of direct runoff) are frequently confounded as T_C, T_L and/or T_P. Due to the difficulty in estimating the centroid values from above-mentioned hyetographs and hydrographs, other T_L estimation techniques have been proposed in literature. Rather than utilising T_L as an input for design flood estimation methods, it is rather utilised as input to the computation of T_C. In utilising T_L characterised as the time from the centroid of effective rainfall to the centroid of direct runoff, T_C and T_L are normally related by $T_C = 1.417T_L$ (McCuen, 2009). In T_L characterised as the time from the centroid of effective rainfall to the time of the peak discharge, the proportionality ratio increases to 1.667 (McCuen, 2009). However, in contradiction, Schultz (1964) demonstrated that for small catchments in Lesotho and South Africa, $T_L \approx T_C$. Likewise, Gericke and Smithers (2016; 2017) demonstrated that $T_P \approx T_C$ at medium to large catchments in South Africa, yet the significance of the T_L proportionality ratio ($x = 1.667$), *i.e.* $T_L = 0.6T_C$, was not confirmed.

1.3 Purpose of Study

The overall purpose of this study is to investigate and establish the suitability of the currently recommended time parameter definitions and proportionality ratios for small catchments in larger sub-catchment areas (exceeding 50 km²) of the Modder-Riet River Catchment (MRRC) in South Africa.

1.3.1 Research aims

The overall research aim is to estimate time parameter proportionality ratios from observed rainfall and streamflow data using a simplified convolution process and the seven different time parameter definitions currently recognised in hydrological literature. The time parameters T_C, T_L and T_P are individually estimated using the various time variables obtained from observed rainfall hyetographs and streamflow hydrographs to establish average time parameter proportionality ratios at a catchment level. The latter average time parameter proportionality ratios would then not only confirm or reject the current proportionality ratios of $T_C = 1.417T_L$ and $T_C = 1.667T_L$, but it would also serve as confirmation or rejection of the preliminary findings of Gericke and Smithers (2014; 2016; 2017), *i.e.* $T_P \approx T_C \approx T_L$ at medium to large catchment scales. It is also envisaged, as an additional research aim, to determine the association between the average time parameters (and/or average time parameter proportionality ratios) and the average event spatial distribution (S_e), average peak discharge (Q_P) and the average distance (L) between the rainfall station (where the maximum rainfall depth was recorded) and the catchment outlet.

1.3.2 Assumptions

This study is based on the following assumptions:

(a) **Assumption 1:** Time variables for an individual event (either from a hyetograph or hydrograph) cannot always be measured directly from autographic records owing to the difficulties in determining the start time, end time, and temporal and spatial distribution of effective rainfall and direct runoff.

(b) **Assumption 2:** Poorly synchronised rainfall and streamflow observations can contribute to inaccurate estimates of time parameters using a simplified convolution process.

(c) **Assumption 3:** Time parameter proportionality ratios equal unity in large catchments, *i.e.* $T_P \approx T_C \approx T_L \approx 1$.

(d) **Assumption 4:** The baseflow separation methodology applied in this study is regarded as the most appropriate method to be used in the MRRC.

1.3.3 Specific objectives

To achieve the research aims, the specific objectives are to:

(a) Conduct a comprehensive literature review;

(b) Establish a rainfall and streamflow database for the MRRC;

(c) Develop a toolkit in the Microsoft Excel environment which automates the estimation procedures associated with the temporal characteristics of hyetograph-hydrograph responses;

(d) Analyse the rainfall and streamflow data;

(e) Estimate the time variables and time parameters from the observed data sets using a simplified convolution process and the time parameter definitions currently recognised in hydrological literature; and

(f) Estimate average time parameter proportionality ratios at a catchment level.

1.4 Limitations of Study

In principle all the time parameter definitions in the hydrological literature are reliant on the conceptual definition of T_C; nevertheless, it is also important to note that all these definitions are based on time variables with an associated probability distribution or degree of uncertainty. Apart from these inherent uncertainties, the lack of sub-daily rainfall data in the MRRC could also be regarded as a limitation of the study. However, the time parameter proportionality ratios under investigation, *i.e.* $T_C = 1.417T_L$ and $T_C = 1.667T_L$, are both based centroid values obtained from using a simplified convolution process, whereas, the latter centroid values denote 'average values' which are deemed to be more stable time variables representative

of the catchment response time in larger catchments where flood volumes are central to the design (McCuen, 2009; Gericke and Smithers, 2017). Hence, these centroid-based time parameters are supposedly not significantly influenced by the time series interval, *i.e.* daily as opposed to sub-daily rainfall data.

1.5 Outline of Dissertation Structure

The remainder of this dissertation is organised as follows:

Chapter 2 presents a comprehensive literature review of the time parameters commonly used to express the catchment response time with the focus on the generally accepted time parameter definitions and proportionality ratios applicable to small catchments. Methods used to analyse hyetograph-hydrograph relationships are also discussed.

Chapter 3 provides an overview of the location and characteristics of the study area (MRRC).

Chapter 4 contains the detailed methodology adopted in meeting the specific objectives of this study and includes the: (i) extraction and analyses of rainfall and streamflow data, (ii) assessment of time parameters based on the temporal relationship between average compounded hyetographs and hydrographs in each catchment, and (iii) establishment of event-specific and average proportionality ratios between time parameters at a catchment level. The development of a toolkit in the Microsoft Excel environment which automates the estimation procedures associated with the temporal characteristics of the hyetograph-hydrograph responses as listed in (i) to (iii), is also included in this chapter.

Chapter 5 presents the results based on the methodology described in Chapter 4, with some further discussions included in both Chapters 5 and 6.

Chapter 6 provides the conclusions and general recommendations for future research.

CHAPTER 2: LITERATURE REVIEW

The literature review firstly focuses on the comparative analysis of the relationship between rainfall hyetographs and the resulting streamflow hydrographs to enable the identification of time variables and the estimation of time parameters. Thereafter, the focus is on catchment response time estimation methods, with specific reference to the time parameter definitions and proportionality ratios internationally accepted as applicable to small catchments. Lastly, the application of the different time parameters in design flood estimation, as well as the applicability and possible transfer thereof to larger catchments, are discussed.

2.1 Analysis of Hyetograph-Hydrograph Relationships

Understanding the nature of catchment response to rainfall input is at the core of applied hydrological applications, *e.g.* design flood estimation, water resources management, and catchment parameter estimation. Catchment response reflects how a catchment converts rainfall into runoff, and it incorporates the influence of numerous catchment characteristics, *e.g.* catchment geomorphology, channel geomorphology, soils, land-use and vegetation, and developmental and climatological variables. Catchment response is normally studied using a comparative analysis of the temporal and spatial characteristics of a rainfall hyetograph and the resulting streamflow hydrograph (Dingman, 2002). Indices such as the peak discharge, runoff volume, baseflow index, recession constant and response time could be obtained from rainfall hyetographs and streamflow hydrographs to provide first-order information to comprehend the rainfall-runoff relationship in a particular catchment (Holton and Overton, 1963; Potter and Faulkner, 1987; Ferguson and Suckling, 1990; Jones and Grant, 1996; Elsenbeer and Vertessy, 2000; Sujono *et al*., 2004; Dow, 2007).

2.1.1 Time variables

Time variables can be estimated from the spatial and temporal distributions of rainfall hyetographs and streamflow hydrographs. To estimate these time variables, hydrograph analyses based on the separation of: (i) total runoff hydrographs into direct runoff and baseflow, (ii) rainfall hyetographs into initial abstraction, losses and

effective rainfall, and (iii) the identification of the rainfall-runoff transfer function, are required. A complex process is used to transform the effective rainfall into direct runoff through a synthetic transfer function based on the principle of linear super-positioning, *e.g.* multiplication, translation and addition (Chow *et al.,* 1988; McCuen, 2005).

Effective rainfall hyetographs can be estimated from rainfall hyetographs in two separate ways, contingent upon whether observed data are available or not. In situations where both observed rainfall and streamflow data are available, index methods such as the: (i) Phi-index method, where the index equals the average rainfall intensity above which the effective rainfall volume equals the direct runoff volume, and (ii) constant-percentage method, where losses are proportionate to the rainfall intensity and the effective rainfall volume equals the direct runoff volume, can be used (McCuen, 2005). However, in ungauged catchments, the partitioning of rainfall losses should be based on infiltration methods, which account for infiltration and other losses individually. The Soil Conservation Service (SCS) runoff curve number (*CN*) method is internationally the most commonly used (Chow *et al*., 1988).

In general, time variables obtained from hyetographs include the peak rainfall intensity, the centroid of effective rainfall and the end time of the rainfall event. Hydrograph-based time variables generally include the peak discharge, the start of direct runoff, the centroid of direct runoff and the inflection point on the hydrograph recession limb (McCuen, 2009).

2.1.2 Time parameters

In considering observed rainfall and streamflow data in gauged catchments, time parameters are normally defined by the difference between two interrelated observed time variables (McCuen, 2009), which represent individual events on either a hyetograph or hydrograph. In small catchment areas (A) up to 50 km², the difference between two interrelated observed time variables is estimated using a simplified convolution process between a single rainfall hyetograph and resulting single-peaked hydrograph. In medium to large heterogeneous catchment areas,

typically ranging from 50 km² to 35 000 km², a similar convolution process is required where the temporal relationship between a catchment rainfall hyetograph, which may be derived from numerous rainfall stations, and the resulting outflow hydrograph, is established (Gericke and Smithers, 2017).

The analysis of hyetograph-hydrograph relationships to obtain time variables and time parameters is often done manually, relying on visual examination and interpretation. As a result, considerable time is required to implement these analyses and in general, results could be regarded as inconsistent and subjective. In contrast, automated hydrograph analyses provide objective and consistent results (White and Sloto, 1990). Former automated tools for hydrograph analyses primarily focussed on the selection of hydrograph characteristics and the incorporation of baseflow separation, recession analyses and direct runoff estimation (Arnold *et al*., 1995; Sloto and Crouse, 1996; Rutledge, 1998; Chapman, 1999; Lim *et al*., 2005; Piggott *et al*., 2005). However, the use of automated tools to extract and analyse rainfall hyetographs, is not common practice and most of the rainfall-based time variables are extracted manually. In essence, none of the automated tools developed include both rainfall hyetograph and streamflow hydrograph characteristics, while the relationship between rainfall-based and runoff-based time variables is not defined. Hence, the need to develop an automated tool for hyetograph-hydrograph analyses was identified as one of the specific objectives in this study.

2.2 Catchment Response Time Estimation Methods

Almost all design flood estimation methods require at least one time parameter, *e.g.* T_C, T_L and/or T_P as input. Traditionally, time parameters have numerous theoretical or computational definitions, and T_L is sometimes expressed in terms of T_C. Different researchers (*e.g.* McCuen *et al.,* 1984; Schmidt and Schulze, 1984; Simas, 1996; McCuen, 2005; Jena and Tiwari, 2006; Hood *et al*., 2007; Fang *et al*., 2008; McCuen, 2009) have utilised the difference between the corresponding values of time variables to define two unique time parameters, namely T_C and T_L. Apart from the latter two time parameters, other time parameters, *e.g.* T_P and the hydrograph time base (T_B) are also often considered.

The theoretical definitions of T_C, T_L and T_P are detailed in the following sections.

2.2.1 Time of concentration

Numerous definitions are documented in the literature to define T_C. The most commonly used, conceptual and physically-based definition of T_C is the time required for runoff, due to effective rainfall, with a uniform spatial and temporal distribution over a catchment, to contribute to the peak discharge at the catchment outlet. In other words, the time required for a 'water particle' to flow from the most remote catchment boundary along the longest watercourse to the catchment outlet (Kirpich, 1940; McCuen *et al.,* 1984; McCuen, 2005; USDA NRCS, 2010; SANRAL, 2013).

In utilising such a conceptual definition, the computational definition of T_C is accordingly the distance travelled along the principle flow path, which is partitioned into sections of sensibly uniform hydraulic characteristics, divided by the average flow velocity in each of the sections (McCuen, 2009). The current common practice is to divide the principal flow path into sections of overland flow and principle conduit or channel flow, after which, the travel time in the various sections are computed separately and totalled. The second theoretical definition of T_C is related to the temporal distribution of rainfall and runoff, where T_C is characterised as the time between the start of effective rainfall and the resulting peak discharge. Various computational definitions have been proposed to estimate T_C from observed rainfall and runoff data. The following definitions, as illustrated in Figure 2.1, are occasionally used to estimate T_C from observed hyetographs and hydrographs (McCuen, 2009):

(a) The time from the end of effective rainfall to the inflection point on the hydrograph recession limb, *i.e.* the end of direct runoff; however, this is also the definition used by Clark (1945) to define T_L;
(b) The time from the centroid of effective rainfall to the peak discharge; however, this is also the definition used by Snyder (1938) to define T_L;
(c) The time from the maximum rainfall intensity to the peak discharge; or
(d) The time from the start of direct runoff (rising limb of hydrograph) to the peak discharge.

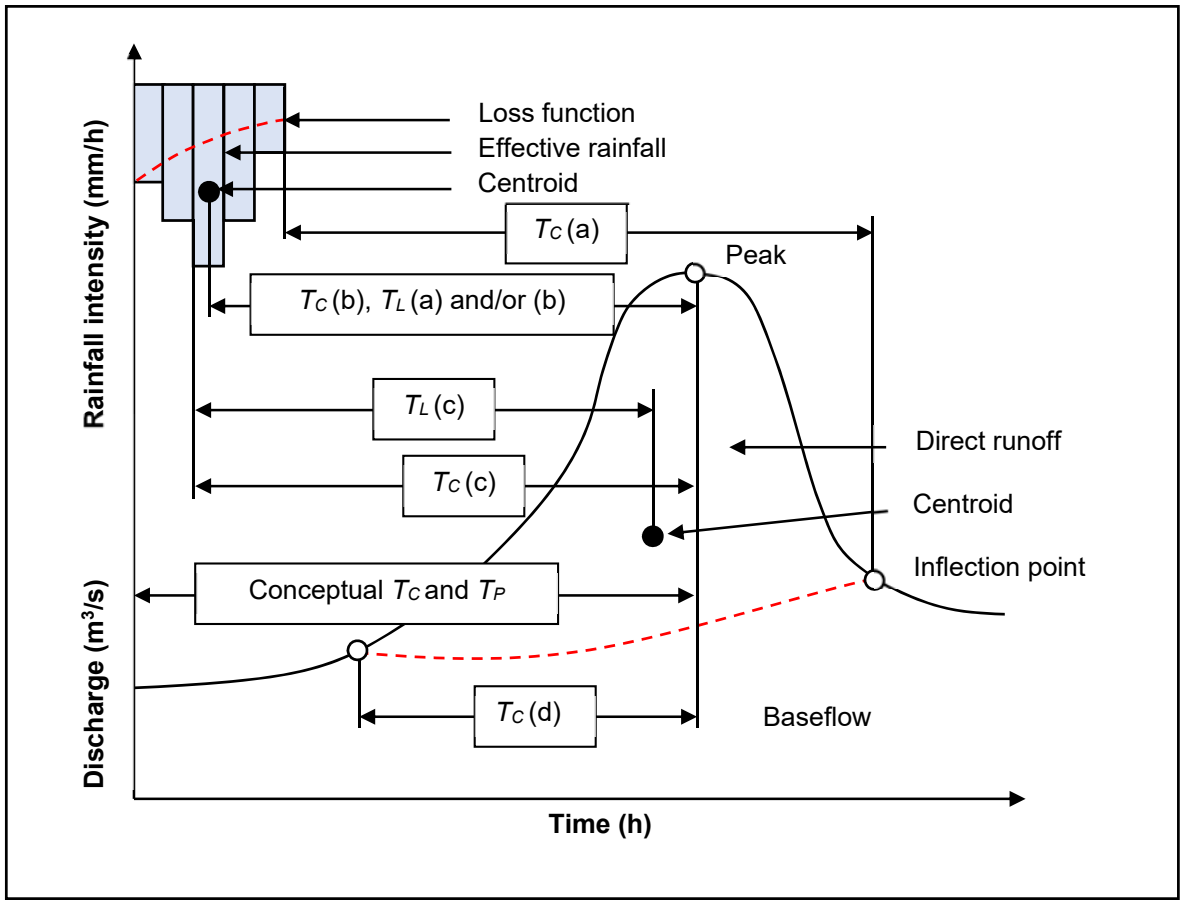

Figure 2.1: Schematic diagram illustrative of the different time parameter definitions and relationships (after Gericke and Smithers, 2014)

In South Africa, the South African National Roads Agency Limited (SANRAL) endorses the use of T_C definition (d) (SANRAL, 2013), but in principle all these definitions are reliant on the conceptual definition of T_C. It is also important to note that all the definitions listed in (a) to (d) are based on time variables with an associated probability distribution or degree of uncertainty. The centroid values denote 'average values' and are therefore deemed to be more stable time variables representative of the catchment response, especially in larger catchments where flood volumes are central to the design (McCuen, 2009). In comparison to large catchments, the time variables associated with peak rainfall intensities and peak discharge are regarded as the best estimate of the catchment response in smaller catchments where the exact occurrence of the peak discharge is of more significance.

McCuen (2009) analysed 41 hyetograph-hydrograph datasets from 20 catchment areas ranging from 1 to 60 ha in the United States of America (USA). The results from floods estimated using the Rational and/or NRCS TR-55 methods signified that the T_C based on the conceptual definition and principal flow path characteristics considerably underestimate the temporal distribution of runoff, and that T_C should be increased with a factor of 1.56 in order to correctly reflect the timing of runoff from the entire catchment, while the T_C based on T_C definition (b), proved to be the most accurate and was therefore recommended.

2.2.2 Lag time

Theoretically, T_L is generally described as the time between the centroid of effective rainfall and the peak discharge of the resultant hydrograph, which is the same as T_C definition (b) as shown in Figure 2.1. Computationally, T_L can be estimated as a weighted T_C value when, for a given rainfall event, the catchment is separated into sub-areas and the travel times from the centroid of each sub-area to the catchment outlet are determined by the relationship expressed in Equation (2.1) (USDA NRCS, 2010).

$$T_L = \frac{\sum(A_i Q_i T_i)}{\sum(A_i Q_i)} \qquad (2.1)$$

where:

T_L = lag time (h),

A_i = incremental catchment area/sub-area (km^2),

Q_i = incremental runoff from A_i (mm), and

T_i = travel time from the centroid of A_i to the catchment outlet (h).

In flood hydrology, T_L is generally not estimated with Equation (2.1). As an alternative, either empirical or analytical techniques are used to establish the correlation between the response time and meteorological and geomorphological parameters of a catchment. Hydrological literature frequently fails to clearly differentiate between T_C and T_L, particularly when observed data (hyetographs and hydrographs) are used to estimate these time parameters. The variations between

time variables from numerous points on the hyetographs to numerous points on the resultant hydrographs are sometimes misconstrued as T_C.

The following definitions, as illustrated in Figure 2.1, are used to estimate T_L from observed hyetographs and hydrographs (Heggen, 2003):

(a) The time from the centroid of effective rainfall to the time of the peak discharge of direct runoff;
(b) The time from the centroid of effective rainfall to the time of the peak discharge of total runoff; or
(c) The time from the centroid of effective rainfall to the centroid of direct runoff.

As in the case of T_C, T_L is also based on uncertain and inconsistent time variables. Nevertheless, the T_L definitions (a) to (c) detailed above are based on centroid values and are therefore regarded as more stable time variables illustrative of the catchment response time in larger catchments. Pullen (1969) also highlighted that T_L is favoured as a measure of catchment response time, particularly due to the integration of storm duration in the different definitions. Definitions (a) to (c) are commonly used to define T_L, (*e.g.* Simas, 1996; Hood *et al.*, 2007; Folmar and Miller, 2008; Pavlovic and Moglen, 2008), despite of the fact that T_L definition (b) is occasionally also used to define T_C.

Due to the difficulty in estimating the centroid values of hyetographs and hydrographs, alternative T_L estimation techniques have been proposed in literature. Instead of utilising T_L as an input for design flood estimation methods, it is preferably utilised as input to the computation of T_C. In using T_L definition (c), T_C and T_L are related by $T_C = 1.417T_L$ (McCuen, 2009). In T_L definitions (a) and (b), the proportionality ratio increases to 1.667 (McCuen, 2009). However, in contradiction to above-mentioned proportionality ratios, Schultz (1964) demonstrated that $T_L \approx T_C$ in small catchments in Lesotho and South Africa.

2.2.3 Time to peak

The T_P, which is utilised in numerous hydrological applications, can be defined as the time from the beginning of effective rainfall to the peak discharge in a single-peaked hydrograph (McCuen *et al*., 1984; USDA SCS, 1985; Linsley *et al*., 1988; Seybert, 2006). However, this is also the theoretical definition used for T_C (*cf.* Figure 2.1). T_P is likewise in some cases characterised as the time interval between the centroid of the effective rainfall and the peak discharge of direct runoff (Heggen, 2003); however, this is also one of the definitions used to define T_C and T_L utilising T_C definition (b) and T_L definition (c), respectively. As indicated by Ramser (1927), T_P is considered to be synonymous with T_C and both these time parameters are reasonably constant for a particular catchment. In contrast, Bell and Kar (1969) demonstrated that these time parameters are not constant and vary in the range of between 40% and 200% from the median value.

2.3 Application of Time Parameters in Design Flood Estimation

In ungauged catchments, catchment response time parameters are estimated utilising either empirically or hydraulically-based methods; however, analytical or semi-analytical methods are also occasionally used (McCuen *et al.*, 1984; McCuen, 2009). Empirical methods are commonly used by practitioners to estimate the catchment response time and almost 95% of all the methods developed internationally, are empirically-based (Gericke and Smithers, 2014). Conversely, most of these methods are related to and calibrated for small catchments, with only the research of Thomas *et al.* (2000) applicable to catchment areas of up to 1 280 km² and the research of Johnstone and Cross (1949), Pullen (1969), Mimikou (1984), Watt and Chow (1985), and Sabol (2008) focussing on larger catchments of up to 5 000 km².

Regrettably, in South Africa none of the empirical T_C estimation methods suggested for general use was developed and calibrated using local data. In small, flat catchments with overland flow being dominant, the use of the Kerby equation (Kerby, 1959) is suggested, while the empirical United States Bureau of Reclamation (USBR) equation (USBR, 1973) is utilised to estimate T_C as channel

flow in a defined watercourse (SANRAL, 2013). Both the Kerby and USBR equations were developed and calibrated in the USA for catchment areas less than 4 ha and 45 ha, respectively (McCuen *et al.*, 1984). Thus, practitioners in South Africa commonly apply these 'recommended methods' beyond their limits, both in terms of spatial extent and their original developmental regions, without using any local correction factors (Gericke and Smithers, 2014).

The empirical estimates of T_L utilised in South Africa are constrained to the group of equations developed by the Hydrological Research Unit (HRU; Pullen, 1969); the United States Department of Agriculture Natural Resource Conservation Service (USDA NRCS), previously known as the USDA Soil Conservation Service (USDA SCS, 1985) and SCS-SA (Schmidt and Schulze, 1984) equations. Both the HRU and Schmidt-Schulze T_L equations were locally developed and calibrated. The HRU methodology is prescribed for catchment areas less than 5 000 km², while the Schmidt-Schulze (SCS-SA) methodology is restricted to small catchment areas less than 30 km².

The SCS-Mockus method is the only empirical method used in South Africa to estimate T_P based on the Synthetic Unit Hydrograph (SUH) research conducted by Snyder (1938), while Mockus (1957; cited by Viessman *et al.*, 1989) developed the SCS SUHs from dimensionless unit hydrographs, as acquired from numerous hydrographs in catchments of different sizes and geographical localities.

In using event-based deterministic design flood estimation methods in ungauged catchments, T_C, T_L and T_P are generally used to estimate the catchment response time. T_C is not only the most commonly used time parameter in event-based design flood estimation methods (SANRAL, 2013; Gericke and Smithers, 2014), but it is also applied in continuous simulation modelling, (*e.g.* USACE, 2001; Neitsch *et al.*, 2005; Smithers *et al.*, 2013). T_C is primarily used to estimate the critical storm duration of a particular design rainfall event which serves as input to deterministic methods, *i.e.* the Rational and Standard Design Flood (SDF) methods, while T_L is utilised as input to the deterministic SCS and SUH methods.

The concurrent use of the various time parameter definitions and proportionality ratios as recommended in the literature, as well as the inherent procedural limitations of the traditional simplified convolution process when applied in medium to large catchments, combined with the absence of both continuously recorded rainfall data and available direct measurements of rainfall and runoff relationships at these catchment scales, has not just curtailed the establishment of objective time parameter estimation procedures in South Africa, but also had a direct impact on design flood estimation (Gericke, 2016).

An overview of the location and characteristics of the study area (MRRC) is provided in the next chapter.

CHAPTER 3: STUDY AREA

This chapter provides and overview of the location and characteristics of the MRRC.

3.1 Location and General Characteristics

South Africa is demarcated into 22 primary drainage regions, which are further sub-divided into 148 secondary drainage regions. The MRRC comprises of the C5 secondary drainage region located within primary drainage region C (Midgley *et al*., 1994). The MRRC, as shown in Figure 3.1, covers 34 795 km^2 and is located between 28°25' and 30°17' S and 23°49' and 27°00' E (DWAF, 1995). The Modder and Riet Rivers are the principal river reaches in the MRRC and discharge into the Orange-Vaal River drainage system (Midgley *et al*., 1994).

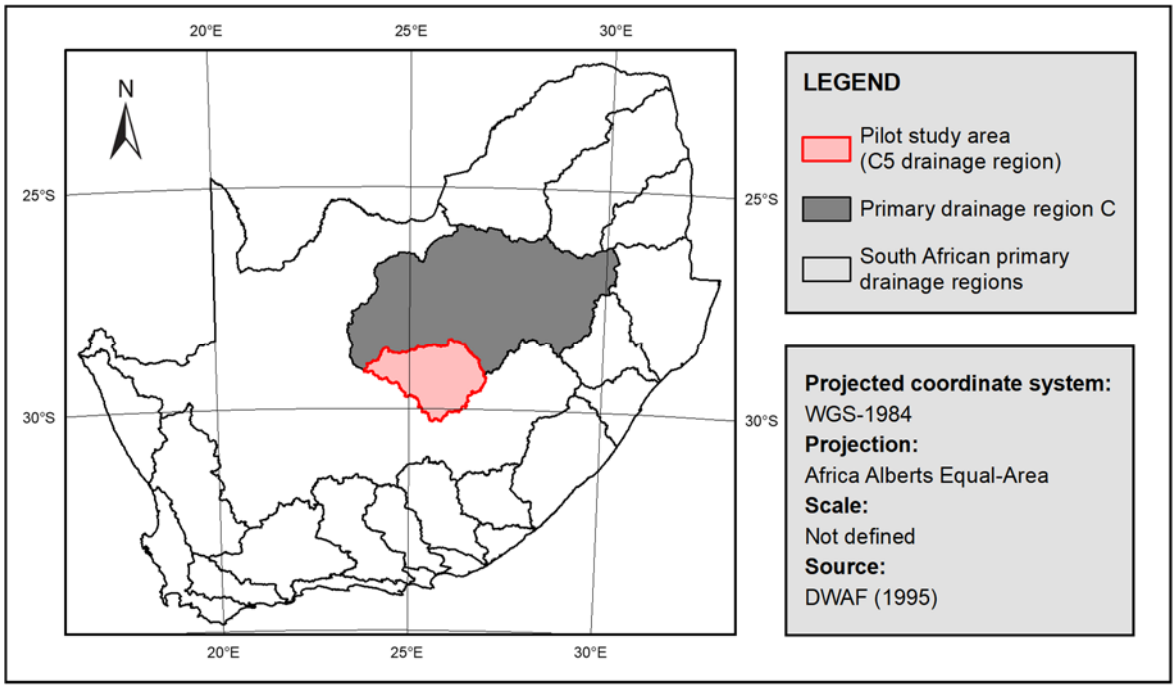

Figure 3.1: Location of the MRRC (C5 secondary drainage region) (after Gericke and Smithers, 2014)

The native vegetation consists of Grassland of the Interior Plateau, False Karoo and Karoo. Agricultural land is the largest human-induced modification in the rural areas, while residential and suburban areas govern the urban areas (CSIR, 2001). Practically, 99.1% of the MRRC comprises of rural areas, while 0.7% and 0.2% denote urban areas and water bodies, respectively (DWAF, 1995). The landscape

is gentle with slopes between 2.4 and 5.5% (USGS, 2016), while water has a tendency to pool easily; hence, affecting the attenuation and translation of floods.

3.2 Climate

The weather of central South Africa is moderate to hot in summer, with the long-term minimum and maximum averages varying between 12°C and 30°C, respectively, while the winter months are characterised by long-term minimum and maximum average temperatures of between -3°C and 18°C (Midgley *et al.*, 1994). The Mean Annual Evaporation (MAE) varies from 1 600 mm (where the Modder River originates) to 2 200 mm (downstream of the convergence of the Modder and Riet Rivers). Evaporation intensifies from the east to west, while the rainfall decreases from east to west (Midgley *et al.*, 1994).

In the MRRC, the average Mean Annual Precipitation (MAP) is 424 mm, varying from 275 mm in the west to 685 mm in the east (Lynch, 2004). The rainfall is primarily classified as convective rainfall, which is regarded as highly variable in both time and space. The rainy season commences in early September and ends in mid-April with a dry winter.

3.3 Rainfall Monitoring Network

There are 185 South African Weather Services (SAWS) daily rainfall stations located within the boundaries of the MRRC. However, currently, there are only 40 active SAWS rainfall stations available in the MRRC, while only 169 SAWS rainfall stations, as shown in Figure 3.2, proved to have adequate historical data both in terms of record length and data quality to conduct this study. It is apparent from the rainfall monitoring network in Figure 3.2 that it is more condensed in the mid-eastern parts than in the north-western parts of the MRRC (Pietersen, 2016).

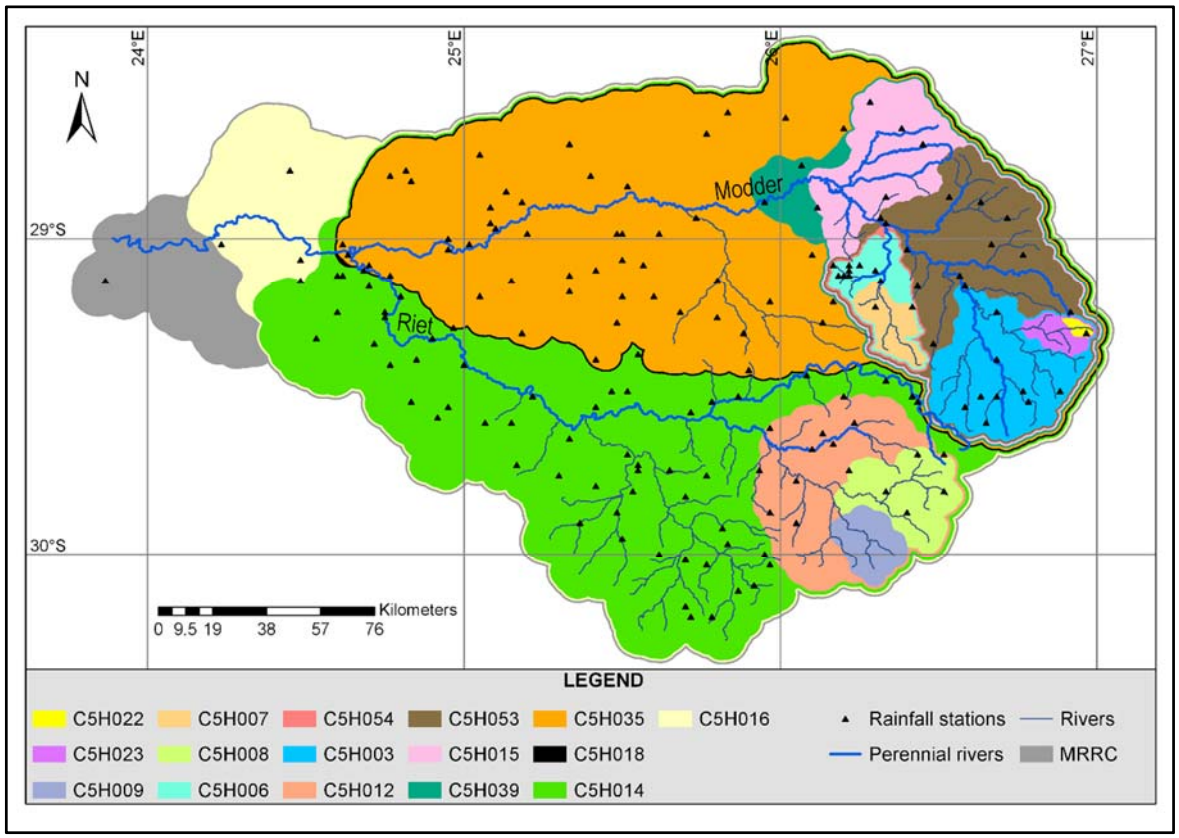

Figure 3.2: Location of the daily SAWS rainfall stations within the sub-catchments of the MRRC

3.4 Flow-gauging Network

There are 16 gauged sub-catchment areas ranging between 39 km^2 and 33 278 km^2 in the MRRC. The sub-catchments are regarded as 'gauged', since Department of Water and Sanitation (DWS) flow-gauging stations are located at the outlet of each sub-catchment. The layout of each sub-catchment, the river network and location of each individual flow-gauging station are shown in Figure 3.3.

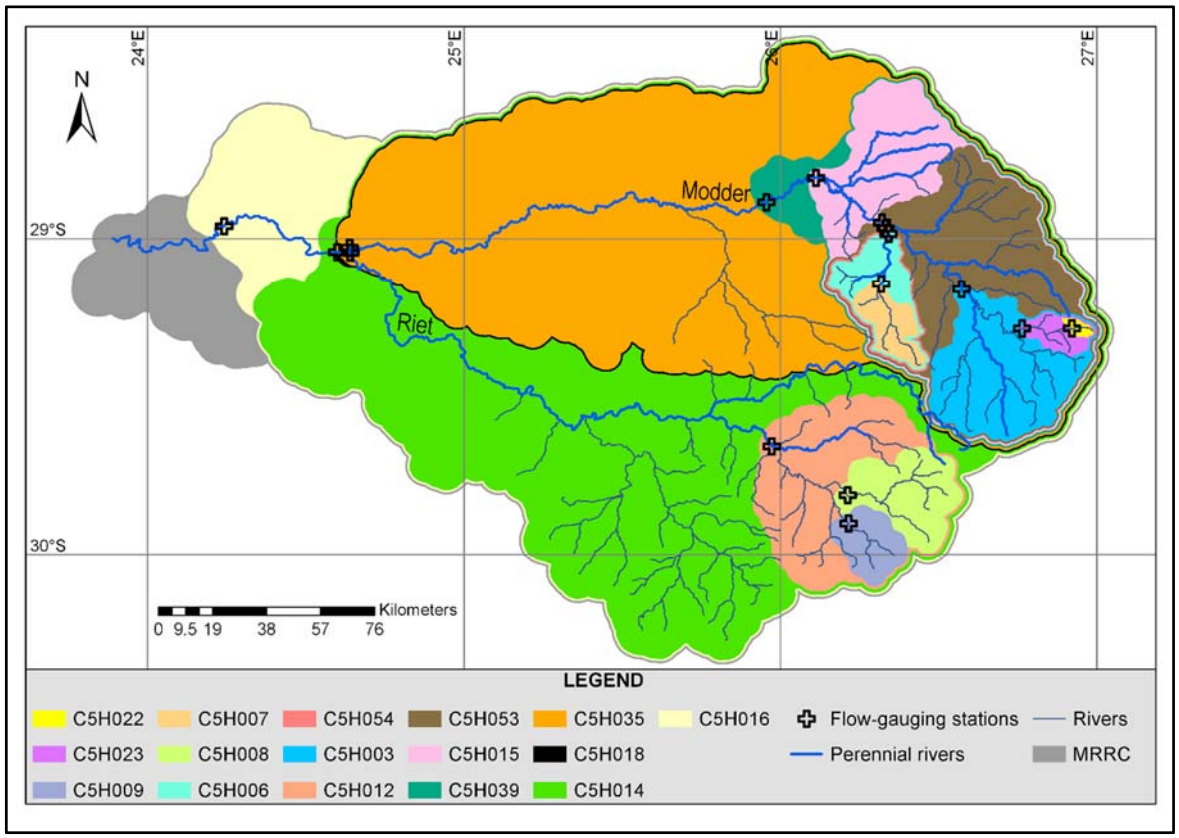

Figure 3.3: Location of the DWS flow-gauging stations and sub-catchments in the MRRC

The methodology adopted in meeting the specific objectives of this study are discussed in the next chapter.

CHAPTER 4: METHODOLOGY

This chapter presents the methodology adopted to estimate time variables, time parameters and time parameter proportionality ratios from observed rainfall-runoff data sets using a simplified convolution process and the currently recommended time parameter definitions. A flow diagram (*cf.* Figure 4.1) is included in this chapter to provide a general overview of the procedural steps followed to estimate the time variables, time parameters and time parameter proportionality ratios. The development of an Automated Toolkit and the associated working processes thereof to aid in the analyses of the observed rainfall-runoff data, are also included.

4.1 Establishment of Rainfall Database

A daily rainfall database was established by evaluating, preparing and extracting daily rainfall data from the SAWS and the Agricultural Research Council - Institute for Soil, Climate and Water (ARC-ISCW) rainfall stations present in the MRRC. In total, 169 rainfall stations were used due to a lack of data from 16 stations within the MRRC.

The SAWS is a respected scientific voice on weather and climate related issues. In terms of forecasting, the SAWS, through its widespread network of surface and atmospheric weather observation stations and remote weather observation networks (satellite, radar, lightning detection network and CCTV cameras), is able to monitor weather conditions and as required, issue alerts of adverse weather conditions as mandated by the SAWS Act, 2001 (Act No. 8 of 2001), as amended in 2013 (SAWS, 2019). The SAWS stations are manufactured in accordance with the World Meteorological Organization (WMO) specifications standards (SAWS, 2019). The SAWS collates, maintains and runs a quality control process of South Africa's meteorological and climatological data and associated information. These archived data sets consist of (SAWS, 2019):

(a) Daily rainfall values since 1836;

(b) Daily surface observations for all stations, but for selected stations since 1884;

(c) Hourly data of wind direction, wind speed, temperature, humidity, pressure and solar radiation from 1950 onwards;
(d) Upper-air sounding data since 1961;
(e) Marine data from 1975 on-wards;
(f) Forecasting data since 1990;
(g) Satellite data since 1992; and
(h) Radar data since 1994.

The SAWS daily rainfall database typically consists of aggregated catchment specific samples of daily and sub-daily (where available) rainfall stations present in the MRRC as previously used by Smithers and Schulze (2000a; 2000b), Lynch (2004) and Pietersen (2016).

The ARC-ISCW Agrometeorology Programme (AgroMet) maintains an operational agro-climate network of weather stations (approximately 500) and a climate database in South Africa (ARC, 2019). Hourly, daily, monthly, yearly or long-term average data are available. According to Kaempffer and Germishuyse (2009), AgroMet has a countrywide weather station network that has been installed since 1940 with the aim of satisfying the climatological requirements of the agricultural sector. The AgroMet weather station network has approximately 100 mechanical and 530 automatic weather stations (Kaempffer and Germishuyse, 2009). AgroMet actively expands the automatic weather station (AWS) network on an on-going basis. AgroMet also uses the basic WMO standards as a guideline and all AWS's are monitored and calibrated at regular intervals and calibration reports are filed as metadata for future reference (Kaempffer and Germishuyse, 2009). The ARC-ISCW daily rainfall database contains only up-to-date samples of the daily rainfall stations present in the MRRC.

The DWS meteorological stations in the MRRC were not considered to extend the rainfall data series as it cannot be confirmed whether these stations use the basic WMO standards as a guideline, and whether they are monitored and calibrated at regular intervals, since the DWS is not mandated to monitor weather conditions in South Africa.

The Daily Rainfall Extraction Utility (DREU; Lynch, 2004) was used for the extraction of all the daily rainfall data series. Infilling of missing rainfall data to extend the rainfall data series was not considered. In cases where inactive SAWS rainfall stations lacked data, data from the ARC-ISCW database were combined with the SAWS database as far as possible to extend the rainfall data series. The ARC-ISCW stations used to extend the data series of inactive SAWS stations were in close proximity to the inactive stations. A list of all 169 SAWS rainfall stations with coordinates were sent to the ARC-ISCW. The ARC-ISCW only found 35 stations that were in close proximity to the SAWS rainfall stations. In other words, this denoted that only the data series from 35 stations out of the 169 SAWS stations could be extended.

The Geographical Information Systems (GIS) feature classes (shape files) containing the spatial features of the complete daily rainfall database were generated in the ArcGIS™ 10.1 environment. During the analyses, care was taken to ensure that all the stations within a sub-catchment contributed to the rainfall data. In cases where missing rainfall data are present during the analyses, the Automated Toolkit developed (*cf.* Section 4.3), would caution the user about the presence of a negative Phi-index and that an alternative rainfall-runoff event needs to be selected.

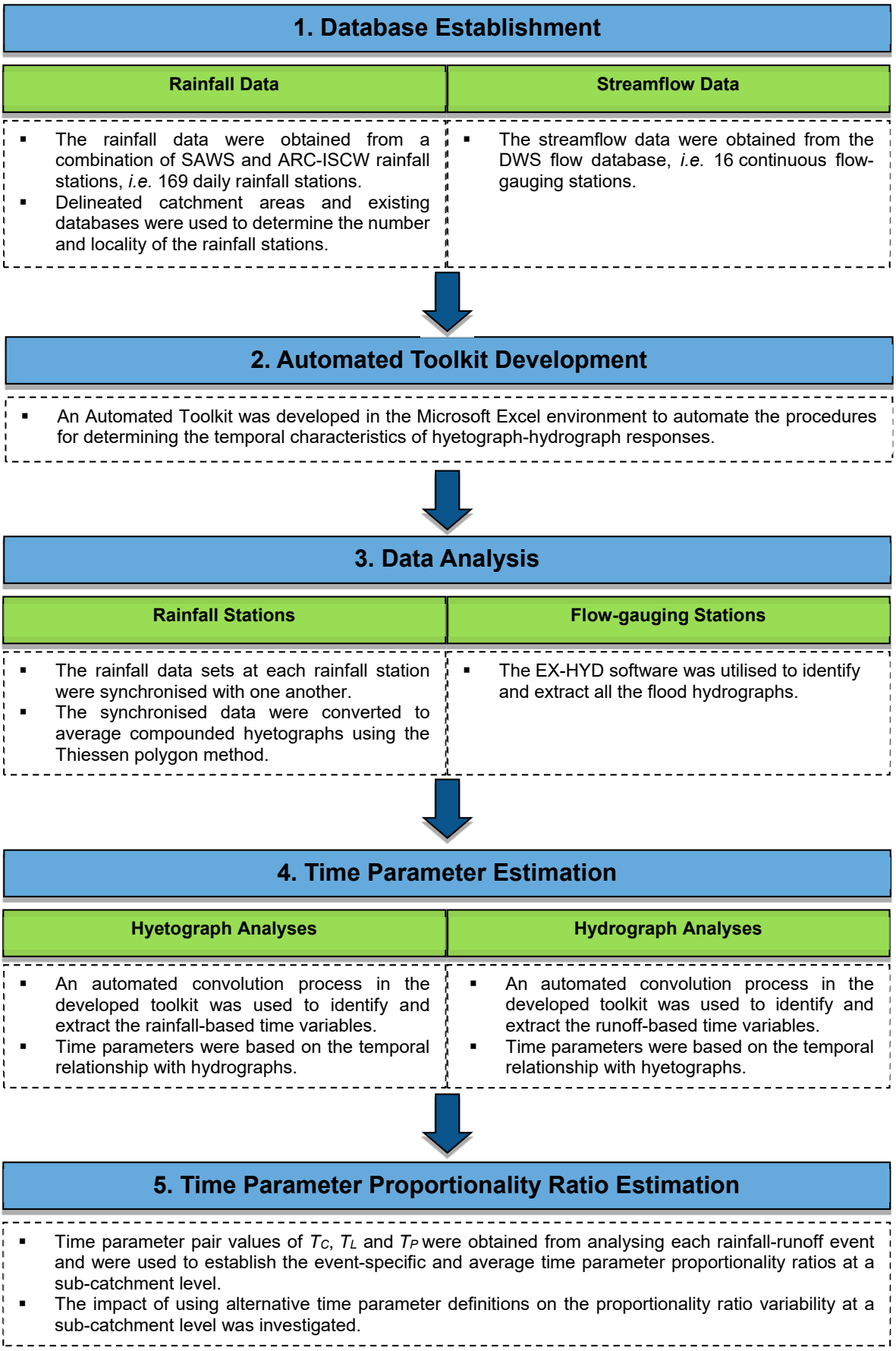

Figure 4.1: Schematic flow diagram illustrative of the implemented methodology

4.1.1 Synchronisation of rainfall data

The degree of synchronisation between the point rainfall data sets at each rainfall station was established by considering recorded rainfall with mutual time intervals. The rainfall data series at each rainfall station was firstly exported and converted to a Microsoft Excel file format (*e.g.* *.xlsx). Thereafter, the rainfall data files were imported to the Automated Toolkit (*cf.* Section 4.3). In essence, a number of logic and synchronisation functions are available in the Visual Basic for Applications (imbedded in Microsoft Excel) environment to enable the automatic synchronisation of daily rainfall data, *e.g.* 'INDEX' and 'MATCH'. The 'INDEX' function returns a value or a reference of a cell at the intersection of a particular row and column within a given range, while the 'MATCH' function returns the relative position of an item in an array that matches a specific value in a specified order. The use of the Automated Toolkit ensured that large data sets from numerous rainfall stations within a particular sub-catchment could be synchronised within minutes.

The details of each daily rainfall station in terms of location and distance from the sub-catchment outlet (L) are listed in Table A.1, Appendix A.

4.1.2 Averaging of observed rainfall data

In the calculation of total quantities of rainfall over large areas, the frequency of storms and their contribution to single rainfall stations are unknown. Therefore, it is necessary to convert numerous observed point rainfall depths to provide an average rainfall depth over a certain area (Wilson, 1990). All the various methods proposed for the averaging of point rainfall depths over an area were considered in this study. However, Gericke and Du Plessis (2011) confirmed that there is a high degree of association (r^2 values > 0.9) between the various averaging methods when applied to the MRRC, with percentage differences < 17%. The latter results actually confirmed the even spatial distribution of the rainfall stations and the relatively flat topography of the MRRC (Gericke and Du Plessis, 2011). Based on these findings and in conjunction with the large amount of data and computations required, the Thiessen polygon method was selected as the most suitable method to use. The weighting procedure as applicable to the Thiessen polygon method [Eq. (4.1)] defines the zone of influence of each rainfall station by drawing lines between pairs

of stations, bisecting the lines with perpendiculars. The total area enclosed within the polygon formed by these intersecting perpendiculars has rainfall of the same amount as the enclosed rainfall station (Wilson, 1990).

$$\overline{P} = \sum \frac{A_S P_i}{A_T} \quad (4.1)$$

where:

$\overline{P}$ = average rainfall depth (mm),
A_S = area of the polygon surrounding a particular rainfall station (km^2),
A_T = total catchment area (km^2), and
P_i = point rainfall depth at a particular rainfall station (mm).

In essence, the Thiessen polygon method was used in each sub-catchment to convert the individual point rainfall hyetographs into an average catchment rainfall hyetograph using the *Create Thiessen Polygons* tool in the *Proximity* toolset contained in the *Analysis Tools* toolbox of ArcGIS™. The boundary of the resultant Thiessen polygons was selected in each case by the applicable sub-catchment boundary (polygon feature class). Thereafter, the areas of the polygons surrounding the stations within each sub-catchment was exported and converted to a Thiessen weight using the total sub-catchment area. The Thiessen weights were then utilised to approximate each rainfall station's contribution to the daily point rainfall within each sub-catchment.

4.2 Establishment of Streamflow Database

A streamflow database was established by evaluating, preparing and extracting primary flow data from the DWS flow database for the 16 continuous flow-gauging stations present in the MRRC. The screening criteria used to select the stations for the analyses include the following:

(a) **Stations common to previous flood studies:** Sixteen continuous flow-gauging stations used by Gericke and Smithers (2018) present in the MRRC were considered.

(b) **Record length:** Only streamflow records longer than 10 years were considered; as a result, one of the 16 flow-gauging stations did not meet the

criteria. However, this flow-gauging station met the criteria as stipulated in (a) and (c); hence it was included in the analysis. This also ensured that a consistent approach is followed when the event-specific and average time parameter proportionality ratios are estimated at a sub-catchment level.

(c) **Catchment area:** In addition to above-listed criteria, the catchment areas of the selected flow-gauging stations should cover the range of sub-catchment areas present in the MRRC.

The details of the 16 flow-gauging stations as included in the streamflow database are listed in Table 4.1. The average data record length of all the flow-gauging stations is 46 years (Gericke and Smithers, 2018).

Table 4.1: Information of sub-catchments as included in the streamflow database (after Gericke and Smithers, 2018)

Sub-catchment	Area (km²)	Record length		
		Start	End	Years
C5H003	1 641	1918	2013	95
C5H006	676	1922	1926	4
C5H007	346	1923	2013	90
C5H008	598	1931	1986	55
C5H009	189	1931	1986	55
C5H012	2 366	1936	2013	77
C5H014	31 283	1938	2013	75
C5H015	5 939	1949	1983	34
C5H016	33 278	1953	1999	46
C5H018	17 361	1960	1999	39
C5H022	39	1980	2013	33
C5H023	185	1983	2008	25
C5H035	17 359	1989	2013	24
C5H039	6 331	1970	2013	43
C5H053	4 569	1999	2013	14
C5H054	687	1995	2013	18

4.2.1 Extraction of flood hydrograph data

The next stage involved the identification and extraction of complete flood hydrographs from the primary flow data sets. The Flood Hydrograph Extraction Software (EX-HYD) developed by Görgens *et al.* (2007) was used to assist in identifying and extracting complete flood hydrographs. Complete flood hydrographs

were extracted using the following selection criteria as proposed by Gericke and Smithers (2017; 2018):

(a) **Truncation levels:** Only flood events larger than the smallest annual maximum flood event on record were extracted. Consequently, all minor events were excluded, while all the flood events retained were characterised as multiple events being selected in a specific hydrological year. This approach resulted in a partial duration series (PDS) of independent flood peaks above a certain level.

(b) **Start/end time of flood hydrographs:** Flood peaks and flood volumes for the same event were obtained by extracting complete hydrographs. Initially, a large number of streamflow data points prior the start of a hydrograph, identified by physical inspection where the flow changes from nearly constant or declining values to rapidly increasing values, were included in order to identify the potential start of direct runoff. Thereafter, it was acknowledged that, by definition, the volume of effective rainfall is equal to the volume of direct runoff. Therefore, when separating a hydrograph into direct runoff and baseflow using a recursive filtering method, the separation point could be regarded as the start of direct runoff which coincides with the start of effective rainfall.

(c) **Extrapolation of rising and recession limbs to zero baseflow line:** In some cases, due to the nature of the data, the above-mentioned starting point identified by physical inspection as the lowest recording, did not necessarily coincide with the baseflow starting point as identified using the recursive filtering techniques. In such cases, a similar approach as followed by Görgens *et al.* (2007) was adopted, where a straight vertical line extrapolation from the identified starting point to the zero baseflow line was applied to enable the estimation of direct runoff volumes.

4.3 Development of Automated Toolkit

One of the specific objectives of this study is to develop a toolkit in the Microsoft Excel environment to automate the procedures of estimating the temporal characteristics of hyetograph-hydrograph responses. The Automated Toolkit consists of a collection of functions required to estimate the temporal characteristics

from rainfall and streamflow records, including: (i) baseflow separation, (ii) time variable identification and estimation, (iii) time parameter estimation and, (iv) the estimation of time parameter proportionality ratios.

Typically, the following modules are available in the Automated Toolkit:

(a) General catchment information;
(b) Processing of observed daily rainfall data;
(c) Extracted streamflow data;
(d) Analyses and plotting of hyetograph-hydrograph relationships; and
(e) Exporting of individual hyetograph-hydrograph pairs and summary of results.

The function for baseflow separation is based on the Hydrograph Analysis Tool (HAT) developed by Gericke (2016), while the remaining functions are proposed as a mechanism to extract compounded catchment hyetographs from multiple rainfall stations with mutual or synchronised events of recorded rainfall. The EX-HYD software developed by Görgens *et al*. (2007) was used to assist in identifying and extracting the complete flood hydrographs (*cf.* Section 4.2.1); hence, this function was not included in the toolkit. The Automated Toolkit attempts to mimic the typical convolution procedure practitioners would follow to visually inspect and interpret hyetograph-hydrograph data sets. Rainfall and streamflow data are exported to corresponding modules in the toolkit, followed by the working processes and analyses as summarised in Figure 4.2.

A detailed discussion of the processes shown in Figure 4.2 to analyse rainfall hyetographs and streamflow hydrographs, is included in Sections 4.4 and 4.5, respectively.

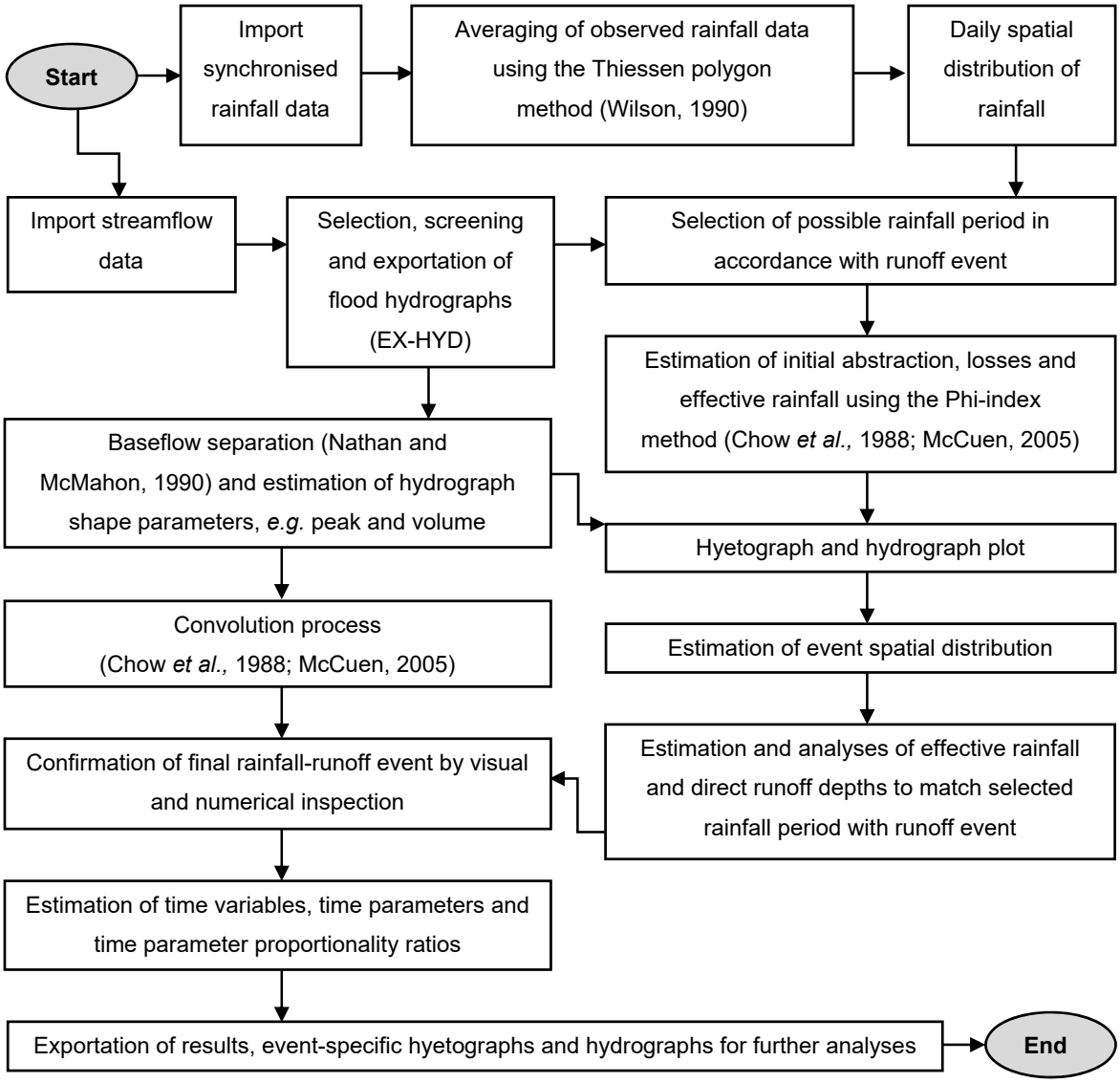

Figure 4.2: Schematic flow diagram illustrative of the working processes included in the Automated Toolkit

4.4 Analyses of Hyetographs

In order to analyse rainfall hyetographs, the associated runoff events (as discussed in Section 4.2.1) need to be identified first. Consequently, a Visual Basic search algorithm was employed to identify the causal rainfall event in a window spanning *n* days before the start of the identified runoff event to the time of the last streamflow recording, where *n* is a user-defined parameter. For example, if *n* is set as 12 days, all rainfall records located in the window 12 days before the start of the runoff event to the last streamflow recording will be identified. The rainfall event starts at the first zero rainfall record in the search window and ends at the last zero recording.

Subsequently, after the averaging of observed rainfall data per rainfall station and the synchronisation of mutual time interval rainfall-runoff events, the daily spatial distribution of any rainfall event could be estimated using Equation (4.2):

$$S_d = \frac{\sum A_T TW_i}{A_T} \text{ x } 100 \qquad (4.2)$$

where:

S_d = daily spatial distribution (%),

A_T = total catchment area (km^2), and

TW_i = Thiessen weight of each rainfall station that contributed to the daily rainfall.

During a rainfall event, not all the rainfall contributes to direct runoff. Initial abstractions, *e.g.* evaporation, transpiration, depression, detention, infiltration and interception by vegetation, reduce the effective runoff producing rainfall that a catchment receives. The Phi-index method [Eq. (4.3)] was used to yield an effective rainfall hyetograph.

$$I = \frac{P_T - Q_D}{t} \qquad (4.3)$$

where:

I = Phi-index (mm/h),

P_T = total rainfall (mm),

Q_D = direct runoff, which equals the effective rainfall (mm), and

t = time period during which effective rainfall occurred (h).

Hence, Equation (4.3) enabled the plotting of possible hyetograph-hydrograph combinations to ultimately translate the effective runoff producing rainfall into direct runoff using a simplified convolution process as shown in Figure 4.3. The average (weighted) rainfall intensity (*y*-axis) is plotted against time (*x*-axis). The Phi-index is shown as a horizontal dashed line. The area above the horizontal dashed line represents the effective rainfall. The area below the horizontal dashed line represents all the losses. The selection of an appropriate hyetograph-hydrograph

event is characterised by the effective rainfall being equal to the direct runoff (as obtained from the baseflow separation applied to the hydrographs in Section 4.5). In cases where the effective rainfall and direct runoff volumes are not in equilibrium, an alternative rainfall period is selected and the process is repeated until equilibrium is reached. In each case, the event spatial distribution [Eq. (4.4)] is also automatically estimated for each rainfall period.

$$S_e = \sum \left[\left(\frac{P_i}{\sum_{i=0}^{r-1} P_i} \right) S_{di} \right] \times 100 \qquad (4.4)$$

where:

S_e = event spatial distribution (%),

i = number of frequency,

P_i = weighted daily rainfall (mm),

$\sum_{i=0}^{r-1} P_i$ = cumulative frequency of weighted daily rainfall (mm),

r = range of frequency, and

S_{di} = daily spatial distribution (%).

The application of Equation (4.4) and matching of rainfall-runoff events with corresponding effective rainfall and direct runoff volumes are discussed in the next section. However, it is important to note that the identification and estimation of time variables *e.g.* start of effective rainfall (t_{er0}), centroid of effective rainfall (t_{erc}), end of effective rainfall (t_{ere}), and time of maximum rainfall (t_{rmax}) for each rainfall-runoff event, are already possible at this stage.

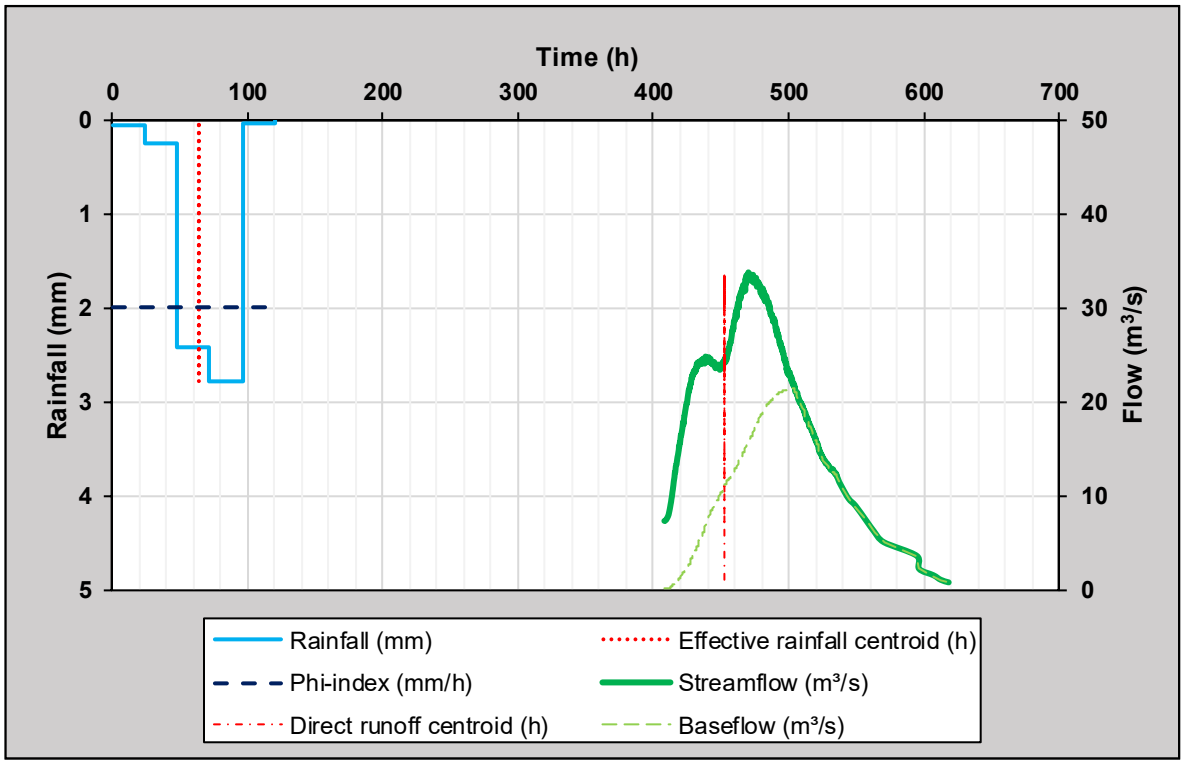

Figure 4.3: Example of a simplified convolution process with a compounded catchment hyetograph and resulting hydrograph

4.5 Analyses of Hydrographs

The convolution process required to assess the time parameters, *e.g.* T_C, T_L and T_P, was based on the temporal relationship between an average compounded catchment hyetograph and a corresponding hydrograph in each sub-catchment. Conceptually, the proposed procedure is based on the definition that the volume of effective rainfall equals the volume of direct runoff when a hydrograph is separated into direct runoff and baseflow. The separation point on the hydrograph is also regarded as the start of direct runoff which coincides with the start of effective rainfall.

A number of methods, *e.g.* graphical, recursive digital filters, frequency-duration, and recession analysis have been proposed in the literature to separate direct runoff and baseflow (Nathan and McMahon, 1990; Arnold *et al.*, 1995; Smakhtin, 2001; McCuen, 2005). According to Smakhtin (2001), the most well-known and widely used recursive filtering methods are those developed by Nathan and McMahon (1990) and Chapman (1999). Smakhtin and Watkins (1997)

also adopted the methodology as proposed by Nathan and McMahon (1990) with some modifications in a national-scale study in South Africa. Smakhtin and Watkins (1997) established that a fixed α-parameter value of 0.995 is suitable for most catchments in South Africa, although in some catchments, α-parameter values of 0.997 proved to be more appropriate. Hughes *et al.* (2003) also highlighted that a fixed β-parameter value of 0.5 could be used with daily time-step data, since there is more than enough flexibility in the setting of the α-parameter value to achieve an acceptable result. Consequently, a fixed α-parameter value = 0.995 and β-parameter value = 0.5 were used in this study.

Hence, based on these recommendations, as well as the need for consistency and reproducibility, Equation (4.5) as proposed by Nathan and McMahon (1990) and adopted by Smakhtin and Watkins (1997), was used in this study. Figure 4.3 (*cf.* Section 4.4) is also illustrative of a typical baseflow separation.

$$Q_{Dxi} = \alpha Q_{Dx(i-1)} + \beta(1+\alpha)(Q_{Txi} - Q_{Tx(i-1)}) \quad (4.5)$$

where:

Q_{Dxi} = filtered direct runoff at time step i, which is subject to $Q_{Dxi} \geq 0$ for time i (m^3/s),

α, β = filter parameters, and

Q_{Txi} = total streamflow (*i.e.* direct runoff plus baseflow) at time step i (m^3/s).

As discussed in Section 4.4, the volumes of effective rainfall and direct runoff need to be in equilibrium when a causal rainfall event of appropriate duration prior to the resulting runoff event is selected. This was done by matching the direct runoff depth (Q_D) with the effective rainfall depth (P_E) in Equation (4.6).

$$P_E = \frac{\sum\left[\frac{Q_{Dxi} + Q_{Dx(i-1)}}{2} \times \Delta T_{xi}\right]}{(A_T \times 1000)S_e} \quad (4.6)$$

where:

P_E = effective rainfall (mm),

A_T = total catchment area (km^2),

Q_{Dxi} = filtered direct runoff at time step i, which is subject to $Q_{Dxi} \geq 0$ for time i (m^3/s),

S_e = event spatial distribution (%), and

ΔT_{xi} = absolute change in time at time step i (seconds).

As a result, time variables *e.g.* start of total runoff (t_{q0}), time of peak discharge (t_{qpk}), centroid of direct runoff (t_{qc}), and time of the inflection point on the recession limb (t_{ip}) could be identified and estimated for each rainfall-runoff event at a sub-catchment level.

4.6 Estimation of Time Parameters and Proportionality Ratios

In considering the observed hyetograph-hydrograph data and the associated time variables established in Sections 4.4 and 4.5, respectively, time parameters were estimated using the Automated Toolkit. The time parameters are based on the seven different theoretical time parameter definitions introduced and discussed in Sections 2.2.1 to 2.2.3, Chapter 2.

Table 4.2 provides a summary of the different time variables, Time Parameter (TP) equations and Time Parameter Proportionality Ratio (TPPR) estimation procedures included in the Automated Toolkit.

It is evident from Table 4.2 that the toolkit includes a series of functions to estimate event-based time variables from both rainfall and streamflow data. The time parameter pair values, *e.g.* T_C, T_L and T_P obtained from analysing each rainfall-runoff event were used to establish the event-specific and average proportionality ratios between these time parameters at a sub-catchment level using the equations listed in Table 4.2. The effect of using alternative time parameter definitions on the proportionality ratio variability was also investigated.

Table 4.2: Summative description of time variables, TP equations and TPPR estimation procedures included in the Automated Toolkit. The letter in brackets () is used as cross-reference to the time parameter definitions (a) to (d) as defined and described in Chapter 2 (*cf.* Figure 2.1)

Symbol	Equation	Description
t_{er0}	-	Start of effective rainfall
t_{erc}	-	Centroid of effective rainfall
t_{ere}	-	End of effective rainfall
t_{rmax}	-	Time of maximum rainfall
t_{q0}	-	Start of total runoff
t_{qpk}	-	Time of peak discharge
t_{qc}	-	Centroid of direct runoff
t_{ip}	-	Time of inflection point on the recession limb
T_C (a)	$t_{ip} - t_{ere}$	Time of concentration definition (a)
T_C (b) & T_L (a/b)	$t_{qpk} - t_{erc}$	Time of concentration definition (b) and lag time definition (a/b)
T_C (c)	$t_{qpk} - t_{rmax}$	Time of concentration definition (c)
T_L (c)	$t_{qc} - t_{erc}$	Lag time definition (c)
T_C (d)	$t_{qpk} - t_{q0}$	Time of concentration definition (d)
TPPR 1	$\frac{T_C(a)}{T_L(a\,or\,b)}$	Time Parameter Proportionality Ratio (1)
TPPR 2	$\frac{T_C(b)}{T_L(a\,or\,b)}$	Time Parameter Proportionality Ratio (2)
TPPR 3	$\frac{T_C(c)}{T_L(a\,or\,b)}$	Time Parameter Proportionality Ratio (3)
TPPR 4	$\frac{T_C(d)}{T_L(a\,or\,b)}$	Time Parameter Proportionality Ratio (4)
TPPR 5	$\frac{T_C(a)}{T_L(c)}$	Time Parameter Proportionality Ratio (5)
TPPR 6	$\frac{T_C(b)}{T_L(c)}$	Time Parameter Proportionality Ratio (6)
TPPR 7	$\frac{T_C(c)}{T_L(c)}$	Time Parameter Proportionality Ratio (7)
TPPR 8	$\frac{T_C(d)}{T_L(c)}$	Time Parameter Proportionality Ratio (8)

The next chapter provides the results based on the methodology adopted in this chapter.

CHAPTER 5: RESULTS AND DISCUSSION

In this chapter, the research results are presented and discussed with reference to the research aim, *i.e.* the estimation of time parameter proportionality ratios from observed rainfall and streamflow data using a simplified convolution process and the seven different time parameter definitions currently recognised in international literature.

5.1 Analyses of Rainfall Data

The catchment area (A), number of rainfall stations (N_X), and the average record length (R_L) of the observed rainfall data used in each of the 16 sub-catchments of the MRRC are listed in Table 5.1. The average period of record for observed rainfall data ranged from 1901 to 2001.

Table 5.1: Details of rainfall stations as included in the MRRC rainfall database

Sub-catchment	A (km^2)	N_X	R_L (years)
C5H003	1 641	15	54
C5H006	676	18	50
C5H007	346	8	46
C5H008	598	6	46
C5H009	189	3	39
C5H012	2 366	21	52
C5H014	31 283	165	51
C5H015	5 939	46	52
C5H016	33 278	168	51
C5H018	17 361	99	52
C5H022	39	N/A	N/A (insufficient data)
C5H023	185	N/A	N/A (insufficient data)
C5H035	17 359	99	52
C5H039	6 331	47	52
C5H053	4 569	40	51
C5H054	687	18	50

From Table 5.1 it is evident that sub-catchments C5H022 and C5H023 could not be analysed, since the rainfall data are insufficient to match the complete flood hydrographs identified and extracted for the specific periods under consideration. As highlighted in Chapter 4, Thiessen polygons were generated for each individual sub-catchment to provide Thiessen weights for the estimation of each rainfall station's contribution to the daily point and average catchment rainfall in a particular

sub-catchment. A summary of the rainfall stations and corresponding Thiessen weights at a sub-catchment level in the MRRC are listed in Table A.2, Appendix A.

5.2 Analyses of Streamflow Data

A total of 1 134 complete flood hydrographs or runoff events were extracted from the primary flow data sets, with between 13 and 117 individual flood hydrographs per flow-gauging station/sub-catchment. The number of runoff events and the period of record extracted for each flow-gauging station/sub-catchment are listed in Table 5.2.

Table 5.2: Number of runoff events extracted from each data period at a sub-catchment level in the MRRC

Sub-catchment	Period of record	Number of runoff events
C5H003	1918/07/01 to 2013/06/26	104
C5H006	1922/11/13 to 1926/12/31	16
C5H007	1923/10/01 to 2013/08/06	92
C5H008	1931/04/01 to 1986/04/01	117
C5H009	1931/03/01 to 1986/05/11	13
C5H012	1936/04/01 to 2013/02/13	82
C5H014	1938/10/17 to 2013/07/25	30
C5H015	1949/01/01 to 1983/11/22	92
C5H016	1953/02/01 to 1999/03/10	108
C5H018	1960/02/23 to 1999/03/15	84
C5H022	1980/10/14 to 2013/10/24	69
C5H023	1983/06/04 to 2008/03/22	77
C5H035	1989/08/03 to 2013/07/23	42
C5H039	1970/11/24 to 2013/08/08	61
C5H053	1999/11/29 to 2013/08/08	70
C5H054	1995/10/18 to 2013/08/08	77

5.3 Hyetograph-Hydrograph Analyses

A total of 394 hyetograph-hydrograph data sets representative of specific rainfall-runoff events were extracted and analysed using the Automated Toolkit (*cf.* Section 4.3, Chapter 4). A summary of the rainfall-runoff events extracted in each sub-catchment of the MRRC, is listed in Table 5.3.

Table 5.3: Number of rainfall-runoff events extracted using the Automated Toolkit

Sub-catchment	Runoff events	Rainfall events	Shortfall
C5H003	104	30	74
C5H006	16	3	13
C5H007	92	40	52
C5H008	117	58	59
C5H009	13	4	9
C5H012	82	6	76
C5H014	30	8	22
C5H015	92	50	42
C5H016	108	65	43
C5H018	84	59	25
C5H022	69	0	69
C5H023	77	0	77
C5H035	42	21	21
C5H039	61	20	41
C5H053	70	12	58
C5H054	77	18	59

It is evident from Table 5.3 that a number of runoff events could not be analysed due to a lack of rainfall data after the year 2001. Hence, this resulted in a shortfall; however, a number of runoff events could also not be analysed due to the difficulty experienced to identify the inflection point on a hydrograph recession limb or due to multi-peaked hydrographs. In essence, only 35% of the extracted runoff events could be analysed, *i.e.* 394 rainfall-runoff events.

Typical examples of the hyetograph-hydrograph events obtained from each sub-catchment are illustrated in Figures 5.1 to Figure 5.14. Additional examples of two hyetograph-hydrograph events per sub-catchment are also illustrated in Figures B.1 to B.28, Appendix B.

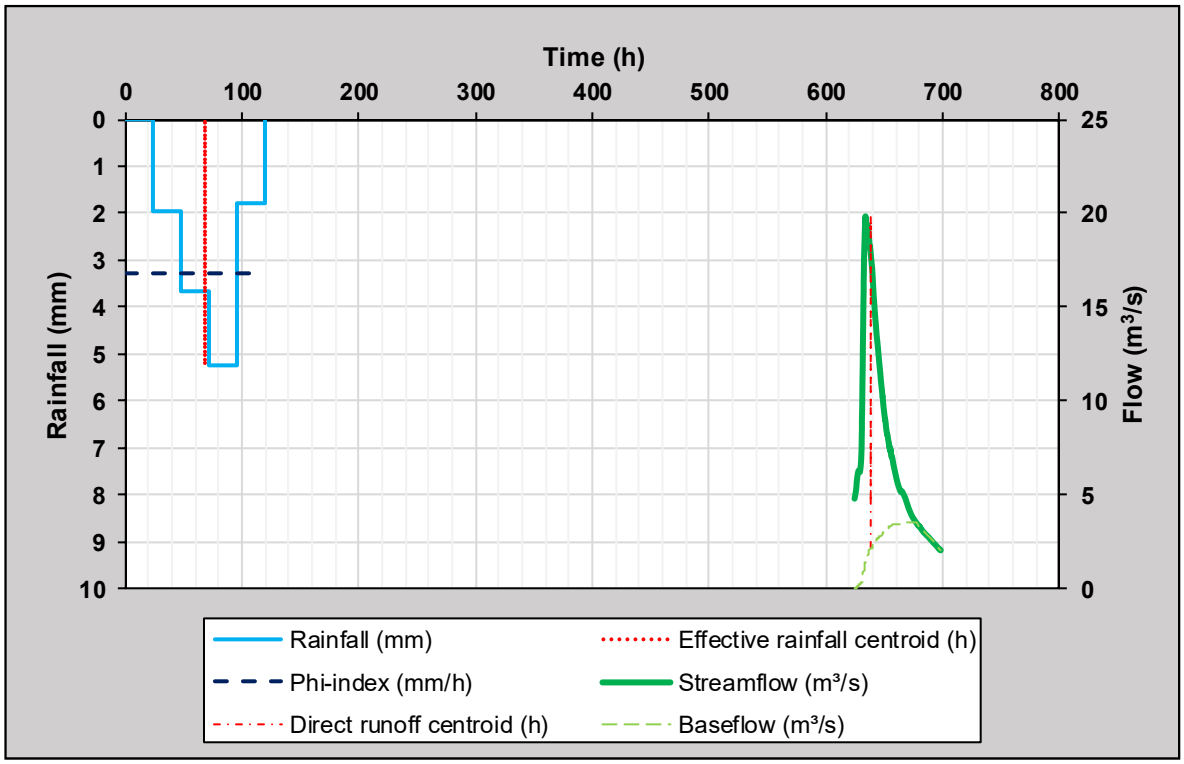

Figure 5.1: Hyetograph-hydrograph event in sub-catchment C5H003

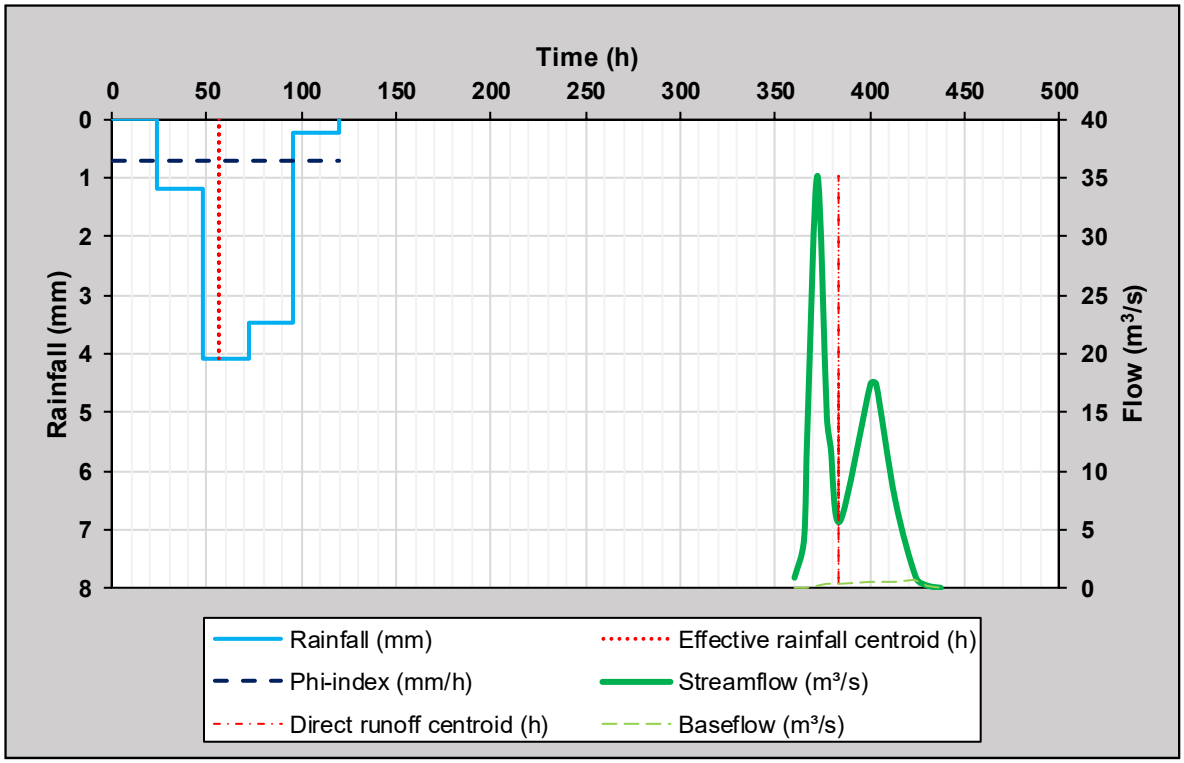

Figure 5.2: Hyetograph-hydrograph event in sub-catchment C5H006

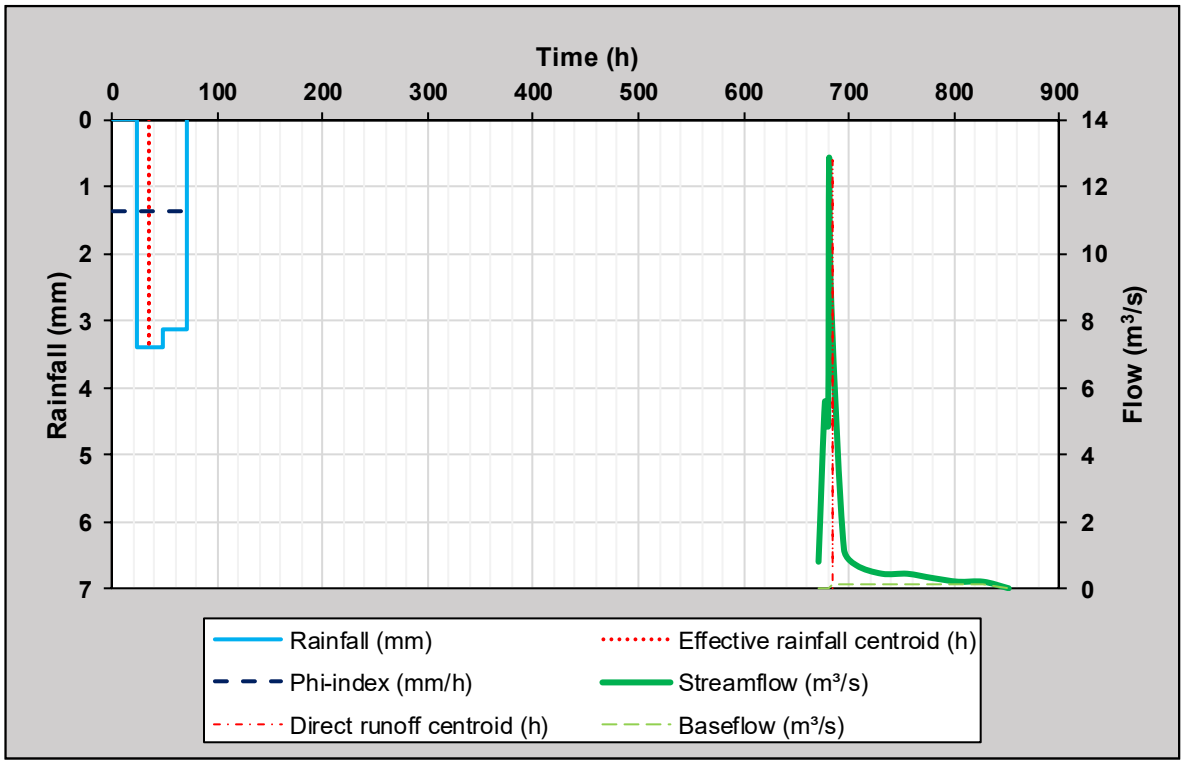

Figure 5.3: Hyetograph-hydrograph event in sub-catchment C5H007

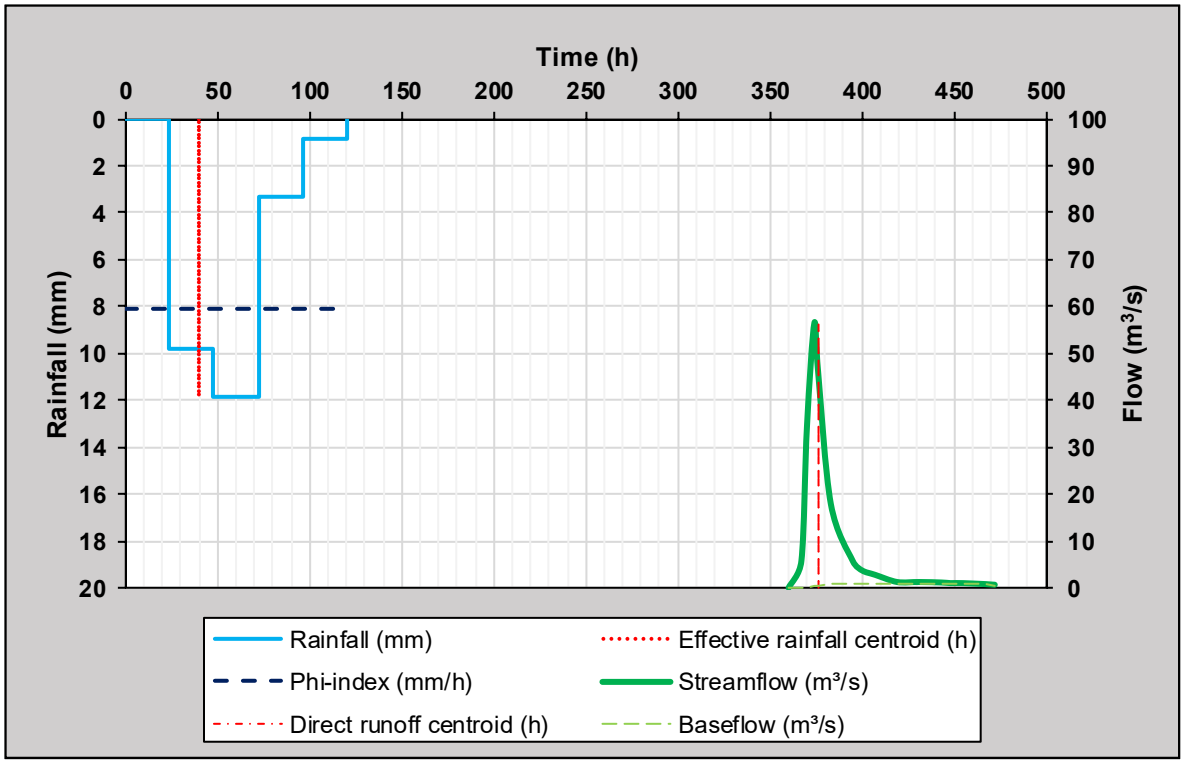

Figure 5.4: Hyetograph-hydrograph event in sub-catchment C5H008

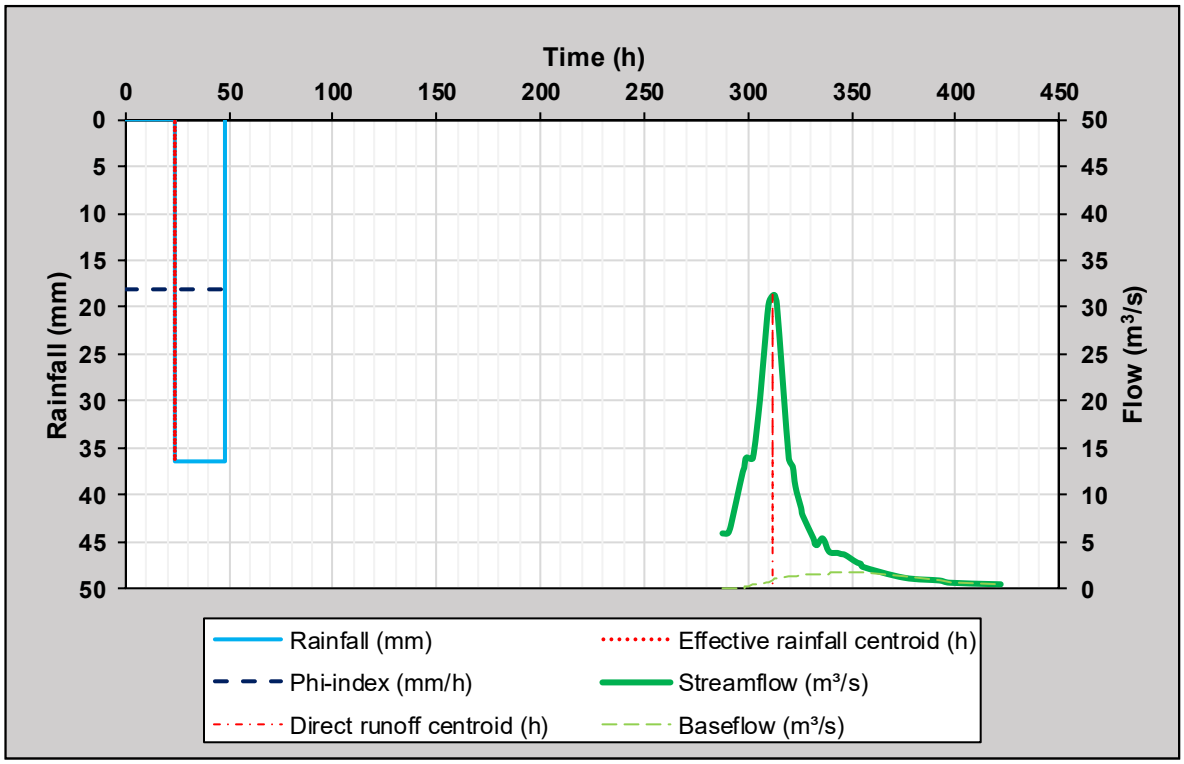

Figure 5.5: Hyetograph-hydrograph event in sub-catchment C5H009

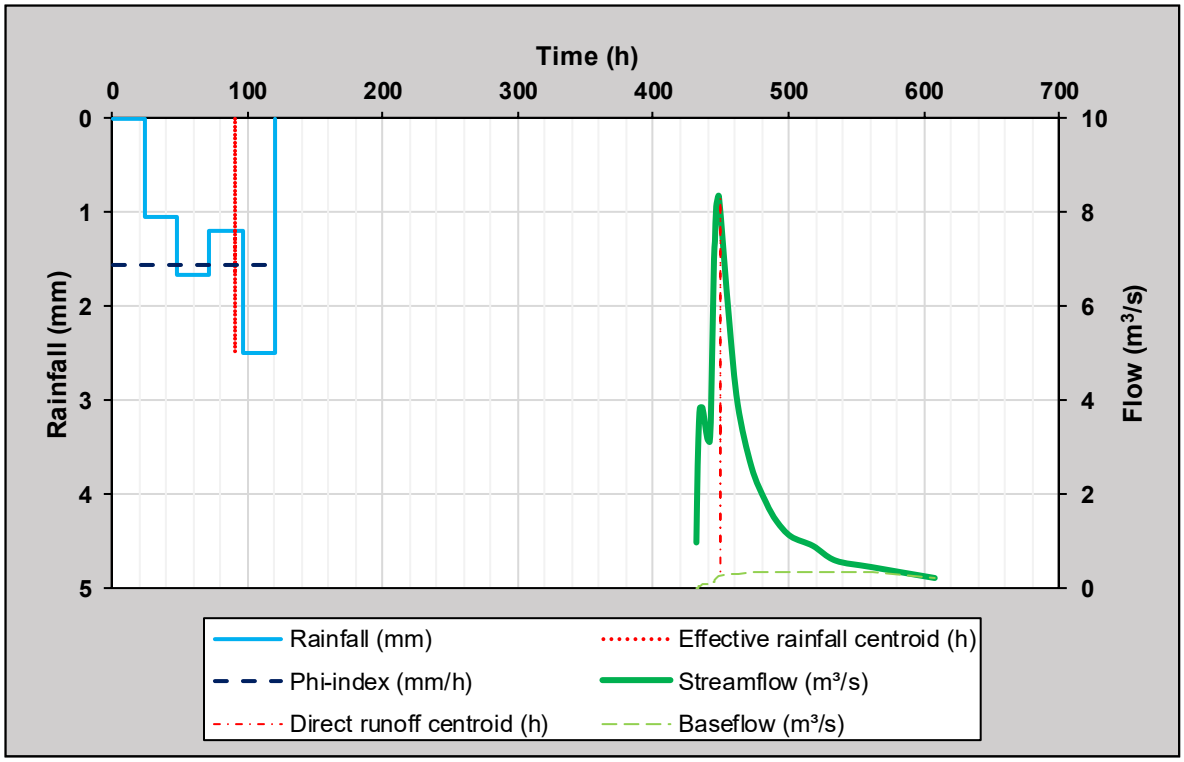

Figure 5.6: Hyetograph-hydrograph event in sub-catchment C5H012

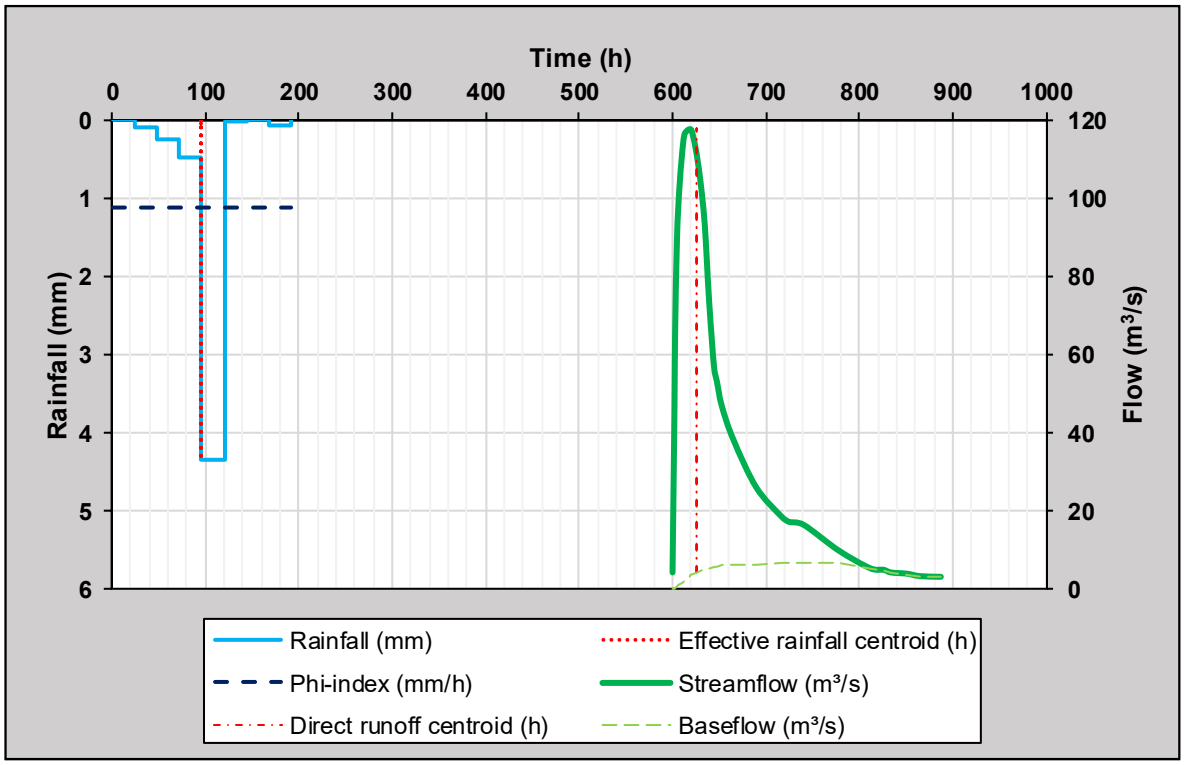

Figure 5.7: Hyetograph-hydrograph event for sub-catchment C5H014

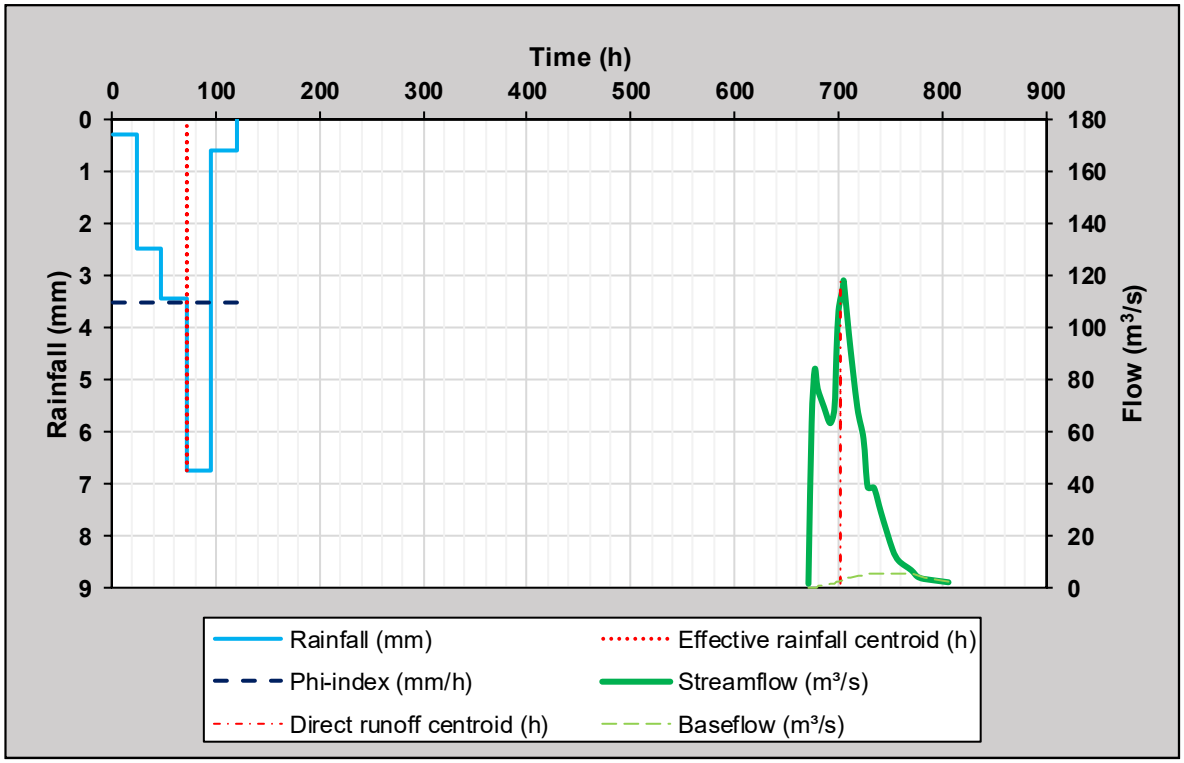

Figure 5.8: Hyetograph-hydrograph event in sub-catchment C5H015

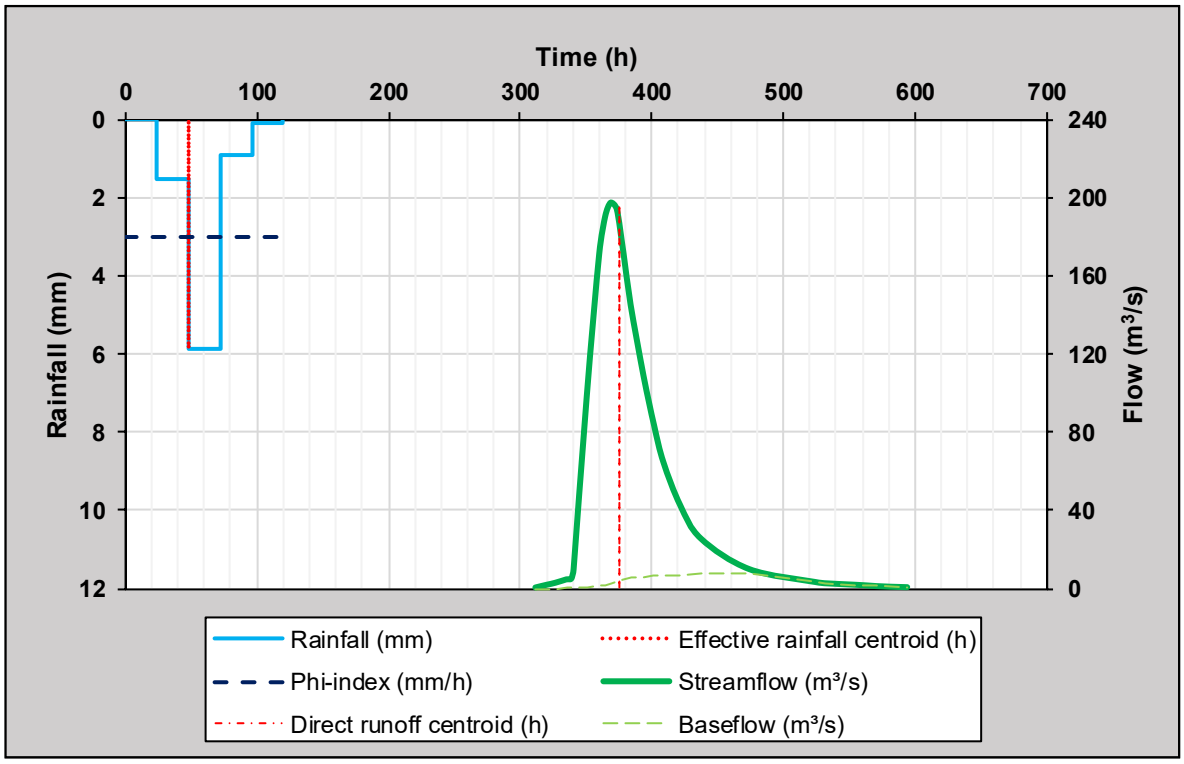

Figure 5.9: Hyetograph-hydrograph event in sub-catchment C5H016

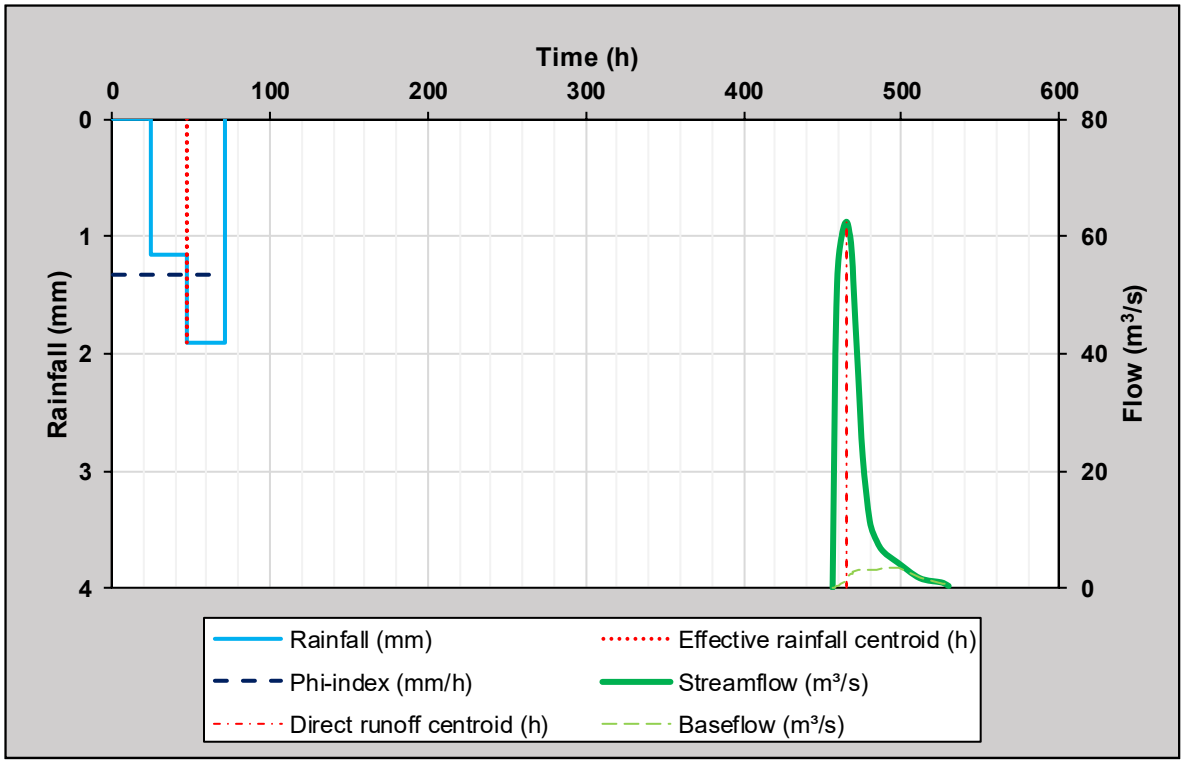

Figure 5.10: Hyetograph-hydrograph event in sub-catchment C5H018

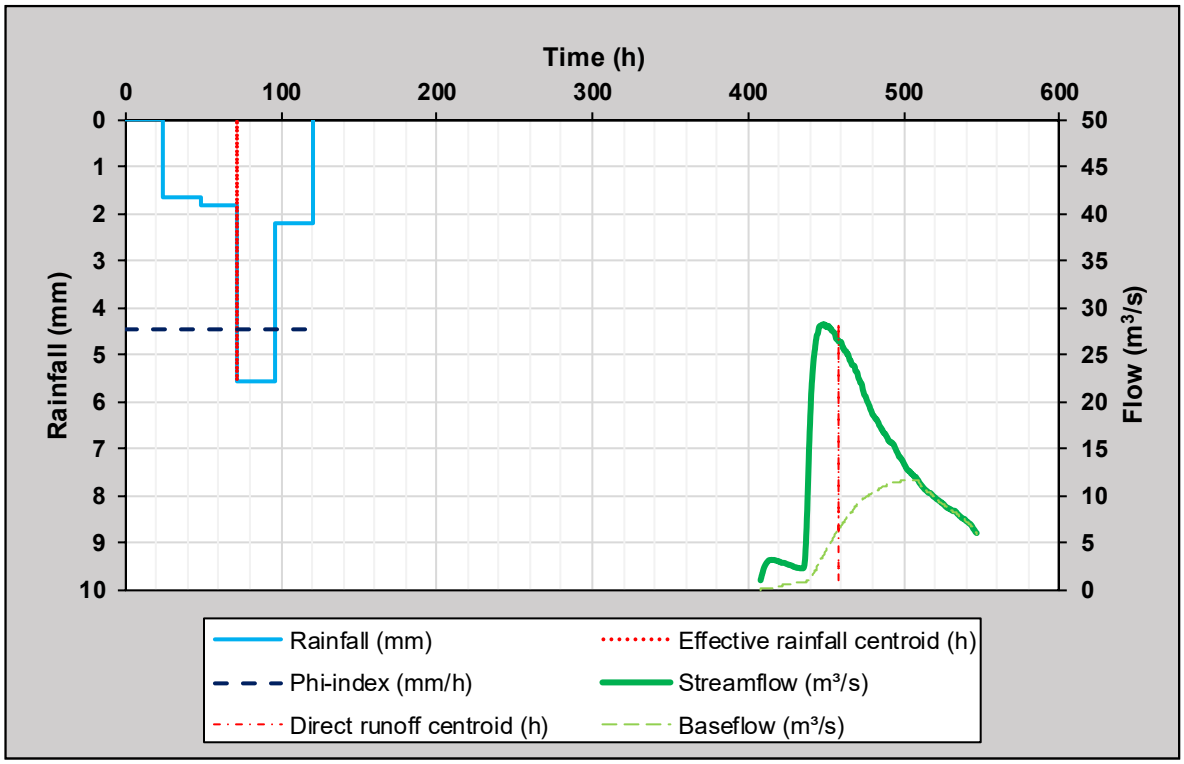

Figure 5.11: Hyetograph-hydrograph event in sub-catchment C5H035

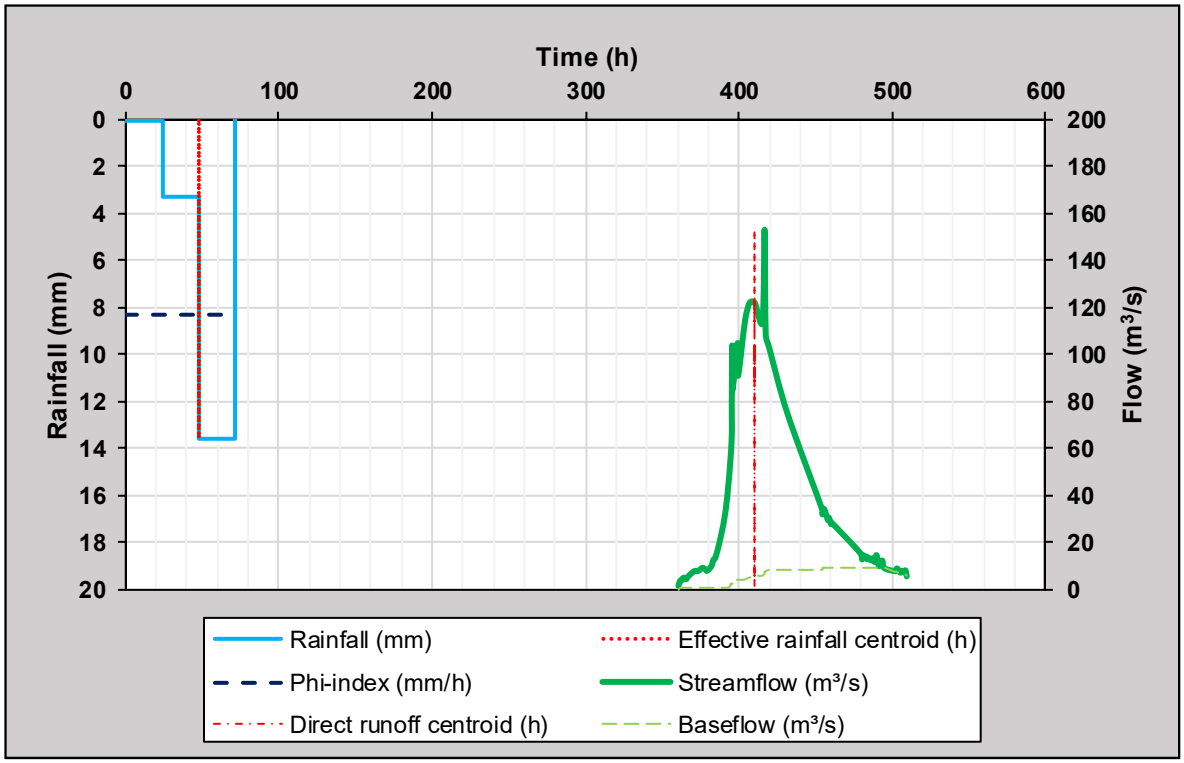

Figure 5.12: Hyetograph-hydrograph event in sub-catchment C5H039

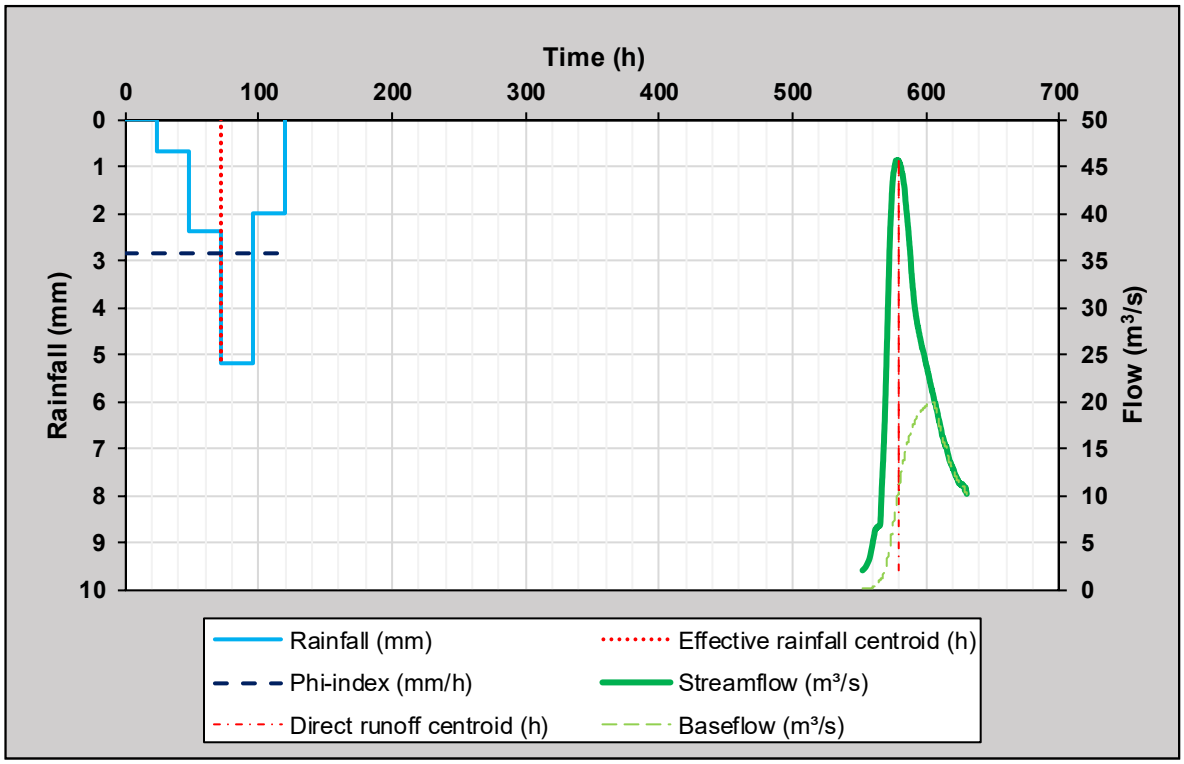

Figure 5.13: Hyetograph-hydrograph event in sub-catchment C5H053

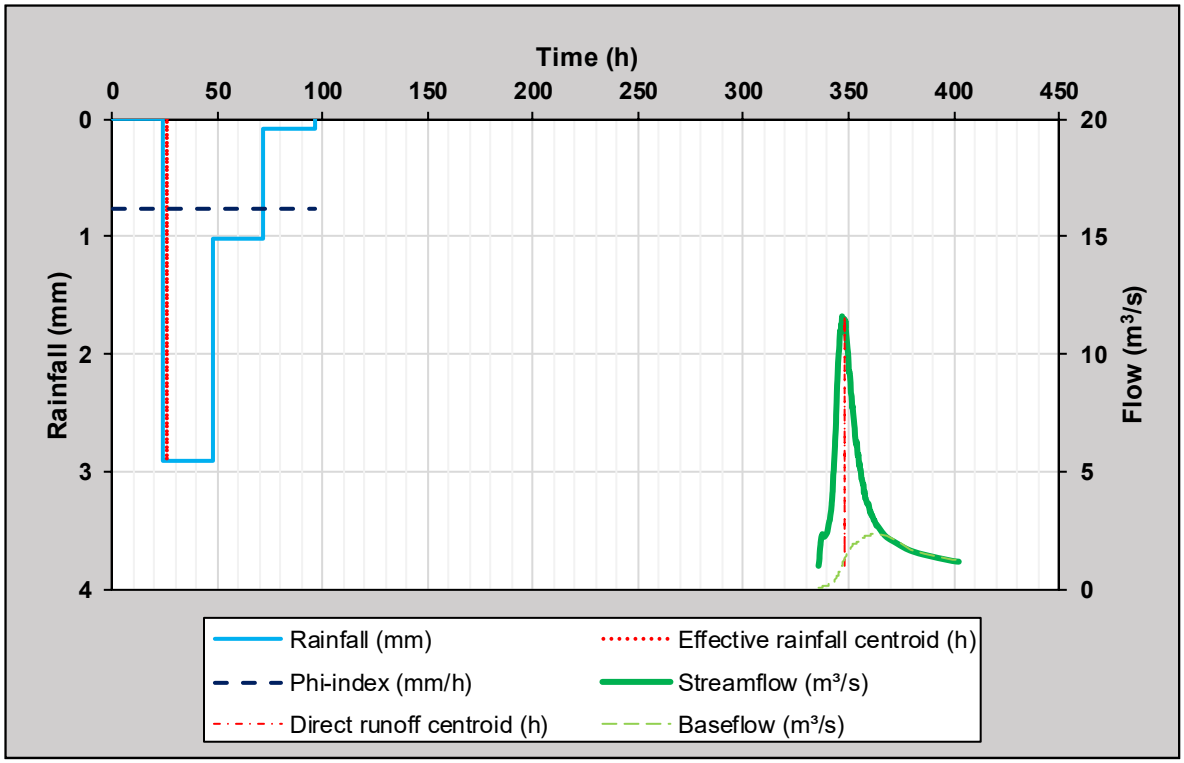

Figure 5.14: Hyetograph-hydrograph event in sub-catchment C5H054

5.4 Estimation of Time Parameters

In considering the analyses of the 394 hyetograph-hydrograph events, it was quite evident that the seven different time parameter definitions contribute to the time parameter variability, which is also influenced by the event spatial distribution (S_e), the variation in peak discharge (Q_P) and the distance (L) between the rainfall station (where the maximum rainfall depth was recorded) and the sub-catchment outlet. In general, the largest Q_P and direct runoff (Q_D) values are associated with the likelihood of the entire sub-catchment receiving rainfall of a high intensity for the critical storm duration, which in principal, represents the conceptual T_C. Shorter response times, *i.e.* lower T_C, T_L and T_P values could be expected to occur when the effective rainfall does not cover the entire catchment, especially when a rainfall event is centred near the outlet of a sub-catchment. In considering the average time parameters listed in Table 5.4 and illustrated in Figure 5.15 to Figure 5.17 for each sub-catchment, it is evident that these average time parameters are in agreement with the preliminary findings of Gericke and Smithers (2017; 2018), *i.e.* $T_P \approx T_C \approx T_L$ at a medium to large catchment level.

Table 5.4: Summary of the average values for time parameters estimated, event spatial distribution (S_e), peak discharge (Q_P) and the distance (L) between the rainfall station (where the maximum rainfall depth was recorded) and the sub-catchment outlet. The letter in brackets [] is used as cross-reference to the time parameter definitions [a] to [d] described in Sections 2.2.1 to 2.2.3, Chapter 2

Sub-catchment	Q_P (m^3/s)	L (km)	S_e (%)	T_C [a] (h)	T_C [b] & T_L [a/b] (h)	T_C [c] (h)	T_L [c] (h)	T_C [d] & T_P (h)
C5H003	22	42	29	442.8	439.8	437.5	440.4	14.3
C5H006	22	44	46	222.0	237.4	240.2	242.9	8.2
C5H007	22	17	63	531.7	540.7	539.8	541.4	8.2
C5H008	40	22	65	437.0	441.4	440.6	443.2	8.6
C5H009	15	18	73	432.7	382.5	382.5	386.0	16.5
C5H012	31	26	22	400.7	409.3	401.6	411.4	5.6
C5H014	110	101	27	563.1	517.8	529.4	541.6	31.4
C5H015	165	55	66	556.1	548.3	546.7	553.8	32.6
C5H016	100	162	31	682.3	654.0	651.9	656.2	41.6
C5H018	115	119	46	628.5	586.0	585.5	591.0	48.1
C5H035	54	110	23	505.6	499.4	499.2	501.3	24.9
C5H039	126	49	55	772.0	776.3	775.5	775.7	57.9
C5H053	77	31	26	430.5	477.2	470.4	475.2	30.4
C5H054	18	21	41	437.4	457.5	454.8	460.7	9.4

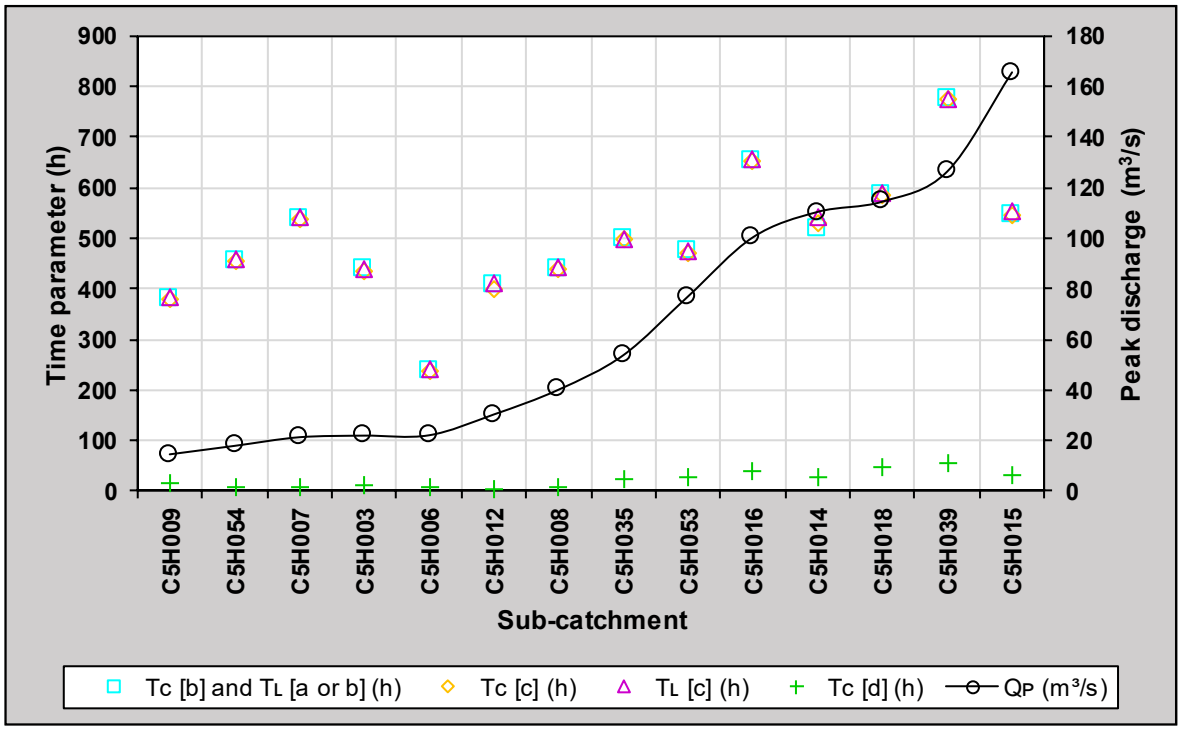

Figure 5.15: Summary of the association between average time parameters (based on different definitions) and the average peak discharge (Q_P) of all rainfall events at a sub-catchment level in the MRRC

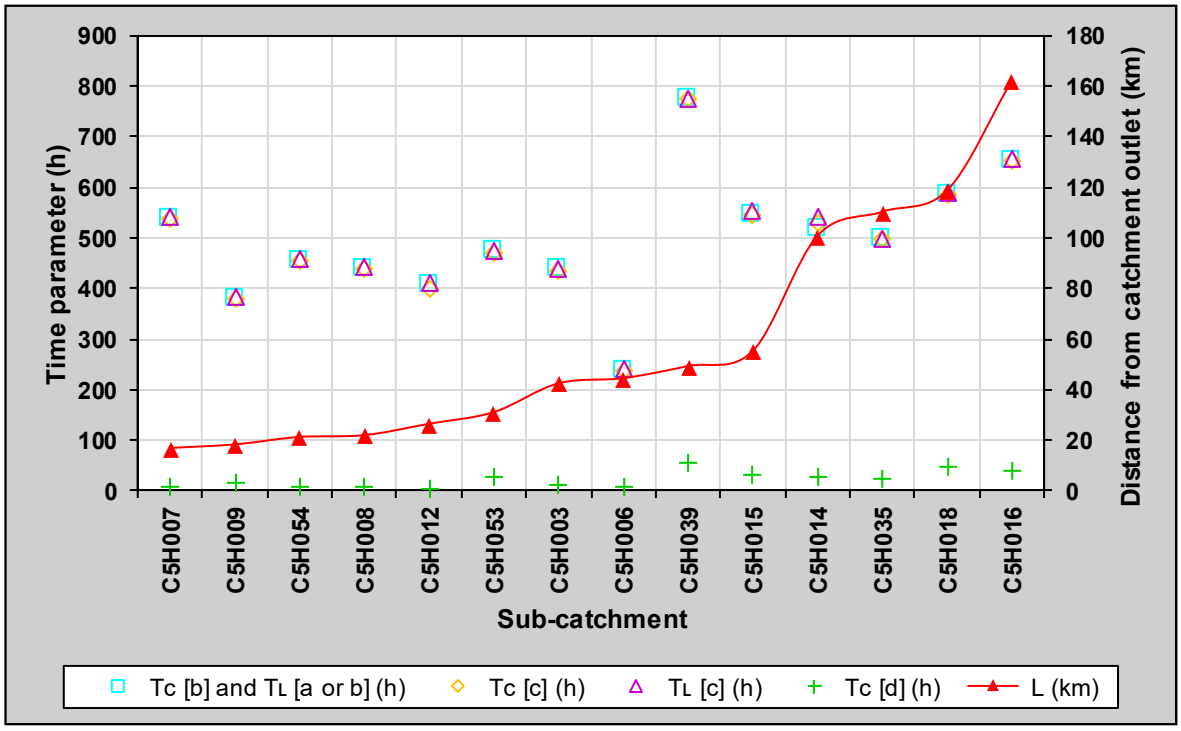

Figure 5.16: Summary of the association between average time parameters (based on different definitions) and the average distance (L) of all rainfall events from the catchment outlet at a sub-catchment level in the MRRC

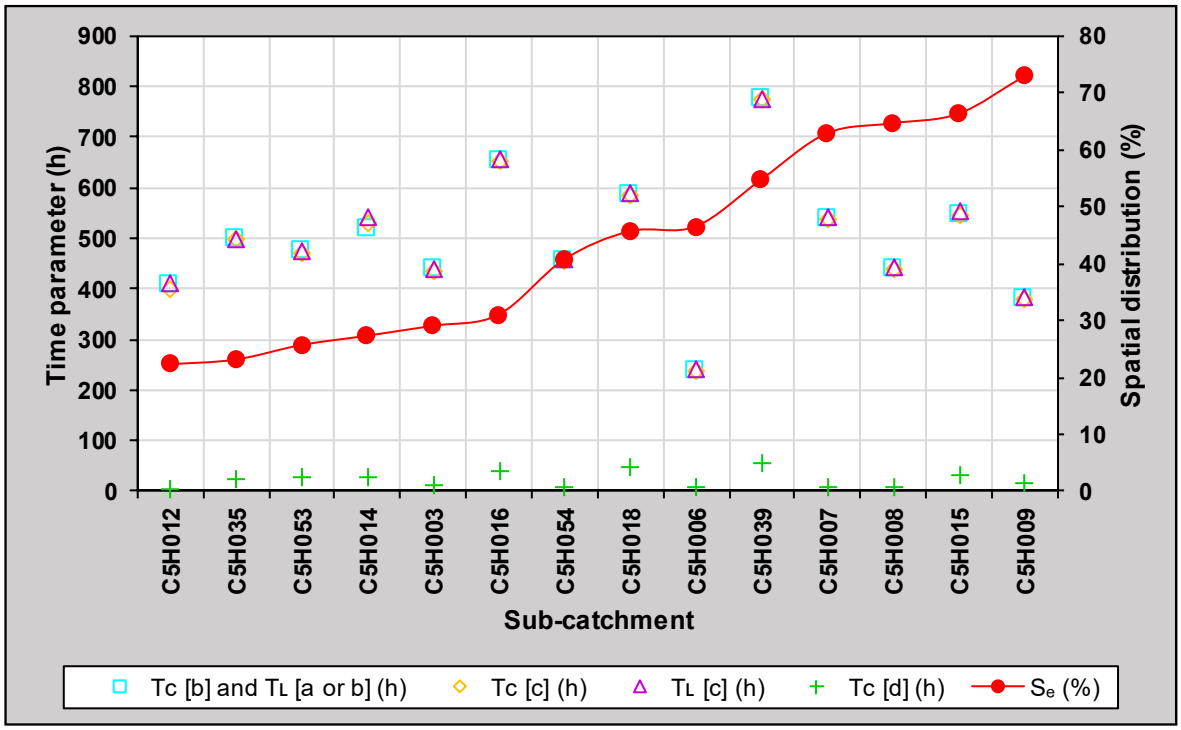

Figure 5.17: Summary of the association between average time parameters (based on different definitions) and the average spatial distribution of all rainfall events (S_e) at a sub-catchment level in the MRRC

Figure 5.15 shows a clear association between average time parameters and the average Q_P values resulting from all the rainfall events at a sub-catchment level in the MRRC. In other words, on average, high time parameter values are typically associated with higher peak discharge values when longer catchment response times are associated with rainfall events with a higher spatial distribution. However, Figure 5.16 does not show a clear association between the average time parameters and the average distance of all rainfall events from the catchment outlet. Figure 5.17 also shows no apparent association between the average time parameters and the average spatial distribution of all the rainfall events. The information presented in Figure 5.15 to Figure 5.17 also shows the insignificance of T_C (d) (*cf.* Section 2.2.1, Chapter 2) when compared to the other T_C definitions. The latter difference could be ascribed to the fact that this definition is also used to define the time to peak for any specific rainfall event, and/or could also be ascribed to the runoff events being wrongfully regarded as baseflow instead of being part of the rising limb of the hydrograph, *i.e.* direct runoff. The event-specific time parameters estimated at a sub-catchment level in the MRRC are listed in Table A.3, Appendix A.

5.4.1 Influence of rainfall event locality on time parameters

An example of the locality analysis results, *i.e.* the establishment of a relationship between the distance of rainfall events from the catchment outlet and the different time parameters in sub-catchment C5H035, is listed in Table 5.5 and illustrated in Figure 5.18, respectively. A summary of the locality analysis results applicable to the entire MRRC is listed in Table A.3, Appendix A and illustrated in Figures B.29 to B.80, Appendix B.

Table 5.5: Example of the association between time parameters (based on different definitions) and the distance (L) of a rainfall event from the catchment outlet in sub-catchment C5H035

Event #	L (km)	Q_P (m^3/s)	T_C [a] (h)	T_C [b] & T_L [a/b] (h)	T_C [c] (h)	T_L [c] (h)	T_C [d] (h)
17	8.5	11.9	477.9	484.7	484.7	486.6	4.7
20	8.5	197.5	356.8	485.7	498.8	485.8	18.8
21	15.9	155.3	287.2	254.4	238.8	218.1	166.8
9	30.3	178.4	174.0	136.4	97.7	177.1	25.7
2	76.1	12.1	187.8	128.0	128.0	142.3	8.0
18	76.1	17.8	1 115.8	1 109.8	1 109.8	1 112.0	5.8
22	76.1	33.7	384.2	406.5	398.2	389.2	62.2
24	82.3	28.2	388.6	376.2	376.2	385.6	40.2
1	84.0	110.6	688.7	766.2	770.3	750.6	98.3
5	95.0	10.6	463.9	490.8	510.4	493.3	6.4
4	95.0	18.1	933.7	779.4	779.4	784.4	11.4
25	95.0	77.1	845.6	942.5	972.6	942.7	12.6
12	117.0	12.6	587.1	555.9	555.9	560.6	3.9
15	117.0	157.5	526.6	520.8	520.8	522.2	16.8
8	142.1	12.1	198.1	148.3	148.3	155.6	4.3
14	171.3	10.9	457.9	443.9	436.5	447.0	4.5
13	194.8	18.7	232.4	201.1	201.1	206.3	9.1
3	196.8	12.8	397.7	339.6	339.6	344.3	3.6
19	204.6	30.1	950.0	947.6	946.0	948.2	10.0
23	212.6	12.1	347.8	364.4	364.4	366.3	4.4
11	212.6	15.7	616.3	604.9	604.9	610.0	4.9

Generally, the results in Table 5.5 demonstrate some relationship between the catchment response time and the distance between the main rainfall event (rainfall station that received the maximum rainfall depth) and the sub-catchment outlet (flow-gauging station). In considering all the sub-catchments, an increase in the distance of a rainfall event from the sub-catchment outlet was generally associated with an increase in the time parameter values. However, in some cases due to low

rainfall intensities resulting in lower Q_P values, the time parameter values are higher and the distance from the sub-catchment outlet has no apparent effect on the response time.

Figure 5.18 shows that the time parameters are influenced by the different time parameter definitions and the distance between the rainfall station that received the maximum rainfall depth and the sub-catchment outlet. Typically, rainfall events which occurred close to the sub-catchment outlets are more susceptible to shorter response times.

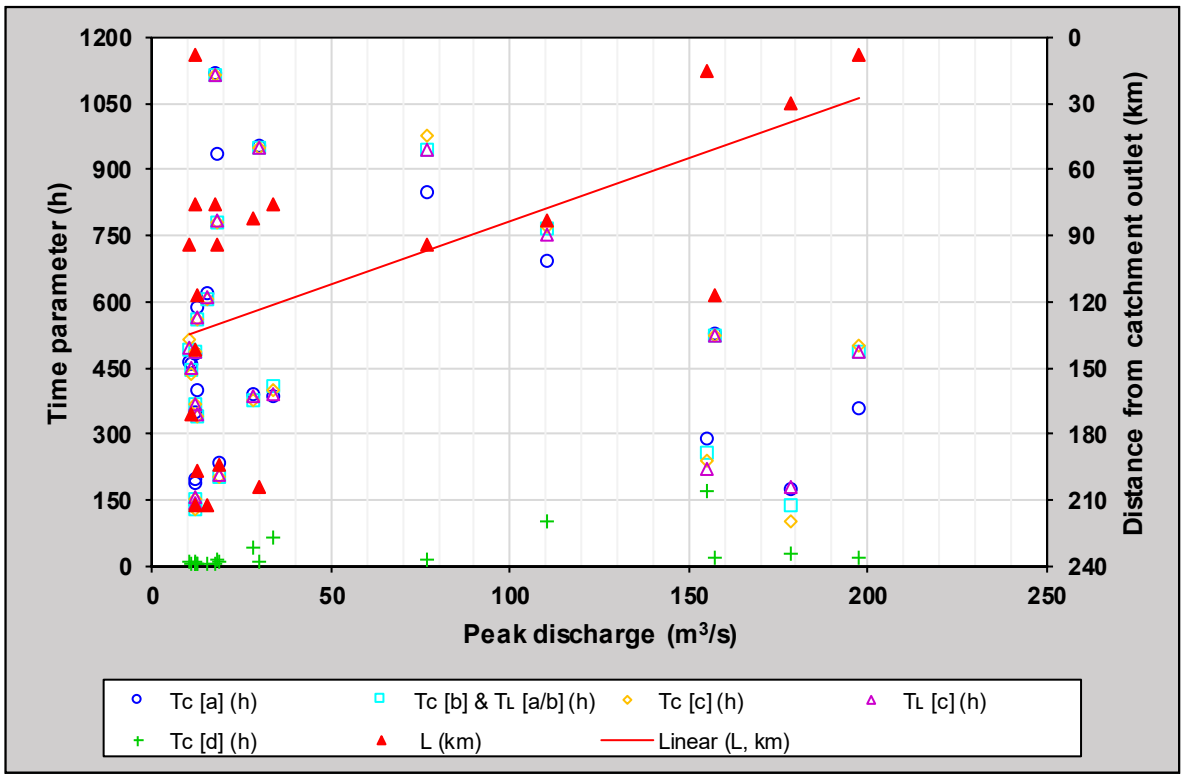

Figure 5.18: Example of the association between time parameters (based on different definitions) and the distance (L) of a rainfall event from the catchment outlet in sub-catchment C5H035

5.4.2 Influence of spatial rainfall distribution on time parameters

An example of the spatial distribution analysis results for the different time parameters in sub-catchment C5H035 is listed in Table 5.6. A summary of the spatial distribution analysis results applicable to the entire MRRC is listed in Table A.3, Appendix A and illustrated in Figures B.29 to B.80, Appendix B.

It is evident from Table 5.6 that the largest Q_P and time parameter values are associated with the likelihood of the entire catchment receiving rainfall for the critical storm duration. Lower time parameter values could be expected when effective rainfall of high intensity does not cover the entire catchment, *i.e.* low S_e values, especially when a storm is centred near the outlet of a sub-catchment. However, in some instances, low rainfall intensities and associated lower peak discharges are ascribed to larger time parameters values, *i.e.* longer response times due to rainfall events having a low spatial distribution more distant from the sub-catchment outlet.

Table 5.6: Example of the association between time parameters (based on different definitions) and the spatial distribution of a rainfall event (S_e) in sub-catchment C5H035

Event #	S_e (%)	Q_P (m^3/s)	T_C [a] (h)	T_C [b] & T_L [a/b] (h)	T_C [c] (h)	T_L [c] (h)	T_C [d] (h)
18	7.9	17.8	1 115.8	1 109.8	1 109.8	1 112.0	5.8
14	9.3	11.0	457.9	444.0	436.5	447.0	4.5
23	11.8	12.1	347.8	364.4	364.4	366.3	4.4
12	13.2	12.6	587.1	555.9	555.9	560.	3.9
17	15.1	11.8	477.9	484.7	484.7	486.6	4.7
13	16.2	18.7	232.4	201.1	201.1	206.3	9.1
24	17.4	28.1	388.6	376.2	376.2	385.6	40.2
19	19.0	30.1	950.0	947.6	946.0	948.2	10.0
5	20.8	10.6	463.9	490.8	510.4	493.4	6.4
25	21.3	77.1	845.6	942.5	972.6	942.7	12.6
8	21.3	12.1	198.1	148.3	148.3	155.6	4.3
22	21.3	33.7	384.2	406.5	398.2	389.2	62.2
3	24.2	12.8	397.7	339.6	339.6	344.3	3.6
15	24.9	157.5	526.6	520.8	520.8	522.2	16.8
20	27.9	197.5	356.8	485.7	498.8	485.8	18.8
2	28.7	12.1	187.8	128.0	128.0	142.3	8.0
1	32.2	110.6	688.7	766.2	770.3	750.6	98.3
21	33.7	155.3	287.2	254.4	238.8	218.1	166.8
4	35.9	18.1	933.7	779.4	779.4	784.4	11.4
11	37.5	15.7	616.3	604.9	604.9	610.0	4.9
9	46.2	178.4	174.0	136.4	97.7	177.1	25.7

Figure 5.19 shows that the time parameter values are influenced by the different time parameter definitions and the spatial distribution of a rainfall event.

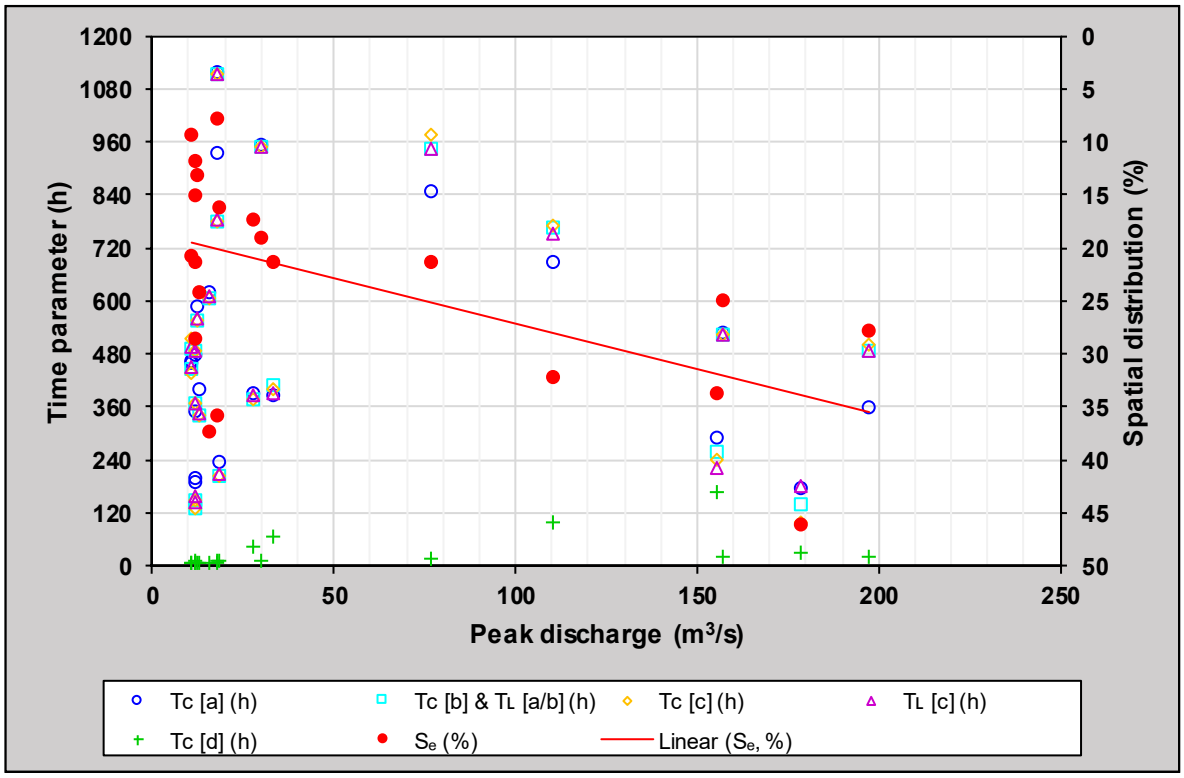

Figure 5.19: Example of the association between time parameters (based on different definitions) and the spatial distribution of a rainfall event (S_e) in sub-catchment C5H035

Hence, based on the above results contained in Tables 5.5 and 5.6, and Figures 5.18 and 5.19, it is evident that time parameters are influenced by the distance of a rainfall event from the catchment outlet, as well as the spatial distribution of such an event. However, a clear relationship could not be found across all sub-catchments, due to the high variability of S_e and L.

5.5 Estimation of Time Parameter Proportionality Ratios

In considering the T_C, T_L and T_P pair values obtained from the 394 hyetograph-hydrograph events, a relatively low variability is evident between the different time parameter proportionality ratios (TPPR 1 to TPPR 8) at a sub-catchment level. In general, where T_L is defined as the time from the centroid of effective rainfall to the peak discharge (McCuen, 2009), T_C and T_L are related by $T_C = 1.003T_L$ (TPPR 1 to TPPR 3, as listed in Table 5.7). In using T_L defined as the time from the centroid of effective rainfall to the centroid of direct runoff (McCuen, 2009), the proportionality ratio reduced to 0.992 (TPPR 5 to TPPR 7, as listed in Table 5.7).

The average time parameter proportionality ratios, in the MRRC, listed in Table 5.7 and presented in Figure 5.20 showed no clear association with the average S_e, average Q_P and average L (distance between the rainfall station where the maximum rainfall depth was recorded and the sub-catchment outlet) values, thus this data were not included. However, the average time parameter proportionality ratios highlighted the insignificance of TPPR 4 and TPPR 8. This is due to the fact that T_C definition (d), as discussed in Section 2.2.1, Chapter 2, is also one of the definitions used to quantify T_P and in general the average values of T_C definition (d) were ± 21 times smaller compared to the other average T_C definition values. In considering the average time parameter proportionality ratios listed in Table 5.7 and illustrated in Figure 5.20 for each sub-catchment, the average time parameter proportionality ratios confirm the preliminary findings of Gericke and Smithers (2017; 2018), *i.e.* $T_P \approx T_C \approx T_L$ at a medium to large catchment level. The event-specific time parameter proportionality ratios estimated at a sub-catchment level in the MRRC are listed in Table A.3, Appendix A.

Table 5.7: Summary of the average time parameter proportionality ratios at a sub-catchment level in the MRRC

Sub-catchment	TPPR 1	TPPR 2	TPPR 3	TPPR 4	TPPR 5	TPPR 6	TPPR 7	TPPR 8
C5H003	1.009	1.000	0.991	0.043	1.007	0.999	0.990	0.043
C5H006	0.928	1.000	1.009	0.034	0.909	0.979	0.987	0.034
C5H007	0.974	1.000	0.998	0.026	0.975	1.001	1.000	0.028
C5H008	0.988	1.000	0.998	0.025	0.982	0.994	0.992	0.025
C5H009	1.133	1.000	1.000	0.046	1.124	0.992	0.992	0.046
C5H012	1.002	1.000	0.975	0.020	0.991	0.990	0.965	0.020
C5H014	1.088	1.000	1.027	0.086	1.037	0.953	0.976	0.081
C5H015	1.030	1.000	0.996	0.064	1.014	0.986	0.983	0.063
C5H016	1.041	1.000	0.996	0.078	1.040	1.000	0.996	0.081
C5H018	1.091	1.000	0.998	0.116	1.073	0.989	0.988	0.113
C5H035	1.060	1.000	0.987	0.074	1.042	0.988	0.977	0.077
C5H039	0.992	1.000	1.004	0.087	0.991	1.000	1.003	0.089
C5H053	0.871	1.000	0.977	0.067	0.874	1.004	0.980	0.068
C5H054	0.955	1.000	0.990	0.034	0.944	0.990	0.980	0.033

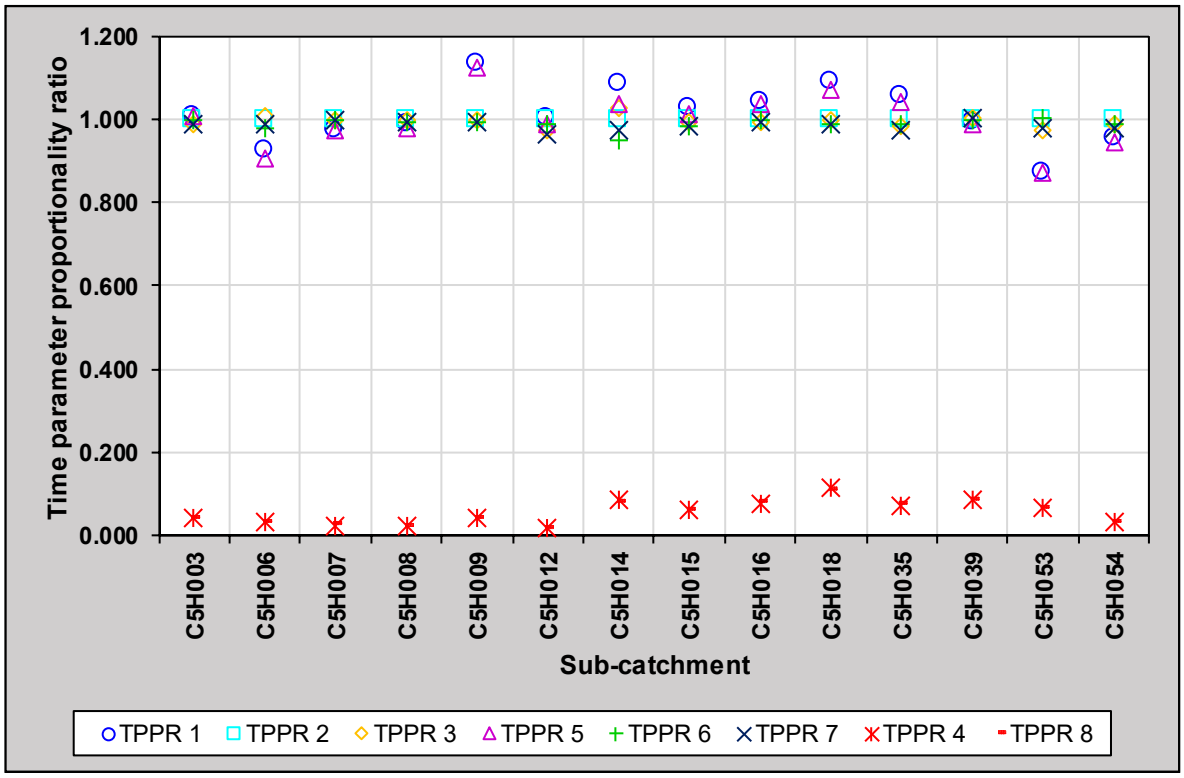

Figure 5.20: Summary of the average time parameter proportionality ratios at a sub-catchment level in the MRRC

5.5.1 Influence of rainfall event locality on time parameter proportionality ratios

An example of the locality analysis results, *i.e.* the establishment of a relationship between the distance of rainfall events from the catchment outlet and the different time parameter proportionality ratios in sub-catchment C5H035, is listed in Table 5.8 and illustrated in Figure 5.21, respectively. A summary of the locality analysis results applicable to the entire MRRC is listed in Table A.3, Appendix A and illustrated in Figures B.29 to B.80, Appendix B.

Generally, the results in Table 5.8 do not demonstrate a clear relationship between the time parameter proportionality ratios and the distance between the main rainfall event (rainfall station that received the maximum rainfall depth) and the sub-catchment outlet (flow-gauging station). However, it is quite evident that T_C and T_L are related by $T_C \approx T_L$, where TPPR 1 – 3 ≈ TPPR 5 – 6, irrespective of the distance between the main rainfall event and the sub-catchment outlet.

Table 5.8: Example of the association between time parameter proportionality ratios and the distance (L) of a rainfall event from the catchment outlet in sub-catchment C5H035

Event #	L (km)	Q_P (m^3/s)	TPPR 1	TPPR 2	TPPR 3	TPPR 4	TPPR 5	TPPR 6	TPPR 7	TPPR 8
17	8.5	11.9	0.986	1.000	1.000	0.010	0.982	0.996	0.996	0.010
20	8.5	197.5	0.735	1.000	1.027	0.039	0.734	1.000	1.027	0.039
21	15.9	155.3	1.129	1.000	0.939	0.656	1.317	1.167	1.095	0.765
9	30.3	178.4	1.276	1.000	0.716	0.188	0.982	0.770	0.552	0.145
2	76.1	12.1	1.467	1.000	1.000	0.063	1.320	0.899	0.899	0.056
18	76.1	17.8	1.005	1.000	1.000	0.005	1.003	0.998	0.998	0.005
22	76.1	33.7	0.945	1.000	0.979	0.153	0.987	1.045	1.023	0.160
24	82.3	28.2	1.033	1.000	1.000	0.107	1.008	0.976	0.976	0.104
1	84.0	110.6	0.899	1.000	1.005	0.128	0.918	1.021	1.026	0.131
5	95.0	10.6	0.945	1.000	1.040	0.013	0.940	0.995	1.035	0.013
4	95.0	18.1	1.198	1.000	1.000	0.015	1.190	0.994	0.994	0.015
25	95.0	77.1	0.897	1.000	1.032	0.013	0.897	1.000	1.032	0.013
12	117.0	12.6	1.056	1.000	1.000	0.007	1.047	0.992	0.992	0.007
15	117.0	157.5	1.011	1.000	1.000	0.032	1.008	0.997	0.997	0.032
8	142.1	12.1	1.336	1.000	1.000	0.029	1.273	0.953	0.953	0.028
14	171.3	10.9	1.031	1.000	0.983	0.010	1.024	0.993	0.977	0.010
13	194.8	18.7	1.156	1.000	1.000	0.045	1.126	0.975	0.975	0.044
3	196.8	12.8	1.171	1.000	1.000	0.011	1.155	0.987	0.987	0.010
19	204.6	30.1	1.002	1.000	0.998	0.011	1.002	0.999	0.998	0.011
23	212.6	12.1	0.954	1.000	1.000	0.012	0.950	0.995	0.995	0.012
11	212.6	15.7	1.019	1.000	1.000	0.008	1.010	0.992	0.992	0.008

In considering Figure 5.21, it is clearly evident that there is no apparent relationship between the Q_P values, time parameter proportionality ratios, and the distance between the rainfall station that received the maximum rainfall depth and the sub-catchment outlet. Due to the insignificance of TPPR 4 and TPPR 8, the proportionality ratios are not plotted in Figure 5.21.

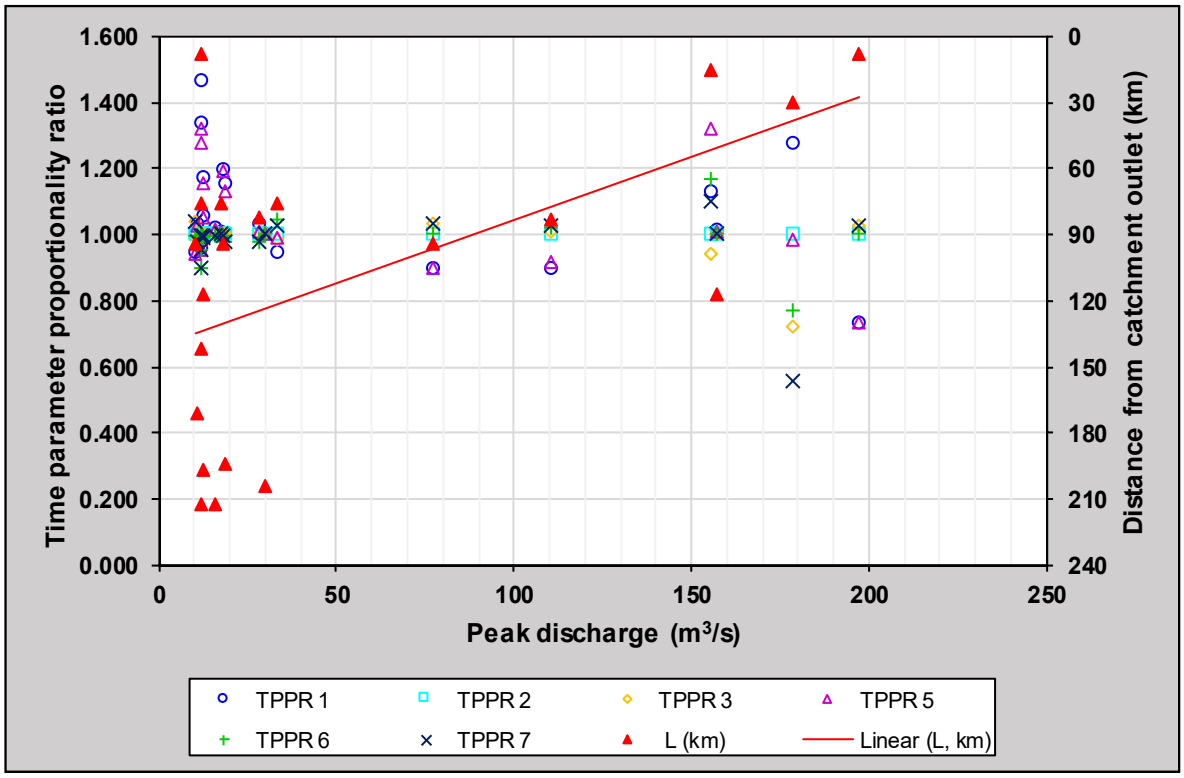

Figure 5.21: Example of the association between time parameter proportionality ratios and the distance (L) of a rainfall event from the catchment outlet in sub-catchment C5H035

5.5.2 Influence of spatial rainfall distribution on time parameter proportionality ratios

An example of the spatial distribution analysis results for the different time parameter proportionality ratios in sub-catchment C5H035 is listed in Table 5.9. A summary of the spatial distribution analysis results applicable to the entire MRRC is listed in Table A.3, Appendix A and illustrated in Figures B.29 to B.80, Appendix B.

Generally, the results in Table 5.9 do not demonstrate a clear relationship between the time parameter proportionality ratios and the S_e values, in other words, the percentage of the sub-catchment area covered by effective rainfall. However, it is quite evident that T_C and T_L are related by $T_C \approx T_L$, where TPPR 1 – 3 ≈ TPPR 5 – 6, irrespective of the spatial distribution of a rainfall event.

Table 5.9: Example of the association between time parameter proportionality ratios and the spatial distribution of a rainfall event (S_e) in sub-catchment C5H035

Event #	S_e (%)	Q_P (m^3/s)	TPPR 1	TPPR 2	TPPR 3	TPPR 4	TPPR 5	TPPR 6	TPPR 7	TPPR 8
18	7.9	17.8	1.005	1.000	1.000	0.005	1.003	0.998	0.998	0.005
14	9.3	11.0	1.031	1.000	0.983	0.010	1.024	0.993	0.977	0.010
23	11.8	12.1	0.954	1.000	1.000	0.012	0.950	0.995	0.995	0.012
12	13.2	12.6	1.056	1.000	1.000	0.007	1.047	0.992	0.992	0.007
17	15.1	11.8	0.986	1.000	1.000	0.010	0.982	0.996	0.996	0.010
13	16.2	18.7	1.156	1.000	1.000	0.045	1.126	0.975	0.975	0.044
24	17.4	28.1	1.033	1.000	1.000	0.107	1.008	0.976	0.976	0.104
19	19.0	30.1	1.002	1.000	0.998	0.011	1.002	0.999	0.998	0.011
5	20.8	10.6	0.945	1.000	1.040	0.013	0.940	0.995	1.035	0.013
25	21.3	77.1	0.897	1.000	1.032	0.013	0.897	1.000	1.032	0.013
8	21.3	12.1	1.336	1.000	1.000	0.029	1.273	0.953	0.953	0.028
22	21.3	33.7	0.945	1.000	0.979	0.153	0.987	1.045	1.023	0.160
3	24.2	12.8	1.171	1.000	1.000	0.011	1.155	0.987	0.987	0.010
15	24.9	157.5	1.011	1.000	1.000	0.032	1.008	0.997	0.997	0.032
20	27.9	197.5	0.735	1.000	1.027	0.039	0.734	1.000	1.027	0.039
2	28.7	12.1	1.467	1.000	1.000	0.063	1.320	0.899	0.899	0.056
1	32.2	110.6	0.899	1.000	1.005	0.128	0.918	1.021	1.026	0.131
21	33.7	155.3	1.129	1.000	0.939	0.656	1.317	1.167	1.095	0.765
4	35.9	18.1	1.198	1.000	1.000	0.015	1.190	0.994	0.994	0.015
11	37.5	15.7	1.019	1.000	1.000	0.008	1.010	0.992	0.992	0.008
9	46.2	178.4	1.276	1.000	0.716	0.188	0.982	0.770	0.552	0.145

The time parameter proportionality ratios depicted in Figure 5.22 demonstrate no direct relationship with the Q_P values and the S_e values at a sub-catchment level. Due to the insignificance of TPPR 4 and TPPR 8, the proportionality ratios are not plotted in Figure 5.22.

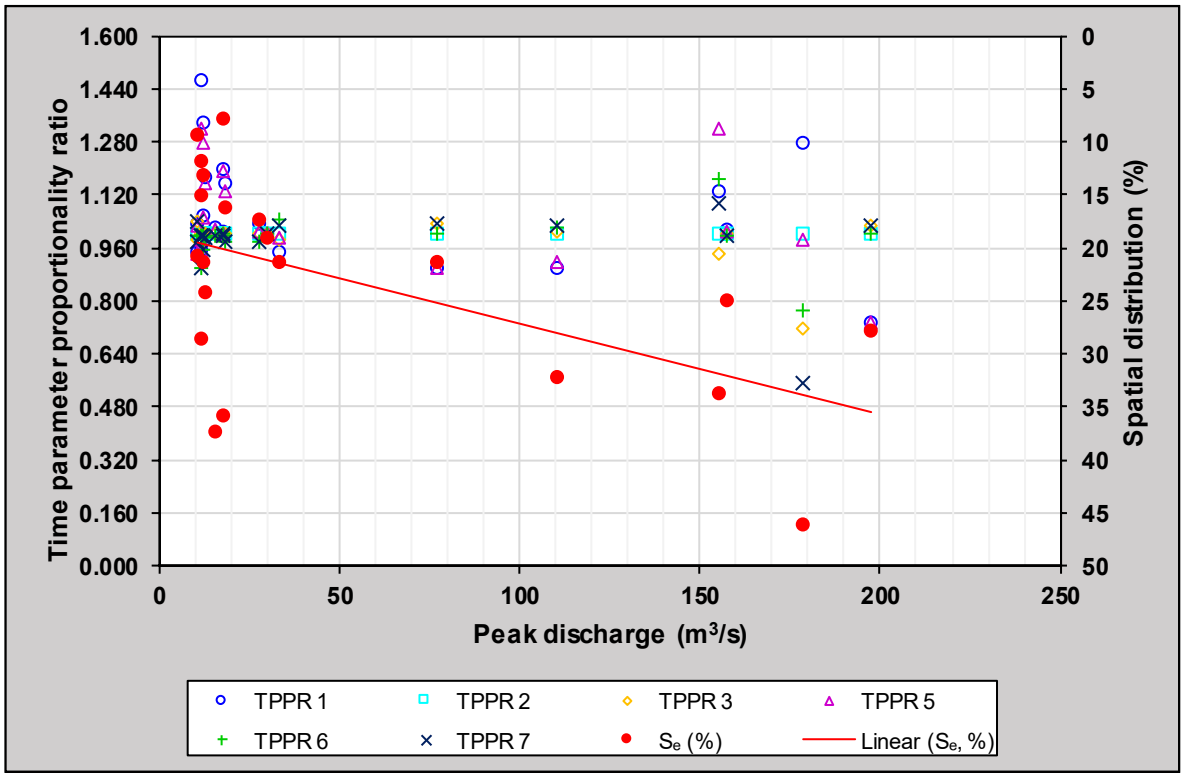

Figure 5.22: Example of the association between time parameter proportionality ratios and the spatial distribution of a rainfall event (S_e) in sub-catchment C5H035

The final conclusions and recommendations for future research are discussed in the next chapter.

CHAPTER 6: CONCLUSIONS AND RECOMMENDATIONS

This chapter contains a synthesised discussion of the research results presented in Chapter 5. The final conclusions and some recommendations for future research are included at the end of this chapter.

6.1 Study Objectives

The overall purpose of this study was to investigate and establish the suitability of the currently recommended time parameter definitions and proportionality ratios for small catchments in larger sub-catchment areas (exceeding 50 km²) of the MRRC in South Africa. The focus was on the estimation of time parameter proportionality ratios from observed rainfall and streamflow data using a simplified convolution process and the seven different time parameter definitions currently recognised in hydrological literature. The time parameters T_C, T_L and T_P were individually estimated using the various time variables obtained from observed hyetographs and hydrographs to establish average time parameter proportionality ratios at a catchment level.

The specific objectives identified to achieve the overall objective of this study are discussed in the subsequent sections.

6.2 Specific Objectives

6.2.1 Analyses of rainfall data

The DREU was successfully used to extract the daily rainfall data series and the number of rainfall stations used in each sub-catchment of the MRRC proved to be sufficient for the required analyses. The general lack of rainfall data not only caused a shortfall in the number of hyetograph-hydrograph events being analysed, but the lack of sub-daily rainfall data also limited the study. However, the time parameter proportionality ratios under investigation, *i.e.* $T_C = 1.417T_L$ and $T_C = 1.667T_L$, are both based centroid values obtained from using a simplified convolution process, whereas, the latter centroid values denote 'average values' which are deemed to be more stable time variables representative of the catchment response time in larger

catchments where flood volumes are central to the design. Hence, these centroid-based time parameters were supposedly not significantly influenced by the time series interval, *i.e.* daily as opposed to sub-daily rainfall data.

The lack of rainfall data from the SAWS stations after the year 2001 is a cause of concern; especially, if the urgent need to enhance design flood estimation research in South Africa is taken into consideration. Apart from the latter research need, the continuous decline in operational rainfall stations in South Africa, from a high number of rainfall stations around 1970 to about only about half of that in 2004 (Pitman, 2011), further exaggerates the situation. Hence, based on the above, it is also evident that the DREU database needs to be updated.

6.2.2 Synchronisation of rainfall data

The Automated Toolkit developed in Microsoft Excel eliminated the concern regarding poorly synchronised rainfall data which can contribute to inaccurate estimates of time parameters using a simplified convolution process. In essence, the Automated Toolkit addressed and overcame most of the problems identified in the study assumptions, *i.e.* Assumptions 1 and 2. In Assumption 1, the direct measurement of time variables from individual events is questioned due to the difficulties in determining the start and end times of an event, in conjunction with the temporal and spatial distribution thereof. In Assumption 2, the possible contribution of poorly synchronised rainfall and streamflow observations to inaccurate estimates of time parameters, is questioned.

6.2.3 Averaging of observed rainfall data

Based on the findings from this study and the preferential use of the Thiessen polygon method in the study conducted by Gericke and Du Plessis (2011), as well as the large amount of data and computations required, the application of the Thiessen polygon method is recommended for future time parameter proportionality ratio studies.

6.2.4 Analyses of streamflow data

The EX-HYD software developed by Görgens *et al.* (2007) and the selection criteria proposed by Gericke and Smithers (2017; 2018) proved to be useful in identifying and extracting complete flood hydrographs.

6.2.5 Hyetograph-hydrograph analyses

In using the Automated Toolkit developed in this study to estimate catchment response time parameters, the response to rainfall could be estimated. In considering the spatial distribution of rainfall events and their distance from the catchment outlet, the Automated Toolkit ensured that the hyetograph-hydrograph analyses are objective and reproducible, and saved considerable labour and time.

The Automated Toolkit also addressed Assumption 4, *i.e.* the baseflow separation methodology applied in this study is regarded as the most appropriate method to be used in the MRRC. This assumption was addressed by the research conducted by Smakhtin and Watkins (1997), which adopted the methodology as proposed by Nathan and McMahon (1990) with some modifications in a national-scale study in South Africa. The latter methodology with modifications was incorporated in the Automated Toolkit.

6.2.6 Estimation of time parameters

The time parameters T_C, T_L and T_P were individually estimated using the various time variables obtained from observed rainfall hyetographs and streamflow hydrographs. The time parameter estimates proved to be highly variable due to the spatial and temporal distribution of rainfall events, variation in peak discharges and the distance of the rainfall events from the catchment outlet. In all the sub-catchments under consideration, the time parameters proved to be uniform, *i.e.* $T_P \approx T_C \approx T_L$. The latter finding is also in agreement with the preliminary findings of Gericke and Smithers (2017; 2018) at a medium to large catchment level.

6.2.7 Estimation of time parameter proportionality ratios

The time parameter proportionality ratios obtained from analysing the pair values of T_C, T_L and T_P for 394 hyetograph-hydrograph events at a large catchment level, were characterised by a relatively low variability between the different time parameter proportionality ratios (TPPR 1 to TPPR 8). In general, where T_L is defined as the time from the centroid of effective rainfall to the peak discharge, T_C and T_L proved to be related by $T_C = 1.003T_L$ (TPPR 1 to TPPR 3). In using T_L defined as the time from the centroid of effective rainfall to the centroid of direct runoff, the proportionality ratio reduced to 0.992 (TPPR 5 to TPPR 7).

Overall, the results showed that T_C and T_L are generally related by $T_C \approx T_L$, where TPPR 1 – 3 ≈ TPPR 5 – 6, regardless of the spatial distribution and distance of the maximum rainfall event from the sub-catchment outlet. These findings are not only in agreement with the preliminary findings of Gericke and Smithers (2017; 2018) at a medium to large catchment scale, but also confirmed Assumption 3, *i.e.* time parameter proportionality ratios equal unity in large catchments.

6.3 Achievement of Objectives and Major Findings

An enhanced methodology was developed to estimate catchment response time parameters and time parameter proportionality ratios at a large catchment level in the MRRC, while considering the spatial distribution of storm events and the distance thereof from the catchment outlet. The major findings are as follows:

(a) Time parameter estimates based on the seven different theoretical time parameter definitions proved to be highly variable due to the spatial and temporal distribution of rainfall events, variation in peak discharges and the distance of the rainfall events from the catchment outlet.
(b) Time parameter proportionality ratios are characterised by a relatively low variability at a larger catchment level in the MRRC.
(c) In this study, where T_L is defined as the time from the centroid of effective rainfall to the peak discharge of direct runoff, T_C and T_L are related by $T_C = 1.003T_L$ and where T_L is defined as the time from the centroid of effective

rainfall to the centroid of direct runoff, the proportionality ratio reduces to 0.992.

(d) In all the sub-catchments under consideration, the preliminary findings of Gericke and Smithers (2016; 2017), *i.e.* $T_P \approx T_C \approx T_L$, were confirmed. In other words, it highlighted that the proportionality ratios currently proposed for small catchments, *i.e.* $T_C = 1.417T_L$ and $T_C = 1.667T_L$, are not applicable at larger catchment levels.

6.4 Recommendations for Future Research

Based on the results obtained, it is recommended that the methodology adopted should be expanded to other catchments in South Africa and internationally by taking cognisance of the following recommendations for future research:

(a) **Daily rainfall disaggregation:** Due to the lack of sub-daily rainfall data at rainfall stations, daily rainfall data should be disaggregated into sub-daily rainfall values using the methodology recommended by Knoesen and Smithers (2008).

(b) **Development of a software interface:** A software interface, *i.e.* further development of the Automated Toolkit, to enable other researchers and/or practitioners to apply the methodology elsewhere, should be developed.

6.5 Conclusions

The estimation of time parameters and time parameter proportionality ratios in large sub-catchments of the MRRC was the objective of this research. The achievement of this objective and the specific objectives, as well as the associated results have been discussed in this chapter to ultimately provide some recommendations for future research. Building upon the critical assessment of the available time parameter definitions and proportionality ratios, it is envisaged that the implementation and expansion of both the identified research values and adopted methodology to other catchments in South Africa and internationally, will ultimately contribute towards improved time parameter estimations at a catchment level. Consequently, the improved time parameter estimations will also result in improved design flood estimations.

CHAPTER 7: REFERENCES

ARC. 2019. Climate Monitoring Services. [Internet]. Agricultural Research Council. Available from: http://www.arc.agric.za/arc-iscw/Pages/Climate-Monitoring-Services.aspx. [Accessed: 1 June 2019].

Arnold, JG, Allen, PM, Muttiah, R, and Bernhardt, G. 1995. Automated base flow separation and recession analysis techniques. *Ground Water* 33 (6): 1010–1018.

Bell, FC and Kar, SO. 1969. Characteristic response times in design flood estimation. *Journal of Hydrology* 8: 173–196. DOI: 10.1016/0022-1694(69)90120-6.

Bondelid, TR, McCuen, RH, and Jackson, TJ. 1982. Sensitivity of SCS models to curve number variation. *Water Resources Bulletin* 20 (2): 337–349.

Chapman, T. 1999. A comparison of algorithms for streamflow recession and baseflow separation. *Hydrological Processes* 13: 701–714.

Chow, VT, Maidment, DR, and Mays, LW. 1988. *Applied Hydrology.* McGraw-Hill, New York, USA.

Clark, CO. 1945. Storage and the unit hydrograph. *Transactions, American Society of Civil Engineers* 110: 1419–1446.

CSIR. 2001. *GIS Data: Classified Raster Data for National Coverage based on 31 Land Cover Types*. National Land Cover Database, Council for Scientific and Industrial Research, Environmentek, Pretoria, RSA.

Dingman, SL. 2002. *Physical Hydrology*. 2nd Ed. Macmillan, New York, USA.

Dow, CL. 2007. Assessing regional land-use/cover influence on New Jersey Pinelands streamflow through hydrograph analysis. *Hydrological Processes* 21: 185–197.

DWAF. 1995. *GIS Data: Drainage Regions of South Africa.* Department of Water Affairs and Forestry, Pretoria, RSA.

Elsenbeer, H and Vertessy, RA. 2000. Stormflow generation and flow path characteristics in an Amazonian rainforest catchment. *Hydrological Processes* 14: 2367–2381.

Fang, X, Thompson, DB, Cleveland, TG, Pradhan, P, and Malla, R. 2008. Time of concentration estimated using watershed parameters by automated and manual methods. *Journal of Irrigation and Drainage Engineering* 134 (2): 202–211. DOI: 10.1061/(ASCE)0733-9437(2008)134:2(202).

Ferguson, BK and Suckling, PW. 1990. Changing rainfall-runoff relationships in the urbanizing Peachtree Creek Watershed. *Water Resources Bulletin* 26 (2): 313–322.

Folmar, ND and Miller, AC. 2008. Development of an empirical lag time equation. *Journal of Irrigation and Drainage Engineering* 134 (4): 501–506. DOI: 10.1061/(ASCE)0733-9437(2008)134:4(501).

Gericke, OJ. 2016. *Estimation of Catchment Response Time in Medium to Large Catchments in South Africa.* Unpublished PhD Eng. thesis, School of Engineering, Department of Bioresources Engineering, University of KwaZulu-Natal, Pietermaritzburg, RSA.

Gericke, OJ and Du Plessis, JA. 2011. Evaluation of critical storm duration rainfall estimates used in flood hydrology in South Africa. *Water SA* 37 (4): 453–470. DOI: 10.4314/wsa.v37i4.4.

Gericke, OJ and Smithers, JC. 2014. Review of methods used to estimate catchment response time for the purpose of peak discharge estimation. *Hydrological Sciences Journal* 59 (11): 1935–1971. DOI: 10.1080/02626667.2013.866712.

Gericke, OJ and Smithers, JC. 2016. Derivation and verification of empirical catchment response time equations for medium to large catchments in South Africa. *Hydrological Processes* 30 (23): 4384–4404. DOI: 10.1002/hyp.10922.

Gericke, OJ and Smithers, JC. 2017. Direct estimation of catchment response time parameters in medium to large catchments using observed streamflow data. *Hydrological Processes* 31 (5): 1125–1143. DOI: 10.1002/hyp.11102.

Gericke, OJ and Smithers, JC. 2018. An improved and consistent approach to estimate catchment response time: Case study in the C5 drainage region, South Africa. *Journal of Flood Risk Management* 11(2018): S284–S301. DOI: 10.1111/jfr3.12206.

Görgens, AHM, Lyons, S, Hayes, L, Makhabane, M, and Maluleke, D. 2007. *Modernised South African Design Flood Practice in the Context of Dam Safety*. WRC Report No. 1420/2/07. Water Research Commission, Pretoria, RSA.

Heggen, R. 2003. Time of concentration, lag time and time to peak. [Internet]. In: eds. Shrestha, B and Rajbhandari, R. *Proceedings of Regional Training Course: Application of Geo-informatics for Water Resources Management*, 3.1-3.23. International Centre for Integrated Mountain Development, Kathmandu, Nepal. Available from: http://www.hkh-friend.net.np/rhdc/training/lectures/HEGGEN/Tc3.pdf. [Accessed: 15 September 2016].

Holton, HN and Overton, DE. 1963. Analysis and application of simple hydrographs. *Journal of Hydrology* 1: 250–264.

Hood, MJ, Clausen, JC, and Warner, GS. 2007. Comparison of stormwater lag times for low impact and traditional residential development. *Journal of the American Water Resources Association* 43 (4): 1036–1046. DOI: 10.1111/j.1752-1688.2007.00085.x.

Hughes, DA, Hannart, P, and Watkins, D. 2003. Continuous baseflow from time series of daily and monthly streamflow data. *Water SA* 29 (1): 43–48.

Jena, SK and Tiwari, KN. 2006. Modelling synthetic unit hydrograph parameters with geomorphologic parameters of watersheds. *Journal of Hydrology* 319: 1–14. DOI: 10.1016/j.AQ10 jhydrol.2005.03.025.

Johnstone, D and Cross, WP. 1949. *Elements of Applied Hydrology*. Ronald Press, New York, USA.

Jones, JA and Grant, GE. 1996. Peak flow response to clear-cutting and roads in small and large basins. *Water Resource Research* 32 (4): 959–947.

Kaempffer, C and Germishuyse, T. 2009. Climate data at the Agricultural Research Council. [Internet]. Ee.co.za. Available from: https://www.ee.co.za/wp-content/uploads/legacy/PosIT_Apr-May_p_66-68.pdf. [Accessed: 1 June 2019].

Kerby, WS. 1959. Time of concentration for overland flow. *Civil Engineering* 29 (3): 174.

Kirpich, ZP. 1940. Time of concentration of small agricultural watersheds. *Civil Engineering* 10 (6): 362.

Knoesen, JM and Smithers, JC. 2008. The development and assessment of a regionalised daily rainfall disaggregation model for South Africa. *Water SA* 34(3): 323–330.

Linsley, RK, Kohler, MA, and Paulhus, JLH. 1988. *Hydrology for Engineers*. SI Metric Ed. McGraw-Hill, Singapore.

Lim, KJ, Engel, BA, Tang, Z, Choi, J, Kim, K, Muthukrishnan, S, and Tripathy, D. 2005. Automated Web GIS Based Hydrograph Analysis Tool, WHAT. *Journal of the American Water Resource Association* 41 (6): 1407–1416.

Lynch, SD. 2004. *Development of a Raster Database of Annual, Monthly and Daily Rainfall for Southern Africa.* WRC Report No. 1156/1/04. Water Research Commission, Pretoria, RSA.

McCuen, RH. 2005. *Hydrologic Analysis and Design*. 3rd Ed. Prentice-Hall, Upper Saddle River, New York, USA.

McCuen, RH. 2009. Uncertainty analyses of watershed time parameters. *Journal of Hydrologic Engineering* 14 (5): 490–498. DOI: 10.1061/(ASCE)HE.1943-5584.0000011.

McCuen, RH, Wong, SL, and Rawls, WJ. 1984. Estimating urban time of concentration. *Journal of Hydraulic Engineering* 110 (7): 887–904.

Midgley, DC, Pitman, WV and Middleton, BJ. 1994. *Surface Water Resources of South Africa*. Volume 2, Drainage Region C, Vaal: Appendices. WRC Report 298/2.1/94. Water Research Commission, Pretoria, RSA.

Mimikou, M. 1984. Regional relationships between basin size and runoff characteristics. *Hydrological Sciences Journal* 29 (1, 3): 63–73. DOI: 10.1080/02626668409490922.

Mockus, V. 1957. *Use of Storm and Watershed Characteristics in Synthetic Hydrograph Analysis and Application.* United States Department of Agriculture, Soil Conservation Service, Washington, DC, USA.

Nathan, RJ and McMahon, TA. 1990. Evaluation of automated techniques for baseflow and recession analyses. *Water Resources Research* 26 (7): 1465–1473.

Neitsch, SL, Arnold, JG, Kiniry, JR, and Williams, JR. 2005. *Soil and Water Assessment Tool: Theoretical Documentation*. Agricultural Research Service and Blackland Research Center, Temple, Texas, USA.

Pavlovic, SB and Moglen, GE. 2008. Discretization issues in travel time calculations. *Journal of Hydrologic Engineering* 13 (2): 71–79. DOI: 10.1061/(ASCE)1084-0699(2008)13:2(71).

Pietersen, JPJ. 2016. *Areal Reduction Factors for Design Rainfall Estimation in the C5 Secondary Drainage Region of South Africa.* Unpublished M Tech Eng. dissertation, Department of Civil Engineering, Central University of Technology, Free State, Bloemfontein, RSA.

Piggott, AR, Moin, S, and Southam, C. 2005. A revised approach to the UKIH method for the calculation of baseflow. *Hydrological Sciences Journal* 50: 911–920.

Pitman WV. 2011. Overview of water resource assessment in South Africa: Current state and future challenges. *Water SA* 37 (5): 659–664. DOI: 10.4314/wsa.v37i5.3.

Potter, KW and Faulkner, EB. 1987. Catchment response time as predicator of flood quantiles. *Water Resources Bulletin* 25 (5): 857–861.

Pullen, RA. 1969. *Synthetic Unit Graphs for South Africa*. HRU Report No. 3/69. Hydrological Research Unit, University of the Witwatersrand, Johannesburg, RSA.

Ramser, CE. 1927. Runoff from small agricultural areas. *Journal of Agricultural Engineering* 34 (9): 797–823.

Rutledge, AT. 1998. *Computer programs for describing the recession of ground-water discharge and for estimating mean ground-water recharge and discharge from streamflow data*. Report No. 984148: 43. United States Geological Survey Water Resources Investigations, USA.

Sabol, GV. 2008. *Hydrologic Basin Response Parameter Estimation Guidelines*. Dam Safety Report, State of Colorado. Tierra Grande International Incorporated, Scottsdale, AZ, USA.

SANRAL. 2013. *Drainage Manual*. 6th Ed. South African National Roads Agency Limited, Pretoria, RSA.

SAWS. 2019. Our Climate Services – Weather SA Portal. [Internet]. South African Weather Service. Available from: http://www.weathersa.co.za/Home/AboutClimateatSAWS. [Accessed: 1 June 2019].

Schmidt, EJ and Schulze, RE. 1984. *Improved Estimation of Peak Flow Rates using Modified SCS Lag Equations*. ACRU Report No. 17. University of Natal, Department of Agricultural Engineering, Pietermaritzburg, RSA.

Schultz, GA. 1964. *Studies in Flood Hydrograph Synthetisation*. Unpublished MSc dissertation, University of the Witwatersrand, Johannesburg, RSA.

Seybert, TA. 2006. *Stormwater Management for Land Development: Methods and Calculations for Quantity Control.* John Wiley and Sons Incorporated, Hoboken, New Jersey, USA.

Simas, MJC. 1996. *Lag Time Characteristics in Small Watersheds in the United States.* Unpublished PhD Thesis, School of Renewable Resources, University of Arizona, Tucson, USA.

Sloto, RA and Crouse, MY. 1996. *HYSEP: A computer program for streamflow hydrograph analysis*. Report No. 90–4040: 46. United States Geological Survey Water Resources Investigations, USA.

Smakhtin, VU. 2001. Low flow hydrology: A review. *Journal of Hydrology* 240 (2001): 147–186.

Smakhtin, VU and Watkins, DA. 1997. *Low Flow Estimation in South Africa*. WRC Report No. 494/1/97. Water Research Commission, Pretoria, RSA.

Smithers, JC, Chetty, KT, Frezghi, MS, Knoesen, DM, and Tewolde, MH. 2013. Development and assessment of a daily time step continuous simulation modelling approach for design flood estimation at ungauged locations: ACRU model and Thukela Catchment case study. *Water SA* 39 (4): 449–458. DOI: 10.4314/wsa.v39i4.4.

Smithers, JC and Schulze, RE. 2000a. *Development and Evaluation of Techniques for Estimating Short Duration Design Rainfall in South Africa*. WRC Report No. 681/1/00. Water Research Commission, Pretoria, RSA.

Smithers, JC and Schulze, RE. 2000b. *Long Duration Design Rainfall Estimates for South Africa.* WRC Report No. 811/1/00. Water Research Commission, Pretoria, RSA.

Snyder, FF. 1938. Synthetic unit hydrographs. *Transactions of American Geophysical Union* 19: 447.

South African Government. 2019. Water and sanitation: South African Government. [Internet]. South African Government. Available from: https://www.gov.za/about-sa/water-affairs. [Accessed: 1 June 2019].

Sujono, J, Shikasho, S, and Hiramatsu, K. 2004. A comparison of techniques for hydrograph recession analysis. *Hydrological Processes* 18: 403–413.

Thomas, WO, Monde, MC, and Davis, SR. 2000. Estimation of time of concentration for Maryland streams. *Journal of the Transportation Research Board* 1720: 95–99.

USACE. 2001. *HEC-HMS Hydrologic Modelling System: User's Manual, Version 2.2.1.* United States Army Corps of Engineers, Vicksburg, Mississippi, USA.

USBR. 1973. *Design of Small Dams*. 2nd Ed. United States Bureau of Reclamation, Water Resources Technical Publication, Washington, DC, USA.

USDA NRCS. 2010. Time of concentration. In: eds. Woodward, DE *et al*., *National Engineering Handbook*, Ch. 15 (Section 4, Part 630), 1–18. United States Department of Agriculture Natural Resources Conservation Service, Washington, DC, USA.

USDA SCS. 1985. Hydrology. In: eds. Kent, KM *et al*., *National Engineering Handbook*, Ch. 16 (Section 4, Part 630), 1–23. United States Department of Agriculture Soil Conservation Service, Washington, DC, USA.

USGS, 2016. EarthExplorer. [Internet]. United States Geological Survey. Available from: https://earthexplorer.usgs.gov/. [Accessed: 19 September 2016].

Viessman, W, Lewis, GL, and Knapp, JW. 1989. *Introduction to Hydrology*. 3rd Ed. Harper and Row Publishers Incorporated, New York, USA.

Watt, WE and Chow, KCA. 1985. A general expression for basin lag time. *Canadian Journal of Civil Engineering* 12: 294–300.

White, K and Sloto, PA. 1990. *Base flow frequency characteristics of selected Pennsylvanian streams*. Report No. 90-4160: 66. United States Geological Survey Water Resources Investigations, USA.

Wilson, EM. 1990. *Engineering Hydrology.* 4th Ed. Macmillan Press Limited, London, UK.

APPENDIX A: TABULATED INFORMATION AND RESULTS

Table A.1: Details of the daily SAWS rainfall stations located in the MRRC

Sub-catchment	SAWS station number	*L* (km)	Latitude	Longitude	Sub-catchment	SAWS station number	*L* (km)	Latitude	Longitude
C5H003	0262314W	13.5	-29.233333	26.683333	C5H006	0261426W	14.2	-29.083333	26.250000
	0262828W	41.3	-29.300000	26.966667		0261368W	20.1	-29.116667	26.200000
	0232512W	44.5	-29.516667	26.783333		0261367W	19.1	-29.116667	26.216667
	0262690W	46.9	-29.483333	26.883333		0261366W	17.7	-29.100000	26.216667
	0262479W	40.5	-29.483333	26.766667		0261365W	16.4	-29.083333	26.216667
	0232301W	39.2	-29.500000	26.683333		0261307A	21.3	-29.116667	26.183333
	0232275W	47.6	-29.583333	26.650000		0293597A	3.9	-28.950000	26.333333
	0232211W	38.2	-29.500000	26.633333		0261722W	7.9	-29.033333	26.400000
	0232123W	41.4	-29.533333	26.583333	C5H007	0261733W	12.5	-29.216667	26.416667
	0261750W	40.6	-29.500000	26.416667		0261750W	40.7	-29.500000	26.416667
	0231754W	41.8	-29.516667	26.433333		0261597W	34.0	-29.450000	26.333333
	0261890W	21.0	-29.333333	26.483333		0261312W	16.0	-29.200000	26.166667
	0262734W	34.4	-29.233333	26.916667		0261890W	26.5	-29.333333	26.483333
	0262353W	27.0	-29.383333	26.683333		0261548W	1.2	-29.133333	26.316667
	0262129W	1.6	-29.150000	26.583333		0261523W	8.3	-29.216667	26.300000
C5H006	0261733W	26.8	-29.216667	26.416667		0261367W	10.3	-29.116667	26.216667
	0261750W	57.8	-29.500000	26.416667		0231713W	19.1	-29.866667	26.400000
	0261597W	51.8	-29.450000	26.333333		0231761W	25.8	-29.683333	26.433333
	0261312W	29.4	-29.200000	26.166667		0232018W	29.4	-29.800000	26.516667
	0261275W	20.3	-29.083333	26.166667		0232011W	32.7	-29.683333	26.516667
	0261890W	41.2	-29.333333	26.483333		0231588W	11.8	-29.800000	26.333333
	0261789W	20.5	-29.150000	26.433333		0231375W	8.8	-29.733333	26.216667
	0261548W	16.7	-29.133333	26.316667		0231713W	18.3	-29.866667	26.400000
	0261523W	26.1	-29.216667	26.300000		0231114W	15.9	-29.900000	26.050000
	0261517W	13.5	-29.100000	26.300000		0231588W	16.2	-29.800000	26.333333

Table A.1: Continued

Sub-catchment	SAWS station number	*L* (km)	Latitude	Longitude	Sub-catchment	SAWS station number	*L* (km)	Latitude	Longitude
C5H012	0231713W	47.3	-29.866667	26.400000	C5H014	0293007W	146.0	-28.616667	26.016667
	0231761W	44.6	-29.683333	26.433333		0293514W	172.4	-28.566667	26.283333
	0230816W	6.5	-29.600000	25.966667		0294417W	206.3	-28.933333	26.716667
	0201843W	41.7	-30.033333	25.966667		0293622W	169.9	-28.866667	26.333333
	0231114W	27.9	-29.900000	26.050000		0292051W	92.3	-28.833333	25.516667
	0230810W	38.1	-30.000000	25.950000		0291323W	59.5	-28.883333	25.183333
	0230774W	23.2	-29.866667	25.966667		0257878W	15.1	-29.133333	24.483333
	0261750W	46.4	-29.500000	26.416667		0258581W	25.0	-29.183333	24.800000
	0261597W	41.9	-29.450000	26.333333		0259348W	63.5	-29.300000	25.183333
	0232018W	54.8	-29.800000	26.516667		0260163W	98.5	-29.183333	25.600000
	0232011W	52.6	-29.683333	26.516667		0260882W	134.0	-29.200000	25.966667
	0231754W	47.2	-29.516667	26.433333		0261733W	177.6	-29.216667	26.416667
	0231588W	38.2	-29.800000	26.333333		0262314W	203.5	-29.233333	26.683333
	0231395W	26.5	-29.583333	26.233333		0262828W	231.6	-29.300000	26.966667
	0231375W	25.0	-29.733333	26.216667		0232512W	218.3	-29.516667	26.783333
	0231361W	28.1	-29.500000	26.200000		0231761W	191.5	-29.683333	26.433333
	0231279W	18.8	-29.650000	26.166667		0230816W	146.4	-29.600000	25.966667
	0231247W	16.2	-29.616667	26.133333		0230011W	113.9	-29.683333	25.516667
	0231161W	12.3	-29.666667	26.100000		0229215W	80.4	-29.583333	25.150000
	0231076W	14.2	-29.766667	26.050000		0228725W	65.9	-29.566667	24.916667
	0230764W	9.2	-29.733333	25.933333		0230210W	145.0	-30.000000	25.616667
C5H014	0229654W	120.9	-29.900000	25.366667		0201843W	172.2	-30.033333	25.966667
	0231713W	197.0	-29.866667	26.400000		0230349W	137.0	-29.816667	25.700000
	0292833W	132.6	-28.883333	25.950000		0230027W	133.4	-29.950000	25.500000
	0290560W	33.9	-28.816667	24.833333		0229862W	125.4	-29.866667	25.483333

Table A.1: Continued

Sub-catchment	SAWS station number	*L* (km)	Latitude	Longitude	Sub-catchment	SAWS station number	*L* (km)	Latitude	Longitude
C5H014	0201492W	172.2	-30.200000	25.783333	C5H014	0231375W	174.5	-29.733333	26.216667
	0201482W	157.8	-30.033333	25.766667		0231361W	163.4	-29.500000	26.200000
	0201373W	168.0	-30.200000	25.716667		0261146AW	150.4	-29.433333	26.083333
	0201370W	164.2	-30.166667	25.700000		0260660W	133.1	-29.500000	25.866667
	0201361W	151.9	-30.016667	25.700000		0231279W	166.3	-29.650000	26.166667
	0231114W	169.8	-29.900000	26.050000		0231247W	161.9	-29.616667	26.133333
	0230810W	168.6	-30.000000	25.950000		0231161W	161.2	-29.666667	26.100000
	0230774W	161.0	-29.866667	25.966667		0231076W	162.0	-29.766667	26.050000
	0230598W	157.6	-29.966667	25.833333		0230764W	150.4	-29.733333	25.933333
	0230566W	152.8	-29.916667	25.816667		0260030W	101.6	-29.483333	25.516667
	0201756W	173.4	-30.100000	25.916667		0230542W	126.4	-29.516667	25.783333
	0201637W	171.1	-30.116667	25.866667		0230466W	137.8	-29.750000	25.766667
	0262690W	226.9	-29.483333	26.883333		0230363W	122.2	-29.550000	25.716667
	0262479W	215.9	-29.483333	26.766667		0230254W	127.5	-29.733333	25.650000
	0232301W	208.5	-29.500000	26.683333		0230074W	119.9	-29.733333	25.550000
	0232275W	207.7	-29.583333	26.650000		0230073W	118.8	-29.716667	25.550000
	0232211W	203.8	-29.500000	26.633333		0230048W	123.6	-29.800000	25.533333
	0232123W	200.0	-29.533333	26.583333		0229737W	114.3	-29.783333	25.416667
	0261750W	183.5	-29.500000	26.416667		0229723W	96.3	-29.533333	25.416667
	0261597W	174.2	-29.450000	26.333333		0229571W	97.4	-29.483333	25.466667
	0232018W	203.9	-29.800000	26.516667		0259390A	78.6	-29.500000	25.216667
	0232011W	199.0	-29.683333	26.516667		0229579W	96.9	-29.633333	25.333333
	0231754W	185.5	-29.516667	26.433333		0229555W	103.9	-29.750000	25.300000
	0231588W	187.9	-29.800000	26.333333		0229344W	93.0	-29.716667	25.166667
	0231395W	169.5	-29.583333	26.233333		0229124W	75.3	-29.583333	25.066667

Table A.1: Continued

Sub-catchment	SAWS station number	*L* (km)	Latitude	Longitude	Sub-catchment	SAWS station number	*L* (km)	Latitude	Longitude
C5H014	0228783W	64.3	-29.533333	24.950000	C5H014	0260082W	99.1	-29.366667	25.550000
	0228571W	57.4	-29.516667	24.833333		0260004W	87.6	-29.066667	25.500000
	0258218W	8.4	-29.116667	24.616667		0259887W	89.4	-29.266667	25.483333
	0258213A	3.4	-29.050000	24.633333		0259881W	88.9	-29.183333	25.500000
	0258164W	21.2	-29.233333	24.600000		0259743W	87.9	-29.383333	25.416667
	0258157A	8.2	-29.116667	24.600000		0259727W	79.7	-29.100000	25.416667
	0258079W	31.1	-29.316667	24.533333		0261312W	153.3	-29.200000	26.166667
	0258894W	55.6	-29.400000	25.000000		0261275W	152.4	-29.083333	26.166667
	0258827W	44.6	-29.283333	24.966667		0261256W	151.1	-29.266667	26.133333
	0258740W	42.2	-29.316667	24.900000		0261183W	145.9	-29.050000	26.100000
	0258624W	45.0	-29.383333	24.850000		0260715W	132.9	-29.416667	25.900000
	0258474W	42.9	-29.400000	24.766667		0260678W	127.9	-29.300000	25.883333
	0258467W	27.3	-29.250000	24.750000		0260555W	118.9	-29.250000	25.800000
	0258458W	18.2	-29.116667	24.766667		0260519W	117.1	-29.133333	25.800000
	0258434W	25.8	-29.233333	24.750000		0262247W	191.4	-29.116667	26.566667
	0258399W	10.8	-29.083333	24.700000		0261890W	185.7	-29.333333	26.483333
	0258380W	34.3	-29.333333	24.716667		0261789W	178.6	-29.150000	26.433333
	0258339W	15.5	-29.150000	24.700000		0261548W	167.2	-29.133333	26.316667
	0258306W	10.4	-29.100000	24.683333		0261523W	166.3	-29.216667	26.300000
	0259609W	72.7	-29.166667	25.333333		0261517W	165.4	-29.100000	26.300000
	0259578W	71.8	-29.116667	25.333333		0261426W	160.5	-29.083333	26.250000
	0259278W	54.5	-29.133333	25.150000		0261368W	155.8	-29.116667	26.200000
	0259102W	46.5	-29.183333	25.050000		0261367W	157.4	-29.116667	26.216667
	0260314W	107.4	-29.233333	25.683333		0261366W	157.3	-29.100000	26.216667
	0260126W	94.1	-29.083333	25.566667		0261365W	157.3	-29.083333	26.216667

Table A.1: Continued

Sub-catchment	SAWS station number	*L* (km)	Latitude	Longitude	Sub-catchment	SAWS station number	*L* (km)	Latitude	Longitude
C5H014	0261307A	154.2	-29.116667	26.183333	C5H014	0291148W	48.2	-28.950000	25.083333
	0262734W	226.1	-29.233333	26.916667		0291075W	55.8	-28.733333	25.050000
	0262453W	210.7	-29.050000	26.766667		0290887W	35.8	-28.783333	24.816667
	0262353W	205.8	-29.383333	26.683333		0290810W	34.4	-29.000000	24.950000
	0262129W	193.2	-29.150000	26.583333		0290468W	31.5	-28.800000	24.766667
	0294233W	198.7	-28.883333	26.633333		0259002W	40.7	-29.016667	25.016667
	0262271W	201.0	-29.016667	26.666667		0258812W	34.1	-29.033333	24.950000
	0294052W	189.2	-28.866667	26.533333		0258182W	3.3	-29.016667	24.616667
	0293792W	184.2	-28.700000	26.450000		0292606W	129.9	-28.600000	25.833333
	0293597A	169.0	-28.950000	26.333333		0293700W	179.2	-28.650000	26.383333
	0293568W	167.5	-28.933333	26.316667		0293339W	161.9	-28.650000	26.200000
	0261722W	175.1	-29.033333	26.400000	C5H015	0293514W	31.6	-28.566667	26.283333
	0293204W	148.5	-28.900000	26.116667		0294417W	60.5	-28.933333	26.716667
	0293106W	146.1	-28.766667	26.066667		0293622W	22.5	-28.866667	26.333333
	0292461W	121.1	-28.666667	25.766667		0261733W	54.3	-29.216667	26.416667
	0292446W	111.0	-28.933333	25.733333		0262314W	73.0	-29.233333	26.683333
	0292089W	99.2	-28.983333	25.616667		0262828W	99.5	-29.300000	26.966667
	0291899W	86.2	-28.983333	25.483333		0232512W	102.3	-29.516667	26.783333
	0291899A	87.8	-28.983333	25.500000		0262690W	106.1	-29.483333	26.883333
	0291708W	82.5	-28.800000	25.400000		0262479W	98.4	-29.483333	26.766667
	0291582W	81.0	-28.700000	25.333333		0232301W	94.9	-29.500000	26.683333
	0291360W	58.8	-28.983333	25.200000		0232275W	100.8	-29.583333	26.650000
	0291231W	56.2	-28.850000	25.133333		0232211W	92.1	-29.500000	26.633333
	0291178W	49.4	-28.966667	25.100000		0232123W	92.8	-29.533333	26.583333
	0291174W	49.7	-28.900000	25.083333		0261750W	82.5	-29.500000	26.416667

Table A.1: Continued

Sub-catchment	SAWS station number	*L* (km)	Latitude	Longitude	Sub-catchment	SAWS station number	*L* (km)	Latitude	Longitude
C5H015	0261597W	74.6	-29.450000	26.333333	C5H015	0293597A	26.7	-28.950000	26.333333
	0231754W	84.8	-29.516667	26.433333		0293568W	24.3	-28.933333	26.316667
	0261312W	43.9	-29.200000	26.166667		0261722W	37.6	-29.033333	26.400000
	0261275W	31.1	-29.083333	26.166667		0293204W	10.3	-28.900000	26.116667
	0261183W	26.9	-29.050000	26.100000		0293106W	6.4	-28.766667	26.066667
	0262247W	56.0	-29.116667	26.566667		0293700W	31.8	-28.650000	26.383333
	0261890W	68.7	-29.333333	26.483333		0293339W	19.5	-28.650000	26.200000
	0261789W	49.2	-29.150000	26.433333	C5H016	0229654W	150.9	-29.900000	25.366667
	0261548W	41.3	-29.133333	26.316667		0231713W	232.0	-29.866667	26.400000
	0261523W	49.0	-29.216667	26.300000		0292833W	166.4	-28.883333	25.950000
	0261517W	37.3	-29.100000	26.300000		0290560W	59.7	-28.816667	24.833333
	0261426W	33.4	-29.083333	26.250000		0293007W	177.1	-28.616667	26.016667
	0261368W	35.4	-29.116667	26.200000		0293514W	203.7	-28.566667	26.283333
	0261367W	35.8	-29.116667	26.216667		0294417W	240.8	-28.933333	26.716667
	0261366W	34.0	-29.100000	26.216667		0293622W	203.8	-28.866667	26.333333
	0261365W	32.3	-29.083333	26.216667		0292051W	124.9	-28.833333	25.516667
	0261307A	35.0	-29.116667	26.183333		0291323W	92.0	-28.883333	25.183333
	0262734W	91.4	-29.233333	26.916667		0289796W	28.2	-28.783333	24.450000
	0262453W	69.2	-29.050000	26.766667		0257391W	6.3	-29.016667	24.233333
	0262353W	84.7	-29.383333	26.683333		0257878W	30.3	-29.133333	24.483333
	0262129W	59.6	-29.150000	26.583333		0258581W	59.6	-29.183333	24.800000
	0294233W	51.5	-28.883333	26.633333		0259348W	98.9	-29.300000	25.183333
	0262271W	58.8	-29.016667	26.666667		0260163W	134.3	-29.183333	25.600000
	0294052W	41.6	-28.866667	26.533333		0260882W	169.7	-29.200000	25.966667
	0293792W	35.1	-28.700000	26.450000		0261733W	213.2	-29.216667	26.416667

Table A.1: Continued

Sub-catchment	SAWS station number	*L* (km)	Latitude	Longitude	Sub-catchment	SAWS station number	*L* (km)	Latitude	Longitude
C5H016	0262314W	239.1	-29.233333	26.683333	C5H016	0262690W	262.8	-29.483333	26.883333
	0262828W	267.3	-29.300000	26.966667		0262479W	251.8	-29.483333	26.766667
	0232512W	254.2	-29.516667	26.783333		0232301W	244.4	-29.500000	26.683333
	0231761W	227.1	-29.683333	26.433333		0232275W	243.6	-29.583333	26.650000
	0230816W	181.8	-29.600000	25.966667		0232211W	239.7	-29.500000	26.633333
	0230011W	147.4	-29.683333	25.516667		0232123W	235.9	-29.533333	26.583333
	0229215W	112.0	-29.583333	25.150000		0261750W	219.4	-29.500000	26.416667
	0228725W	94.0	-29.566667	24.916667		0261597W	210.2	-29.450000	26.333333
	0230210W	176.3	-30.000000	25.616667		0232018W	239.4	-29.800000	26.516667
	0201843W	205.2	-30.033333	25.966667		0232011W	234.7	-29.683333	26.516667
	0230349W	170.3	-29.816667	25.700000		0231754W	221.4	-29.516667	26.433333
	0230027W	164.1	-29.950000	25.500000		0231588W	223.1	-29.800000	26.333333
	0229862W	156.9	-29.866667	25.483333		0231395W	205.2	-29.583333	26.233333
	0201492W	203.0	-30.200000	25.783333		0231375W	209.8	-29.733333	26.216667
	0201482W	189.8	-30.033333	25.766667		0231361W	199.2	-29.500000	26.200000
	0201373W	198.3	-30.200000	25.716667		0261146AW	186.3	-29.433333	26.083333
	0201370W	194.6	-30.166667	25.700000		0260660W	168.7	-29.500000	25.866667
	0201361W	183.6	-30.016667	25.700000		0231279W	201.8	-29.650000	26.166667
	0231114W	203.9	-29.900000	26.050000		0231247W	197.4	-29.616667	26.133333
	0230810W	201.7	-30.000000	25.950000		0231161W	196.5	-29.666667	26.100000
	0230774W	195.1	-29.866667	25.966667		0231076W	196.8	-29.766667	26.050000
	0230598W	190.4	-29.966667	25.833333		0230764W	185.1	-29.733333	25.933333
	0230566W	185.9	-29.916667	25.816667		0260030W	136.7	-29.483333	25.516667
	0201756W	205.7	-30.100000	25.916667		0230542W	161.8	-29.516667	25.783333
	0201637W	203.1	-30.116667	25.866667		0230466W	171.9	-29.750000	25.766667

Table A.1: Continued

Sub-catchment	SAWS station number	*L* (km)	Latitude	Longitude	Sub-catchment	SAWS station number	*L* (km)	Latitude	Longitude
C5H016	0230363W	157.4	-29.550000	25.716667	C5H016	0258474W	70.6	-29.400000	24.766667
	0230254W	161.3	-29.733333	25.650000		0258467W	58.9	-29.250000	24.750000
	0230074W	153.2	-29.733333	25.550000		0258458W	53.9	-29.116667	24.766667
	0230073W	152.1	-29.716667	25.550000		0258434W	57.9	-29.233333	24.750000
	0230048W	156.1	-29.800000	25.533333		0258399W	46.6	-29.083333	24.700000
	0229737W	146.0	-29.783333	25.416667		0258380W	62.0	-29.333333	24.716667
	0229723W	130.6	-29.533333	25.416667		0258339W	49.3	-29.150000	24.700000
	0229571W	132.3	-29.483333	25.466667		0258306W	45.6	-29.100000	24.683333
	0259390A	112.0	-29.500000	25.216667		0259609W	108.5	-29.166667	25.333333
	0229579W	129.6	-29.633333	25.333333		0259578W	107.5	-29.116667	25.333333
	0229555W	135.0	-29.750000	25.300000		0259278W	90.3	-29.133333	25.150000
	0229344W	122.9	-29.716667	25.166667		0259102W	82.3	-29.183333	25.050000
	0229124W	105.8	-29.583333	25.066667		0260314W	143.3	-29.233333	25.683333
	0228783W	93.7	-29.533333	24.950000		0260126W	129.5	-29.083333	25.566667
	0228571W	84.4	-29.516667	24.833333		0260082W	134.8	-29.366667	25.550000
	0258218W	40.4	-29.116667	24.616667		0260004W	122.9	-29.066667	25.500000
	0258213A	39.3	-29.050000	24.633333		0259887W	125.3	-29.266667	25.483333
	0258164W	46.2	-29.233333	24.600000		0259881W	124.7	-29.183333	25.500000
	0258157A	38.9	-29.116667	24.600000		0259743W	123.4	-29.383333	25.416667
	0258079W	48.7	-29.316667	24.533333		0259727W	115.3	-29.100000	25.416667
	0257845W	26.3	-29.066667	24.483333		0261312W	188.9	-29.200000	26.166667
	0258894W	88.3	-29.400000	25.000000		0261275W	187.6	-29.083333	26.166667
	0258827W	79.0	-29.283333	24.966667		0261256W	186.9	-29.266667	26.133333
	0258740W	75.2	-29.316667	24.900000		0261183W	181.0	-29.050000	26.100000
	0258624W	75.5	-29.383333	24.850000		0260715W	168.8	-29.416667	25.900000

Table A.1: Continued

Sub-catchment	SAWS station number	*L* (km)	Latitude	Longitude	Sub-catchment	SAWS station number	*L* (km)	Latitude	Longitude
C5H016	0260678W	163.8	-29.300000	25.883333	C5H016	0261722W	210.0	-29.033333	26.400000
	0260555W	154.7	-29.250000	25.800000		0293204W	182.6	-28.900000	26.116667
	0260519W	152.7	-29.133333	25.800000		0293106W	179.0	-28.766667	26.066667
	0262247W	226.7	-29.116667	26.566667		0292461W	152.1	-28.666667	25.766667
	0261890W	221.6	-29.333333	26.483333		0292446W	145.1	-28.933333	25.733333
	0261789W	214.0	-29.150000	26.433333		0292089W	133.7	-28.983333	25.616667
	0261548W	202.6	-29.133333	26.316667		0291899W	120.8	-28.983333	25.483333
	0261523W	202.0	-29.216667	26.300000		0291899A	122.4	-28.983333	25.500000
	0261517W	200.7	-29.100000	26.300000		0291708W	114.1	-28.800000	25.400000
	0261426W	195.7	-29.083333	26.250000		0291582W	110.2	-28.700000	25.333333
	0261368W	191.1	-29.116667	26.200000		0291360W	93.2	-28.983333	25.200000
	0261367W	192.8	-29.116667	26.216667		0291231W	87.6	-28.850000	25.133333
	0261366W	192.6	-29.100000	26.216667		0291178W	83.5	-28.966667	25.100000
	0261365W	192.5	-29.083333	26.216667		0291174W	82.1	-28.900000	25.083333
	0261307A	189.5	-29.116667	26.183333		0291148W	81.9	-28.950000	25.083333
	0262734W	261.6	-29.233333	26.916667		0291075W	82.6	-28.733333	25.050000
	0262453W	245.7	-29.050000	26.766667		0290887W	59.3	-28.783333	24.816667
	0262353W	241.6	-29.383333	26.683333		0290810W	69.0	-29.000000	24.950000
	0262129W	228.5	-29.150000	26.583333		0290468W	54.1	-28.800000	24.766667
	0294233W	232.9	-28.883333	26.633333		0259002W	75.6	-29.016667	25.016667
	0262271W	235.9	-29.016667	26.666667		0258812W	69.3	-29.033333	24.950000
	0294052W	223.3	-28.866667	26.533333		0258182W	37.0	-29.016667	24.616667
	0293792W	217.0	-28.700000	26.450000		0292606W	160.2	-28.600000	25.833333
	0293597A	203.5	-28.950000	26.333333		0293700W	211.5	-28.650000	26.383333
	0293568W	201.9	-28.933333	26.316667		0293339W	193.9	-28.650000	26.200000

Table A.1: Continued

Sub-catchment	SAWS station number	*L* (km)	Latitude	Longitude	Sub-catchment	SAWS station number	*L* (km)	Latitude	Longitude
C5H018	0292833W	128.6	-28.883333	25.950000	C5H018	0231361W	159.6	-29.500000	26.200000
	0290560W	31.5	-28.816667	24.833333		0261146AW	146.6	-29.433333	26.083333
	0293007W	142.2	-28.616667	26.016667		0230542W	122.7	-29.516667	25.783333
	0293514W	168.6	-28.566667	26.283333		0258213A	1.0	-29.050000	24.633333
	0294417W	202.3	-28.933333	26.716667		0258827W	41.4	-29.283333	24.966667
	0293622W	165.9	-28.866667	26.333333		0258458W	14.7	-29.116667	24.766667
	0292051W	88.4	-28.833333	25.516667		0258399W	7.3	-29.083333	24.700000
	0291323W	55.7	-28.883333	25.183333		0259609W	68.7	-29.166667	25.333333
	0258581W	21.9	-29.183333	24.800000		0259578W	67.8	-29.116667	25.333333
	0259348W	59.9	-29.300000	25.183333		0259278W	50.5	-29.133333	25.150000
	0260163W	94.5	-29.183333	25.600000		0259102W	42.7	-29.183333	25.050000
	0260882W	130.0	-29.200000	25.966667		0260314W	103.5	-29.233333	25.683333
	0261733W	173.6	-29.216667	26.416667		0260126W	90.1	-29.083333	25.566667
	0262314W	199.5	-29.233333	26.683333		0260082W	95.3	-29.366667	25.550000
	0262828W	227.6	-29.300000	26.966667		0260004W	83.6	-29.066667	25.500000
	0232512W	214.4	-29.516667	26.783333		0259887W	85.5	-29.266667	25.483333
	0262690W	223.0	-29.483333	26.883333		0259881W	84.9	-29.183333	25.500000
	0262479W	212.0	-29.483333	26.766667		0259743W	84.3	-29.383333	25.416667
	0232301W	204.5	-29.500000	26.683333		0259727W	75.7	-29.100000	25.416667
	0232275W	203.9	-29.583333	26.650000		0261312W	149.3	-29.200000	26.166667
	0232211W	199.9	-29.500000	26.633333		0261275W	148.4	-29.083333	26.166667
	0232123W	196.1	-29.533333	26.583333		0261256W	147.1	-29.266667	26.133333
	0261750W	179.6	-29.500000	26.416667		0261183W	141.9	-29.050000	26.100000
	0261597W	170.3	-29.450000	26.333333		0260715W	129.1	-29.416667	25.900000
	0231754W	181.7	-29.516667	26.433333		0260678W	124.0	-29.300000	25.883333

Table A.1: Continued

Sub-catchment	SAWS station number	*L* (km)	Latitude	Longitude	Sub-catchment	SAWS station number	*L* (km)	Latitude	Longitude
C5H018	0260555W	114.9	-29.250000	25.800000	C5H018	0293106W	142.2	-28.766667	26.066667
	0260519W	113.1	-29.133333	25.800000		0292461W	117.4	-28.666667	25.766667
	0262247W	187.4	-29.116667	26.566667		0292446W	107.0	-28.933333	25.733333
	0261890W	181.8	-29.333333	26.483333		0292089W	95.2	-28.983333	25.616667
	0261789W	174.6	-29.150000	26.433333		0291899W	82.2	-28.983333	25.483333
	0261548W	163.2	-29.133333	26.316667		0291899A	83.9	-28.983333	25.500000
	0261523W	162.3	-29.216667	26.300000		0291708W	78.7	-28.800000	25.400000
	0261517W	161.4	-29.100000	26.300000		0291582W	77.5	-28.700000	25.333333
	0261426W	156.5	-29.083333	26.250000		0291360W	54.8	-28.983333	25.200000
	0261368W	151.8	-29.116667	26.200000		0291231W	52.6	-28.850000	25.133333
	0261367W	153.4	-29.116667	26.216667		0291178W	45.5	-28.966667	25.100000
	0261366W	153.3	-29.100000	26.216667		0291174W	46.0	-28.900000	25.083333
	0261365W	153.3	-29.083333	26.216667		0291148W	44.3	-28.950000	25.083333
	0261307A	150.2	-29.116667	26.183333		0291075W	52.7	-28.733333	25.050000
	0262734W	222.1	-29.233333	26.916667		0290887W	33.7	-28.783333	24.816667
	0262453W	206.7	-29.050000	26.766667		0290810W	30.5	-29.000000	24.950000
	0262353W	201.8	-29.383333	26.683333		0290468W	29.8	-28.800000	24.766667
	0262129W	189.1	-29.150000	26.583333		0259002W	36.7	-29.016667	25.016667
	0294233W	194.7	-28.883333	26.633333		0258812W	30.1	-29.033333	24.950000
	0262271W	197.0	-29.016667	26.666667		0258182W	3.8	-29.016667	24.616667
	0294052W	185.2	-28.866667	26.533333		0292606W	126.3	-28.600000	25.833333
	0293792W	180.3	-28.700000	26.450000		0293700W	175.3	-28.650000	26.383333
	0293597A	165.0	-28.950000	26.333333		0293339W	158.1	-28.650000	26.200000
	0293568W	163.5	-28.933333	26.316667	C5H035	0292833W	128.6	-28.883333	25.950000
	0261722W	171.1	-29.033333	26.400000		0290560W	30.3	-28.816667	24.833333
	0293204W	144.5	-28.900000	26.116667		0293007W	141.9	-28.616667	26.016667
	0293106W	142.2	-28.766667	26.066667		0293514W	168.3	-28.566667	26.283333

Table A.1: Continued

Sub-catchment	SAWS station number	*L* (km)	Latitude	Longitude	Sub-catchment	SAWS station number	*L* (km)	Latitude	Longitude
C5H035	0294417W	202.4	-28.933333	26.716667	C5H035	0258827W	42.6	-29.283333	24.966667
	0293622W	165.9	-28.866667	26.333333		0258458W	15.9	-29.116667	24.766667
	0292051W	88.2	-28.833333	25.516667		0258399W	8.5	-29.083333	24.700000
	0291323W	55.4	-28.883333	25.183333		0259609W	69.3	-29.166667	25.333333
	0258581W	23.3	-29.183333	24.800000		0259578W	68.3	-29.116667	25.333333
	0259348W	60.9	-29.300000	25.183333		0259278W	51.1	-29.133333	25.150000
	0260163W	95.0	-29.183333	25.600000		0259102W	43.5	-29.183333	25.050000
	0260882W	130.4	-29.200000	25.966667		0260314W	104.0	-29.233333	25.683333
	0261733W	174.0	-29.216667	26.416667		0260126W	90.4	-29.083333	25.566667
	0262314W	199.9	-29.233333	26.683333		0260082W	96.1	-29.366667	25.550000
	0262828W	228.1	-29.300000	26.966667		0260004W	83.9	-29.066667	25.500000
	0232512W	215.0	-29.516667	26.783333		0259887W	86.2	-29.266667	25.483333
	0262690W	223.6	-29.483333	26.883333		0259881W	85.5	-29.183333	25.500000
	0262479W	212.6	-29.483333	26.766667		0259743W	85.2	-29.383333	25.416667
	0232301W	205.2	-29.500000	26.683333		0259727W	76.1	-29.100000	25.416667
	0232275W	204.6	-29.583333	26.650000		0261312W	149.7	-29.200000	26.166667
	0232211W	200.5	-29.500000	26.633333		0261275W	148.7	-29.083333	26.166667
	0232123W	196.8	-29.533333	26.583333		0261256W	147.6	-29.266667	26.133333
	0261750W	180.3	-29.500000	26.416667		0261183W	142.1	-29.050000	26.100000
	0261597W	171.0	-29.450000	26.333333		0260715W	129.8	-29.416667	25.900000
	0231754W	182.4	-29.516667	26.433333		0260678W	124.6	-29.300000	25.883333
	0231361W	160.3	-29.500000	26.200000		0260555W	115.5	-29.250000	25.800000
	0261146AW	147.3	-29.433333	26.083333		0260519W	113.5	-29.133333	25.800000
	0230542W	123.6	-29.516667	25.783333		0262247W	187.7	-29.116667	26.566667
	0258213A	2.4	-29.050000	24.633333		0261890W	182.3	-29.333333	26.483333

Table A.1: Continued

Sub-catchment	SAWS station number	*L* (km)	Latitude	Longitude	Sub-catchment	SAWS station number	*L* (km)	Latitude	Longitude
C5H035	0261789W	174.9	-29.150000	26.433333	C5H035	0292089W	95.3	-28.983333	25.616667
	0261548W	163.5	-29.133333	26.316667		0291899W	82.3	-28.983333	25.483333
	0261523W	162.8	-29.216667	26.300000		0291899A	83.9	-28.983333	25.500000
	0261517W	161.7	-29.100000	26.300000		0291708W	78.4	-28.800000	25.400000
	0261426W	156.8	-29.083333	26.250000		0291582W	76.9	-28.700000	25.333333
	0261368W	152.1	-29.116667	26.200000		0291360W	54.9	-28.983333	25.200000
	0261367W	153.7	-29.116667	26.216667		0291231W	52.1	-28.850000	25.133333
	0261366W	153.6	-29.100000	26.216667		0291178W	45.4	-28.966667	25.100000
	0261365W	153.5	-29.083333	26.216667		0291174W	45.6	-28.900000	25.083333
	0261307A	150.5	-29.116667	26.183333		0291148W	44.2	-28.950000	25.083333
	0262734W	222.5	-29.233333	26.916667		0291075W	51.8	-28.733333	25.050000
	0262453W	206.9	-29.050000	26.766667		0290887W	32.3	-28.783333	24.816667
	0262353W	202.4	-29.383333	26.683333		0290810W	30.5	-29.000000	24.950000
	0262129W	189.5	-29.150000	26.583333		0290468W	28.3	-28.800000	24.766667
	0294233W	194.8	-28.883333	26.633333		0259002W	36.8	-29.016667	25.016667
	0262271W	197.2	-29.016667	26.666667		0258812W	30.3	-29.033333	24.950000
	0294052W	185.3	-28.866667	26.533333		0258182W	2.5	-29.016667	24.616667
	0293792W	180.2	-28.700000	26.450000		0292606W	125.8	-28.600000	25.833333
	0293597A	165.1	-28.950000	26.333333		0293700W	175.1	-28.650000	26.383333
	0293568W	163.6	-28.933333	26.316667		0293339W	157.8	-28.650000	26.200000
	0261722W	171.3	-29.033333	26.400000	C5H039	0292833W	0.6	-28.883333	25.950000
	0293204W	144.5	-28.900000	26.116667		0293514W	47.7	-28.566667	26.283333
	0293106W	142.1	-28.766667	26.066667		0294417W	74.3	-28.933333	26.716667
	0292461W	117.0	-28.666667	25.766667		0293622W	36.8	-28.866667	26.333333
	0292446W	107.0	-28.933333	25.733333		0261733W	58.0	-29.216667	26.416667

Table A.1: Continued

Sub-catchment	SAWS station number	*L* (km)	Latitude	Longitude	Sub-catchment	SAWS station number	*L* (km)	Latitude	Longitude
C5H039	0262314W	80.6	-29.233333	26.683333	C5H039	0261365W	33.6	-29.083333	26.216667
	0262828W	108.5	-29.300000	26.966667		0261307A	34.0	-29.116667	26.183333
	0232512W	106.7	-29.516667	26.783333		0262734W	101.1	-29.233333	26.916667
	0262690W	112.0	-29.483333	26.883333		0262453W	81.0	-29.050000	26.766667
	0262479W	103.1	-29.483333	26.766667		0262353W	89.8	-29.383333	26.683333
	0232301W	98.3	-29.500000	26.683333		0262129W	67.8	-29.150000	26.583333
	0232275W	102.8	-29.583333	26.650000		0294233W	66.0	-28.883333	26.633333
	0232211W	94.9	-29.500000	26.633333		0262271W	70.7	-29.016667	26.666667
	0232123W	94.4	-29.533333	26.583333		0294052W	56.3	-28.866667	26.533333
	0261750W	81.7	-29.500000	26.416667		0293792W	52.4	-28.700000	26.450000
	0261597W	72.8	-29.450000	26.333333		0293597A	37.5	-28.950000	26.333333
	0231754W	84.2	-29.516667	26.433333		0293568W	35.5	-28.933333	26.316667
	0261312W	40.6	-29.200000	26.166667		0261722W	46.3	-29.033333	26.400000
	0261275W	30.1	-29.083333	26.166667		0293204W	15.8	-28.900000	26.116667
	0261183W	23.1	-29.050000	26.100000		0293106W	17.0	-28.766667	26.066667
	0262247W	64.8	-29.116667	26.566667		0293700W	49.2	-28.650000	26.383333
	0261890W	71.5	-29.333333	26.483333		0293339W	35.3	-28.650000	26.200000
	0261789W	55.0	-29.150000	26.433333	C5H053	0294417W	38.5	-28.933333	26.716667
	0261548W	44.7	-29.133333	26.316667		0293622W	9.2	-28.866667	26.333333
	0261523W	49.8	-29.216667	26.300000		0261733W	31.2	-29.216667	26.416667
	0261517W	41.2	-29.100000	26.300000		0262314W	47.3	-29.233333	26.683333
	0261426W	36.1	-29.083333	26.250000		0262828W	73.9	-29.300000	26.966667
	0261368W	35.1	-29.116667	26.200000		0232512W	77.5	-29.516667	26.783333
	0261367W	36.2	-29.116667	26.216667		0262690W	80.7	-29.483333	26.883333
	0261366W	34.9	-29.100000	26.216667		0262479W	73.5	-29.483333	26.766667

Table A.1: Continued

Sub-catchment	SAWS station number	*L* (km)	Latitude	Longitude	Sub-catchment	SAWS station number	*L* (km)	Latitude	Longitude
C5H053	0232301W	70.7	-29.500000	26.683333	C5H053	0294233W	31.2	-28.883333	26.633333
	0232275W	77.5	-29.583333	26.650000		0262271W	34.5	-29.016667	26.666667
	0232211W	68.4	-29.500000	26.633333		0294052W	22.6	-28.866667	26.533333
	0232123W	69.8	-29.533333	26.583333		0293792W	30.4	-28.700000	26.450000
	0261750W	62.0	-29.500000	26.416667		0293597A	1.2	-28.950000	26.333333
	0261597W	55.8	-29.450000	26.333333		0293568W	1.8	-28.933333	26.316667
	0231754W	64.1	-29.516667	26.433333		0261722W	12.2	-29.033333	26.400000
	0261312W	31.7	-29.200000	26.166667	C5H054	0261733W	29.0	-29.216667	26.416667
	0261275W	21.2	-29.083333	26.166667		0261750W	59.9	-29.500000	26.416667
	0262247W	30.3	-29.116667	26.566667		0261597W	53.7	-29.450000	26.333333
	0261890W	45.6	-29.333333	26.483333		0261312W	30.6	-29.200000	26.166667
	0261789W	24.9	-29.150000	26.433333		0261275W	20.7	-29.083333	26.166667
	0261548W	20.5	-29.133333	26.316667		0261890W	43.3	-29.333333	26.483333
	0261523W	29.9	-29.216667	26.300000		0261789W	22.6	-29.150000	26.433333
	0261517W	17.0	-29.100000	26.300000		0261548W	18.6	-29.133333	26.316667
	0261426W	16.5	-29.083333	26.250000		0261523W	28.0	-29.216667	26.300000
	0261368W	22.1	-29.116667	26.200000		0261517W	15.2	-29.100000	26.300000
	0261367W	21.3	-29.116667	26.216667		0261426W	15.3	-29.083333	26.250000
	0261366W	19.7	-29.100000	26.216667		0261368W	21.1	-29.116667	26.200000
	0261365W	18.1	-29.083333	26.216667		0261367W	20.1	-29.116667	26.216667
	0261307A	23.0	-29.116667	26.183333		0261366W	18.6	-29.100000	26.216667
	0262734W	66.0	-29.233333	26.916667		0261365W	17.2	-29.083333	26.216667
	0262453W	44.8	-29.050000	26.766667		0261307A	22.1	-29.116667	26.183333
	0262353W	59.8	-29.383333	26.683333		0293597A	1.9	-28.950000	26.333333
	0262129W	33.9	-29.150000	26.583333		0261722W	9.9	-29.033333	26.400000

Table A.2: Thiessen weights at a sub-catchment level in the MRRC

Sub-catchment	SAWS station number	Thiessen weight	Weighted area (km²)	Sub-catchment	SAWS station number	Thiessen weight	Weighted area (km²)	Sub-catchment	SAWS station number	Thiessen weight	Weighted area (km²)
C5H003	0262314W	0.120	197.1	C5H006	0261426W	0.057	38.8	C5H012	0231713W	0.153	362.6
	0262828W	0.075	122.3		0261368W	0.017	11.5		0231761W	0.068	161.5
	0232512W	0.073	120.3		0261367W	0.055	36.9		0230816W	0.015	35.4
	0262690W	0.092	150.7		0261366W	0.010	6.7		0201843W	0.023	53.6
	0262479W	0.072	118.5		0261365W	0.009	6.2		0231114W	0.174	411.8
	0232301W	0.048	78.3		0261307A	0.025	16.7		0230810W	0.001	2.1
	0232275W	0.059	96.9		0293597A	0.026	17.3		0230774W	0.020	46.7
	0232211W	0.058	94.8		0261722W	0.043	28.8		0261750W	0.003	6.5
	0232123W	0.082	134.9	C5H007	0261733W	0.210	72.7		0261597W	0.000	0.6
	0261750W	0.000	0.2		0261750W	0.002	0.6		0232018W	0.037	88.5
	0231754W	0.018	28.8		0261597W	0.095	32.8		0232011W	0.004	8.9
	0261890W	0.056	91.6		0261312W	0.004	1.2		0231754W	0.001	3.4
	0262734W	0.058	94.4		0261890W	0.176	61.0		0231588W	0.116	274.6
	0262353W	0.167	274.1		0261548W	0.067	23.1		0231395W	0.073	172.1
	0262129W	0.023	37.6		0261523W	0.442	152.7		0231375W	0.108	255.2
C5H006	0261733W	0.133	90.0		0261367W	0.005	1.7		0231361W	0.001	2.6
	0261750W	0.001	0.6	C5H008	0231713W	0.363	217.1		0231279W	0.031	72.5
	0261597W	0.048	32.8		0231761W	0.089	53.3		0231247W	0.031	72.2
	0261312W	0.010	6.8		0232018W	0.148	88.5		0231161W	0.050	119.3
	0261275W	0.007	4.5		0232011W	0.015	8.9		0231076W	0.078	184.0
	0261890W	0.090	61.0		0231588W	0.320	191.3		0230764W	0.014	32.3
	0261789W	0.032	21.9		0231375W	0.065	38.6	C5H014	0229654W	0.010	323.9
	0261548W	0.115	77.7	C5H009	0231713W	0.728	137.3		0231713W	0.012	362.6
	0261523W	0.227	153.8		0231114W	0.065	12.2		0292833W	0.015	482.7
	0261517W	0.095	64.3		0231588W	0.207	39.0		0290560W	0.008	264.4

Table A.2: Continued

Sub-catchment	SAWS station number	Thiessen weight	Weighted area (km²)	Sub-catchment	SAWS station number	Thiessen weight	Weighted area (km²)	Sub-catchment	SAWS station number	Thiessen weight	Weighted area (km²)
C5H014	0293007W	0.015	454.9	C5H014	0201492W	0.005	141.6	C5H014	0231375W	0.008	255.2
	0293514W	0.008	265.6		0201482W	0.004	121.1		0231361W	0.006	199.7
	0294417W	0.005	163.3		0201373W	0.003	83.8		0261146AW	0.010	314.3
	0293622W	0.010	300.6		0201370W	0.009	269.6		0260660W	0.005	154.3
	0292051W	0.014	452.4		0201361W	0.004	138.8		0231279W	0.002	72.5
	0291323W	0.006	198.9		0231114W	0.013	421.8		0231247W	0.004	116.2
	0257878W	0.002	66.7		0230810W	0.004	109.9		0231161W	0.004	119.4
	0258581W	0.005	167.4		0230774W	0.005	168.7		0231076W	0.006	184.0
	0259348W	0.012	383.6		0230598W	0.003	105.6		0230764W	0.007	231.1
	0260163W	0.005	157.0		0230566W	0.006	176.3		0260030W	0.006	202.6
	0260882W	0.011	335.6		0201756W	0.003	93.0		0230542W	0.007	226.3
	0261733W	0.005	161.4		0201637W	0.004	121.3		0230466W	0.008	244.9
	0262314W	0.010	325.5		0262690W	0.005	150.7		0230363W	0.010	302.7
	0262828W	0.004	122.3		0262479W	0.004	118.5		0230254W	0.006	173.3
	0232512W	0.004	120.3		0232301W	0.003	78.3		0230074W	0.002	50.2
	0231761W	0.007	225.7		0232275W	0.004	121.4		0230073W	0.002	54.1
	0230816W	0.008	262.5		0232211W	0.003	94.8		0230048W	0.004	131.1
	0230011W	0.006	201.8		0232123W	0.005	157.2		0229737W	0.005	161.1
	0229215W	0.005	160.7		0261750W	0.004	121.6		0229723W	0.006	198.2
	0228725W	0.007	211.9		0261597W	0.009	276.0		0229571W	0.003	80.5
	0230210W	0.009	279.0		0232018W	0.003	88.5		0259390A	0.010	320.6
	0201843W	0.005	142.0		0232011W	0.004	140.3		0229579W	0.007	233.7
	0230349W	0.006	194.7		0231754W	0.005	161.8		0229555W	0.007	206.8
	0230027W	0.009	284.4		0231588W	0.009	274.6		0229344W	0.006	176.8
	0229862W	0.003	108.9		0231395W	0.006	193.3		0229124W	0.008	241.9

Table A.2: Continued

Sub-catchment	SAWS station number	Thiessen weight	Weighted area (km²)	Sub-catchment	SAWS station number	Thiessen weight	Weighted area (km²)	Sub-catchment	SAWS station number	Thiessen weight	Weighted area (km²)
C5H014	0228783W	0.004	135.2	C5H014	0260082W	0.009	266.2	C5H014	0261307A	0.001	37.7
	0228571W	0.005	171.8		0260004W	0.003	81.3		0262734W	0.008	247.2
	0258218W	0.001	41.8		0259887W	0.006	175.4		0262453W	0.008	247.3
	0258213A	0.001	46.3		0259881W	0.004	120.6		0262353W	0.009	274.1
	0258164W	0.005	168.4		0259743W	0.009	279.4		0262129W	0.005	165.7
	0258157A	0.001	33.5		0259727W	0.004	139.5		0294233W	0.006	194.3
	0258079W	0.011	338.9		0261312W	0.004	136.1		0262271W	0.006	187.5
	0258894W	0.008	264.5		0261275W	0.002	69.7		0294052W	0.010	323.3
	0258827W	0.006	186.0		0261256W	0.009	271.2		0293792W	0.008	250.2
	0258740W	0.004	131.5		0261183W	0.009	272.0		0293597A	0.004	110.4
	0258624W	0.004	135.7		0260715W	0.007	225.5		0293568W	0.004	117.3
	0258474W	0.004	130.3		0260678W	0.006	195.2		0261722W	0.007	213.8
	0258467W	0.003	87.3		0260555W	0.006	200.5		0293204W	0.010	306.5
	0258458W	0.005	160.2		0260519W	0.011	358.0		0293106W	0.010	304.3
	0258434W	0.002	52.5		0262247W	0.005	164.7		0292461W	0.019	587.9
	0258399W	0.004	123.8		0261890W	0.010	328.0		0292446W	0.014	440.2
	0258380W	0.006	172.4		0261789W	0.004	134.7		0292089W	0.007	216.7
	0258339W	0.002	77.5		0261548W	0.002	77.7		0291899W	0.005	170.9
	0258306W	0.001	28.5		0261523W	0.007	216.5		0291899A	0.003	82.1
	0259609W	0.007	220.3		0261517W	0.002	64.3		0291708W	0.010	319.2
	0259578W	0.005	168.5		0261426W	0.002	63.5		0291582W	0.016	509.7
	0259278W	0.008	239.7		0261368W	0.000	11.7		0291360W	0.008	248.3
	0259102W	0.007	233.6		0261367W	0.001	36.9		0291231W	0.005	153.5
	0260314W	0.008	236.0		0261366W	0.000	6.7		0291178W	0.003	86.0
	0260126W	0.004	131.4		0261365W	0.002	52.0		0291174W	0.005	143.9

Table A.2: Continued

Sub-catchment	SAWS station number	Thiessen weight	Weighted area (km²)	Sub-catchment	SAWS station number	Thiessen weight	Weighted area (km²)	Sub-catchment	SAWS station number	Thiessen weight	Weighted area (km²)
C5H014	0291148W	0.002	47.7	C5H015	0261597W	0.006	32.8	C5H015	0293597A	0.019	110.4
	0291075W	0.010	311.5		0231754W	0.005	28.8		0293568W	0.020	117.3
	0290887W	0.003	89.0		0261312W	0.001	6.8		0261722W	0.036	213.8
	0290810W	0.007	208.0		0261275W	0.003	17.9		0293204W	0.023	139.2
	0290468W	0.005	149.5		0261183W	0.000	0.0		0293106W	0.001	6.5
	0259002W	0.004	125.6		0262247W	0.028	164.7		0293700W	0.040	239.8
	0258812W	0.006	172.2		0261890W	0.055	326.4		0293339W	0.010	56.5
	0258182W	0.003	79.0		0261789W	0.023	134.7	C5H016	0229654W	0.010	323.9
	0292606W	0.005	151.6		0261548W	0.013	77.7		0231713W	0.011	362.6
	0293700W	0.008	239.8		0261523W	0.026	153.8		0292833W	0.015	482.7
	0293339W	0.011	347.5		0261517W	0.011	64.3		0290560W	0.008	264.4
C5H015	0293514W	0.017	101.9		0261426W	0.011	63.5		0293007W	0.014	454.9
	0294417W	0.028	163.3		0261368W	0.002	11.5		0293514W	0.008	265.6
	0293622W	0.051	300.6		0261367W	0.006	36.9		0294417W	0.005	163.3
	0261733W	0.027	161.4		0261366W	0.001	6.7		0293622W	0.009	300.6
	0262314W	0.055	325.5		0261365W	0.009	52.0		0292051W	0.014	452.4
	0262828W	0.021	122.3		0261307A	0.003	16.7		0291323W	0.006	198.9
	0232512W	0.020	120.3		0262734W	0.042	247.2		0289796W	0.024	792.4
	0262690W	0.025	150.7		0262453W	0.042	247.3		0257391W	0.008	265.3
	0262479W	0.020	118.5		0262353W	0.046	274.1		0257878W	0.008	251.7
	0232301W	0.013	78.3		0262129W	0.028	165.7		0258581W	0.005	167.4
	0232275W	0.016	96.9		0294233W	0.033	194.3		0259348W	0.012	383.6
	0232211W	0.016	94.8		0262271W	0.032	187.5		0260163W	0.005	157.0
	0232123W	0.023	134.9		0294052W	0.054	323.3		0260882W	0.010	335.6
	0261750W	0.000	0.8		0293792W	0.042	250.2		0261733W	0.005	161.4

Table A.2: Continued

Sub-catchment	SAWS station number	Thiessen weight	Weighted area (km²)	Sub-catchment	SAWS station number	Thiessen weight	Weighted area (km²)	Sub-catchment	SAWS station number	Thiessen weight	Weighted area (km²)
C5H016	0262314W	0.010	325.5	C5H016	0201637W	0.004	121.3	C5H016	0230542W	0.007	226.3
	0262828W	0.004	122.3		0262690W	0.005	150.7		0230466W	0.007	244.9
	0232512W	0.004	120.3		0262479W	0.004	118.5		0230363W	0.009	302.7
	0231761W	0.007	225.7		0232301W	0.002	78.3		0230254W	0.005	173.3
	0230816W	0.008	262.5		0232275W	0.004	121.4		0230074W	0.002	50.2
	0230011W	0.006	201.8		0232211W	0.003	94.8		0230073W	0.002	54.1
	0229215W	0.005	160.7		0232123W	0.005	157.2		0230048W	0.004	131.1
	0228725W	0.006	211.9		0261750W	0.004	121.6		0229737W	0.005	161.1
	0230210W	0.008	279.0		0261597W	0.008	276.0		0229723W	0.006	198.2
	0201843W	0.004	142.0		0232018W	0.003	88.5		0229571W	0.002	80.5
	0230349W	0.006	194.7		0232011W	0.004	140.3		0259390A	0.010	320.6
	0230027W	0.009	284.4		0231754W	0.005	161.8		0229579W	0.007	233.7
	0229862W	0.003	108.9		0231588W	0.008	274.6		0229555W	0.006	206.8
	0201492W	0.004	141.6		0231395W	0.006	193.3		0229344W	0.005	176.8
	0201482W	0.004	121.1		0231375W	0.008	255.2		0229124W	0.007	241.9
	0201373W	0.003	83.8		0231361W	0.006	199.7		0228783W	0.004	135.2
	0201370W	0.008	269.6		0261146AW	0.009	314.3		0228571W	0.005	171.8
	0201361W	0.004	138.8		0260660W	0.005	154.3		0258218W	0.001	41.8
	0231114W	0.013	421.8		0231279W	0.002	72.5		0258213A	0.002	52.4
	0230810W	0.003	109.9		0231247W	0.003	116.2		0258164W	0.005	168.4
	0230774W	0.005	168.7		0231161W	0.004	119.4		0258157A	0.002	75.3
	0230598W	0.003	105.6		0231076W	0.006	184.0		0258079W	0.010	338.9
	0230566W	0.005	176.3		0230764W	0.007	231.1		0257845W	0.010	316.6
	0201756W	0.003	93.0		0260030W	0.006	202.6		0258894W	0.008	264.5

Table A.2: Continued

Sub-catchment	SAWS station number	Thiessen weight	Weighted area (km²)	Sub-catchment	SAWS station number	Thiessen weight	Weighted area (km²)	Sub-catchment	SAWS station number	Thiessen weight	Weighted area (km²)
C5H016	0258827W	0.006	186.0	C5H016	0261256W	0.008	271.2	C5H016	0293792W	0.008	250.2
	0258740W	0.004	131.5		0261183W	0.008	272.0		0293597A	0.003	110.4
	0258624W	0.004	135.7		0260715W	0.007	225.5		0293568W	0.004	117.3
	0258474W	0.004	130.3		0260678W	0.006	195.2		0261722W	0.006	213.8
	0258467W	0.003	87.3		0260555W	0.006	200.5		0293204W	0.009	306.5
	0258458W	0.005	160.2		0260519W	0.011	358.0		0293106W	0.009	304.3
	0258434W	0.002	52.5		0262247W	0.005	164.7		0292461W	0.018	587.9
	0258399W	0.004	123.8		0261890W	0.010	328.0		0292446W	0.013	440.2
	0258380W	0.005	172.4		0261789W	0.004	134.7		0292089W	0.007	216.7
	0258339W	0.002	77.5		0261548W	0.002	77.7		0291899W	0.005	170.9
	0258306W	0.001	28.5		0261523W	0.007	216.5		0291899A	0.002	82.1
	0259609W	0.007	220.3		0261517W	0.002	64.3		0291708W	0.010	319.2
	0259578W	0.005	168.5		0261426W	0.002	63.5		0291582W	0.015	509.7
	0259278W	0.007	239.7		0261368W	0.000	11.7		0291360W	0.007	248.3
	0259102W	0.007	233.6		0261367W	0.001	36.9		0291231W	0.005	153.5
	0260314W	0.007	236.0		0261366W	0.000	6.7		0291178W	0.003	86.0
	0260126W	0.004	131.4		0261365W	0.002	52.0		0291174W	0.004	143.9
	0260082W	0.008	266.2		0261307A	0.001	37.7		0291148W	0.001	47.7
	0260004W	0.002	81.3		0262734W	0.007	247.2		0291075W	0.009	311.5
	0259887W	0.005	175.4		0262453W	0.007	247.3		0290887W	0.003	89.0
	0259881W	0.004	120.6		0262353W	0.008	274.1		0290810W	0.006	208.0
	0259743W	0.008	279.4		0262129W	0.005	165.7		0290468W	0.009	307.3
	0259727W	0.004	139.5		0294233W	0.006	194.3		0259002W	0.004	125.6
	0261312W	0.004	136.1		0262271W	0.006	187.5		0258812W	0.005	172.2
	0261275W	0.002	69.7		0294052W	0.010	323.3		0258182W	0.009	309.2

Table A.2: Continued

Sub-catchment	SAWS station number	Thiessen weight	Weighted area (km²)	Sub-catchment	SAWS station number	Thiessen weight	Weighted area (km²)	Sub-catchment	SAWS station number	Thiessen weight	Weighted area (km²)
C5H016	0292606W	0.005	151.6	C5H018	0232123W	0.008	134.9	C5H018	0261275W	0.004	69.7
	0293700W	0.007	239.8		0261750W	0.000	0.8		0261256W	0.016	270.7
	0293339W	0.010	347.5		0261597W	0.002	41.1		0261183W	0.016	272.0
C5H018	0292833W	0.028	482.7		0231754W	0.002	28.8		0260715W	0.004	76.0
	0290560W	0.015	264.4		0231361W	0.000	0.2		0260678W	0.011	195.2
	0293007W	0.026	454.9		0261146AW	0.004	66.0		0260555W	0.011	196.3
	0293514W	0.015	265.6		0230542W	0.000	2.0		0260519W	0.021	358.0
	0294417W	0.009	163.3		0258213A	0.001	17.0		0262247W	0.009	164.7
	0293622W	0.017	300.6		0258827W	0.002	26.2		0261890W	0.019	326.4
	0292051W	0.026	452.4		0258458W	0.006	104.2		0261789W	0.008	134.7
	0291323W	0.011	198.9		0258399W	0.006	97.6		0261548W	0.004	77.7
	0258581W	0.001	19.0		0259609W	0.012	216.1		0261523W	0.012	216.5
	0259348W	0.007	115.5		0259578W	0.010	168.5		0261517W	0.004	64.3
	0260163W	0.009	157.0		0259278W	0.014	239.7		0261426W	0.004	63.5
	0260882W	0.019	335.6		0259102W	0.012	216.7		0261368W	0.001	11.7
	0261733W	0.009	161.4		0260314W	0.014	235.9		0261367W	0.002	36.9
	0262314W	0.019	325.5		0260126W	0.008	131.4		0261366W	0.000	6.7
	0262828W	0.007	122.3		0260082W	0.003	56.1		0261365W	0.003	52.0
	0232512W	0.007	120.3		0260004W	0.005	81.3		0261307A	0.002	37.7
	0262690W	0.009	150.7		0259887W	0.009	156.5		0262734W	0.014	247.2
	0262479W	0.007	118.5		0259881W	0.007	120.6		0262453W	0.014	247.3
	0232301W	0.005	78.3		0259743W	0.002	38.1		0262353W	0.016	274.1
	0232275W	0.006	96.9		0259727W	0.008	139.5		0262129W	0.010	165.7
	0232211W	0.005	94.8		0261312W	0.008	136.1		0294233W	0.011	194.3

Table A.2: Continued

Sub-catchment	SAWS station number	Thiessen weight	Weighted area (km²)	Sub-catchment	SAWS station number	Thiessen weight	Weighted area (km²)	Sub-catchment	SAWS station number	Thiessen weight	Weighted area (km²)
C5H018	0262271W	0.011	187.5	C5H018	0258182W	0.003	53.3	C5H035	0261750W	0.000	0.8
	0294052W	0.019	323.3		0292606W	0.009	151.6		0261597W	0.002	41.1
	0293792W	0.014	250.2		0293700W	0.014	239.8		0231754W	0.002	28.8
	0293597A	0.006	110.4		0293339W	0.020	347.5		0231361W	0.000	0.2
	0293568W	0.007	117.3	C5H035	0292833W	0.028	482.7		0261146AW	0.004	66.0
	0261722W	0.012	213.8		0290560W	0.015	264.4		0230542W	0.000	2.0
	0293204W	0.018	306.5		0293007W	0.026	454.9		0258213A	0.001	15.3
	0293106W	0.018	304.3		0293514W	0.015	265.6		0258827W	0.002	26.2
	0292461W	0.034	587.9		0294417W	0.009	163.3		0258458W	0.006	104.2
	0292446W	0.025	440.2		0293622W	0.017	300.6		0258399W	0.006	97.6
	0292089W	0.012	216.7		0292051W	0.026	452.4		0259609W	0.012	216.1
	0291899W	0.010	170.9		0291323W	0.011	198.9		0259578W	0.010	168.5
	0291899A	0.005	82.1		0258581W	0.001	19.0		0259278W	0.014	239.7
	0291708W	0.018	319.2		0259348W	0.007	115.5		0259102W	0.012	216.7
	0291582W	0.029	509.7		0260163W	0.009	157.0		0260314W	0.014	235.9
	0291360W	0.014	248.3		0260882W	0.019	335.6		0260126W	0.008	131.4
	0291231W	0.009	153.5		0261733W	0.009	161.4		0260082W	0.003	56.1
	0291178W	0.005	86.0		0262314W	0.019	325.5		0260004W	0.005	81.3
	0291174W	0.008	143.9		0262828W	0.007	122.3		0259887W	0.009	156.5
	0291148W	0.003	47.7		0232512W	0.007	120.3		0259881W	0.007	120.6
	0291075W	0.018	311.5		0262690W	0.009	150.7		0259743W	0.002	38.1
	0290887W	0.005	89.0		0262479W	0.007	118.5		0259727W	0.008	139.5
	0290810W	0.012	208.0		0232301W	0.005	78.3		0261312W	0.008	136.1
	0290468W	0.009	149.5		0232275W	0.006	96.9		0261275W	0.004	69.7
	0259002W	0.007	125.6		0232211W	0.005	94.8		0261256W	0.016	270.7
	0258812W	0.010	172.2		0232123W	0.008	134.9		0261183W	0.016	272.0

Table A.2: Continued

Sub-catchment	SAWS station number	Thiessen weight	Weighted area (km²)	Sub-catchment	SAWS station number	Thiessen weight	Weighted area (km²)	Sub-catchment	SAWS station number	Thiessen weight	Weighted area (km²)
C5H035	0260715W	0.004	76.0	C5H035	0293204W	0.018	306.5	C5H039	0293622W	0.047	300.6
	0260678W	0.011	195.2		0293106W	0.018	304.3		0261733W	0.025	161.4
	0260555W	0.011	196.3		0292461W	0.034	587.9		0262314W	0.051	325.5
	0260519W	0.021	358.0		0292446W	0.025	440.2		0262828W	0.019	122.3
	0262247W	0.009	164.7		0292089W	0.012	216.7		0232512W	0.019	120.3
	0261890W	0.019	326.4		0291899W	0.010	170.9		0262690W	0.024	150.7
	0261789W	0.008	134.7		0291899A	0.005	82.1		0262479W	0.019	118.5
	0261548W	0.004	77.7		0291708W	0.018	319.2		0232301W	0.012	78.3
	0261523W	0.012	216.5		0291582W	0.029	509.7		0232275W	0.015	96.9
	0261517W	0.004	64.3		0291360W	0.014	248.3		0232211W	0.015	94.8
	0261426W	0.004	63.5		0291231W	0.009	153.5		0232123W	0.021	134.9
	0261368W	0.001	11.7		0291178W	0.005	86.0		0261750W	0.000	0.8
	0261367W	0.002	36.9		0291174W	0.008	143.9		0261597W	0.005	32.8
	0261366W	0.000	6.7		0291148W	0.003	47.7		0231754W	0.005	28.8
	0261365W	0.003	52.0		0291075W	0.018	311.5		0261312W	0.001	6.8
	0261307A	0.002	37.7		0290887W	0.005	89.0		0261275W	0.003	17.9
	0262734W	0.014	247.2		0290810W	0.012	208.0		0261183W	0.000	2.7
	0262453W	0.014	247.3		0290468W	0.009	149.5		0262247W	0.026	164.7
	0262353W	0.016	274.1		0259002W	0.007	125.6		0261890W	0.052	326.4
	0262129W	0.010	165.7		0258812W	0.010	172.2		0261789W	0.021	134.7
	0294233W	0.011	194.3		0258182W	0.003	53.3		0261548W	0.012	77.7
	0262271W	0.011	187.5		0292606W	0.009	151.6		0261523W	0.024	153.8
	0294052W	0.019	323.3		0293700W	0.014	239.8		0261517W	0.010	64.3
	0293792W	0.014	250.2		0293339W	0.020	347.5		0261426W	0.010	63.5
	0293597A	0.006	110.4	C5H039	0292833W	0.014	89.5		0261368W	0.002	11.5
	0293568W	0.007	117.3		0293514W	0.016	101.9		0261367W	0.006	36.9
	0261722W	0.012	213.8		0294417W	0.026	163.3		0261366W	0.001	6.7

Table A.2: Continued

Sub-catchment	SAWS station number	Thiessen weight	Weighted area (km²)	Sub-catchment	SAWS station number	Thiessen weight	Weighted area (km²)	Sub-catchment	SAWS station number	Thiessen weight	Weighted area (km²)
C5H039	0261365W	0.008	52.0	C5H053	0232301W	0.017	78.3	C5H053	0294233W	0.043	194.3
	0261307A	0.003	16.7		0232275W	0.021	96.9		0262271W	0.041	187.5
	0262734W	0.039	247.2		0232211W	0.021	94.8		0294052W	0.052	235.6
	0262453W	0.039	247.3		0232123W	0.030	134.9		0293792W	0.002	7.4
	0262353W	0.043	274.1		0261750W	0.000	0.8		0293597A	0.023	105.9
	0262129W	0.026	165.7		0261597W	0.007	32.8		0293568W	0.001	4.6
	0294233W	0.031	194.3		0231754W	0.006	28.8		0261722W	0.047	213.8
	0262271W	0.030	187.5		0261312W	0.001	6.8	C5H054	0261733W	0.131	90.0
	0294052W	0.051	323.3		0261275W	0.001	4.5		0261750W	0.001	0.6
	0293792W	0.040	250.2		0262247W	0.036	164.7		0261597W	0.048	32.8
	0293597A	0.017	110.4		0261890W	0.071	326.4		0261312W	0.010	6.8
	0293568W	0.019	117.3		0261789W	0.029	134.7		0261275W	0.007	4.5
	0261722W	0.034	213.8		0261548W	0.017	77.7		0261890W	0.089	61.0
	0293204W	0.045	287.9		0261523W	0.034	153.8		0261789W	0.032	21.9
	0293106W	0.018	111.4		0261517W	0.014	64.3		0261548W	0.113	77.7
	0293700W	0.038	239.8		0261426W	0.008	38.8		0261523W	0.224	153.8
	0293339W	0.016	103.4		0261368W	0.003	11.5		0261517W	0.094	64.3
C5H053	0294417W	0.036	163.3		0261367W	0.008	36.9		0261426W	0.056	38.8
	0293622W	0.001	6.7		0261366W	0.001	6.7		0261368W	0.017	11.5
	0261733W	0.035	161.4		0261365W	0.001	6.2		0261367W	0.054	36.9
	0262314W	0.071	325.5		0261307A	0.004	16.7		0261366W	0.010	6.7
	0262828W	0.027	122.3		0262734W	0.054	247.2		0261365W	0.009	6.2
	0232512W	0.026	120.3		0262453W	0.054	247.3		0261307A	0.024	16.7
	0262690W	0.033	150.7		0262353W	0.060	274.1		0293597A	0.041	28.1
	0262479W	0.026	118.5		0262129W	0.036	165.7		0261722W	0.042	28.8

Table A.3: Event-specific time parameters and time parameter proportionality ratios at a sub-catchment level in the MRRC

Sub-catchment	Event #	Q_P (m^3/s)	L (km)	S_e (%)	T_C [a] (h)	T_C [b] & T_L [a/b] (h)	T_C [c] (h)	T_L [c] (h)	T_C [d] (h)	TPPR 1	TPPR 2	TPPR 3	TPPR 4	TPPR 5	TPPR 6	TPPR 7	TPPR 8
C5H003	40	6.0	40.5	22.5	330.8	232.2	232.2	243.0	16.2	1.425	1.000	1.000	0.070	1.362	0.956	0.956	0.067
	41	6.6	47.6	23.9	491.3	411.2	411.2	415.5	3.2	1.195	1.000	1.000	0.008	1.182	0.990	0.990	0.008
	16	6.8	47.6	23.0	382.2	406.1	386.6	408.7	2.6	0.941	1.000	0.952	0.006	0.935	0.994	0.946	0.006
	77	8.4	41.4	18.8	570.0	613.8	603.0	616.7	3.0	0.929	1.000	0.982	0.005	0.924	0.995	0.978	0.005
	24	9.2	40.5	23.0	453.4	458.4	458.4	459.9	2.4	0.989	1.000	1.000	0.005	0.986	0.997	0.997	0.005
	46	9.4	41.4	12.7	451.9	434.3	434.3	437.4	2.3	1.041	1.000	1.000	0.005	1.033	0.993	0.993	0.005
	25	9.5	40.5	26.1	319.2	315.0	321.0	316.5	9.0	1.013	1.000	1.019	0.029	1.009	0.995	1.014	0.028
	33	12.3	40.5	23.7	899.3	843.4	843.4	847.9	3.4	1.066	1.000	1.000	0.004	1.061	0.995	0.995	0.004
	58	13.0	40.5	22.3	361.2	385.2	375.4	384.4	15.4	0.938	1.000	0.975	0.040	0.940	1.002	0.977	0.040
	37	13.3	40.5	34.8	169.6	162.0	151.9	162.4	7.9	1.047	1.000	0.937	0.049	1.045	0.998	0.936	0.049
	51	19.1	41.4	19.4	137.8	145.7	156.0	146.2	12.0	0.946	1.000	1.071	0.082	0.943	0.997	1.067	0.082
	8	19.5	40.5	34.6	439.9	443.0	447.6	445.7	15.6	0.993	1.000	1.010	0.035	0.987	0.994	1.004	0.035
	71	19.9	40.5	33.5	557.2	565.2	561.4	570.4	9.4	0.986	1.000	0.993	0.017	0.977	0.991	0.984	0.016
	11	21.2	47.6	27.2	164.7	178.4	178.4	177.7	10.4	0.923	1.000	1.000	0.058	0.927	1.004	1.004	0.059
	44	23.2	41.4	26.4	382.4	341.2	338.8	343.2	2.8	1.121	1.000	0.993	0.008	1.114	0.994	0.987	0.008
	3	23.3	40.5	39.7	390.8	375.6	375.6	369.4	15.6	1.040	1.000	1.000	0.042	1.058	1.017	1.017	0.042
	43	24.0	41.4	26.1	640.0	627.7	627.7	631.5	3.7	1.020	1.000	1.000	0.006	1.013	0.994	0.994	0.006
	73	24.6	41.4	27.5	382.4	439.2	439.2	441.0	7.2	0.871	1.000	1.000	0.016	0.867	0.996	0.996	0.016
	78	25.6	47.6	21.3	356.6	365.0	365.0	366.8	5.0	0.977	1.000	1.000	0.014	0.972	0.995	0.995	0.014
	45	26.2	47.6	21.3	720.1	680.9	680.9	686.2	8.9	1.058	1.000	1.000	0.013	1.049	0.992	0.992	0.013
	19	26.5	47.6	57.3	426.6	367.9	368.4	349.2	128.4	1.160	1.000	1.001	0.349	1.222	1.053	1.055	0.368
	4	29.0	40.5	38.6	197.7	218.5	208.2	218.2	16.2	0.905	1.000	0.953	0.074	0.906	1.001	0.954	0.074
	67	29.0	40.5	30.5	899.9	931.9	920.8	933.8	8.8	0.966	1.000	0.988	0.009	0.964	0.998	0.986	0.009
	42	29.7	41.4	33.9	995.0	1059.7	1076.5	1047.2	44.5	0.939	1.000	1.016	0.042	0.950	1.012	1.028	0.042
	15	30.9	41.4	34.9	371.9	369.5	368.7	359.2	32.7	1.006	1.000	0.998	0.088	1.035	1.029	1.026	0.091

Table A.3: Continued

Sub-catchment	Event #	Q_P (m^3/s)	L (km)	S_e (%)	T_C [a] (h)	T_C [b] & T_L [a/b] (h)	T_C [c] (h)	T_L [c] (h)	T_C [d] (h)	TPPR 1	TPPR 2	TPPR 3	TPPR 4	TPPR 5	TPPR 6	TPPR 7	TPPR 8
C5H003	10	31.6	38.2	43.1	749.4	728.6	728.6	733.0	8.6	1.029	1.000	1.000	0.012	1.022	0.994	0.994	0.012
	26	34.0	41.4	23.6	172.1	213.7	217.2	214.5	1.2	0.805	1.000	1.016	0.006	0.802	0.996	1.013	0.006
	31	37.8	47.6	31.9	548.1	536.1	536.1	538.9	8.1	1.022	1.000	1.000	0.015	1.017	0.995	0.995	0.015
	52	38.4	41.4	31.8	127.8	123.7	111.8	121.1	15.8	1.033	1.000	0.903	0.128	1.056	1.022	0.924	0.131
	5	60.4	40.5	38.7	193.7	220.3	200.8	224.9	8.8	0.879	1.000	0.912	0.040	0.861	0.979	0.893	0.039
C5H006	10	14.7	17.7	52.0	135.0	149.5	149.5	152.3	5.5	0.903	1.000	1.000	0.037	0.886	0.982	0.982	0.036
	2	17.4	57.8	24.1	227.0	247.0	247.0	249.7	7.0	0.919	1.000	1.000	0.028	0.909	0.989	0.989	0.028
	13	35.2	57.8	63.4	304.0	315.7	324.0	326.7	12.0	0.963	1.000	1.026	0.038	0.930	0.966	0.992	0.037
C5H007	79	8.1	12.5	45.1	402.2	408.8	389.6	410.9	5.6	0.984	1.000	0.953	0.014	0.979	0.995	0.948	0.014
	57	8.3	8.3	55.3	792.3	797.9	797.9	797.6	5.9	0.993	1.000	1.000	0.007	0.993	1.000	1.000	0.007
	38	8.7	40.7	84.2	642.4	668.8	668.8	666.0	20.8	0.961	1.000	1.000	0.031	0.965	1.004	1.004	0.031
	18	11.0	12.5	37.3	152.0	171.0	171.0	170.8	3.0	0.889	1.000	1.000	0.018	0.890	1.001	1.001	0.018
	15	11.5	16.0	28.5	294.4	313.4	313.4	313.9	1.4	0.939	1.000	1.000	0.004	0.938	0.998	0.998	0.004
	31	11.8	8.3	61.2	737.9	739.6	736.7	738.4	16.7	0.998	1.000	0.996	0.023	0.999	1.002	0.998	0.023
	29	12.1	12.5	55.8	138.0	179.8	174.0	181.6	6.0	0.767	1.000	0.968	0.033	0.760	0.990	0.958	0.033
	73	12.2	12.5	22.9	527.2	557.4	557.4	559.0	5.4	0.946	1.000	1.000	0.010	0.943	0.997	0.997	0.010
	9	12.8	12.5	42.8	756.0	646.9	658.0	648.9	10.0	1.169	1.000	1.017	0.015	1.165	0.997	1.014	0.015
	55	13.0	8.3	68.6	355.1	339.4	339.4	340.9	3.4	1.046	1.000	1.000	0.010	1.042	0.996	0.996	0.010
	41	13.0	40.7	80.2	786.1	796.6	796.6	790.4	28.6	0.987	1.000	1.000	0.036	0.995	1.008	1.008	0.036
	16	13.9	12.5	53.1	430.6	487.8	491.6	483.9	11.6	0.883	1.000	1.008	0.024	0.890	1.008	1.016	0.024
	36	14.3	12.5	65.1	469.3	509.5	509.5	508.7	5.5	0.921	1.000	1.000	0.011	0.923	1.002	1.002	0.011
	77	14.3	12.5	21.0	574.0	577.4	577.4	578.6	1.4	0.994	1.000	1.000	0.002	0.992	0.998	0.998	0.002
	65	14.5	8.3	58.8	502.6	507.7	509.2	509.9	5.2	0.990	1.000	1.003	0.010	0.986	0.996	0.999	0.010
	20	14.7	10.3	83.6	680.0	679.0	679.0	677.8	7.0	1.001	1.000	1.000	0.010	1.003	1.002	1.002	0.010
	7	15.0	26.5	42.2	642.0	719.5	722.0	721.1	2.0	0.892	1.000	1.003	0.003	0.890	0.998	1.001	0.003

Table A.3: Continued

Sub-catchment	Event #	Q_P (m^3/s)	L (km)	S_e (%)	T_C [a] (h)	T_C [b] & T_L [a/b] (h)	T_C [c] (h)	T_L [c] (h)	T_C [d] (h)	TPPR 1	TPPR 2	TPPR 3	TPPR 4	TPPR 5	TPPR 6	TPPR 7	TPPR 8
C5H007	42	15.9	8.3	87.6	918.0	906.3	918.0	909.7	6.0	1.013	1.000	1.013	0.007	1.009	0.996	1.009	0.007
	19	16.1	34.0	34.3	172.6	192.6	192.6	192.9	0.6	0.896	1.000	1.000	0.003	0.895	0.999	0.999	0.003
	64	16.6	12.5	86.2	789.1	797.2	797.2	800.8	5.2	0.990	1.000	1.000	0.007	0.985	0.995	0.995	0.006
	21	18.1	40.7	60.3	630.2	630.8	630.8	630.7	6.8	0.999	1.000	1.000	0.011	0.999	1.000	1.000	0.011
	40	19.5	16.0	65.7	618.7	587.7	587.7	589.6	11.7	1.053	1.000	1.000	0.020	1.049	0.997	0.997	0.020
	63	19.7	12.5	65.1	349.3	341.6	341.6	343.2	5.6	1.023	1.000	1.000	0.016	1.018	0.995	0.995	0.016
	49	21.2	8.3	44.5	607.2	580.7	580.7	582.5	4.7	1.046	1.000	1.000	0.008	1.042	0.997	0.997	0.008
	33	22.4	34.0	77.8	821.1	819.0	819.0	822.2	3.0	1.003	1.000	1.000	0.004	0.999	0.996	0.996	0.004
	37	22.8	40.7	65.3	893.7	894.5	894.5	895.3	6.5	0.999	1.000	1.000	0.007	0.998	0.999	0.999	0.007
	26	23.9	8.3	83.0	555.0	585.0	585.0	582.4	9.0	0.949	1.000	1.000	0.015	0.953	1.004	1.004	0.015
	23	23.9	26.5	83.8	406.0	391.0	391.0	394.0	7.0	1.038	1.000	1.000	0.018	1.030	0.992	0.992	0.018
	22	24.6	10.3	70.9	272.4	313.0	313.0	313.2	1.0	0.870	1.000	1.000	0.003	0.870	0.999	0.999	0.003
	56	26.5	12.5	92.6	747.5	800.1	800.1	802.1	8.1	0.934	1.000	1.000	0.010	0.932	0.998	0.998	0.010
	66	27.4	12.5	79.9	140.7	150.6	150.6	151.1	6.6	0.934	1.000	1.000	0.044	0.931	0.996	0.996	0.044
	24	31.7	8.3	55.1	779.4	793.4	793.4	794.3	1.4	0.982	1.000	1.000	0.002	0.981	0.999	0.999	0.002
	10	33.3	26.5	63.0	741.0	752.0	752.0	756.3	8.0	0.985	1.000	1.000	0.011	0.980	0.994	0.994	0.011
	48	33.6	12.5	73.0	356.0	339.9	339.9	349.5	3.9	1.047	1.000	1.000	0.011	1.019	0.973	0.973	0.011
	67	33.6	8.3	49.6	223.9	249.1	249.1	249.0	9.1	0.899	1.000	1.000	0.037	0.899	1.000	1.000	0.037
	45	36.2	16.0	72.3	132.4	129.3	137.6	111.3	65.6	1.024	1.000	1.064	0.507	1.190	1.162	1.236	0.589
	11	43.6	12.5	58.9	680.0	698.0	698.0	698.8	2.0	0.974	1.000	1.000	0.003	0.973	0.999	0.999	0.003
	17	44.2	12.5	66.9	358.0	386.1	364.4	389.4	4.4	0.927	1.000	0.944	0.011	0.919	0.992	0.936	0.011
	60	50.4	8.3	78.2	560.1	604.5	580.7	611.0	4.7	0.926	1.000	0.961	0.008	0.917	0.989	0.950	0.008
	12	51.1	26.5	92.3	632.0	583.7	585.0	587.1	9.0	1.083	1.000	1.002	0.015	1.076	0.994	0.996	0.015
C5H008	88	9.3	19.1	51.2	472.3	478.4	478.4	471.1	22.4	0.987	1.000	1.000	0.047	1.003	1.015	1.015	0.048
	56	11.4	29.4	68.8	336.0	346.0	346.0	347.4	10.0	0.971	1.000	1.000	0.029	0.967	0.996	0.996	0.029
	5	11.9	19.1	76.0	539.0	578.0	578.0	578.8	2.0	0.933	1.000	1.000	0.003	0.931	0.999	0.999	0.003

Table A.3: Continued

Sub-catchment	Event #	Q_P (m^3/s)	L (km)	S_e (%)	T_C [a] (h)	T_C [b] & T_L [a/b] (h)	T_C [c] (h)	T_L [c] (h)	T_C [d] (h)	TPPR 1	TPPR 2	TPPR 3	TPPR 4	TPPR 5	TPPR 6	TPPR 7	TPPR 8
C5H008	70	12.4	19.1	43.9	304.0	338.0	338.0	339.6	2.0	0.899	1.000	1.000	0.006	0.895	0.995	0.995	0.006
	66	12.4	29.4	47.2	658.5	652.5	652.5	654.7	4.5	1.009	1.000	1.000	0.007	1.006	0.997	0.997	0.007
	65	12.4	19.1	36.3	798.0	794.0	794.0	797.3	2.0	1.005	1.000	1.000	0.003	1.001	0.996	0.996	0.003
	33	12.4	8.8	40.3	705.0	721.0	721.0	722.4	1.0	0.978	1.000	1.000	0.001	0.976	0.998	0.998	0.001
	87	12.6	19.1	36.3	537.1	535.7	535.7	535.9	7.7	1.003	1.000	1.000	0.014	1.002	1.000	1.000	0.014
	32	13.4	29.4	23.7	138.0	129.0	129.0	134.2	9.0	1.070	1.000	1.000	0.070	1.028	0.961	0.961	0.067
	89	13.5	19.1	51.4	577.7	577.1	577.1	580.0	1.1	1.001	1.000	1.000	0.002	0.996	0.995	0.995	0.002
	50	15.4	11.8	33.5	246.0	266.0	266.0	269.1	2.0	0.925	1.000	1.000	0.008	0.914	0.988	0.988	0.007
	96	16.1	19.1	51.1	366.8	363.0	363.0	366.0	3.0	1.010	1.000	1.000	0.008	1.002	0.992	0.992	0.008
	19	16.5	11.8	46.8	882.0	867.0	867.0	873.2	3.0	1.017	1.000	1.000	0.003	1.010	0.993	0.993	0.003
	98	17.4	19.1	51.1	242.6	218.8	218.8	226.4	2.8	1.109	1.000	1.000	0.013	1.071	0.966	0.966	0.012
	54	17.6	19.1	57.5	385.0	389.0	389.0	391.6	5.0	0.990	1.000	1.000	0.013	0.983	0.993	0.993	0.013
	46	17.6	19.1	68.3	760.0	774.0	774.0	775.8	6.0	0.982	1.000	1.000	0.008	0.980	0.998	0.998	0.008
	29	18.7	29.4	92.0	448.0	466.0	466.0	469.3	10.0	0.961	1.000	1.000	0.021	0.955	0.993	0.993	0.021
	86	19.4	19.1	61.4	456.0	432.0	432.0	386.8	120.0	1.056	1.000	1.000	0.278	1.179	1.117	1.117	0.310
	85	19.9	29.4	51.1	847.0	677.0	677.0	696.8	5.0	1.251	1.000	1.000	0.007	1.215	0.972	0.972	0.007
	82	20.4	19.1	36.3	419.0	366.0	366.0	366.9	6.0	1.145	1.000	1.000	0.016	1.142	0.997	0.997	0.016
	60	24.5	8.8	57.5	496.0	506.0	506.0	509.5	2.0	0.980	1.000	1.000	0.004	0.973	0.993	0.993	0.004
	95	24.5	19.1	73.2	165.0	165.7	174.9	168.7	6.9	0.996	1.000	1.056	0.042	0.978	0.982	1.037	0.041
	106	24.7	19.1	42.0	155.7	145.2	127.4	150.1	7.4	1.072	1.000	0.878	0.051	1.037	0.967	0.849	0.049
	27	25.7	19.1	82.2	600.0	628.0	628.0	628.7	4.0	0.955	1.000	1.000	0.006	0.954	0.999	0.999	0.006
	97	28.2	19.1	65.6	239.0	246.8	246.8	249.2	6.8	0.968	1.000	1.000	0.028	0.959	0.990	0.990	0.027
	7	29.4	32.7	86.5	800.0	819.0	819.0	821.2	3.0	0.977	1.000	1.000	0.004	0.974	0.997	0.997	0.004
	35	32.0	11.8	40.9	104.0	124.0	124.0	124.7	4.0	0.839	1.000	1.000	0.032	0.834	0.994	0.994	0.032
	17	33.3	29.4	55.7	902.0	914.0	914.0	915.8	2.0	0.987	1.000	1.000	0.002	0.985	0.998	0.998	0.002

Table A.3: Continued

Sub-catchment	Event #	Q_P (m^3/s)	L (km)	S_e (%)	T_C [a] (h)	T_C [b] & T_L [a/b] (h)	T_C [c] (h)	T_L [c] (h)	T_C [d] (h)	TPPR 1	TPPR 2	TPPR 3	TPPR 4	TPPR 5	TPPR 6	TPPR 7	TPPR 8
C5H008	83	34.5	29.4	51.1	459.0	418.0	418.0	420.5	10.0	1.098	1.000	1.000	0.024	1.092	0.994	0.994	0.024
	41	34.6	29.4	93.5	258.0	266.0	266.0	269.2	2.0	0.970	1.000	1.000	0.008	0.959	0.988	0.988	0.007
	23	34.6	29.4	57.2	632.0	626.0	626.0	631.7	2.0	1.010	1.000	1.000	0.003	1.000	0.991	0.991	0.003
	22	34.6	29.4	67.7	488.0	508.0	508.0	511.0	4.0	0.961	1.000	1.000	0.008	0.955	0.994	0.994	0.008
	71	35.9	29.4	51.1	472.0	482.0	482.0	482.6	2.0	0.979	1.000	1.000	0.004	0.978	0.999	0.999	0.004
	36	35.9	29.4	69.9	596.0	630.0	630.0	629.9	6.0	0.946	1.000	1.000	0.010	0.946	1.000	1.000	0.010
	28	35.9	29.4	89.7	696.0	720.2	724.0	723.9	4.0	0.966	1.000	1.005	0.006	0.961	0.995	1.000	0.006
	55	37.3	29.4	57.5	414.0	434.0	434.0	434.5	2.0	0.954	1.000	1.000	0.005	0.953	0.999	0.999	0.005
	14	37.3	25.8	92.5	698.0	742.0	742.0	738.9	22.0	0.941	1.000	1.000	0.030	0.945	1.004	1.004	0.030
	111	37.7	19.1	77.6	166.7	191.9	204.9	197.4	12.9	0.869	1.000	1.068	0.067	0.844	0.972	1.038	0.065
	84	39.6	19.1	61.2	385.0	299.0	299.0	315.3	11.0	1.288	1.000	1.000	0.037	1.221	0.948	0.948	0.035
	79	42.2	19.1	73.4	277.0	288.5	295.0	289.1	7.0	0.960	1.000	1.022	0.024	0.958	0.998	1.020	0.024
	61	44.3	19.1	73.7	662.0	652.7	662.0	657.6	14.0	1.014	1.000	1.014	0.021	1.007	0.992	1.007	0.021
	73	49.4	29.4	50.2	365.0	382.6	386.0	382.1	26.0	0.954	1.000	1.009	0.068	0.955	1.001	1.010	0.068
	49	50.2	11.8	44.8	232.0	242.8	242.0	243.8	2.0	0.956	1.000	0.997	0.008	0.952	0.996	0.993	0.008
	16	56.2	8.8	96.7	732.0	746.0	746.0	747.9	2.0	0.981	1.000	1.000	0.003	0.979	0.997	0.997	0.003
	80	56.3	19.1	86.3	335.0	333.6	326.0	335.9	14.0	1.004	1.000	0.977	0.042	0.997	0.993	0.970	0.042
	105	60.5	19.1	65.1	294.9	272.4	272.4	274.4	8.4	1.083	1.000	1.000	0.031	1.075	0.993	0.993	0.031
	62	67.7	8.8	75.3	304.0	322.9	314.0	326.2	2.0	0.941	1.000	0.972	0.006	0.932	0.990	0.963	0.006
	78	70.5	19.1	98.2	507.0	531.6	531.6	535.0	3.6	0.954	1.000	1.000	0.007	0.948	0.994	0.994	0.007
	53	75.0	29.4	48.3	581.0	636.9	625.0	640.3	1.0	0.912	1.000	0.981	0.002	0.907	0.995	0.976	0.002
	69	77.9	29.4	80.0	414.0	429.9	410.0	430.6	2.0	0.963	1.000	0.954	0.005	0.961	0.998	0.952	0.005
	26	84.9	29.4	93.5	196.0	199.0	199.0	200.4	7.0	0.985	1.000	1.000	0.035	0.978	0.993	0.993	0.035
	4	86.3	29.4	79.2	223.0	252.3	254.0	251.1	14.0	0.884	1.000	1.007	0.056	0.888	1.005	1.012	0.056
	59	87.6	29.4	48.5	288.0	304.2	322.0	307.2	10.0	0.947	1.000	1.058	0.033	0.937	0.990	1.048	0.033

Table A.3: Continued

Sub-catchment	Event #	Q_P (m^3/s)	L (km)	S_e (%)	T_C [a] (h)	T_C [b] & T_L [a/b] (h)	T_C [c] (h)	T_L [c] (h)	T_C [d] (h)	TPPR 1	TPPR 2	TPPR 3	TPPR 4	TPPR 5	TPPR 6	TPPR 7	TPPR 8
C5H008	34	99.0	19.1	99.4	310.0	336.0	315.0	337.3	3.0	0.923	1.000	0.938	0.009	0.919	0.996	0.934	0.009
	3	99.0	29.4	61.6	138.0	146.0	146.0	147.3	2.0	0.945	1.000	1.000	0.014	0.937	0.991	0.991	0.014
	42	104.6	29.4	89.5	248.0	252.0	252.0	254.4	12.0	0.984	1.000	1.000	0.048	0.975	0.991	0.991	0.047
	13	104.6	11.8	99.9	74.0	75.0	75.0	77.2	3.0	0.987	1.000	1.000	0.040	0.958	0.971	0.971	0.039
	8	105.6	11.8	83.5	320.0	360.4	340.0	359.2	28.0	0.888	1.000	0.943	0.078	0.891	1.003	0.947	0.078
C5H009	3	4.2	18.3	72.7	587.4	496.2	496.2	500.7	16.2	1.184	1.000	1.000	0.033	1.173	0.991	0.991	0.032
	11	6.8	18.3	72.7	298.5	247.6	247.6	250.4	7.6	1.206	1.000	1.000	0.031	1.192	0.989	0.989	0.030
	10	17.4	18.3	72.7	537.4	497.1	497.1	504.9	17.1	1.081	1.000	1.000	0.034	1.064	0.985	0.985	0.034
	8	31.3	18.3	72.7	307.5	289.2	289.2	288.0	25.2	1.063	1.000	1.000	0.087	1.068	1.004	1.004	0.088
C5H012	13	7.2	38.1	9.4	1014.4	1009.7	1009.7	1011.4	1.7	1.005	1.000	1.000	0.002	1.003	0.998	0.998	0.002
	8	8.3	38.1	35.9	442.0	357.8	352.7	358.0	16.7	1.235	1.000	0.986	0.047	1.235	1.000	0.985	0.047
	44	10.5	54.8	12.3	451.8	557.7	553.8	561.1	1.8	0.810	1.000	0.993	0.003	0.805	0.994	0.987	0.003
	6	18.0	9.2	18.2	124.3	122.0	122.0	125.3	2.0	1.019	1.000	1.000	0.016	0.992	0.974	0.974	0.016
	22	50.5	9.2	23.7	233.7	285.5	248.6	286.7	8.6	0.818	1.000	0.871	0.030	0.815	0.996	0.867	0.030
	7	89.1	9.2	34.4	138.2	123.0	123.0	126.0	3.0	1.124	1.000	1.000	0.024	1.096	0.976	0.976	0.024
C5H014	12	22.9	133.4	8.9	1116.6	1110.8	1110.8	1114.2	6.8	1.005	1.000	1.000	0.006	1.002	0.997	0.997	0.006
	4	24.8	98.5	30.9	790.5	792.9	786.3	842.8	18.3	0.997	1.000	0.992	0.023	0.938	0.941	0.933	0.022
	16	27.9	132.6	17.9	318.4	287.2	286.0	297.3	22.0	1.109	1.000	0.996	0.077	1.071	0.966	0.962	0.074
	5	114.6	8.4	28.2	901.0	666.5	655.1	715.6	79.1	1.352	1.000	0.983	0.119	1.259	0.931	0.915	0.111
	10	117.6	121.1	23.3	586.3	520.7	520.7	529.8	16.7	1.126	1.000	1.000	0.032	1.107	0.983	0.983	0.032
	6	143.8	10.4	35.7	355.6	389.3	511.9	440.0	55.9	0.913	1.000	1.315	0.144	0.808	0.885	1.163	0.127
	14	144.1	150.4	21.3	112.2	120.4	115.0	123.2	19.0	0.932	1.000	0.955	0.158	0.911	0.977	0.933	0.154
	2	288.2	150.4	52.5	324.3	254.6	249.1	270.4	33.1	1.274	1.000	0.978	0.130	1.200	0.942	0.921	0.122
C5H015	58	22.1	32.3	38.0	864.0	864.0	864.0	872.4	24.0	1.000	1.000	1.000	0.028	0.990	0.990	0.990	0.028
	2	25.7	73.0	59.4	512.0	560.0	560.0	565.8	8.0	0.914	1.000	1.000	0.014	0.905	0.990	0.990	0.014
	30	28.4	31.6	26.5	366.0	366.0	366.0	366.5	6.0	1.000	1.000	1.000	0.016	0.999	0.999	0.999	0.016

Table A.3: Continued

Sub-catchment	Event #	Q_P (m^3/s)	L (km)	S_e (%)	T_C [a] (h)	T_C [b] & T_L [a/b] (h)	T_C [c] (h)	T_L [c] (h)	T_C [d] (h)	TPPR 1	TPPR 2	TPPR 3	TPPR 4	TPPR 5	TPPR 6	TPPR 7	TPPR 8
C5H015	29	28.4	59.6	40.8	870.0	896.2	896.2	899.0	8.2	0.971	1.000	1.000	0.009	0.968	0.997	0.997	0.009
	33	40.0	60.5	53.5	384.0	418.7	410.0	425.9	26.0	0.917	1.000	0.979	0.062	0.902	0.983	0.963	0.061
	21	40.6	58.8	58.0	516.0	379.5	386.0	397.2	26.0	1.360	1.000	1.017	0.069	1.299	0.955	0.972	0.065
	92	41.3	26.9	39.1	685.4	595.5	603.6	601.9	27.6	1.151	1.000	1.014	0.046	1.139	0.989	1.003	0.046
	81	45.8	54.3	45.3	481.7	512.8	512.8	515.0	8.8	0.939	1.000	1.000	0.017	0.935	0.996	0.996	0.017
	72	48.1	73.0	60.4	582.9	536.8	525.1	543.2	21.1	1.086	1.000	0.978	0.039	1.073	0.988	0.967	0.039
	24	50.8	92.8	59.2	796.0	765.0	765.0	780.5	21.0	1.041	1.000	1.000	0.027	1.020	0.980	0.980	0.027
	34	59.3	37.6	38.4	402.0	378.4	387.0	382.7	27.0	1.062	1.000	1.023	0.071	1.050	0.989	1.011	0.071
	36	65.5	22.5	52.5	336.0	363.6	354.0	370.4	18.0	0.924	1.000	0.974	0.050	0.907	0.982	0.956	0.049
	11	67.3	19.5	72.6	782.0	751.5	746.0	736.9	74.0	1.041	1.000	0.993	0.098	1.061	1.020	1.012	0.100
	64	68.2	32.3	45.0	786.8	704.4	699.7	754.1	3.7	1.117	1.000	0.993	0.005	1.043	0.934	0.928	0.005
	57	70.9	31.6	81.0	389.0	431.0	485.0	439.0	53.0	0.903	1.000	1.125	0.123	0.886	0.982	1.105	0.121
	44	85.2	31.6	67.1	342.0	397.7	389.0	367.9	77.0	0.860	1.000	0.978	0.194	0.930	1.081	1.057	0.209
	83	85.5	26.9	56.8	594.5	679.8	660.3	652.5	84.3	0.875	1.000	0.971	0.124	0.911	1.042	1.012	0.129
	17	88.3	73.0	63.8	228.0	166.0	166.0	185.7	22.0	1.373	1.000	1.000	0.133	1.228	0.894	0.894	0.118
	68	89.2	84.7	44.5	718.2	732.3	736.5	743.3	16.5	0.981	1.000	1.006	0.023	0.966	0.985	0.991	0.022
	3	97.3	41.6	62.3	368.0	364.0	364.0	380.0	4.0	1.011	1.000	1.000	0.011	0.968	0.958	0.958	0.011
	59	110.4	35.1	64.7	456.0	493.2	533.0	543.5	5.0	0.925	1.000	1.081	0.010	0.839	0.907	0.981	0.009
	49	110.4	31.6	56.6	571.0	516.4	456.0	519.7	48.0	1.106	1.000	0.883	0.093	1.099	0.994	0.877	0.092
	14	117.5	49.2	93.1	788.0	830.0	830.0	822.8	86.0	0.949	1.000	1.000	0.104	0.958	1.009	1.009	0.105
	4	117.5	82.5	94.5	651.0	634.0	634.0	630.1	34.0	1.027	1.000	1.000	0.054	1.033	1.006	1.006	0.054
	54	120.9	60.5	60.0	1008.0	984.0	984.0	989.6	24.0	1.024	1.000	1.000	0.024	1.019	0.994	0.994	0.024
	48	138.0	49.0	65.7	876.0	642.0	642.0	651.2	66.0	1.364	1.000	1.000	0.103	1.345	0.986	0.986	0.101
	91	141.9	26.7	75.7	496.7	522.3	522.3	506.6	42.3	0.951	1.000	1.000	0.081	0.981	1.031	1.031	0.084
	12	143.1	98.4	64.0	576.0	528.8	516.0	537.2	36.0	1.089	1.000	0.976	0.068	1.072	0.984	0.960	0.067

Table A.3: Continued

Sub-catchment	Event #	Q_P (m^3/s)	L (km)	S_e (%)	T_C [a] (h)	T_C [b] & T_L [a/b] (h)	T_C [c] (h)	T_L [c] (h)	T_C [d] (h)	TPPR 1	TPPR 2	TPPR 3	TPPR 4	TPPR 5	TPPR 6	TPPR 7	TPPR 8
C5H015	53	150.2	35.4	86.4	960.0	953.8	963.0	953.4	75.0	1.006	1.000	1.010	0.079	1.007	1.000	1.010	0.079
	31	150.2	10.3	92.2	438.0	416.0	416.0	422.7	8.0	1.053	1.000	1.000	0.019	1.036	0.984	0.984	0.019
	80	153.9	92.1	55.7	256.4	207.9	205.7	212.9	13.7	1.233	1.000	0.990	0.066	1.204	0.976	0.966	0.064
	66	157.6	59.6	85.5	753.2	797.9	797.9	798.5	29.9	0.944	1.000	1.000	0.037	0.943	0.999	0.999	0.037
	15	182.5	41.6	77.2	797.0	839.3	833.0	848.2	17.0	0.950	1.000	0.992	0.020	0.940	0.989	0.982	0.020
	87	184.6	84.7	60.5	164.9	107.5	107.5	113.2	11.5	1.534	1.000	1.000	0.107	1.457	0.950	0.950	0.102
	20	198.3	84.7	62.0	474.0	443.9	447.0	474.4	15.0	1.068	1.000	1.007	0.034	0.999	0.936	0.942	0.032
	7	203.3	82.5	68.7	566.0	509.0	509.0	517.4	5.0	1.112	1.000	1.000	0.010	1.094	0.984	0.984	0.010
	10	221.3	31.6	73.7	178.0	186.0	176.0	196.1	8.0	0.957	1.000	0.946	0.043	0.908	0.948	0.897	0.041
	43	249.0	92.8	43.1	456.0	444.8	440.0	444.2	32.0	1.025	1.000	0.989	0.072	1.026	1.001	0.990	0.072
	42	249.0	59.6	55.5	744.0	707.7	711.0	723.1	87.0	1.051	1.000	1.005	0.123	1.029	0.979	0.983	0.120
	40	255.0	31.6	73.6	438.0	427.8	422.0	439.0	14.0	1.024	1.000	0.986	0.033	0.998	0.974	0.961	0.032
	78	272.3	100.8	61.0	802.0	855.8	848.7	864.9	32.7	0.937	1.000	0.992	0.038	0.927	0.989	0.981	0.038
	63	285.9	100.8	89.5	905.0	935.5	935.5	906.5	143.5	0.967	1.000	1.000	0.153	0.998	1.032	1.032	0.158
	26	295.2	84.8	61.6	574.0	606.0	606.0	608.0	6.0	0.947	1.000	1.000	0.010	0.944	0.997	0.997	0.010
	8	331.2	60.5	90.6	287.0	322.7	322.0	327.3	10.0	0.890	1.000	0.998	0.031	0.877	0.986	0.984	0.031
	25	353.3	84.7	83.3	258.0	240.0	240.0	255.1	24.0	1.075	1.000	1.000	0.100	1.012	0.941	0.941	0.094
	55	356.9	73.0	89.5	312.0	344.4	342.0	340.0	54.0	0.906	1.000	0.993	0.157	0.918	1.013	1.006	0.159
	46	356.9	22.5	88.8	720.0	690.5	672.0	697.1	24.0	1.043	1.000	0.973	0.035	1.033	0.991	0.964	0.034
	45	407.7	6.4	89.8	648.0	689.9	688.0	687.3	40.0	0.939	1.000	0.997	0.058	0.943	1.004	1.001	0.058
	50	523.8	49.0	88.0	240.0	266.6	259.0	268.2	43.0	0.900	1.000	0.972	0.161	0.895	0.994	0.966	0.160
	38	589.3	74.6	98.5	408.0	409.4	401.0	409.0	41.0	0.997	1.000	0.979	0.100	0.997	1.001	0.980	0.100
C5H016	80	10.3	185.1	20.6	739.8	745.7	745.7	748.2	1.7	0.992	1.000	1.000	0.002	0.989	0.997	0.997	0.002
	101	10.5	251.8	5.7	182.9	209.0	198.3	208.6	6.3	0.875	1.000	0.949	0.030	0.877	1.002	0.951	0.030
	99	11.1	240.8	7.4	159.7	173.5	173.5	173.5	5.5	0.920	1.000	1.000	0.032	0.920	1.000	1.000	0.032

Table A.3: Continued

Sub-catchment	Event #	Q_P (m^3/s)	L (km)	S_e (%)	T_C [a] (h)	T_C [b] & T_L [a/b] (h)	T_C [c] (h)	T_L [c] (h)	T_C [d] (h)	TPPR 1	TPPR 2	TPPR 3	TPPR 4	TPPR 5	TPPR 6	TPPR 7	TPPR 8
C5H016	60	12.3	169.7	12.4	861.0	869.8	869.8	873.7	5.8	0.990	1.000	1.000	0.007	0.985	0.996	0.996	0.007
	96	12.4	26.3	17.0	879.5	893.6	893.6	892.7	5.6	0.984	1.000	1.000	0.006	0.985	1.001	1.001	0.006
	47	12.9	93.7	35.0	313.3	317.6	317.6	320.1	5.6	0.986	1.000	1.000	0.018	0.979	0.992	0.992	0.017
	105	13.6	189.8	18.7	825.1	824.8	824.8	826.7	8.8	1.000	1.000	1.000	0.011	0.998	0.998	0.998	0.011
	24	13.8	198.3	17.3	989.3	894.2	894.2	917.5	6.2	1.106	1.000	1.000	0.007	1.078	0.975	0.975	0.007
	71	14.1	192.5	16.9	691.3	677.5	677.5	679.5	5.5	1.020	1.000	1.000	0.008	1.017	0.997	0.997	0.008
	89	15.3	81.9	20.0	522.8	534.4	539.8	520.5	83.8	0.978	1.000	1.010	0.157	1.005	1.027	1.037	0.161
	83	16.4	110.2	21.6	719.3	701.5	701.5	703.6	5.5	1.025	1.000	1.000	0.008	1.022	0.997	0.997	0.008
	73	16.9	37.0	18.8	913.2	964.5	964.5	966.8	4.5	0.947	1.000	1.000	0.005	0.945	0.998	0.998	0.005
	87	17.6	251.8	18.4	874.1	844.3	844.3	847.4	4.3	1.035	1.000	1.000	0.005	1.032	0.996	0.996	0.005
	72	17.8	152.1	6.3	934.7	939.0	963.8	941.5	3.8	0.995	1.000	1.026	0.004	0.993	0.997	1.024	0.004
	100	17.9	235.9	16.2	321.2	340.8	340.8	340.1	52.8	0.942	1.000	1.000	0.155	0.945	1.002	1.002	0.155
	38	19.7	177.1	25.7	668.5	677.2	677.1	682.3	5.1	0.987	1.000	1.000	0.008	0.980	0.992	0.992	0.007
	82	20.4	90.3	20.0	311.6	292.2	292.2	294.8	4.2	1.066	1.000	1.000	0.014	1.057	0.991	0.991	0.014
	84	20.6	189.8	21.1	852.9	866.8	868.3	869.3	4.3	0.984	1.000	1.002	0.005	0.981	0.997	0.999	0.005
	48	20.6	147.4	7.5	558.0	618.1	652.3	620.4	4.3	0.903	1.000	1.055	0.007	0.899	0.996	1.051	0.007
	53	20.8	58.9	23.9	454.7	459.0	459.0	461.1	3.0	0.991	1.000	1.000	0.007	0.986	0.995	0.995	0.007
	51	20.8	243.6	10.4	1053.6	1072.5	1060.7	1073.7	4.7	0.982	1.000	0.989	0.004	0.981	0.999	0.988	0.004
	43	21.3	201.7	17.9	781.2	803.4	803.4	803.4	11.4	0.972	1.000	1.000	0.014	0.972	1.000	1.000	0.014
	69	21.4	54.1	13.2	308.9	355.6	364.1	358.4	4.1	0.869	1.000	1.024	0.012	0.862	0.992	1.016	0.011
	61	24.8	251.8	24.7	366.8	364.0	364.0	366.1	4.0	1.008	1.000	1.000	0.011	1.002	0.994	0.994	0.011
	81	24.9	205.2	27.3	304.5	318.7	318.7	319.6	6.7	0.955	1.000	1.000	0.021	0.953	0.997	0.997	0.021
	86	26.8	163.8	46.6	865.5	847.4	847.4	849.0	7.4	1.021	1.000	1.000	0.009	1.019	0.998	0.998	0.009
	90	27.3	81.9	24.6	454.3	436.1	436.1	439.5	4.1	1.042	1.000	1.000	0.009	1.034	0.992	0.992	0.009
	15	31.9	181.8	50.2	792.0	696.0	696.0	706.8	48.0	1.138	1.000	1.000	0.069	1.120	0.985	0.985	0.068

Table A.3: Continued

Sub-catchment	Event #	Q_P (m^3/s)	L (km)	S_e (%)	T_C [a] (h)	T_C [b] & T_L [a/b] (h)	T_C [c] (h)	T_L [c] (h)	T_C [d] (h)	TPPR 1	TPPR 2	TPPR 3	TPPR 4	TPPR 5	TPPR 6	TPPR 7	TPPR 8
C5H016	34	32.2	211.5	19.8	1386.8	1422.3	1422.3	1421.2	6.3	0.975	1.000	1.000	0.004	0.976	1.001	1.001	0.004
	88	33.6	239.4	16.1	839.8	826.1	822.4	827.5	6.4	1.017	1.000	0.995	0.008	1.015	0.998	0.994	0.008
	75	34.1	177.1	9.3	809.1	742.6	739.1	753.0	19.1	1.090	1.000	0.995	0.026	1.075	0.986	0.982	0.025
	52	34.3	211.5	28.5	654.1	651.4	651.4	654.5	3.4	1.004	1.000	1.000	0.005	0.999	0.995	0.995	0.005
	27	37.4	136.7	23.2	883.0	717.0	710.0	741.1	14.0	1.231	1.000	0.990	0.020	1.192	0.968	0.958	0.019
	68	38.0	189.8	20.6	434.5	436.8	436.8	439.4	4.8	0.995	1.000	1.000	0.011	0.989	0.994	0.994	0.011
	74	40.3	88.3	18.6	754.6	693.4	675.7	701.9	3.7	1.088	1.000	0.975	0.005	1.075	0.988	0.963	0.005
	20	42.3	203.5	51.3	978.2	836.2	836.2	831.0	92.2	1.170	1.000	1.000	0.110	1.177	1.006	1.006	0.111
	29	42.7	203.7	59.0	470.8	443.0	443.0	453.9	11.0	1.063	1.000	1.000	0.025	1.037	0.976	0.976	0.024
	40	55.6	203.7	20.6	272.4	249.8	249.8	252.8	9.8	1.090	1.000	1.000	0.039	1.077	0.988	0.988	0.039
	26	55.9	211.5	29.8	874.9	736.0	747.3	766.1	3.3	1.189	1.000	1.015	0.004	1.142	0.961	0.975	0.004
	39	61.7	240.8	34.1	615.9	650.5	650.5	655.4	26.5	0.947	1.000	1.000	0.041	0.940	0.993	0.993	0.040
	33	62.1	154.7	29.0	751.6	665.5	665.5	662.9	89.5	1.129	1.000	1.000	0.134	1.134	1.004	1.004	0.135
	92	66.1	136.7	36.1	1003.4	800.8	818.0	814.2	266.0	1.253	1.000	1.021	0.332	1.232	0.984	1.005	0.327
	78	67.0	213.2	51.1	482.1	437.4	425.6	387.1	185.6	1.102	1.000	0.973	0.424	1.245	1.130	1.099	0.479
	77	74.7	122.9	29.6	1192.2	1142.7	1149.8	1151.1	21.8	1.043	1.000	1.006	0.019	1.036	0.993	0.999	0.019
	32	76.4	192.5	47.9	912.9	852.8	852.8	848.0	60.8	1.070	1.000	1.000	0.071	1.077	1.006	1.006	0.072
	108	97.9	152.1	22.8	645.0	540.9	540.9	549.5	12.9	1.192	1.000	1.000	0.024	1.174	0.984	0.984	0.023
	91	107.4	136.7	22.5	489.8	358.9	358.9	371.1	94.9	1.365	1.000	1.000	0.264	1.320	0.967	0.967	0.256
	21	113.3	75.5	50.5	1173.3	1107.7	1107.7	1108.0	51.7	1.059	1.000	1.000	0.047	1.059	1.000	1.000	0.047
	106	122.5	189.8	38.8	1058.7	931.9	943.1	975.5	31.1	1.136	1.000	1.012	0.033	1.085	0.955	0.967	0.032
	4	132.2	169.7	35.3	985.0	853.0	770.0	857.3	26.0	1.155	1.000	0.903	0.030	1.149	0.995	0.898	0.030
	37	147.8	154.7	29.8	220.9	244.2	244.2	242.7	28.2	0.905	1.000	1.000	0.115	0.910	1.006	1.006	0.116
	30	166.4	179.0	60.5	729.0	748.7	748.7	745.5	28.7	0.974	1.000	1.000	0.038	0.978	1.004	1.004	0.038
	41	174.3	239.1	60.9	395.2	408.7	408.7	382.8	96.7	0.967	1.000	1.000	0.237	1.032	1.068	1.068	0.253

Table A.3: Continued

Sub-catchment	Event #	Q_P (m^3/s)	L (km)	S_e (%)	T_C [a] (h)	T_C [b] & T_L [a/b] (h)	T_C [c] (h)	T_L [c] (h)	T_C [d] (h)	TPPR 1	TPPR 2	TPPR 3	TPPR 4	TPPR 5	TPPR 6	TPPR 7	TPPR 8
C5H016	63	187.1	152.1	61.4	401.4	343.0	320.2	289.3	272.2	1.170	1.000	0.934	0.794	1.387	1.186	1.107	0.941
	17	190.1	203.7	14.8	672.0	633.4	624.0	654.6	24.0	1.061	1.000	0.985	0.038	1.027	0.968	0.953	0.037
	56	196.9	136.7	38.0	353.8	321.0	321.0	328.0	57.0	1.102	1.000	1.000	0.178	1.079	0.979	0.979	0.174
	12	217.2	46.6	59.9	552.0	468.0	468.0	479.2	108.0	1.179	1.000	1.000	0.231	1.152	0.977	0.977	0.225
	35	219.3	185.1	45.9	796.6	834.1	838.2	832.1	22.2	0.955	1.000	1.005	0.027	0.957	1.002	1.007	0.027
	95	277.2	70.6	42.0	793.8	674.5	669.9	697.6	117.9	1.177	1.000	0.993	0.175	1.138	0.967	0.960	0.169
	31	278.9	192.5	49.3	617.7	668.1	675.3	646.4	147.3	0.925	1.000	1.011	0.220	0.956	1.033	1.045	0.228
	93	328.1	201.8	55.6	1215.7	1108.6	1074.4	1119.6	114.4	1.097	1.000	0.969	0.103	1.086	0.990	0.960	0.102
	65	385.9	146.0	61.9	676.2	526.5	527.9	536.1	119.9	1.284	1.000	1.003	0.228	1.261	0.982	0.985	0.224
	2	420.4	57.9	42.3	514.0	507.4	502.0	497.8	70.0	1.013	1.000	0.989	0.138	1.032	1.019	1.008	0.141
	22	553.9	37.0	45.7	460.7	481.7	459.0	477.1	75.0	0.956	1.000	0.953	0.156	0.966	1.010	0.962	0.157
	23	844.0	203.5	87.8	583.1	706.2	686.6	697.9	62.6	0.826	1.000	0.972	0.089	0.836	1.012	0.984	0.090
C5H018	78	31.3	165.0	24.6	557.2	373.4	382.3	362.7	118.3	1.492	1.000	1.024	0.317	1.536	1.030	1.054	0.326
	43	32.2	142.2	54.0	578.2	384.1	340.3	433.8	28.3	1.505	1.000	0.886	0.074	1.333	0.885	0.785	0.065
	52	33.6	77.5	16.3	825.8	867.6	867.6	868.2	3.6	0.952	1.000	1.000	0.004	0.951	0.999	0.999	0.004
	21	36.8	94.5	41.2	99.0	83.0	83.0	91.0	11.0	1.193	1.000	1.000	0.133	1.088	0.912	0.912	0.121
	4	36.8	174.6	53.0	145.0	101.0	101.0	111.1	5.0	1.436	1.000	1.000	0.050	1.305	0.909	0.909	0.045
	23	38.3	142.2	37.4	568.0	673.5	664.0	657.2	40.0	0.843	1.000	0.986	0.059	0.864	1.025	1.010	0.061
	66	38.6	128.6	15.7	782.8	795.8	795.8	798.0	3.8	0.984	1.000	1.000	0.005	0.981	0.997	0.997	0.005
	1	39.9	181.7	37.3	716.0	662.7	672.0	663.8	48.0	1.080	1.000	1.014	0.072	1.079	0.998	1.012	0.072
	35	42.9	130.0	19.5	855.4	857.3	857.3	848.1	17.3	0.998	1.000	1.000	0.020	1.009	1.011	1.011	0.020
	6	43.5	159.6	28.1	403.0	404.1	395.0	414.6	11.0	0.997	1.000	0.978	0.027	0.972	0.975	0.953	0.027
	53	44.8	1.0	33.9	563.6	558.1	558.1	560.3	6.1	1.010	1.000	1.000	0.011	1.006	0.996	0.996	0.011
	48	50.1	202.3	22.8	213.5	199.5	199.5	200.2	7.5	1.070	1.000	1.000	0.038	1.067	0.997	0.997	0.037
	61	52.8	50.5	23.0	820.6	841.7	845.1	843.0	5.1	0.975	1.000	1.004	0.006	0.973	0.999	1.002	0.006

Table A.3: Continued

Sub-catchment	Event #	Q_P (m^3/s)	L (km)	S_e (%)	T_C [a] (h)	T_C [b] & T_L [a/b] (h)	T_C [c] (h)	T_L [c] (h)	T_C [d] (h)	TPPR 1	TPPR 2	TPPR 3	TPPR 4	TPPR 5	TPPR 6	TPPR 7	TPPR 8
C5H018	64	52.9	77.5	30.1	518.9	514.4	514.4	513.6	10.4	1.009	1.000	1.000	0.020	1.010	1.002	1.002	0.020
	47	53.1	128.6	41.1	1690.0	1455.7	1443.8	1483.9	3.8	1.161	1.000	0.992	0.003	1.139	0.981	0.973	0.003
	49	54.0	67.8	16.9	141.8	161.9	151.7	164.3	7.7	0.876	1.000	0.937	0.048	0.863	0.985	0.923	0.047
	45	54.6	50.5	27.8	441.6	445.8	445.8	442.7	13.8	0.991	1.000	1.000	0.031	0.997	1.007	1.007	0.031
	59	55.7	212.0	32.0	675.3	677.4	677.4	678.7	5.4	0.997	1.000	1.000	0.008	0.995	0.998	0.998	0.008
	60	56.0	203.9	35.8	286.5	306.5	306.5	302.3	18.5	0.935	1.000	1.000	0.060	0.948	1.014	1.014	0.061
	71	59.0	196.1	39.6	1154.3	1173.9	1176.1	1169.2	24.1	0.983	1.000	1.002	0.021	0.987	1.004	1.006	0.021
	5	59.2	7.3	55.5	1046.0	870.0	870.0	881.3	6.0	1.202	1.000	1.000	0.007	1.187	0.987	0.987	0.007
	57	59.3	196.1	34.4	626.7	631.5	631.5	632.5	7.5	0.992	1.000	1.000	0.012	0.991	0.998	0.998	0.012
	34	60.0	75.7	44.2	895.8	784.9	789.5	805.6	45.5	1.141	1.000	1.006	0.058	1.112	0.974	0.980	0.056
	36	60.8	212.0	40.1	348.8	367.0	367.0	369.1	7.0	0.950	1.000	1.000	0.019	0.945	0.994	0.994	0.019
	56	61.1	180.3	34.7	242.8	223.0	223.0	223.4	7.0	1.089	1.000	1.000	0.031	1.087	0.998	0.998	0.031
	69	61.2	83.6	48.2	723.8	711.1	711.1	711.2	15.1	1.018	1.000	1.000	0.021	1.018	1.000	1.000	0.021
	58	61.7	146.6	39.3	781.6	800.8	800.8	803.8	8.8	0.976	1.000	1.000	0.011	0.972	0.996	0.996	0.011
	73	62.0	1.0	37.1	292.3	264.6	275.9	264.9	11.9	1.105	1.000	1.043	0.045	1.103	0.999	1.041	0.045
	72	62.3	141.9	50.9	665.4	679.3	679.3	685.1	7.3	0.980	1.000	1.000	0.011	0.971	0.991	0.991	0.011
	63	62.5	50.5	36.3	425.6	416.9	416.9	417.5	8.9	1.021	1.000	1.000	0.021	1.020	0.999	0.999	0.021
	24	62.8	202.3	46.2	754.5	642.5	642.5	660.5	18.5	1.174	1.000	1.000	0.029	1.142	0.973	0.973	0.028
	50	62.9	36.7	46.4	163.8	153.0	153.0	153.5	9.0	1.071	1.000	1.000	0.059	1.067	0.997	0.997	0.059
	70	64.2	128.6	18.9	725.9	719.7	727.8	722.6	7.8	1.009	1.000	1.011	0.011	1.005	0.996	1.007	0.011
	74	66.9	44.3	32.3	440.5	420.2	420.2	423.3	12.2	1.048	1.000	1.000	0.029	1.041	0.993	0.993	0.029
	22	68.7	114.9	41.2	240.0	176.0	176.0	193.7	32.0	1.364	1.000	1.000	0.182	1.239	0.909	0.909	0.165
	67	69.3	124.0	61.1	664.0	645.8	645.8	640.4	21.8	1.028	1.000	1.000	0.034	1.037	1.008	1.008	0.034
	19	69.7	31.5	40.8	1176.0	909.6	904.0	943.0	88.0	1.293	1.000	0.994	0.097	1.247	0.965	0.959	0.093
	11	85.6	175.3	38.3	740.0	721.6	732.0	736.2	12.0	1.025	1.000	1.014	0.017	1.005	0.980	0.994	0.016

Table A.3: Continued

Sub-catchment	Event #	Q_P (m^3/s)	L (km)	S_e (%)	T_C [a] (h)	T_C [b] & T_L [a/b] (h)	T_C [c] (h)	T_L [c] (h)	T_C [d] (h)	TPPR 1	TPPR 2	TPPR 3	TPPR 4	TPPR 5	TPPR 6	TPPR 7	TPPR 8
C5H018	18	87.9	77.5	72.5	744.0	480.0	480.0	502.0	24.0	1.550	1.000	1.000	0.050	1.482	0.956	0.956	0.048
	2	87.9	159.6	43.9	384.0	352.8	356.0	351.5	116.0	1.089	1.000	1.009	0.329	1.092	1.004	1.013	0.330
	80	89.1	180.3	54.8	1033.5	985.7	985.7	1000.5	97.7	1.048	1.000	1.000	0.099	1.033	0.985	0.985	0.098
	25	91.5	199.5	67.4	96.0	60.5	60.5	74.1	84.5	1.587	1.000	1.000	1.397	1.295	0.816	0.816	1.140
	82	100.2	7.3	42.2	997.5	855.9	979.7	909.9	19.7	1.165	1.000	1.145	0.023	1.096	0.941	1.077	0.022
	51	101.3	128.6	39.0	485.3	484.0	484.0	485.3	4.0	1.003	1.000	1.000	0.008	1.000	0.997	0.997	0.008
	79	118.4	1.0	65.5	1270.5	1066.7	1065.6	1100.6	249.6	1.191	1.000	0.999	0.234	1.154	0.969	0.968	0.227
	7	119.2	170.3	47.7	745.0	694.0	697.0	694.9	49.0	1.074	1.000	1.004	0.071	1.072	0.999	1.003	0.071
	83	144.1	141.9	46.4	1014.9	1019.4	1008.2	982.2	120.2	0.996	1.000	0.989	0.118	1.033	1.038	1.026	0.122
	3	152.7	199.5	79.2	172.0	148.0	148.0	146.5	28.0	1.162	1.000	1.000	0.189	1.174	1.010	1.010	0.191
	38	156.9	199.5	64.0	1211.1	1071.6	1060.1	1018.9	292.1	1.130	1.000	0.989	0.273	1.189	1.052	1.040	0.287
	17	210.8	153.3	63.5	646.0	628.5	638.0	612.4	62.0	1.028	1.000	1.015	0.099	1.055	1.026	1.042	0.101
	40	237.9	36.7	64.7	595.1	542.0	535.2	536.5	103.2	1.098	1.000	0.987	0.190	1.109	1.010	0.998	0.192
	8	261.9	94.5	78.7	584.0	768.8	792.0	669.0	240.0	0.760	1.000	1.030	0.312	0.873	1.149	1.184	0.359
	81	285.0	82.2	59.5	304.7	229.9	225.0	243.4	57.0	1.325	1.000	0.979	0.248	1.252	0.945	0.924	0.234
	30	319.1	94.5	94.8	1344.0	925.3	816.0	1136.5	120.0	1.452	1.000	0.882	0.130	1.183	0.814	0.718	0.106
	77	323.8	180.3	55.3	416.1	425.0	436.2	411.4	100.2	0.979	1.000	1.026	0.236	1.011	1.033	1.060	0.244
	9	330.5	30.5	90.6	578.5	671.8	662.5	652.1	62.5	0.861	1.000	0.986	0.093	0.887	1.030	1.016	0.096
	39	379.0	196.1	73.8	984.7	938.0	916.3	927.0	172.3	1.050	1.000	0.977	0.184	1.062	1.012	0.988	0.186
	12	395.6	3.8	50.8	356.0	432.0	432.0	429.8	24.0	0.824	1.000	1.000	0.056	0.828	1.005	1.005	0.056
	76	698.0	117.4	64.1	127.4	121.3	121.0	109.7	97.0	1.050	1.000	0.997	0.800	1.161	1.106	1.103	0.884
C5H035	5	10.6	95.0	20.8	463.9	490.8	510.4	493.3	6.4	0.945	1.000	1.040	0.013	0.940	0.995	1.035	0.013
	14	11.0	171.3	9.3	457.9	443.9	436.5	447.0	4.5	1.031	1.000	0.983	0.010	1.024	0.993	0.977	0.010
	17	11.8	8.5	15.1	477.9	484.7	484.7	486.6	4.7	0.986	1.000	1.000	0.010	0.982	0.996	0.996	0.010
	23	12.1	212.6	11.8	347.8	364.4	364.4	366.3	4.4	0.954	1.000	1.000	0.012	0.950	0.995	0.995	0.012

Table A.3: Continued

Sub-catchment	Event #	Q_P (m^3/s)	L (km)	S_e (%)	T_C [a] (h)	T_C [b] & T_L [a/b] (h)	T_C [c] (h)	T_L [c] (h)	T_C [d] (h)	TPPR 1	TPPR 2	TPPR 3	TPPR 4	TPPR 5	TPPR 6	TPPR 7	TPPR 8
C5H035	2	12.1	76.1	28.7	187.8	128.0	128.0	142.3	8.0	1.467	1.000	1.000	0.063	1.320	0.899	0.899	0.056
	8	12.1	142.1	21.3	198.1	148.3	148.3	155.6	4.3	1.336	1.000	1.000	0.029	1.273	0.953	0.953	0.028
	12	12.6	117.0	13.2	587.1	555.9	555.9	560.6	3.9	1.056	1.000	1.000	0.007	1.047	0.992	0.992	0.007
	3	12.8	196.8	24.2	397.7	339.6	339.6	344.2	3.6	1.171	1.000	1.000	0.011	1.155	0.987	0.987	0.010
	11	15.7	212.6	37.5	616.3	604.9	604.9	610.0	4.9	1.019	1.000	1.000	0.008	1.010	0.992	0.992	0.008
	18	17.8	76.1	7.9	1115.8	1109.8	1109.8	1112.0	5.8	1.005	1.000	1.000	0.005	1.003	0.998	0.998	0.005
	4	18.1	95.0	35.9	933.7	779.4	779.4	784.4	11.4	1.198	1.000	1.000	0.015	1.190	0.994	0.994	0.015
	13	18.7	194.8	16.2	232.4	201.1	201.1	206.3	9.1	1.156	1.000	1.000	0.045	1.126	0.975	0.975	0.044
	24	28.1	82.3	17.4	388.6	376.2	376.2	385.6	40.2	1.033	1.000	1.000	0.107	1.008	0.976	0.976	0.104
	19	30.1	204.6	19.0	950.0	947.6	946.0	948.2	10.0	1.002	1.000	0.998	0.011	1.002	0.999	0.998	0.011
	22	33.7	76.1	21.3	384.2	406.5	398.2	389.2	62.2	0.945	1.000	0.979	0.153	0.987	1.045	1.023	0.160
	25	77.1	95.0	21.3	845.6	942.5	972.6	942.7	12.6	0.897	1.000	1.032	0.013	0.897	1.000	1.032	0.013
	1	110.6	83.9	32.2	688.7	766.2	770.3	750.6	98.3	0.899	1.000	1.005	0.128	0.918	1.021	1.026	0.131
	21	155.3	15.9	33.7	287.2	254.4	238.8	218.1	166.8	1.129	1.000	0.939	0.656	1.317	1.167	1.095	0.765
	15	157.5	117.0	24.9	526.6	520.8	520.8	522.2	16.8	1.011	1.000	1.000	0.032	1.008	0.997	0.997	0.032
	9	178.4	30.3	46.2	174.0	136.4	97.7	177.1	25.7	1.276	1.000	0.716	0.188	0.982	0.770	0.552	0.145
	20	197.5	8.5	27.9	356.8	485.7	498.8	485.8	18.8	0.735	1.000	1.027	0.039	0.734	1.000	1.027	0.039
C5H039	21	29.6	58.0	53.5	446.4	379.2	409.3	439.1	49.3	1.177	1.000	1.079	0.130	1.017	0.864	0.932	0.112
	41	36.0	66.0	56.8	1344.0	1207.8	1200.0	1225.3	120.0	1.113	1.000	0.994	0.099	1.097	0.986	0.979	0.098
	26	49.9	102.8	24.7	627.9	649.2	649.2	649.4	1.2	0.967	1.000	1.000	0.002	0.967	1.000	1.000	0.002
	40	51.0	23.1	44.0	1190.0	1191.9	1191.9	1191.3	39.9	0.998	1.000	1.000	0.033	0.999	1.000	1.000	0.033
	27	65.7	23.1	57.1	922.7	899.3	877.0	909.5	37.0	1.026	1.000	0.975	0.041	1.015	0.989	0.964	0.041
	37	65.9	94.4	52.0	461.1	542.0	553.4	527.2	73.4	0.851	1.000	1.021	0.135	0.875	1.028	1.050	0.139
	38	66.4	89.8	27.8	1066.1	1134.7	1134.7	1128.5	30.7	0.940	1.000	1.000	0.027	0.945	1.006	1.006	0.027
	28	68.1	0.6	34.5	714.4	735.3	735.3	732.0	15.3	0.972	1.000	1.000	0.021	0.976	1.005	1.005	0.021

Table A.3: Continued

Sub-catchment	Event #	Q_P (m^3/s)	L (km)	S_e (%)	T_C [a] (h)	T_C [b] & T_L [a/b] (h)	T_C [c] (h)	T_L [c] (h)	T_C [d] (h)	TPPR 1	TPPR 2	TPPR 3	TPPR 4	TPPR 5	TPPR 6	TPPR 7	TPPR 8
C5H039	43	70.3	23.1	61.9	1230.9	1200.4	1173.1	1200.0	93.1	1.025	1.000	0.977	0.078	1.026	1.000	0.978	0.078
	39	70.7	37.5	56.3	1071.8	1120.5	1119.8	1113.6	15.8	0.957	1.000	0.999	0.014	0.962	1.006	1.006	0.014
	33	72.7	0.6	31.9	522.7	583.8	583.8	585.1	7.8	0.895	1.000	1.000	0.013	0.893	0.998	0.998	0.013
	32	77.5	23.1	39.0	891.0	928.4	937.6	921.2	25.6	0.960	1.000	1.010	0.028	0.967	1.008	1.018	0.028
	2	79.5	58.0	43.6	505.8	517.1	505.2	524.5	1.2	0.978	1.000	0.977	0.002	0.964	0.986	0.963	0.002
	1	100.5	47.7	59.9	707.6	740.0	740.0	735.6	20.0	0.956	1.000	1.000	0.027	0.962	1.006	1.006	0.027
	12	141.7	66.0	53.7	293.9	276.4	284.3	281.7	20.3	1.063	1.000	1.028	0.073	1.043	0.981	1.009	0.072
	29	153.2	0.6	59.0	421.3	368.3	368.3	362.4	56.3	1.144	1.000	1.000	0.153	1.163	1.016	1.016	0.155
	14	194.6	37.5	89.4	1346.0	1265.0	1235.2	1234.9	251.2	1.064	1.000	0.976	0.199	1.090	1.024	1.000	0.203
	17	266.5	94.9	74.7	364.3	420.4	457.6	440.6	73.6	0.867	1.000	1.088	0.175	0.827	0.954	1.039	0.167
	6	362.5	47.7	96.0	400.0	438.7	417.9	383.2	201.9	0.912	1.000	0.953	0.460	1.044	1.145	1.091	0.527
	3	505.4	89.8	79.1	912.6	927.3	936.7	929.1	24.7	0.984	1.000	1.010	0.027	0.982	0.998	1.008	0.027
C5H053	23	24.2	12.2	15.4	260.8	314.1	316.6	317.0	4.6	0.830	1.000	1.008	0.015	0.823	0.991	0.999	0.015
	26	33.5	77.5	11.6	624.2	636.6	636.6	637.1	12.6	0.981	1.000	1.000	0.020	0.980	0.999	0.999	0.020
	15	34.0	12.2	24.4	903.0	914.4	914.4	913.0	26.4	0.988	1.000	1.000	0.029	0.989	1.002	1.002	0.029
	12	36.0	77.5	26.3	519.8	589.6	645.6	574.9	117.6	0.882	1.000	1.095	0.199	0.904	1.026	1.123	0.205
	9	40.2	22.1	18.3	569.2	574.0	574.0	578.6	22.0	0.992	1.000	1.000	0.038	0.984	0.992	0.992	0.038
	8	41.1	12.2	23.4	259.4	291.0	291.0	292.5	3.0	0.891	1.000	1.000	0.010	0.887	0.995	0.995	0.010
	20	45.6	31.2	27.6	486.2	505.0	505.0	507.4	25.0	0.963	1.000	1.000	0.050	0.958	0.995	0.995	0.049
	16	48.9	22.1	35.1	350.4	425.5	343.0	402.6	79.0	0.824	1.000	0.806	0.186	0.870	1.057	0.852	0.196
	6	98.8	31.2	21.8	309.4	340.5	325.8	342.7	13.8	0.909	1.000	0.957	0.041	0.903	0.994	0.951	0.040
	24	145.4	31.2	25.6	103.6	148.5	138.0	147.0	18.0	0.698	1.000	0.929	0.121	0.705	1.010	0.939	0.122
	11	171.6	12.2	48.0	566.4	633.5	621.4	631.2	21.4	0.894	1.000	0.981	0.034	0.897	1.004	0.985	0.034
	3	206.8	31.2	30.9	213.0	353.7	333.8	359.1	21.8	0.602	1.000	0.944	0.062	0.593	0.985	0.930	0.061

Table A.3: Continued

Sub-catchment	Event #	Q_P (m^3/s)	L (km)	S_e (%)	T_C [a] (h)	T_C [b] & T_L [a/b] (h)	T_C [c] (h)	T_L [c] (h)	T_C [d] (h)	TPPR 1	TPPR 2	TPPR 3	TPPR 4	TPPR 5	TPPR 6	TPPR 7	TPPR 8
C5H054	16	10.8	1.9	41.3	479.6	517.6	517.6	517.1	13.6	0.927	1.000	1.000	0.026	0.928	1.001	1.001	0.026
	20	11.6	9.9	26.3	267.8	320.7	323.2	321.5	11.2	0.835	1.000	1.008	0.035	0.833	0.998	1.005	0.035
	9	11.9	21.1	41.2	1124.8	1090.6	1090.6	1097.6	10.6	1.031	1.000	1.000	0.010	1.025	0.994	0.994	0.010
	17	12.6	29.0	20.2	812.0	821.1	821.0	822.2	5.0	0.989	1.000	1.000	0.006	0.988	0.999	0.999	0.006
	15	12.8	21.1	45.4	643.2	653.4	653.4	654.9	5.4	0.984	1.000	1.000	0.008	0.982	0.998	0.998	0.008
	29	13.8	21.1	23.1	181.2	170.6	170.6	172.7	2.6	1.062	1.000	1.000	0.015	1.049	0.988	0.988	0.015
	34	14.0	1.9	30.4	287.6	290.8	290.8	293.7	2.8	0.989	1.000	1.000	0.010	0.979	0.990	0.990	0.010
	1	14.9	28.0	49.1	670.6	677.4	677.4	684.9	5.4	0.990	1.000	1.000	0.008	0.979	0.989	0.989	0.008
	23	16.0	21.1	31.2	695.8	799.8	799.8	801.4	7.8	0.870	1.000	1.000	0.010	0.868	0.998	0.998	0.010
	13	16.6	29.0	49.2	238.8	268.8	268.8	277.1	4.8	0.888	1.000	1.000	0.018	0.862	0.970	0.970	0.017
	6	18.7	28.0	45.8	506.6	518.4	518.4	524.1	14.4	0.977	1.000	1.000	0.028	0.967	0.989	0.989	0.027
	32	19.4	29.0	30.8	279.4	310.2	310.2	308.7	22.2	0.901	1.000	1.000	0.072	0.905	1.005	1.005	0.072
	24	22.6	21.1	41.3	250.8	344.7	299.8	345.2	11.8	0.728	1.000	0.870	0.034	0.727	0.999	0.869	0.034
	18	24.0	29.0	31.2	547.4	556.8	556.8	558.9	4.8	0.983	1.000	1.000	0.009	0.979	0.996	0.996	0.009
	8	24.8	21.1	45.4	123.8	111.8	111.8	120.4	15.8	1.107	1.000	1.000	0.141	1.029	0.929	0.929	0.131
	10	27.7	21.1	49.3	236.0	226.8	226.8	231.3	10.8	1.041	1.000	1.000	0.048	1.020	0.981	0.981	0.047
	27	28.1	21.1	45.0	419.8	440.2	440.2	446.7	8.2	0.954	1.000	1.000	0.019	0.940	0.985	0.985	0.018
	7	28.4	28.0	86.5	107.8	115.5	108.8	115.0	12.8	0.933	1.000	0.942	0.111	0.937	1.005	0.946	0.111

APPENDIX B: GRAPHICAL INFORMATION AND RESULTS

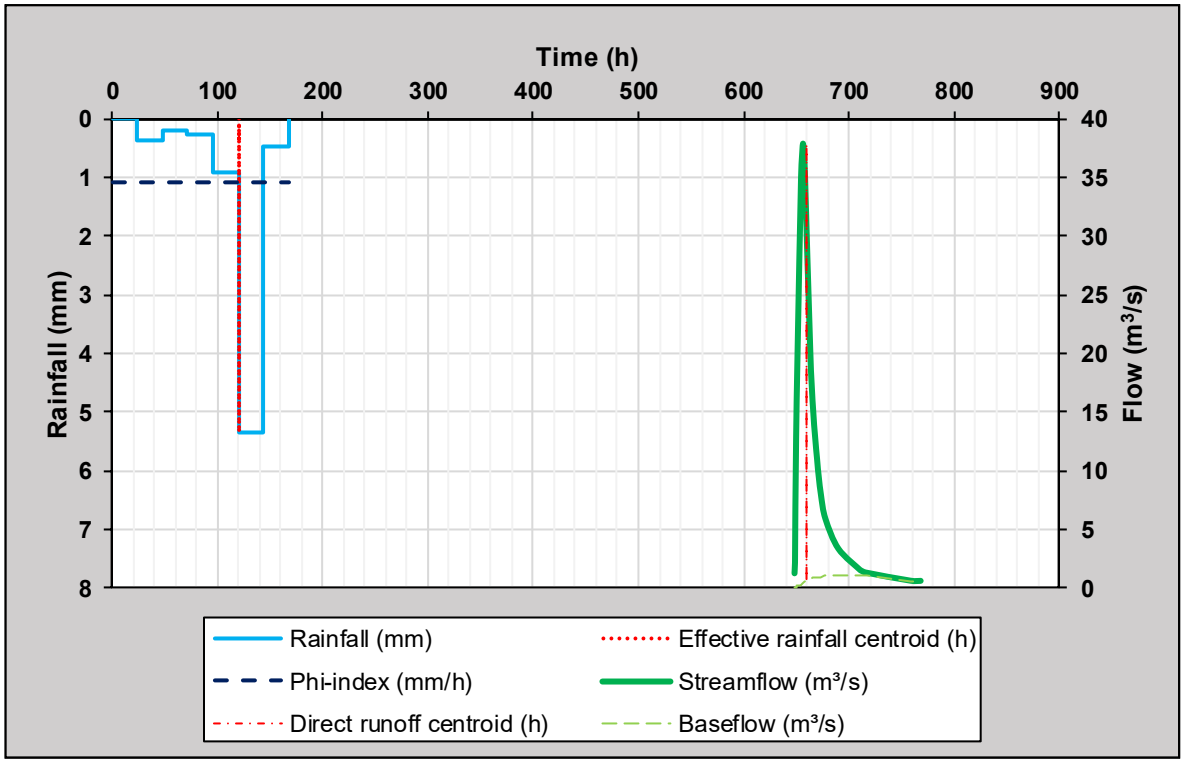

Figure B.1: Hyetograph-hydrograph event 31 in sub-catchment C5H003

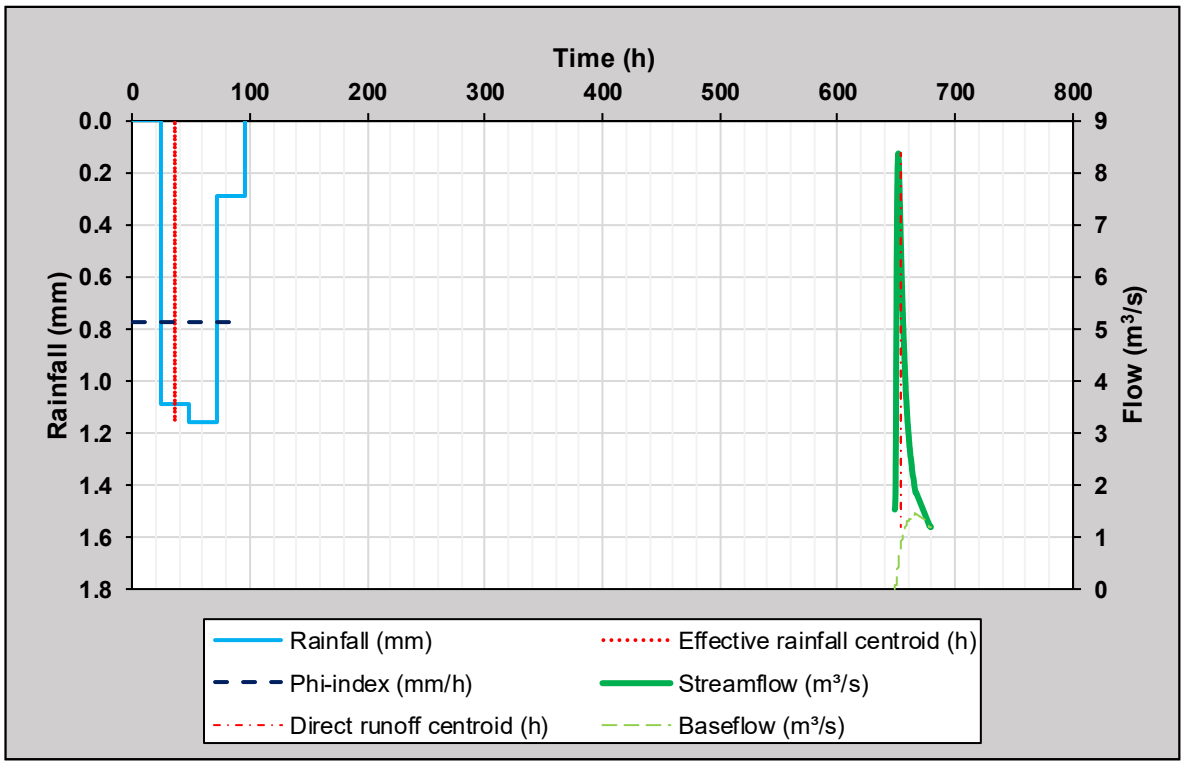

Figure B.2: Hyetograph-hydrograph event 77 in sub-catchment C5H003

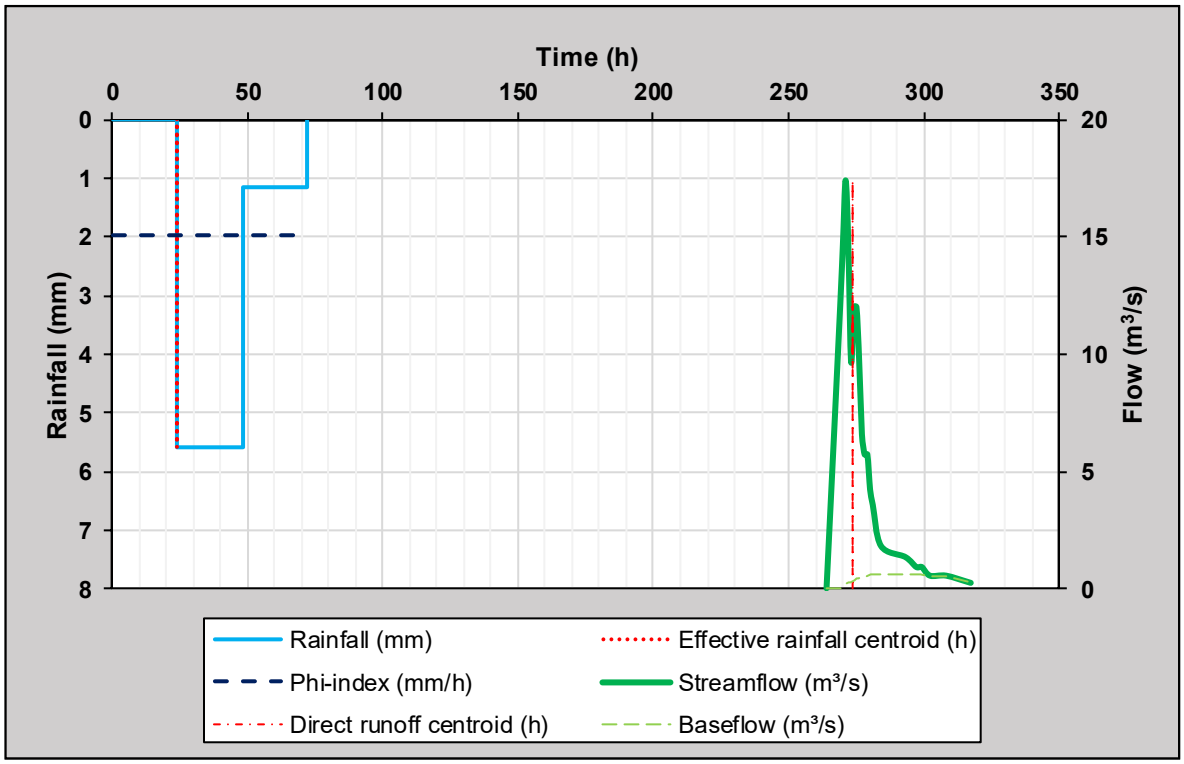

Figure B.3: Hyetograph-hydrograph event 2 in sub-catchment C5H006

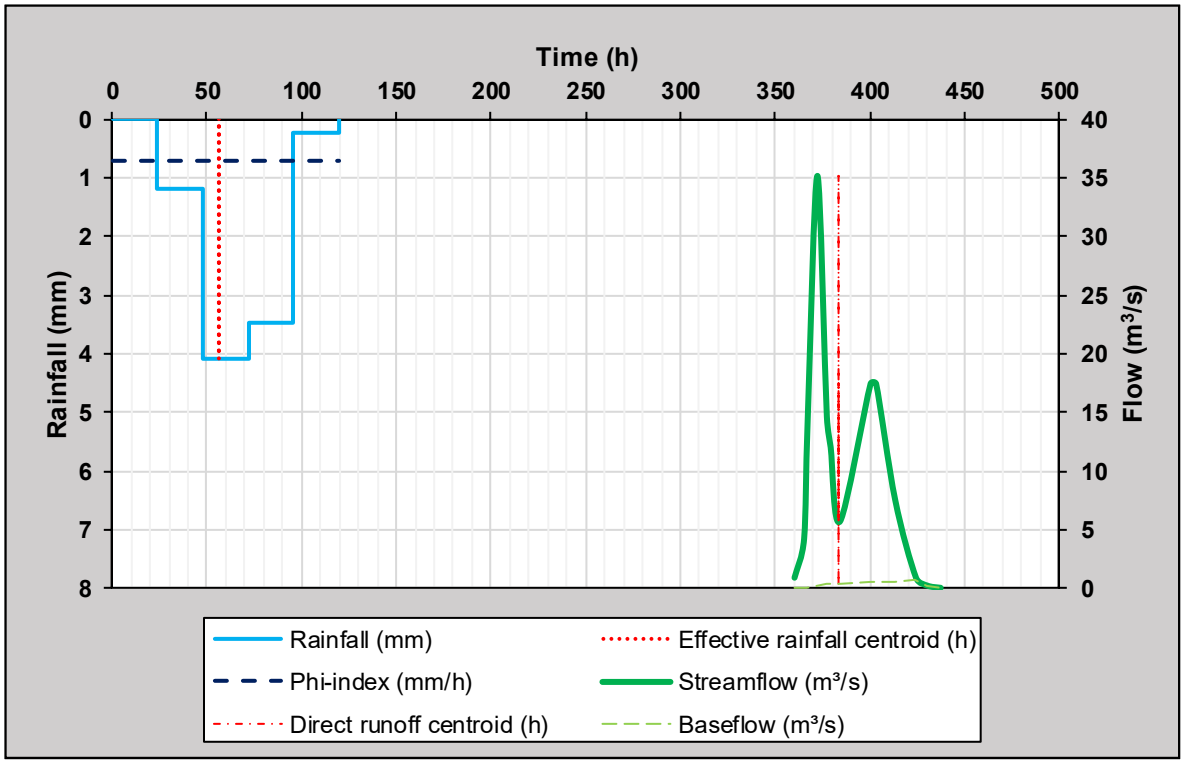

Figure B.4: Hyetograph-hydrograph event 13 in sub-catchment C5H006

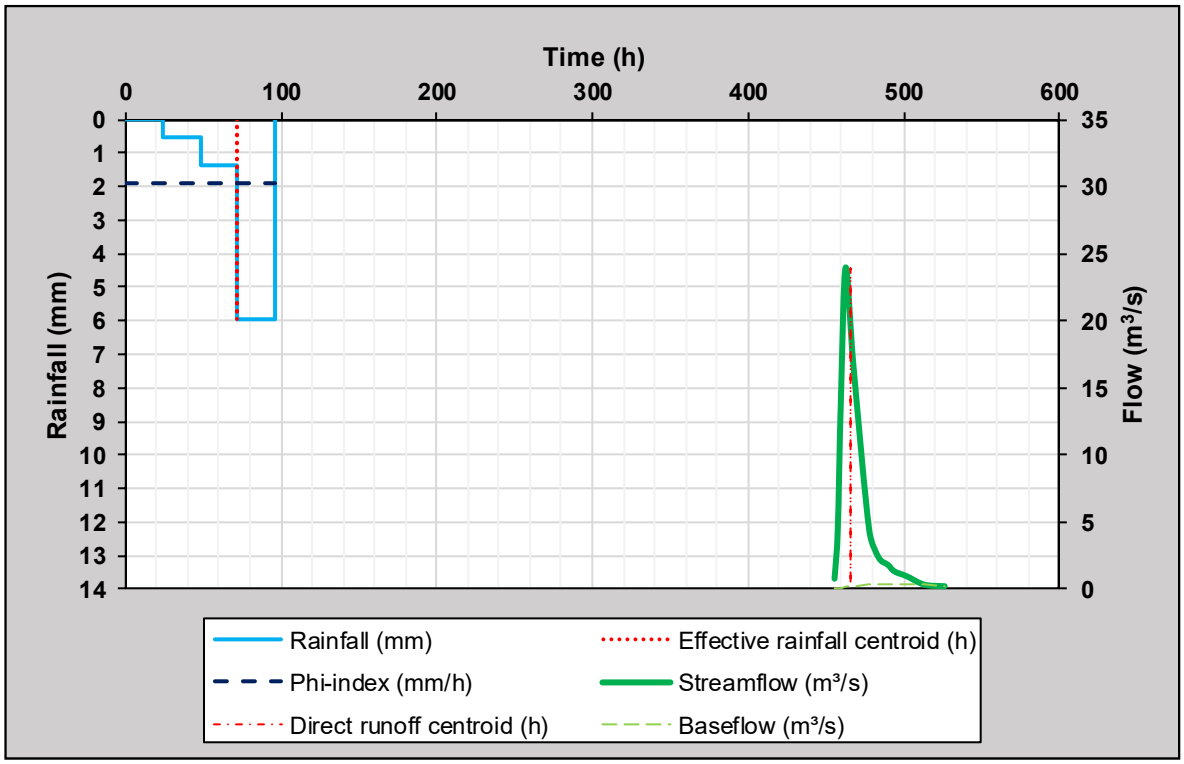

Figure B.5: Hyetograph-hydrograph event 23 in sub-catchment C5H007

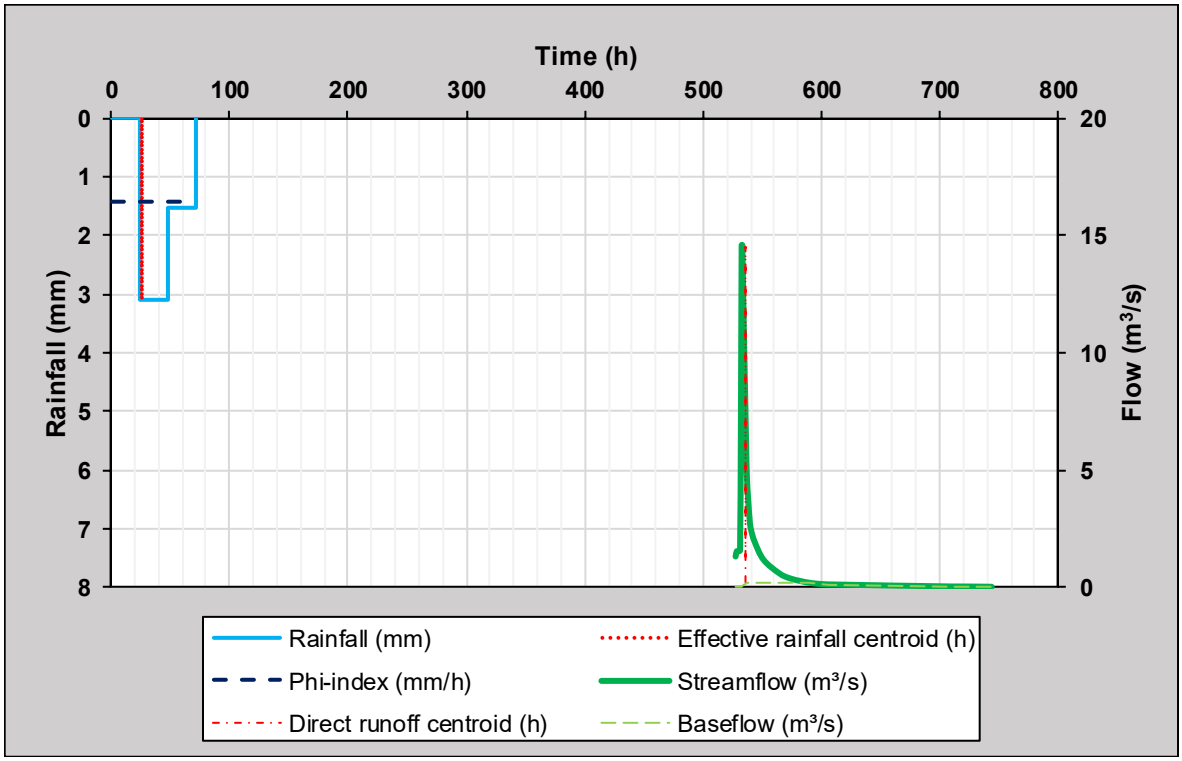

Figure B.6: Hyetograph-hydrograph event 65 in sub-catchment C5H007

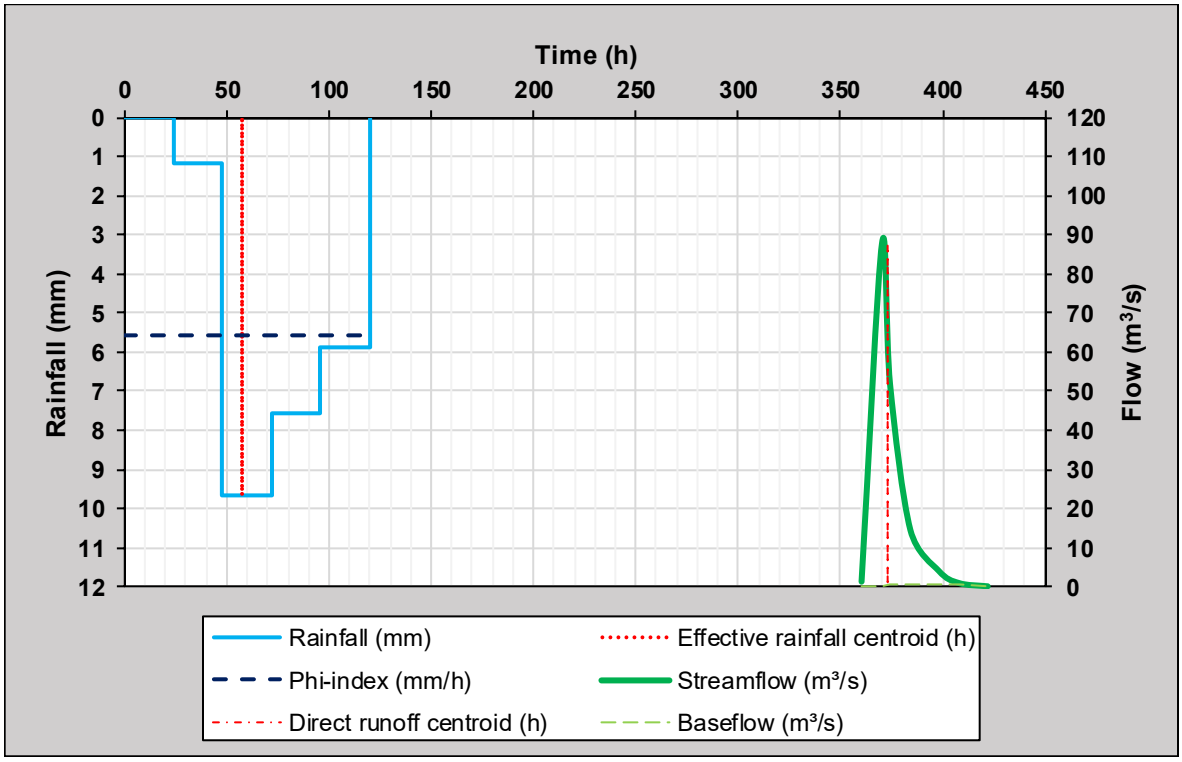

Figure B.7: Hyetograph-hydrograph event 59 in sub-catchment C5H008

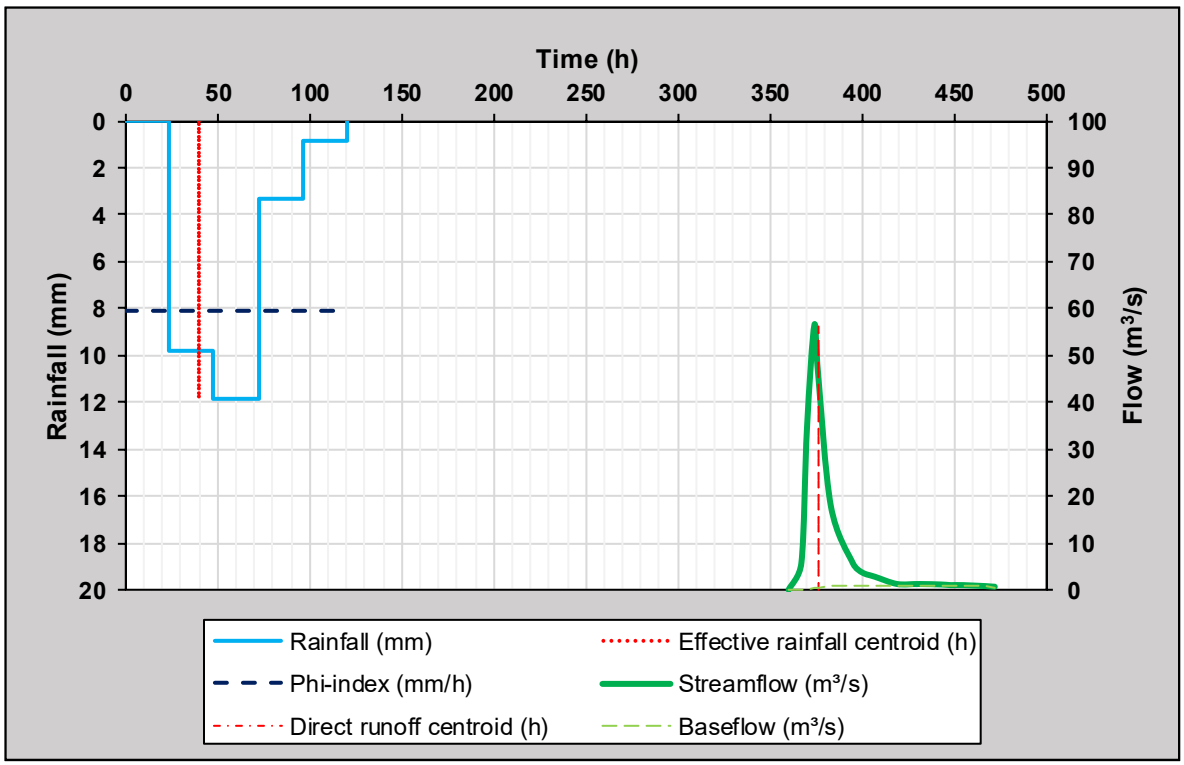

Figure B.8: Hyetograph-hydrograph event 80 in sub-catchment C5H008

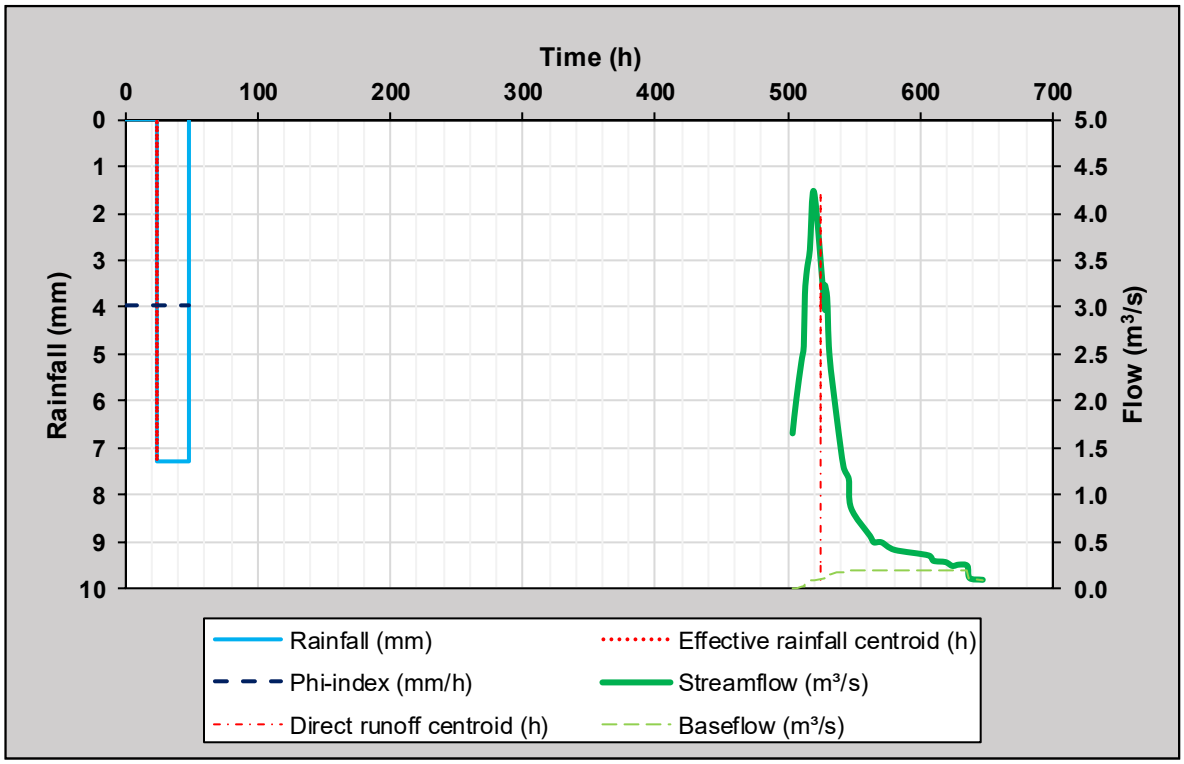

Figure B.9: Hyetograph-hydrograph event 3 in sub-catchment C5H009

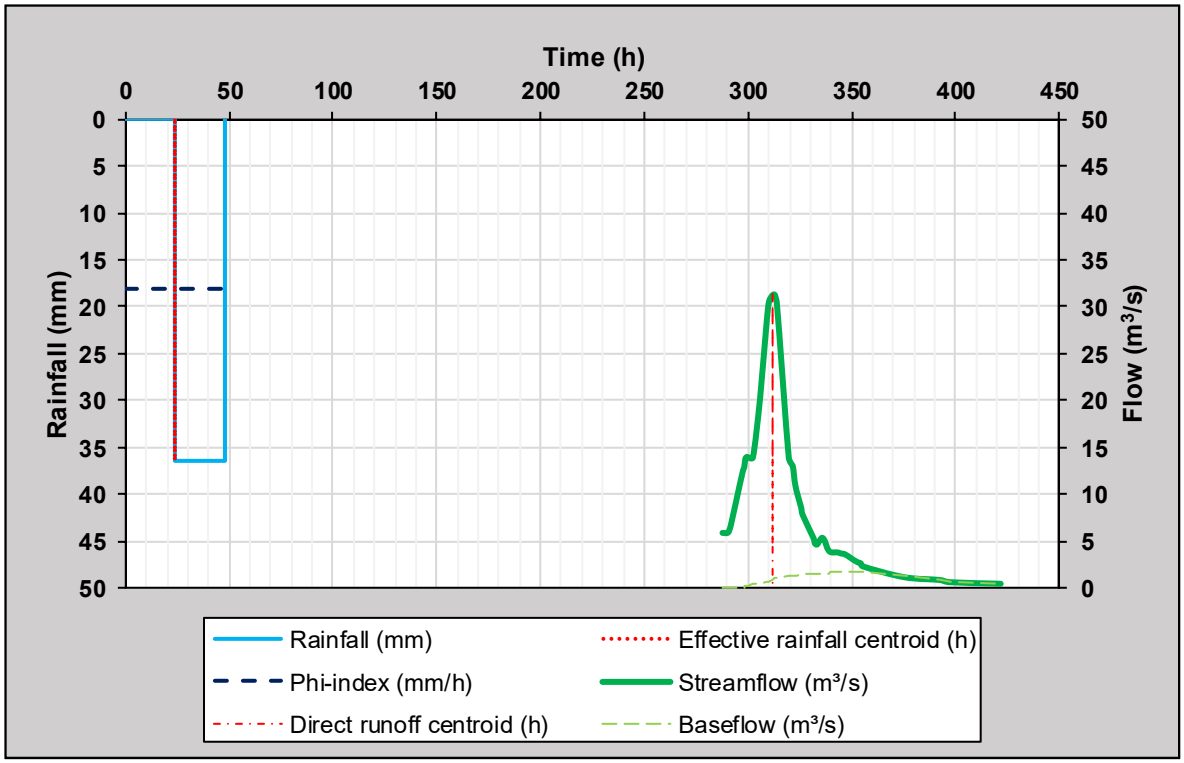

Figure B.10: Hyetograph-hydrograph event 8 in sub-catchment C5H009

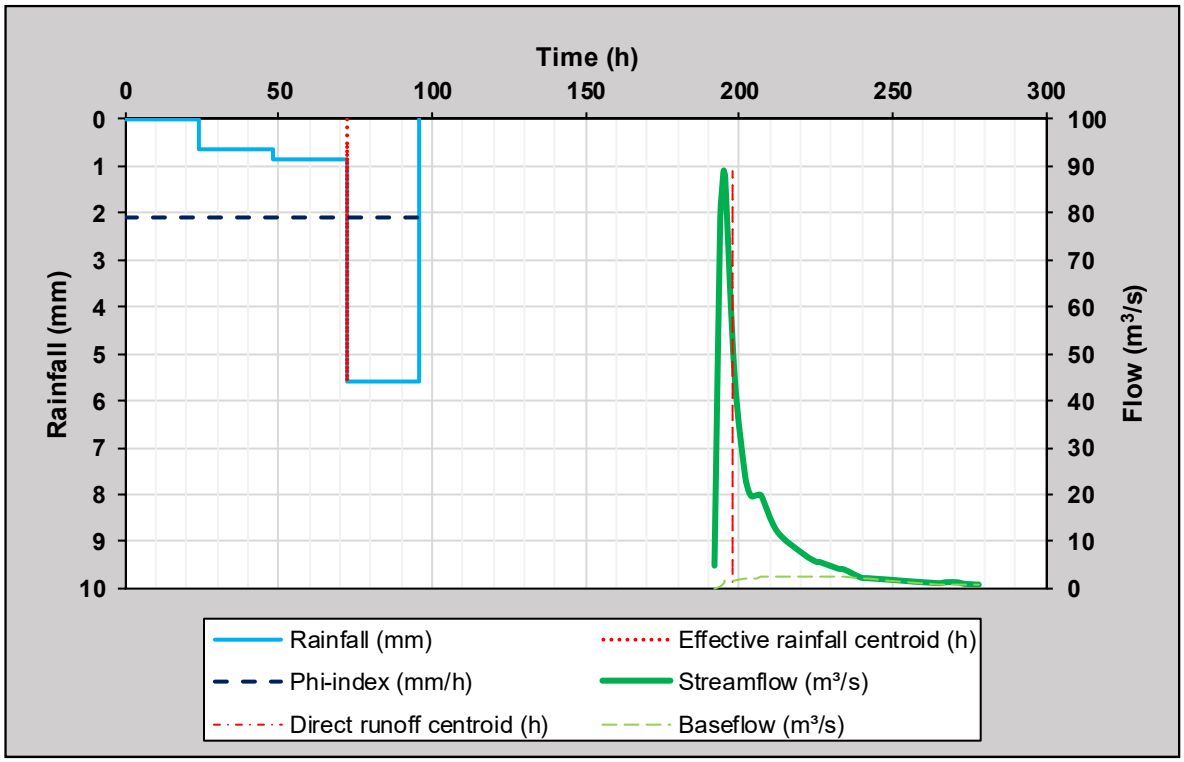

Figure B.11: Hyetograph-hydrograph event 7 in sub-catchment C5H012

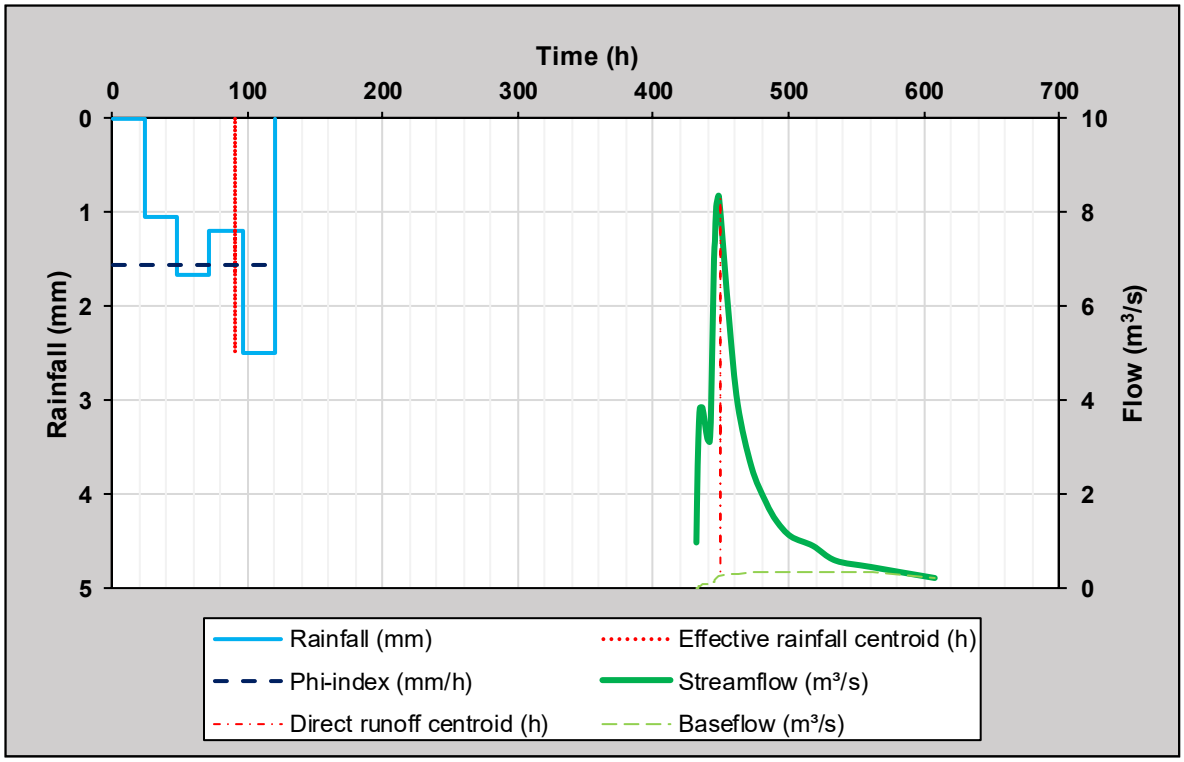

Figure B.12: Hyetograph-hydrograph event 8 in sub-catchment C5H012

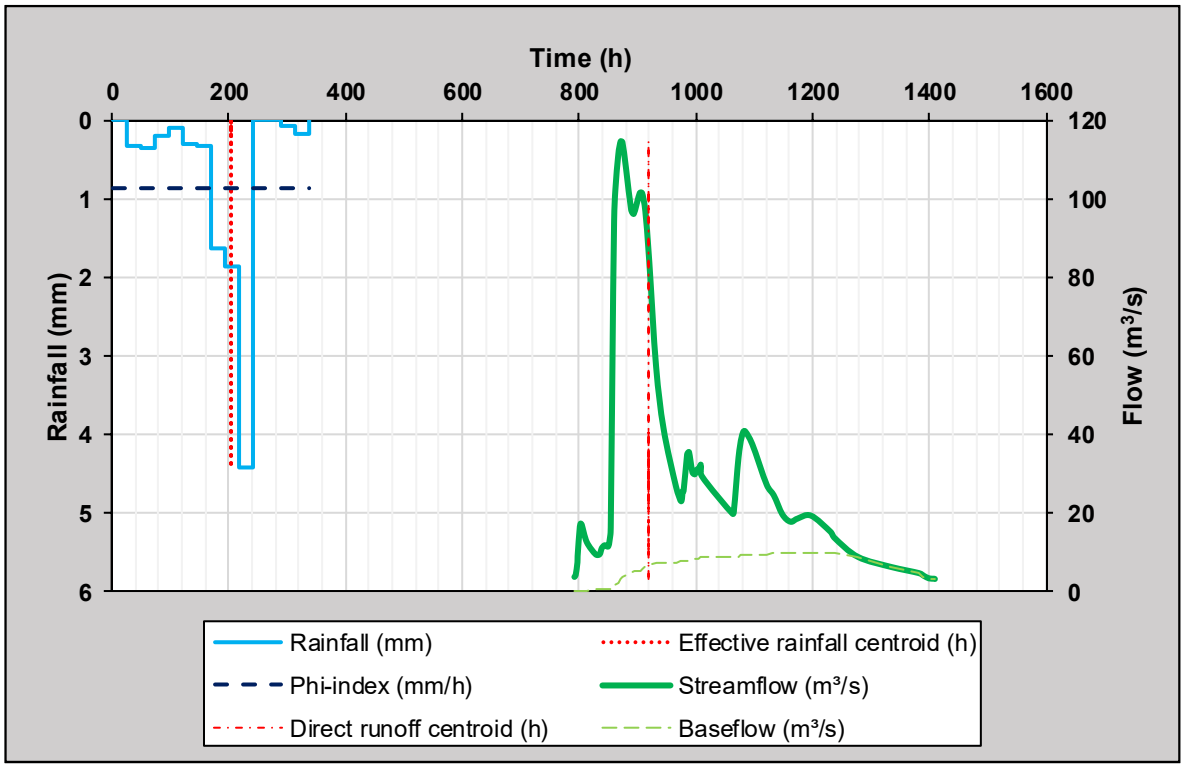

Figure B.13: Hyetograph-hydrograph event 5 in sub-catchment C5H014

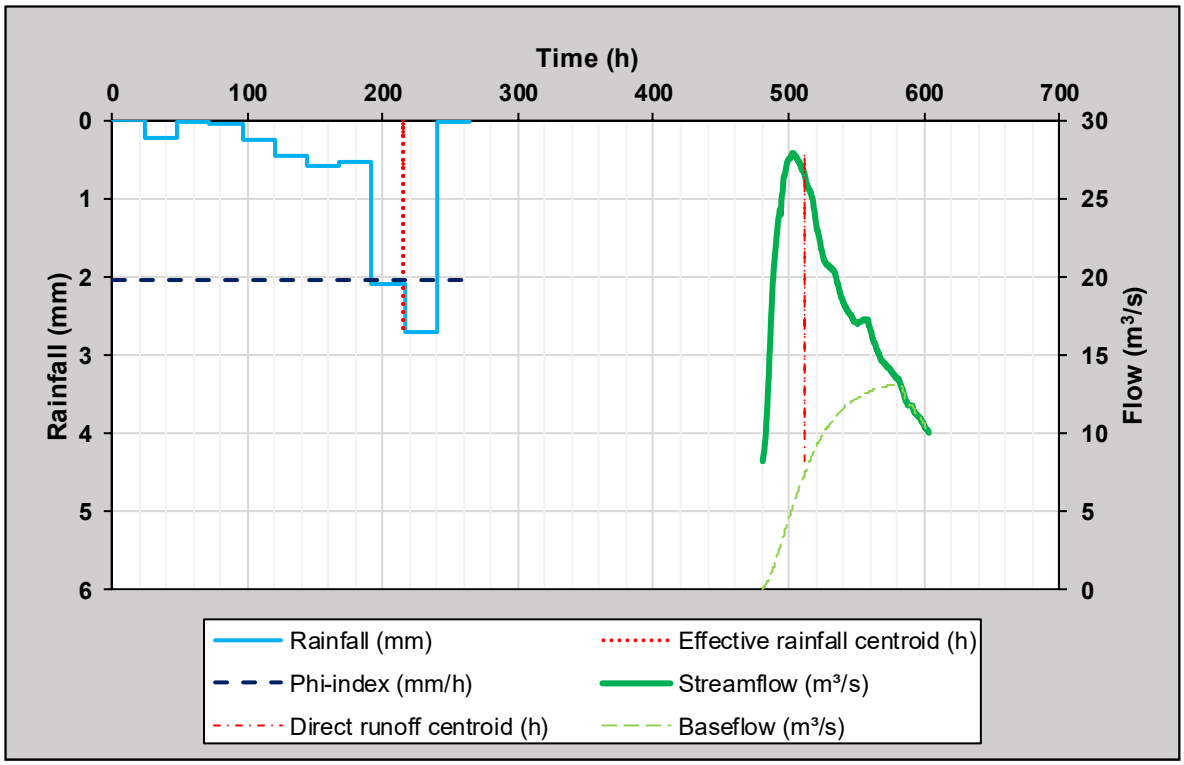

Figure B.14: Hyetograph-hydrograph event 16 in sub-catchment C5H014

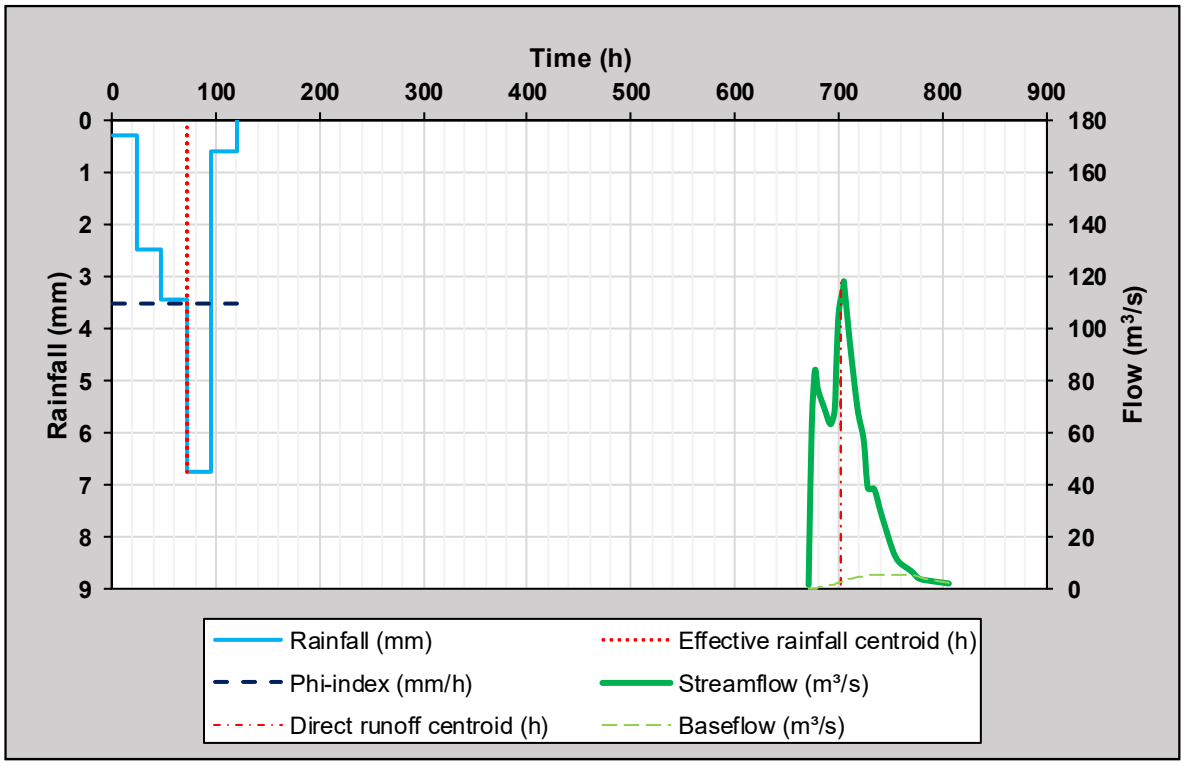

Figure B.15: Hyetograph-hydrograph event 4 in sub-catchment C5H015

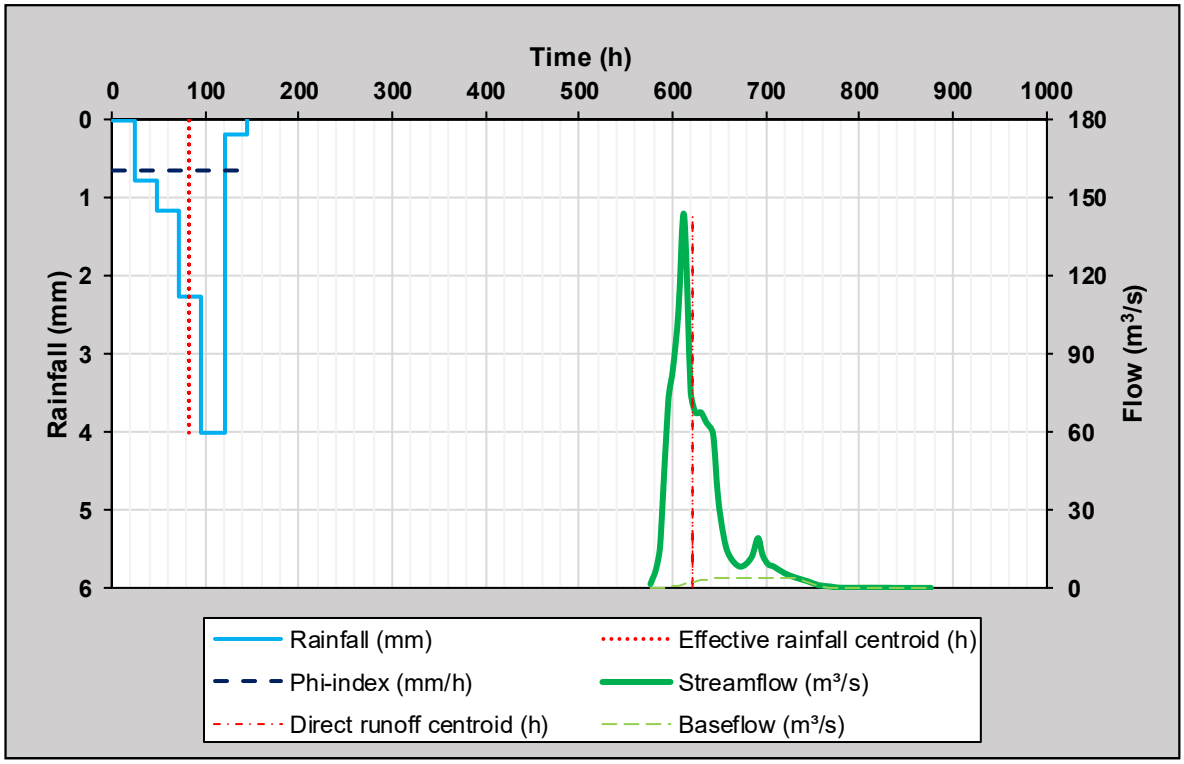

Figure B.16: Hyetograph-hydrograph event 12 in sub-catchment C5H015

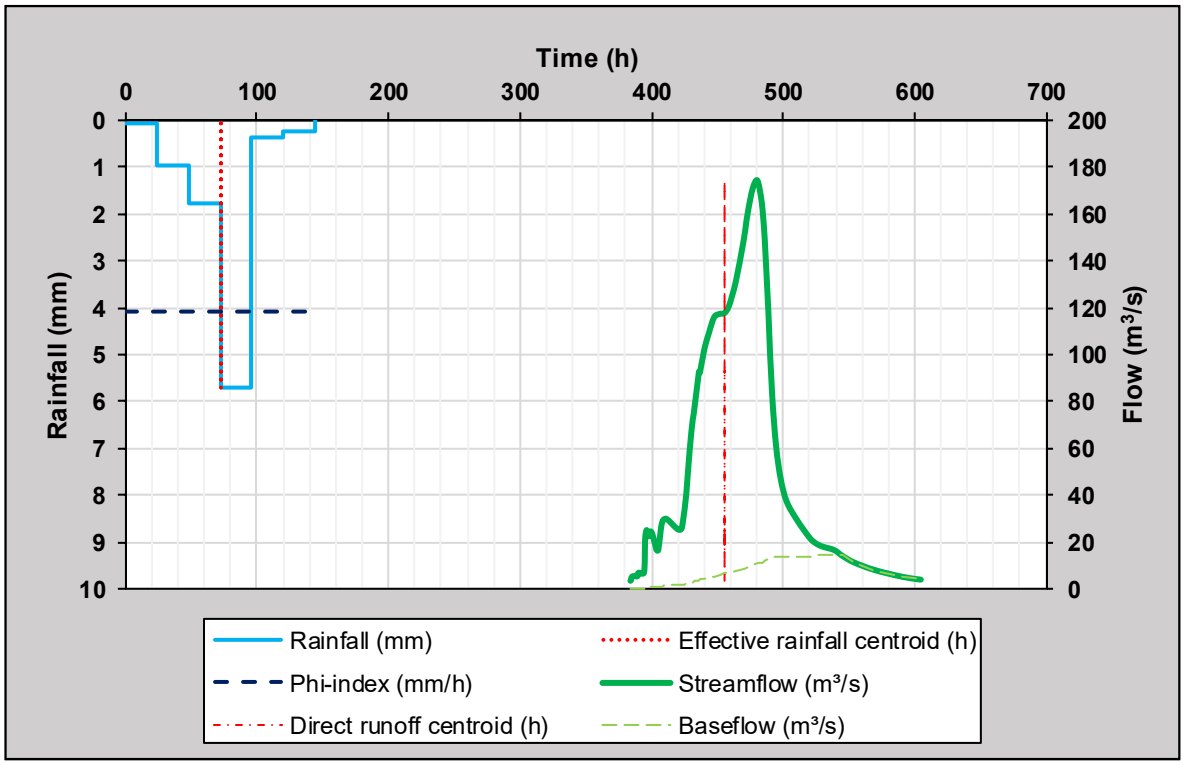

Figure B.17: Hyetograph-hydrograph event 41 in sub-catchment C5H016

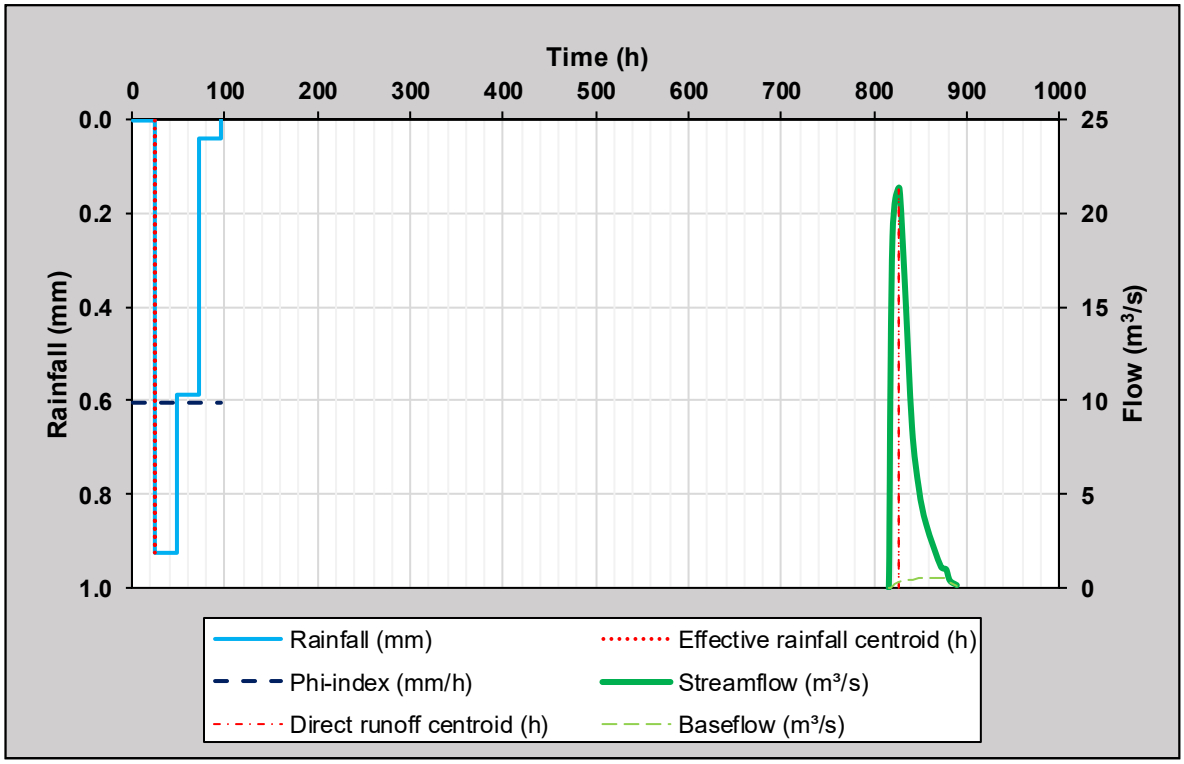

Figure B.18: Hyetograph-hydrograph event 43 in sub-catchment C5H016

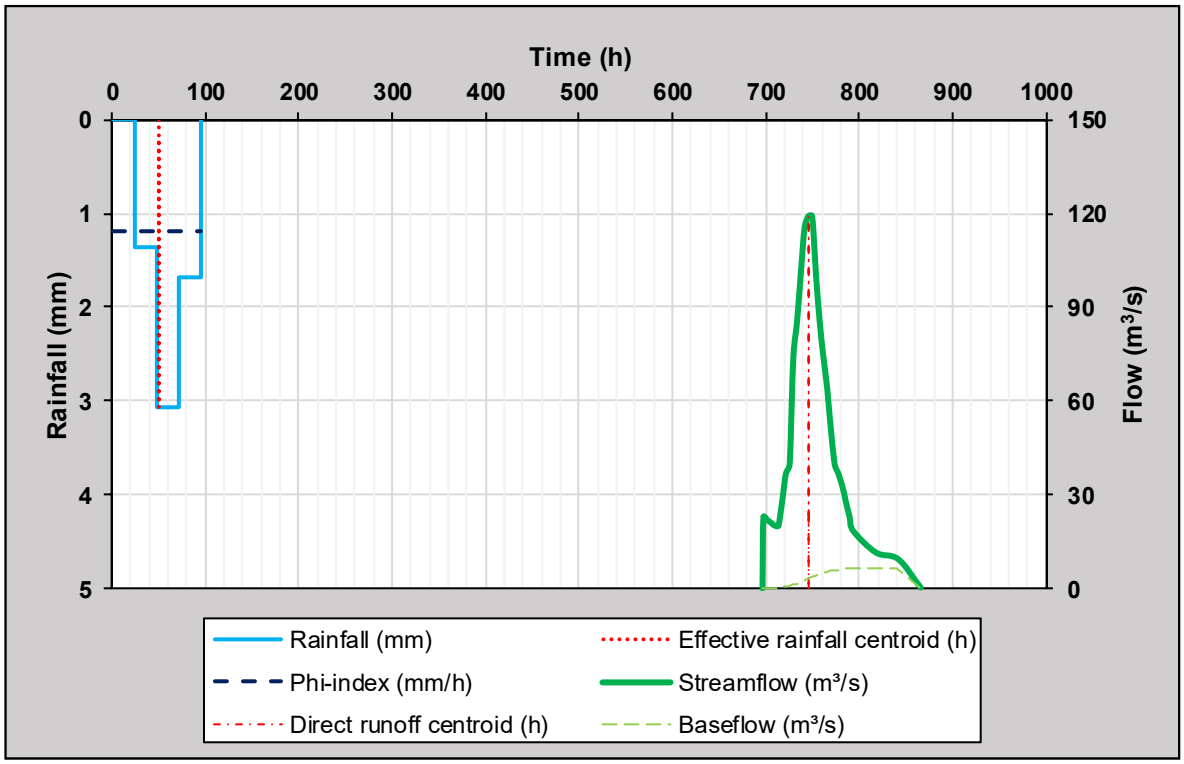

Figure B.19: Hyetograph-hydrograph event 7 in sub-catchment C5H018

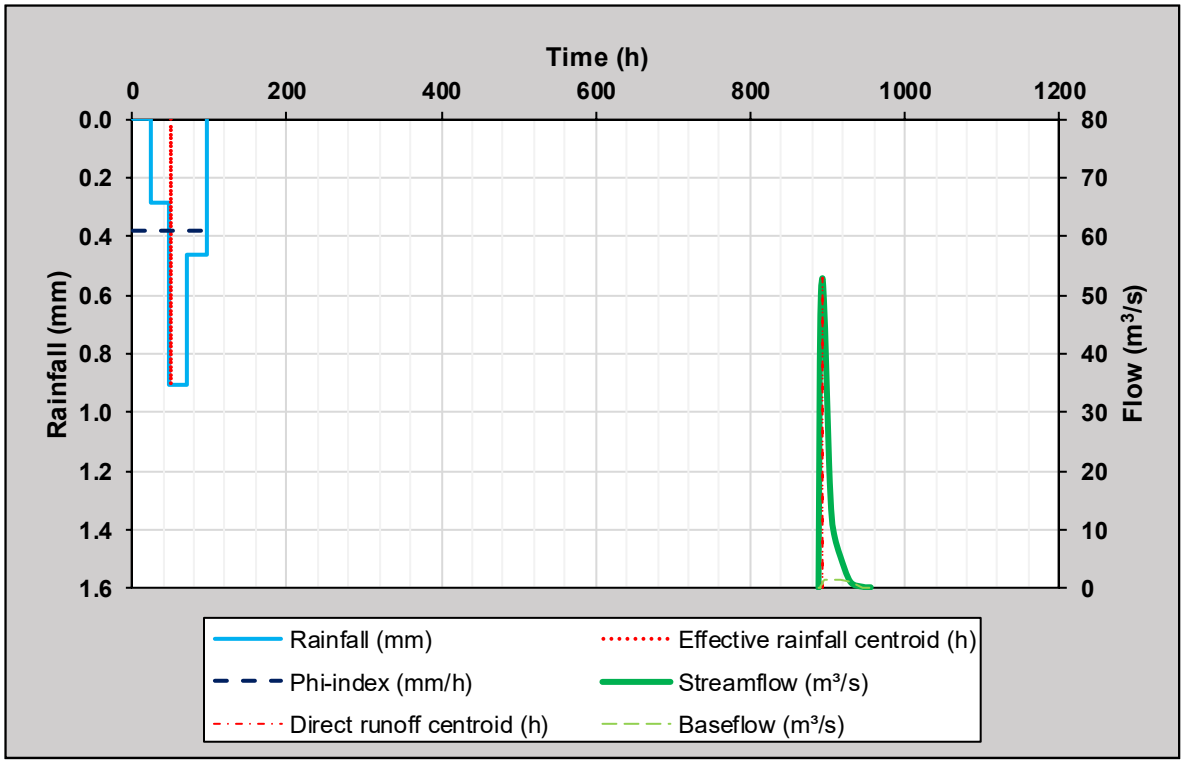

Figure B.20: Hyetograph-hydrograph event 61 in sub-catchment C5H018

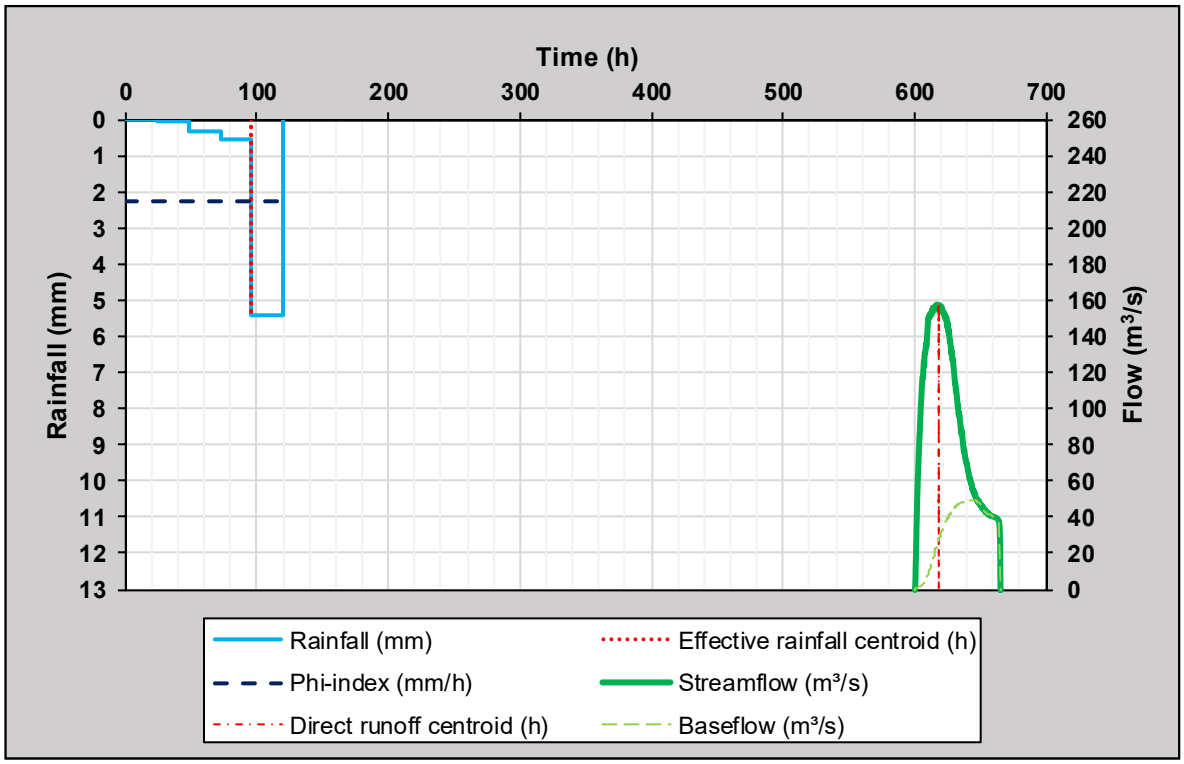

Figure B.21: Hyetograph-hydrograph event 15 in sub-catchment C5H035

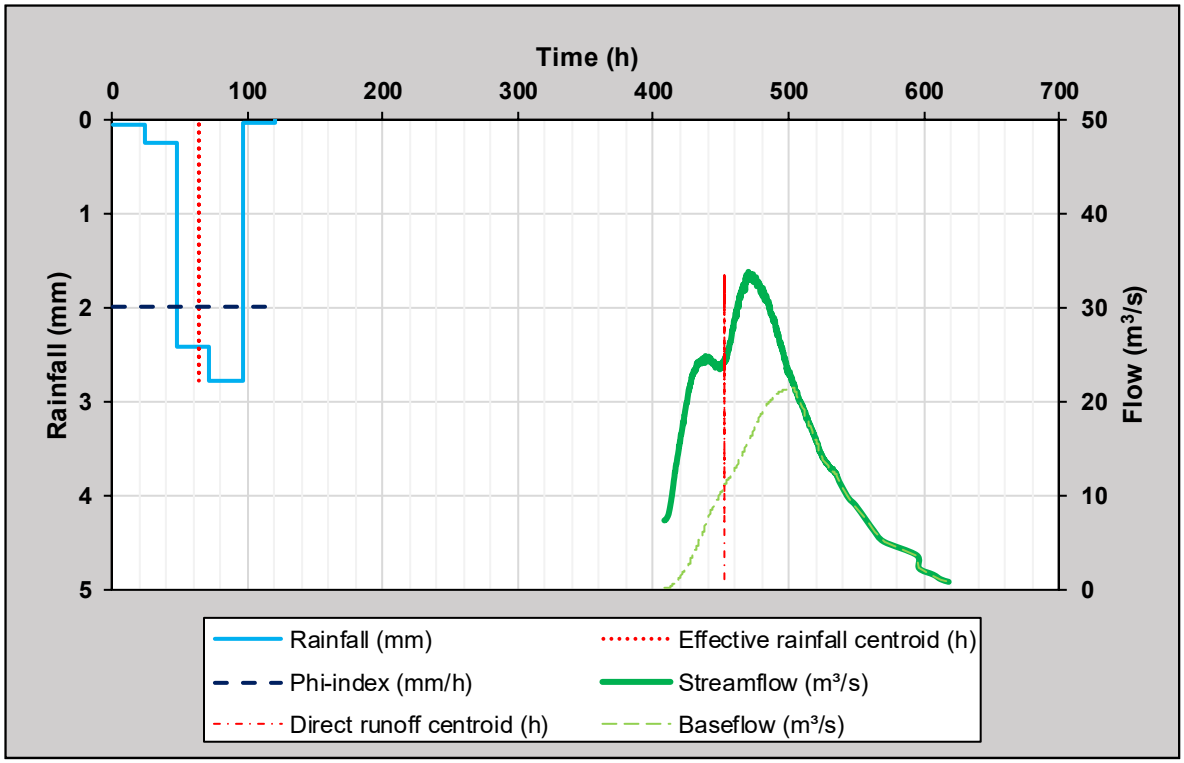

Figure B.22: Hyetograph-hydrograph event 22 in sub-catchment C5H035

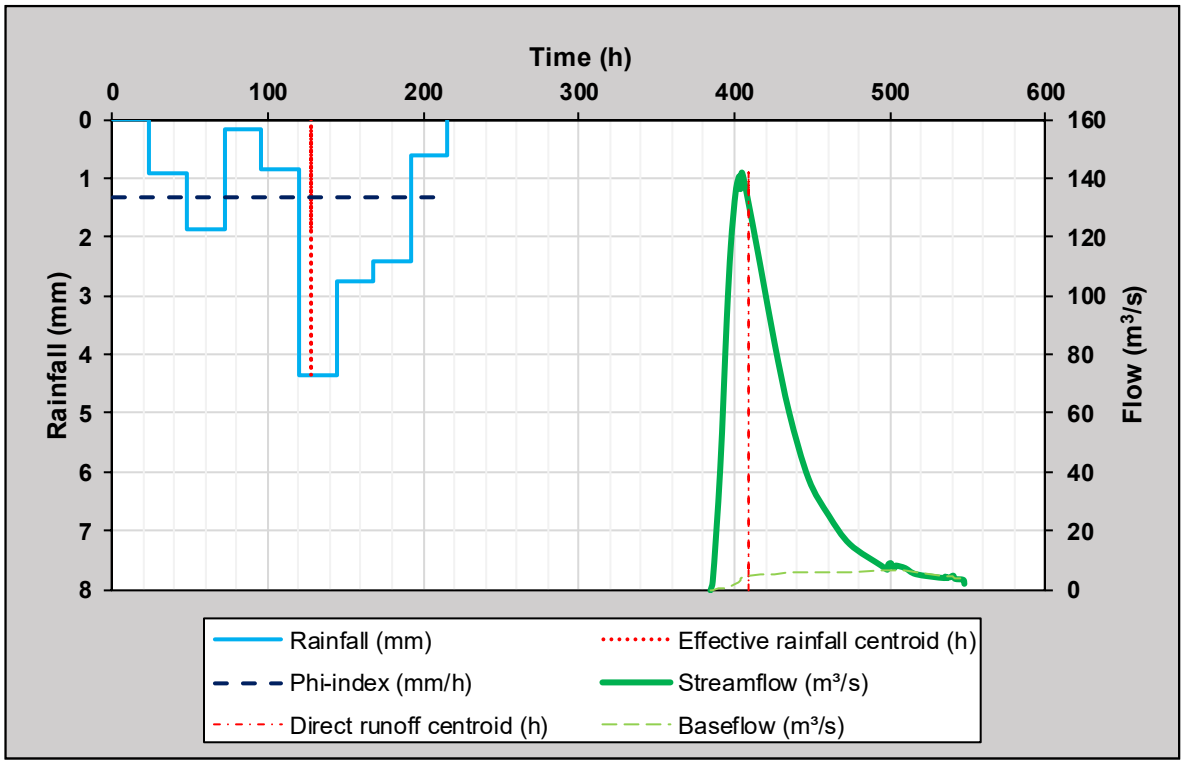

Figure B.23: Hyetograph-hydrograph event 12 in sub-catchment C5H039

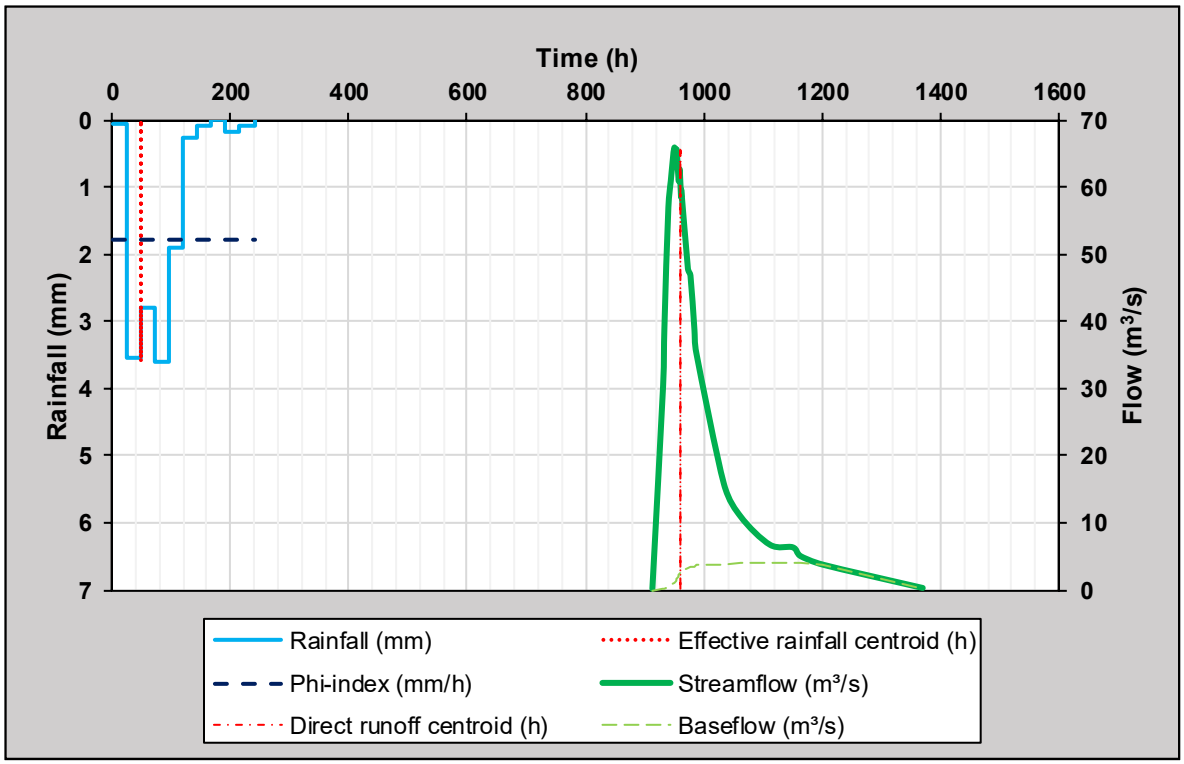

Figure B.24: Hyetograph-hydrograph event 27 in sub-catchment C5H039

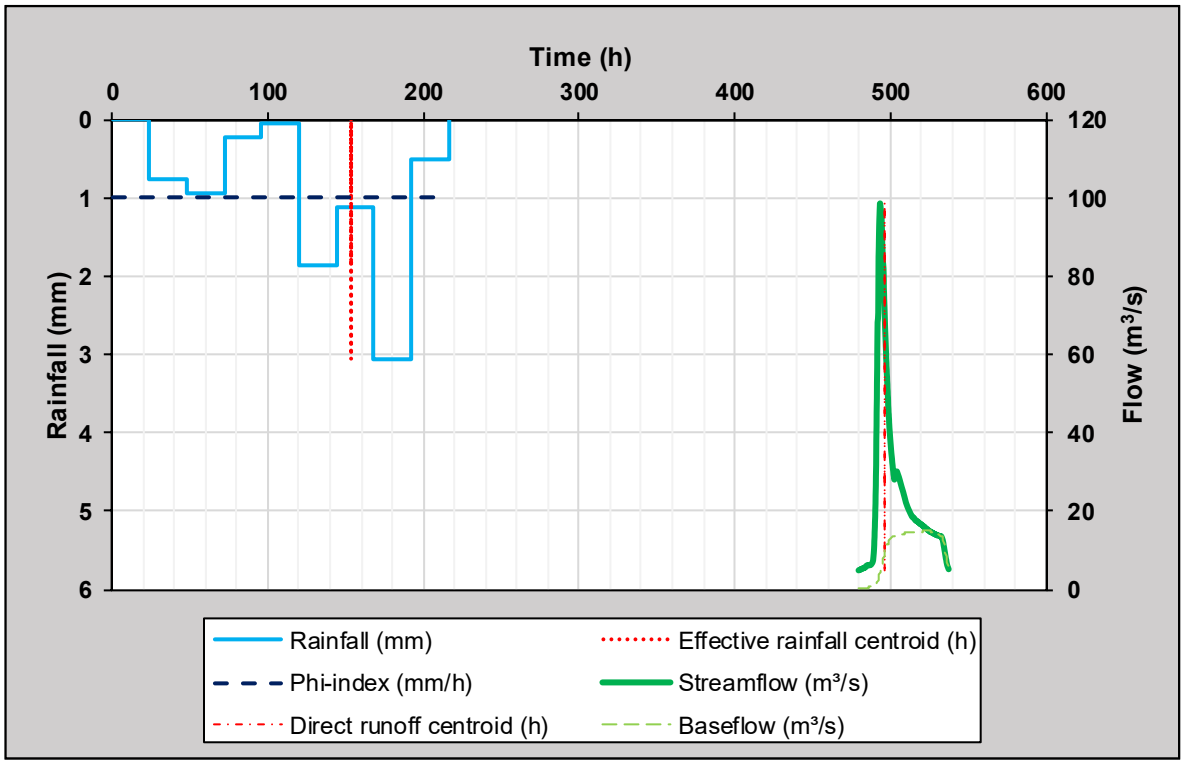

Figure B.25: Hyetograph-hydrograph event 6 in sub-catchment C5H053

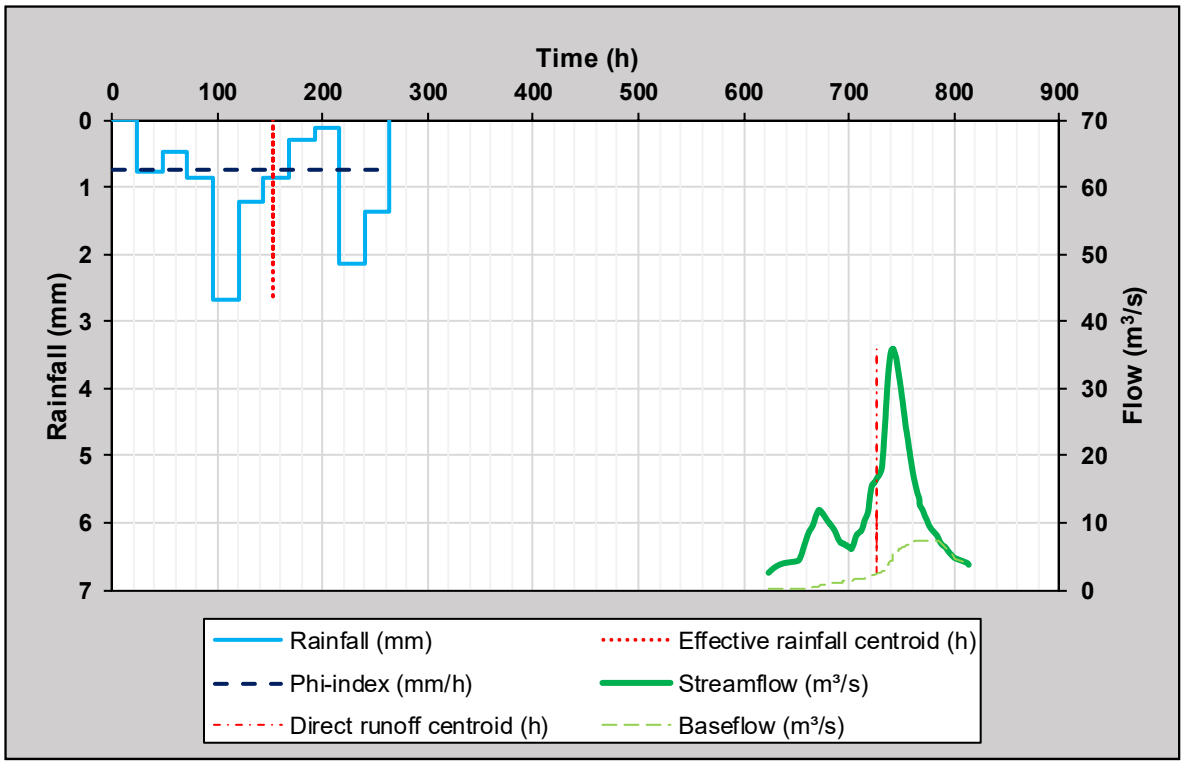

Figure B.26: Hyetograph-hydrograph event 12 in sub-catchment C5H053

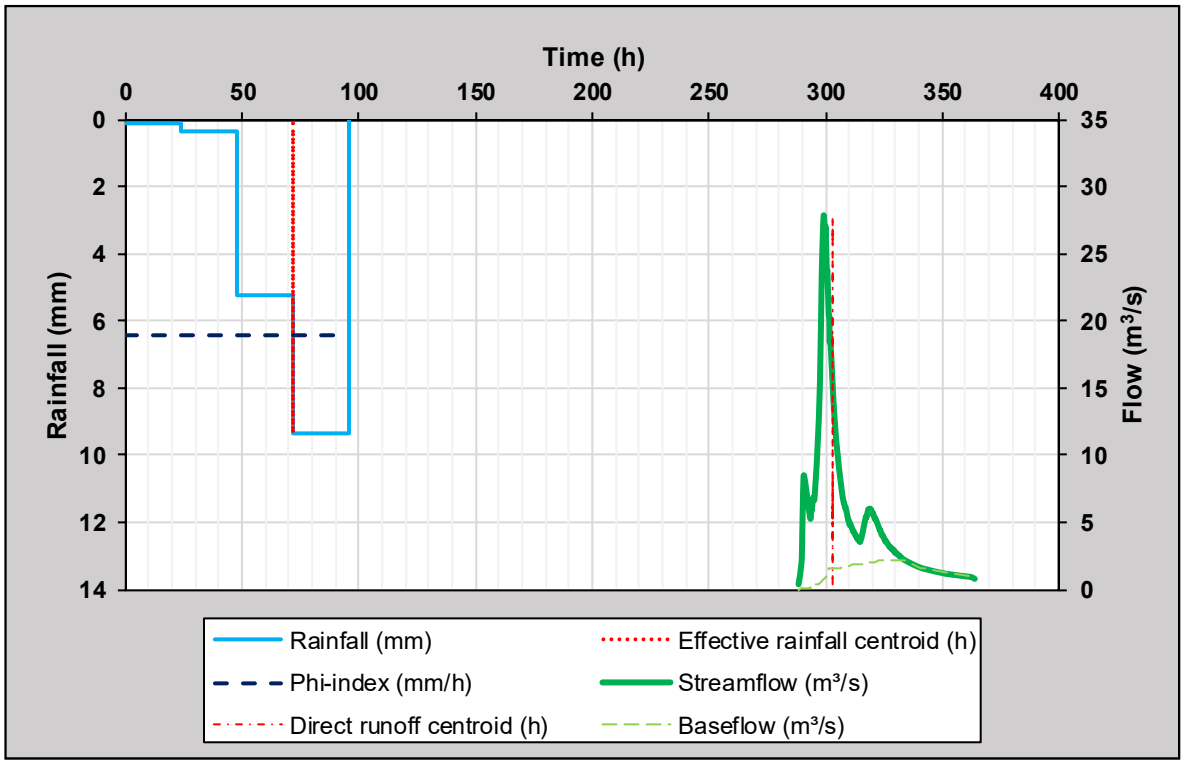

Figure B.27: Hyetograph-hydrograph event 10 in sub-catchment C5H054

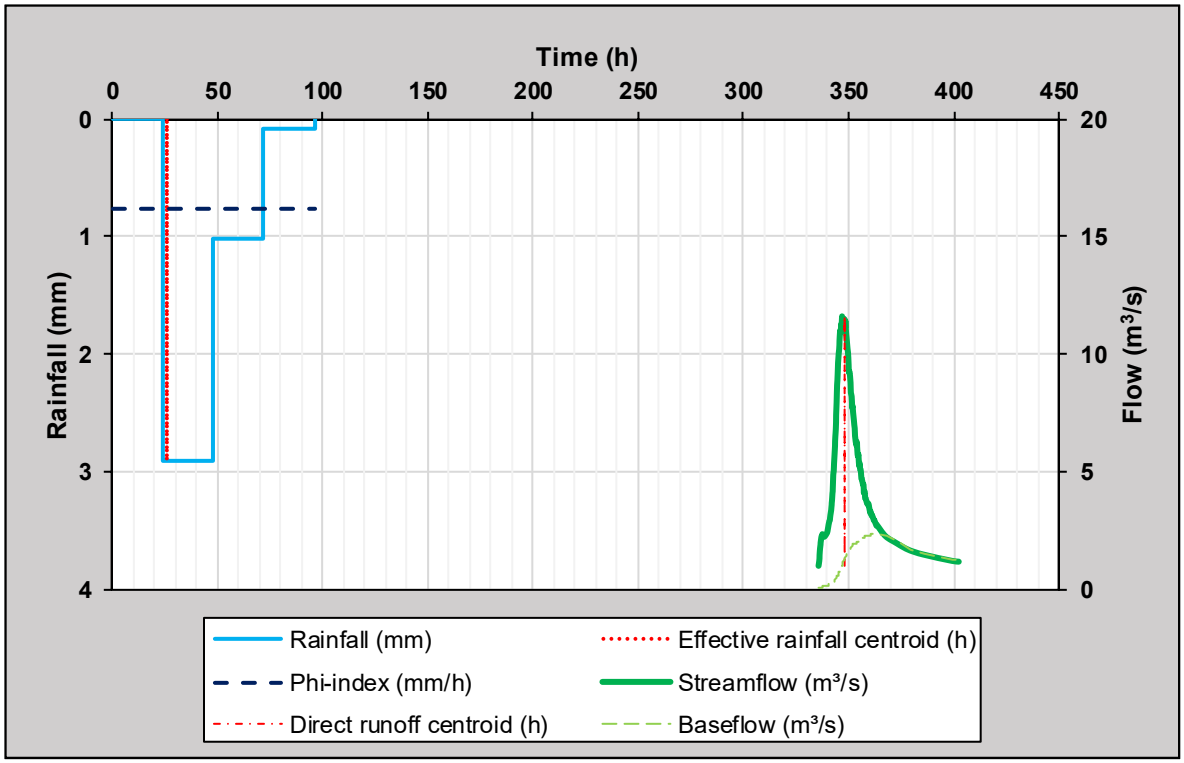

Figure B.28: Hyetograph-hydrograph event 20 in sub-catchment C5H054

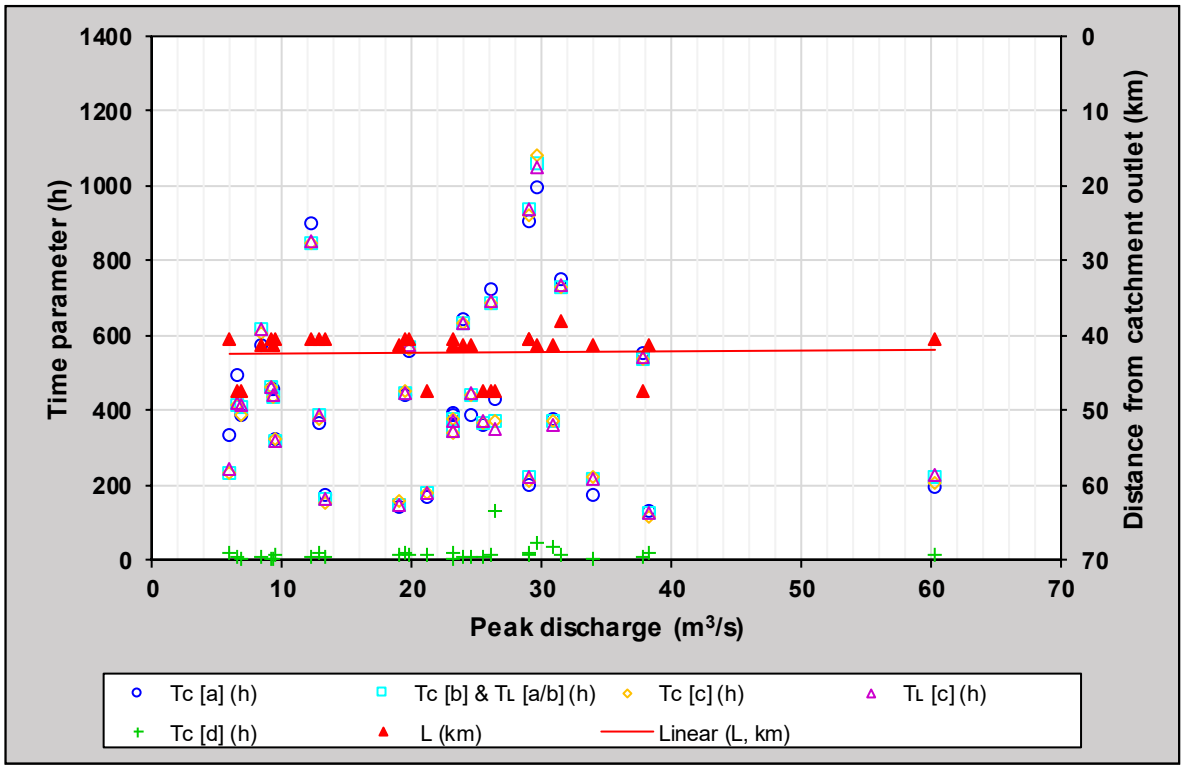

Figure B.29: Time parameters versus the distance (*L*) of a rainfall event from the catchment outlet in sub-catchment C5H003

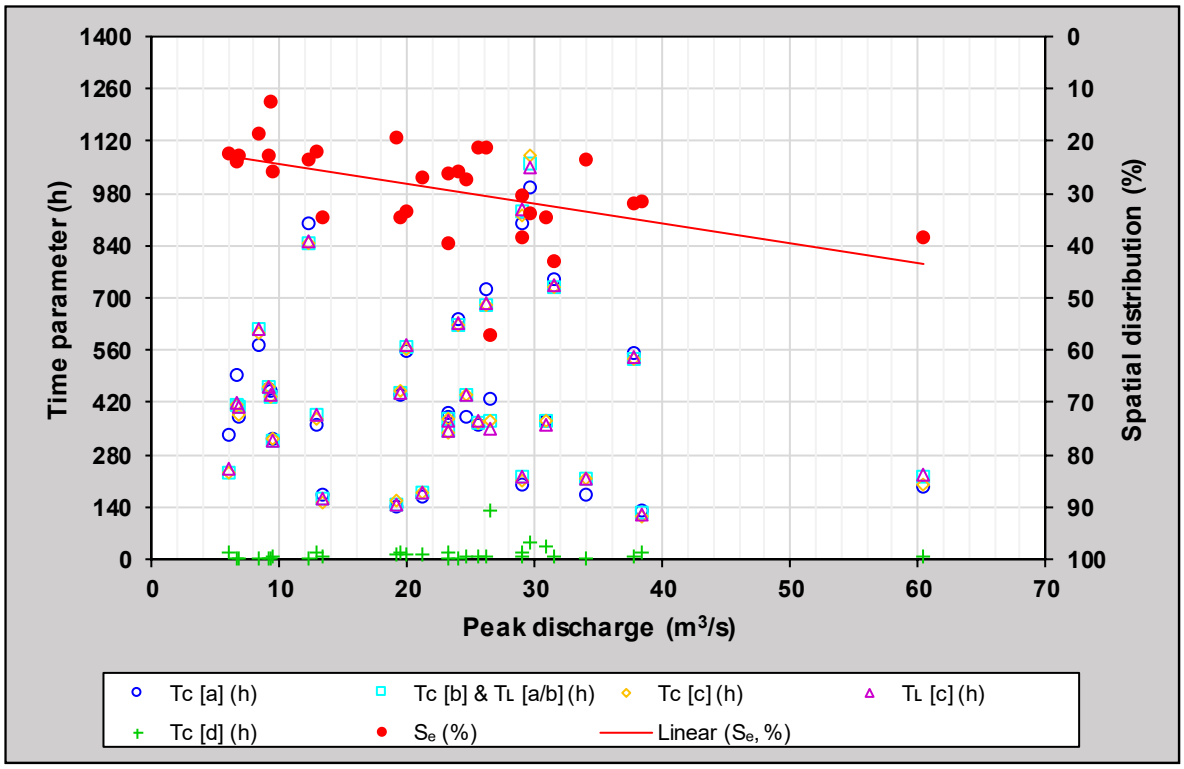

Figure B.30: Time parameters versus the spatial distribution of a rainfall event (S_e) in sub-catchment C5H003

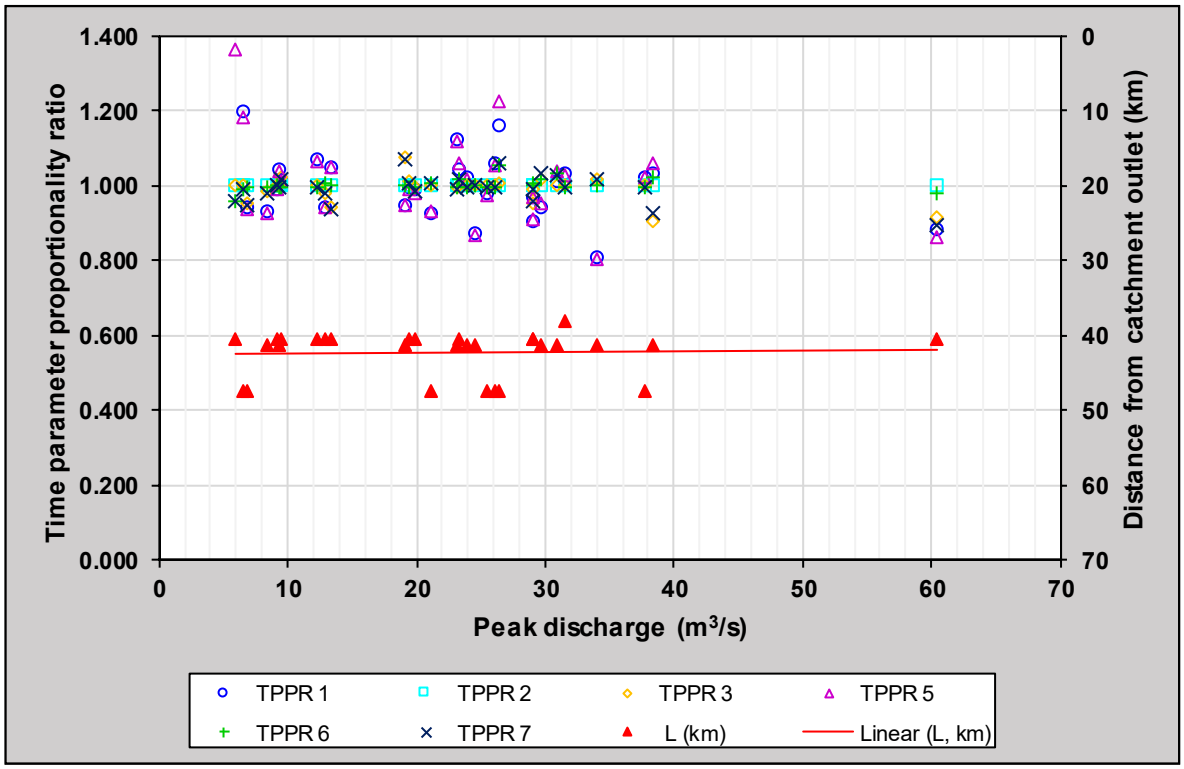

Figure B.31: Time parameter proportionality ratios versus the distance (L) of a rainfall event from the catchment outlet in sub-catchment C5H003

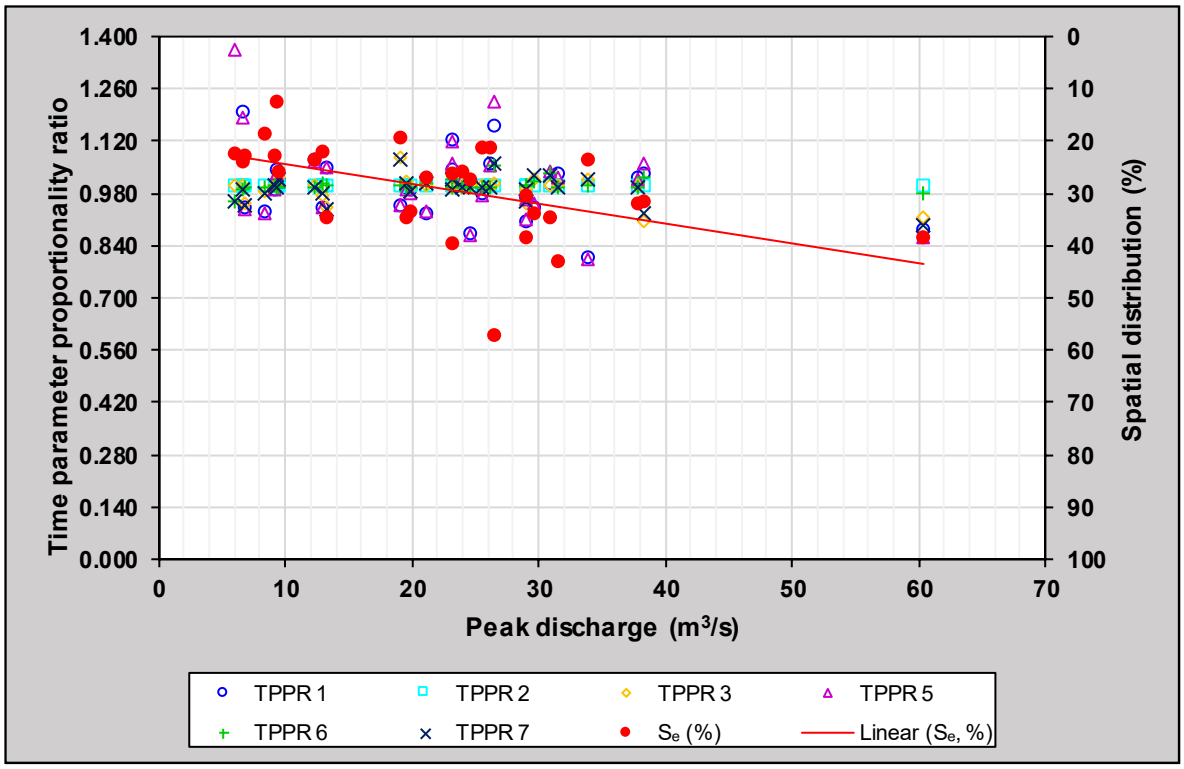

Figure B.32: Time parameter proportionality ratios versus the spatial distribution of a rainfall event (S_e) in sub-catchment C5H003

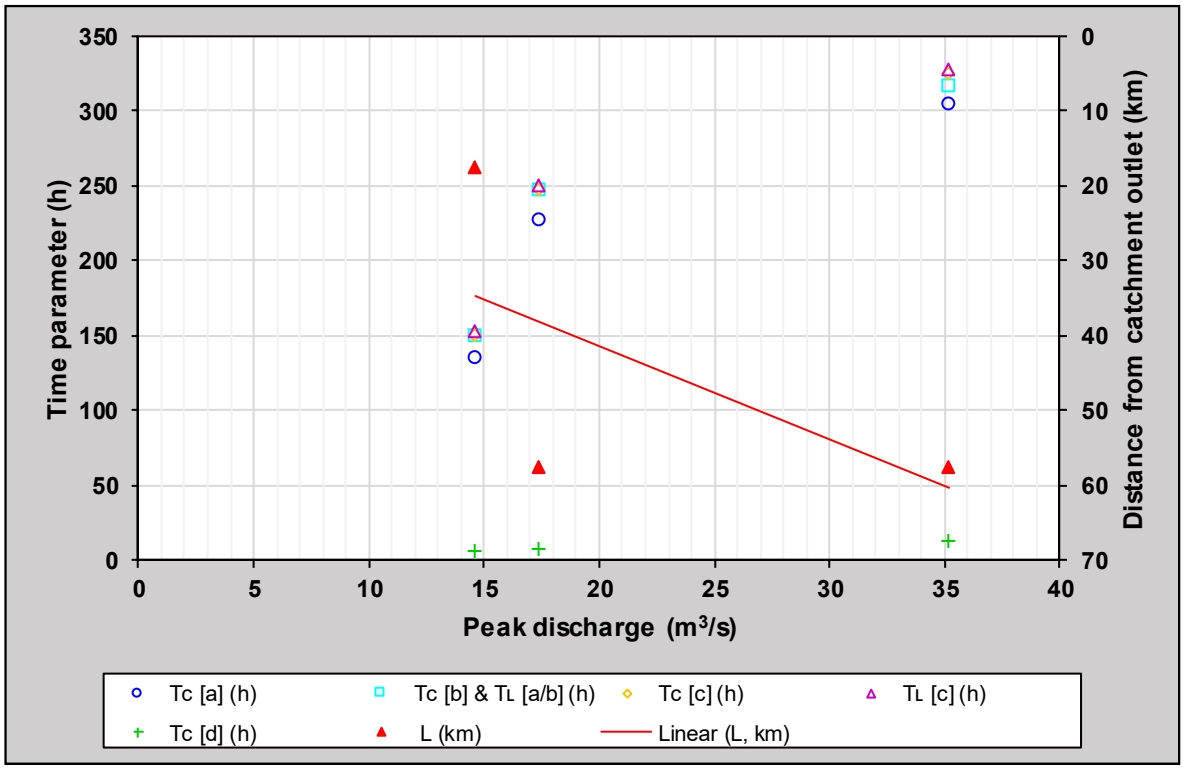

Figure B.33: Time parameters versus the distance (*L*) of a rainfall event from the catchment outlet in sub-catchment C5H006

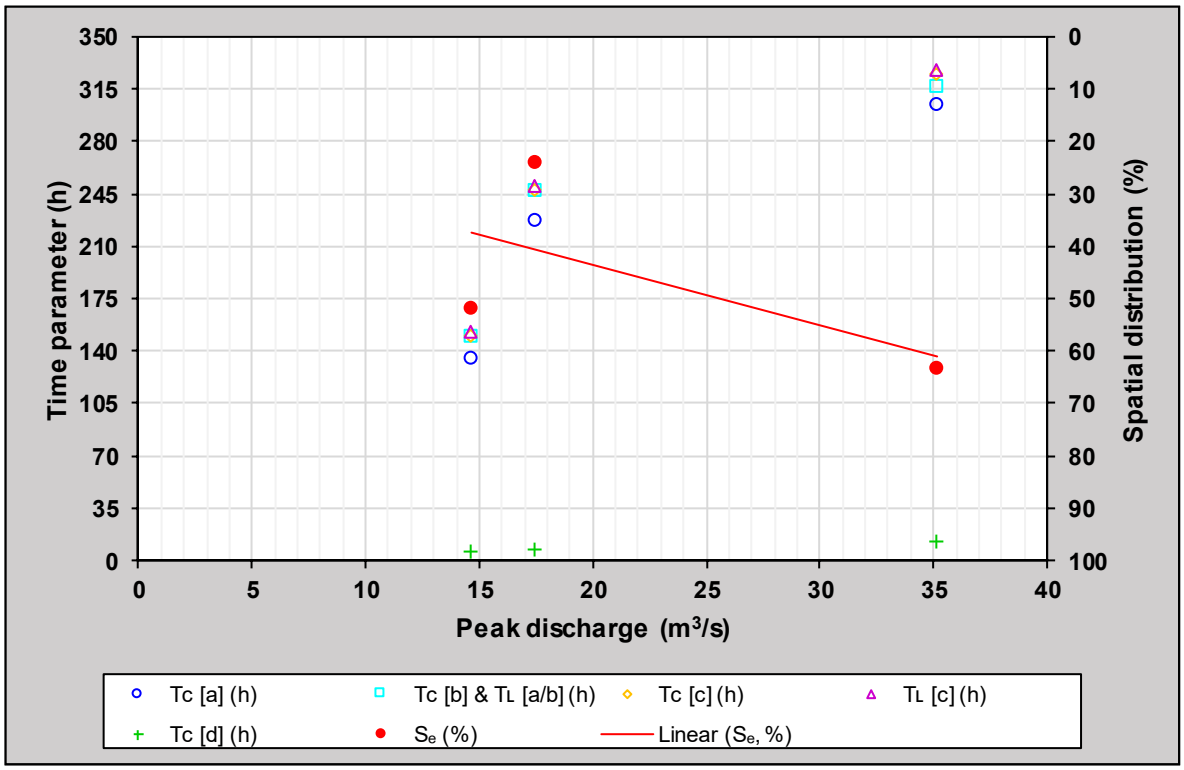

Figure B.34: Time parameters versus the spatial distribution of a rainfall event (S_e) in sub-catchment C5H006

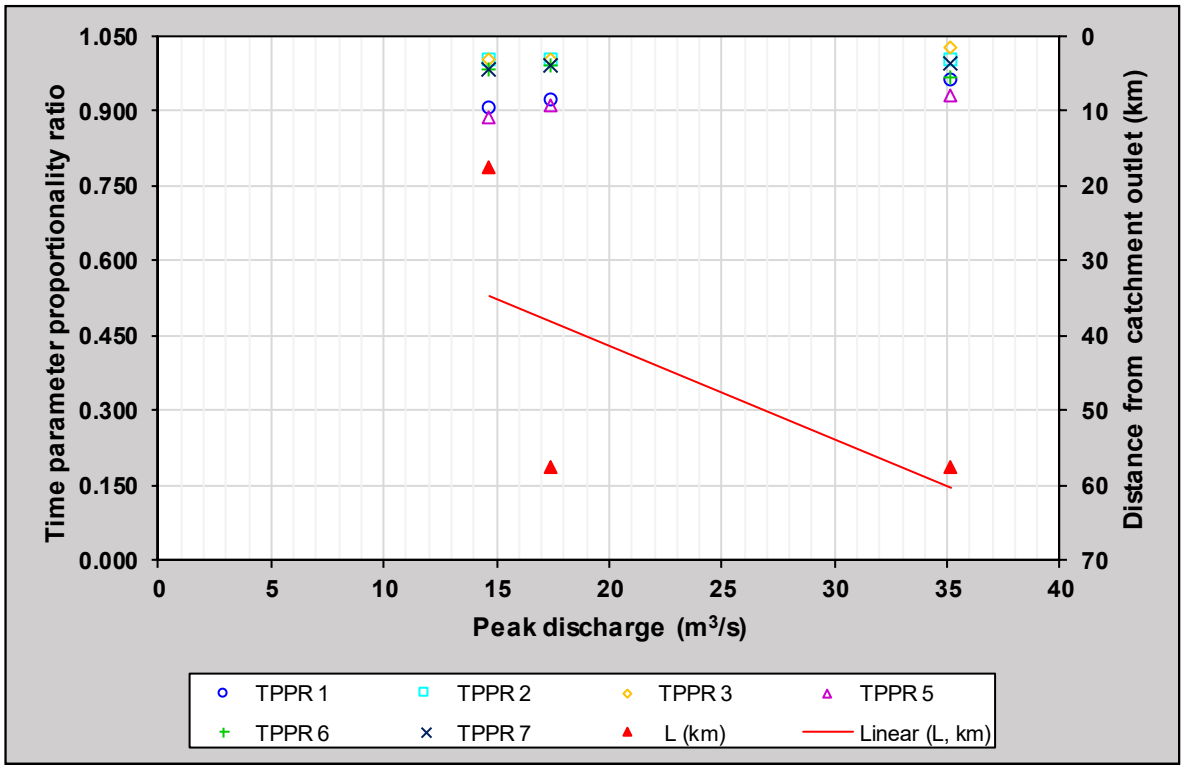

Figure B.35: Time parameter proportionality ratios versus the distance (L) of a rainfall event from the catchment outlet in sub-catchment C5H006

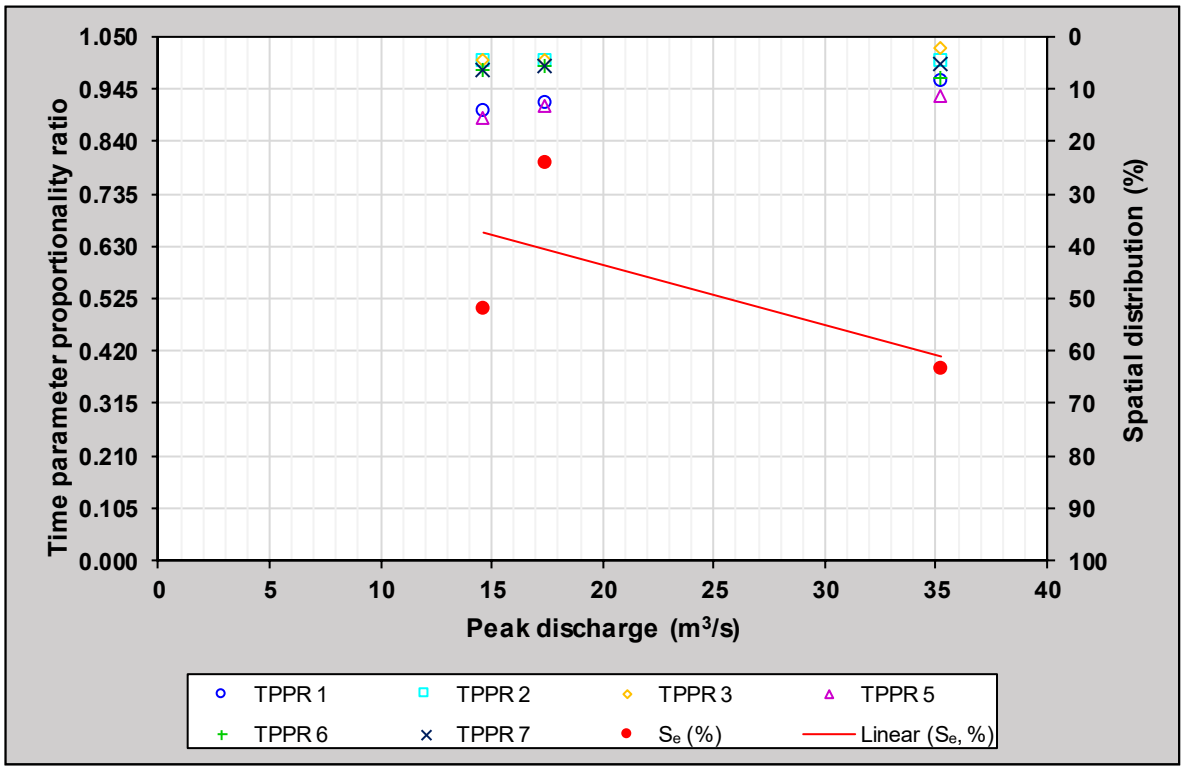

Figure B.36: Time parameter proportionality ratios versus the spatial distribution of a rainfall event (S_e) in sub-catchment C5H006

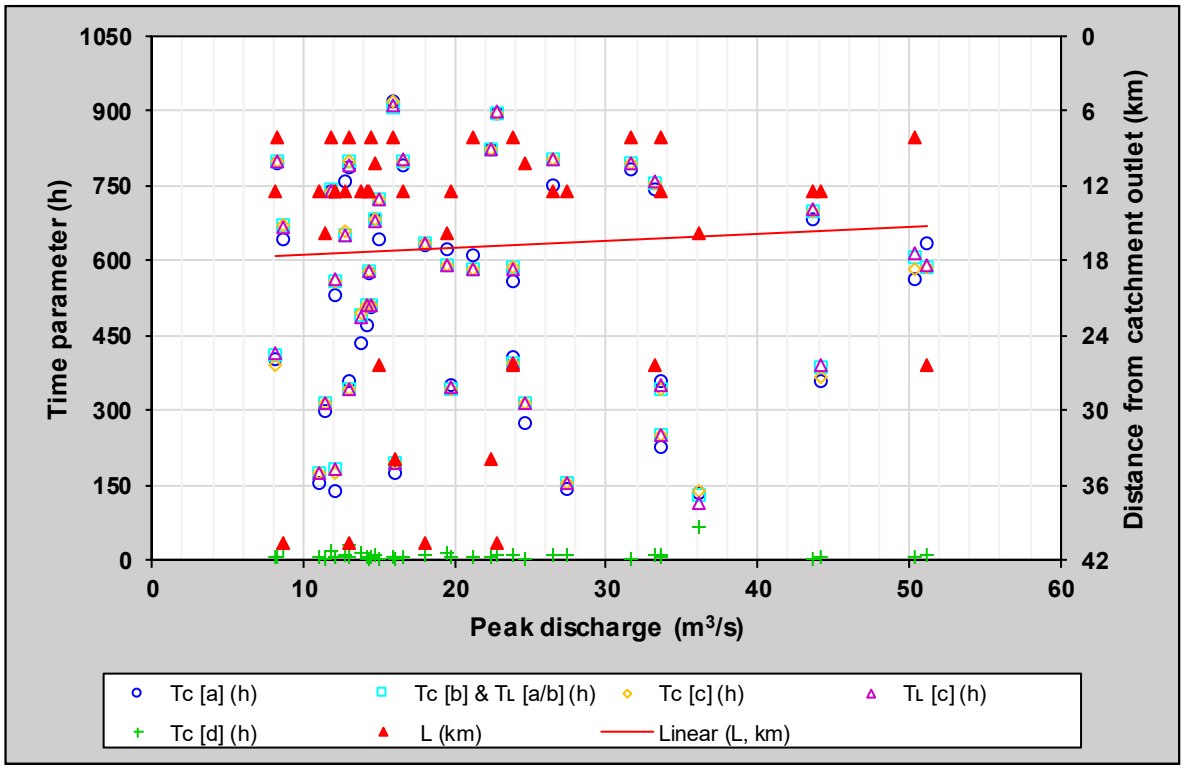

Figure B.37: Time parameters versus the distance (*L*) of a rainfall event from the catchment outlet in sub-catchment C5H007

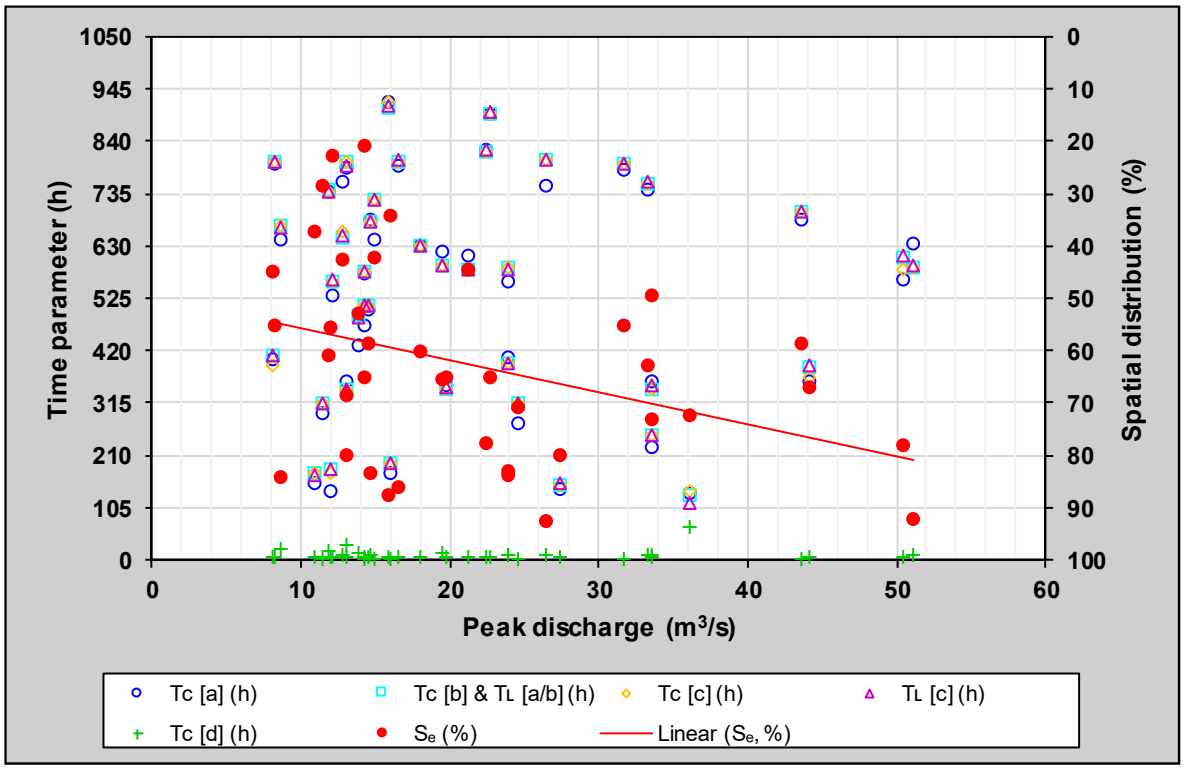

Figure B.38: Time parameters versus the spatial distribution of a rainfall event (S_e) in sub-catchment C5H007

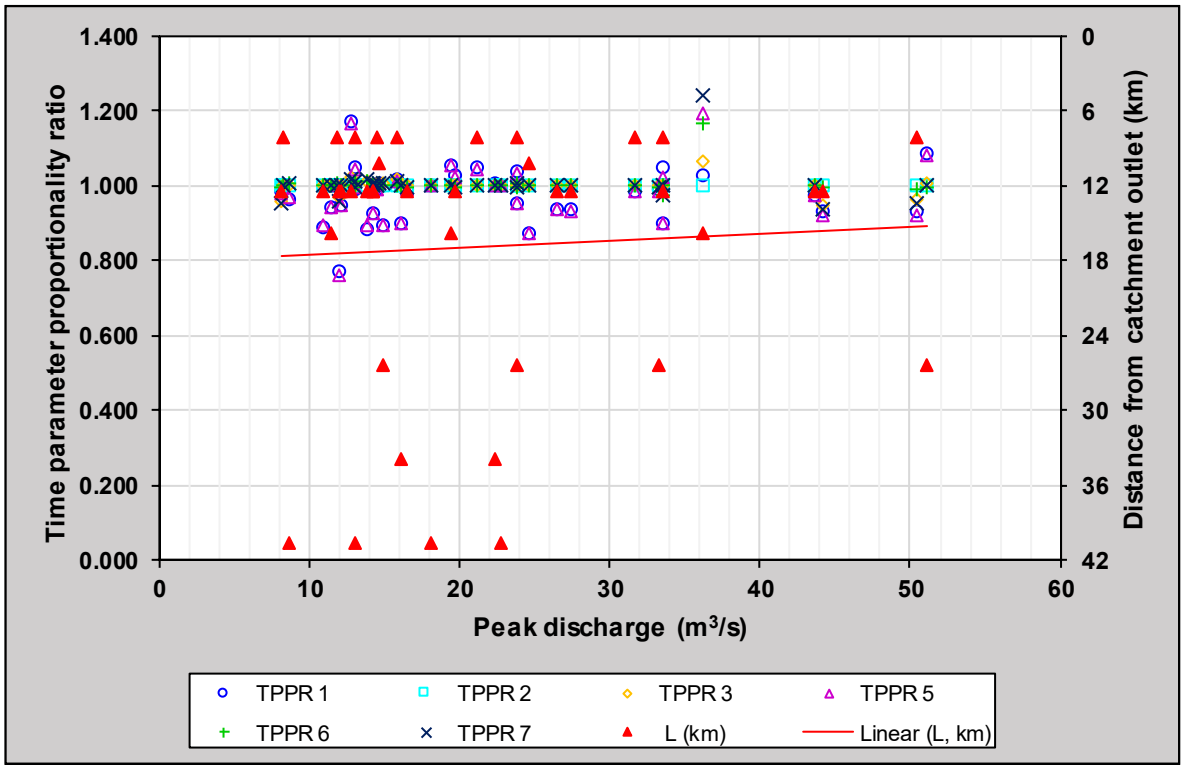

Figure B.39: Time parameter proportionality ratios versus the distance (L) of a rainfall event from the catchment outlet in sub-catchment C5H007

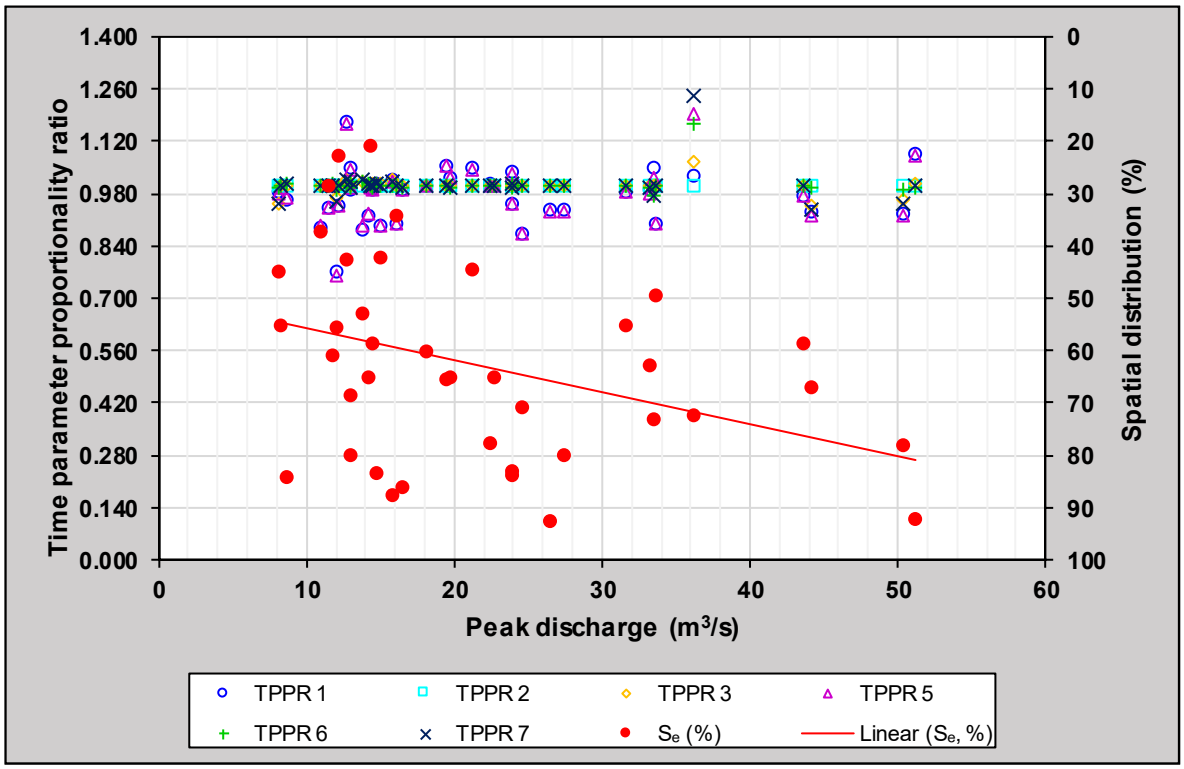

Figure B.40: Time parameter proportionality ratios versus the spatial distribution of a rainfall event (S_e) in sub-catchment C5H007

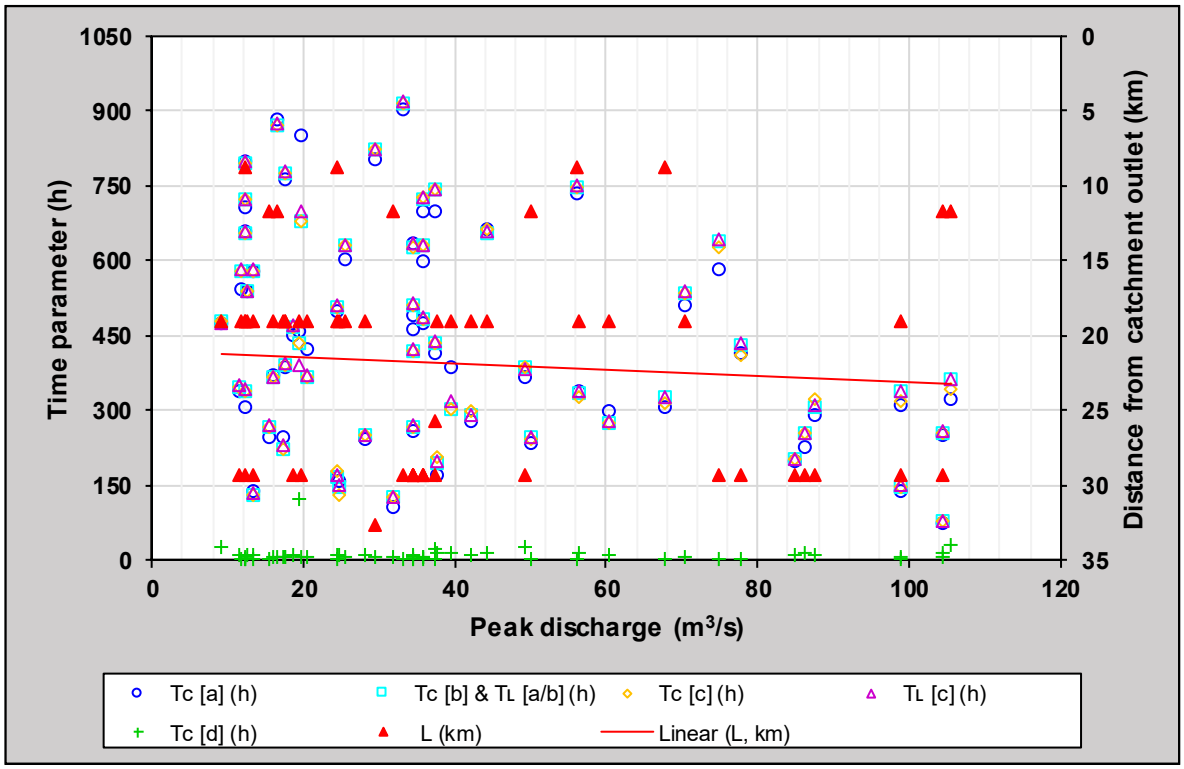

Figure B.41: Time parameters versus the distance (L) of a rainfall event from the catchment outlet in sub-catchment C5H008

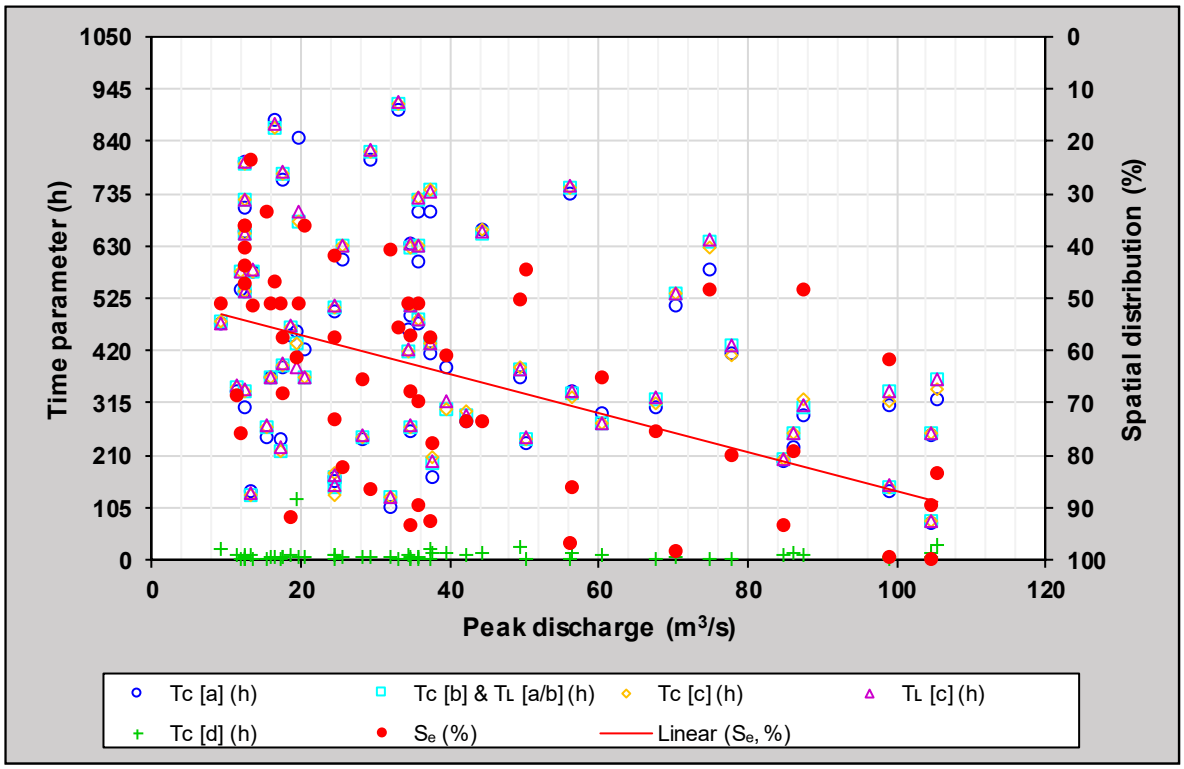

Figure B.42: Time parameters versus the spatial distribution of a rainfall event (S_e) in sub-catchment C5H008

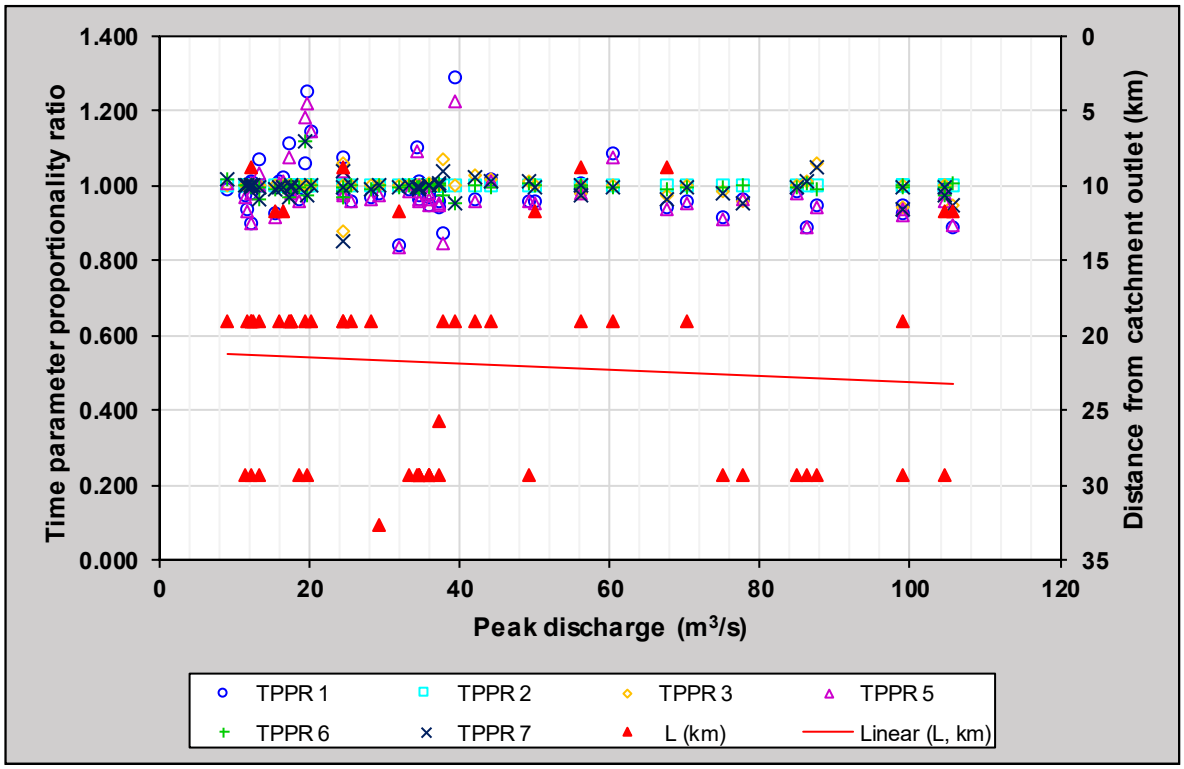

Figure B.43: Time parameter proportionality ratios versus the distance (L) of a rainfall event from the catchment outlet in sub-catchment C5H008

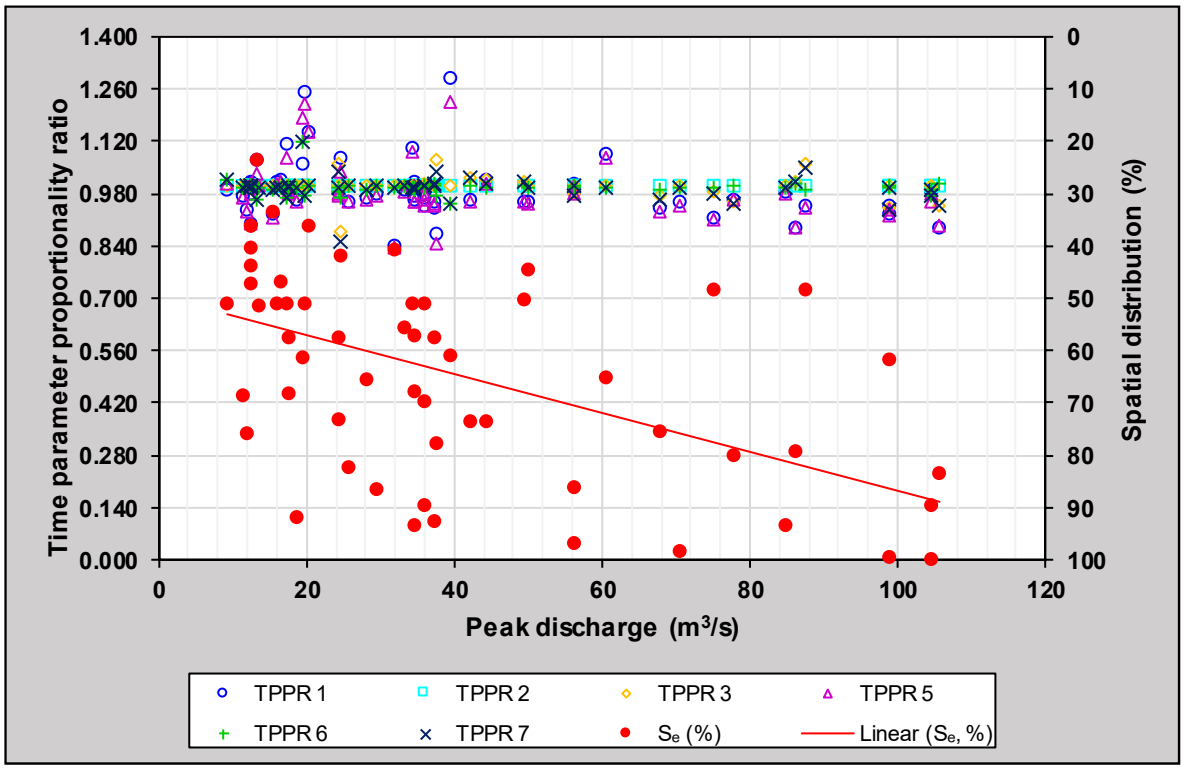

Figure B.44: Time parameter proportionality ratios versus the spatial distribution of a rainfall event (S_e) in sub-catchment C5H008

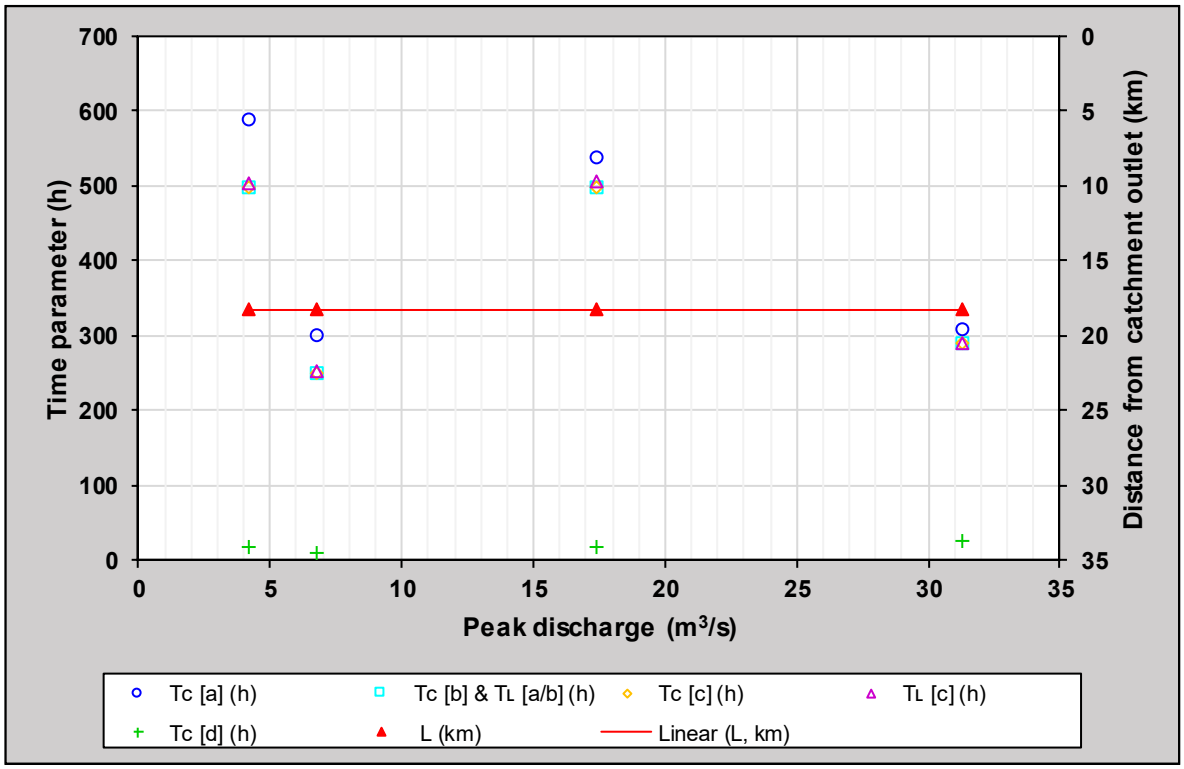

Figure B.45: Time parameters versus the distance (*L*) of a rainfall event from the catchment outlet in sub-catchment C5H009

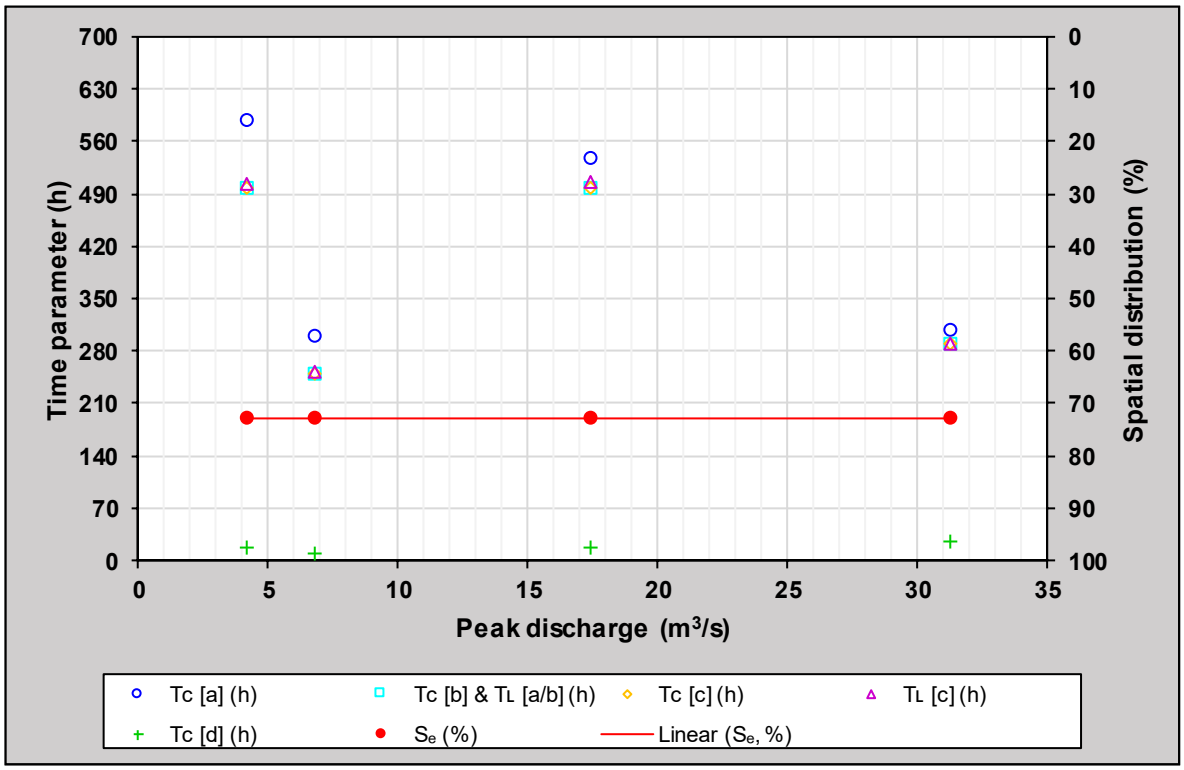

Figure B.46: Time parameters versus the spatial distribution of a rainfall event (S_e) in sub-catchment C5H009

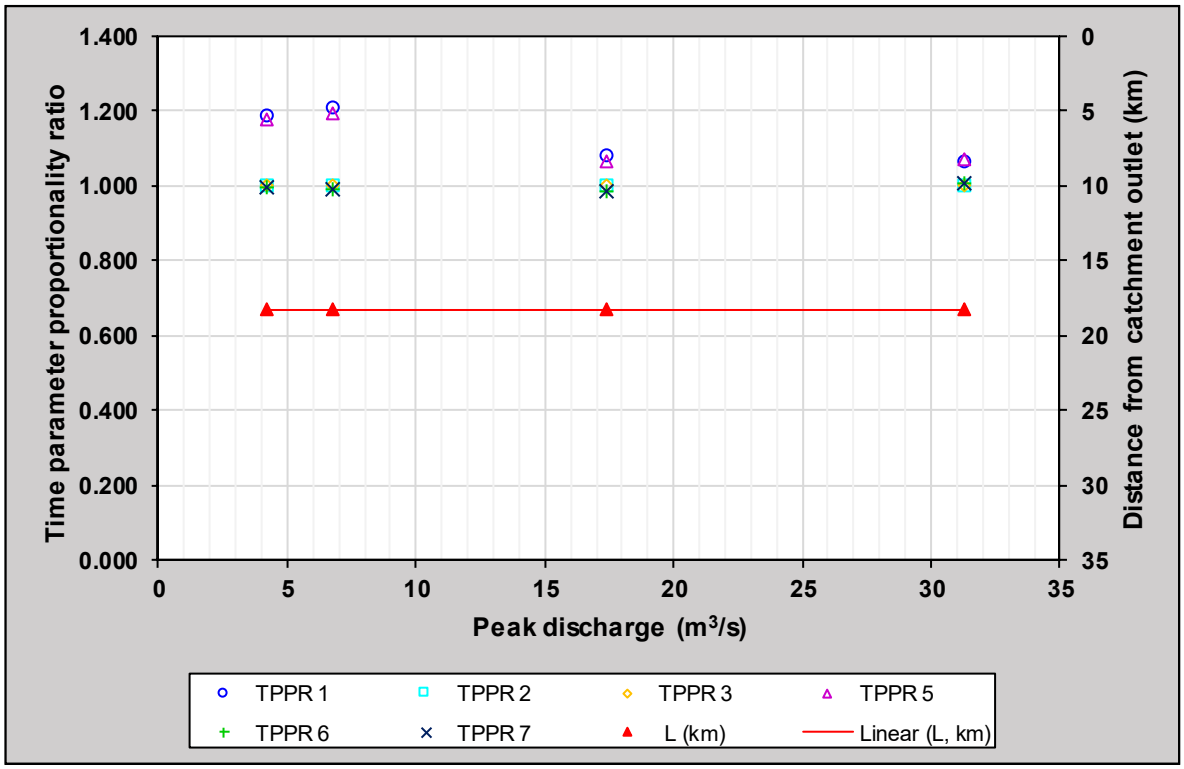

Figure B.47: Time parameter proportionality ratios versus the distance (L) of a rainfall event from the catchment outlet in sub-catchment C5H009

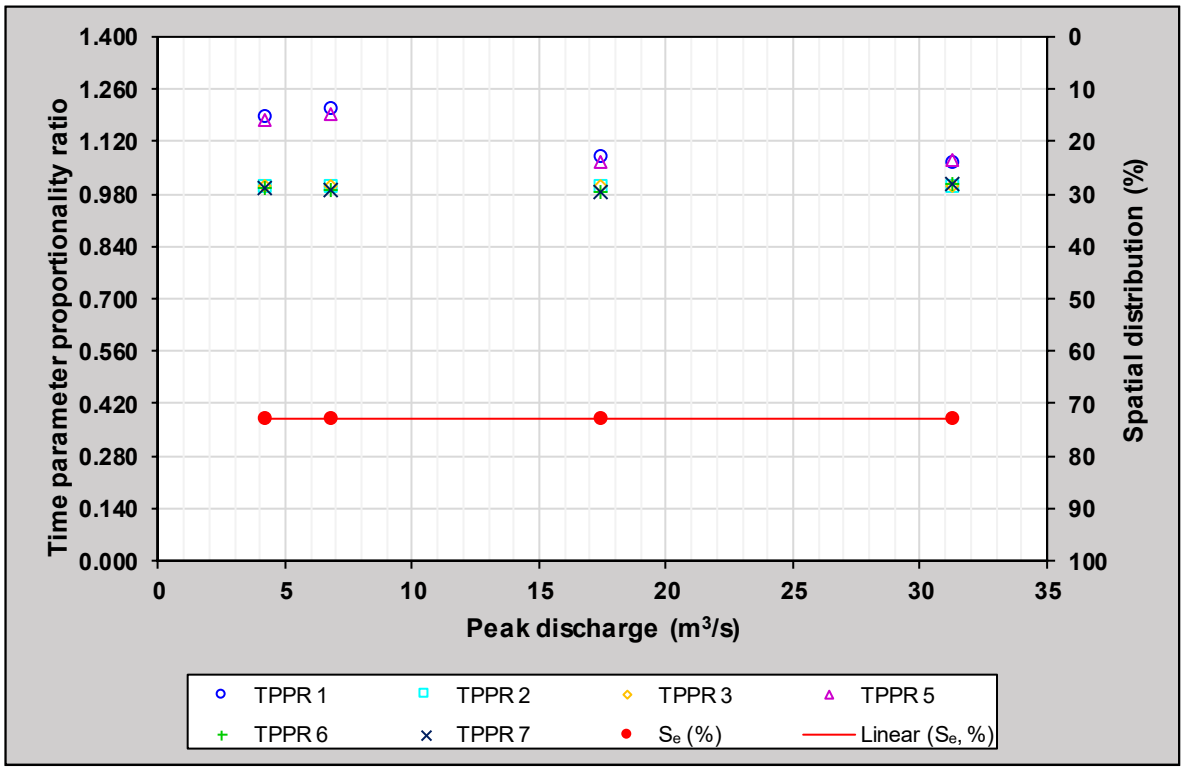

Figure B.48: Time parameter proportionality ratios versus the spatial distribution of a rainfall event (S_e) in sub-catchment C5H009

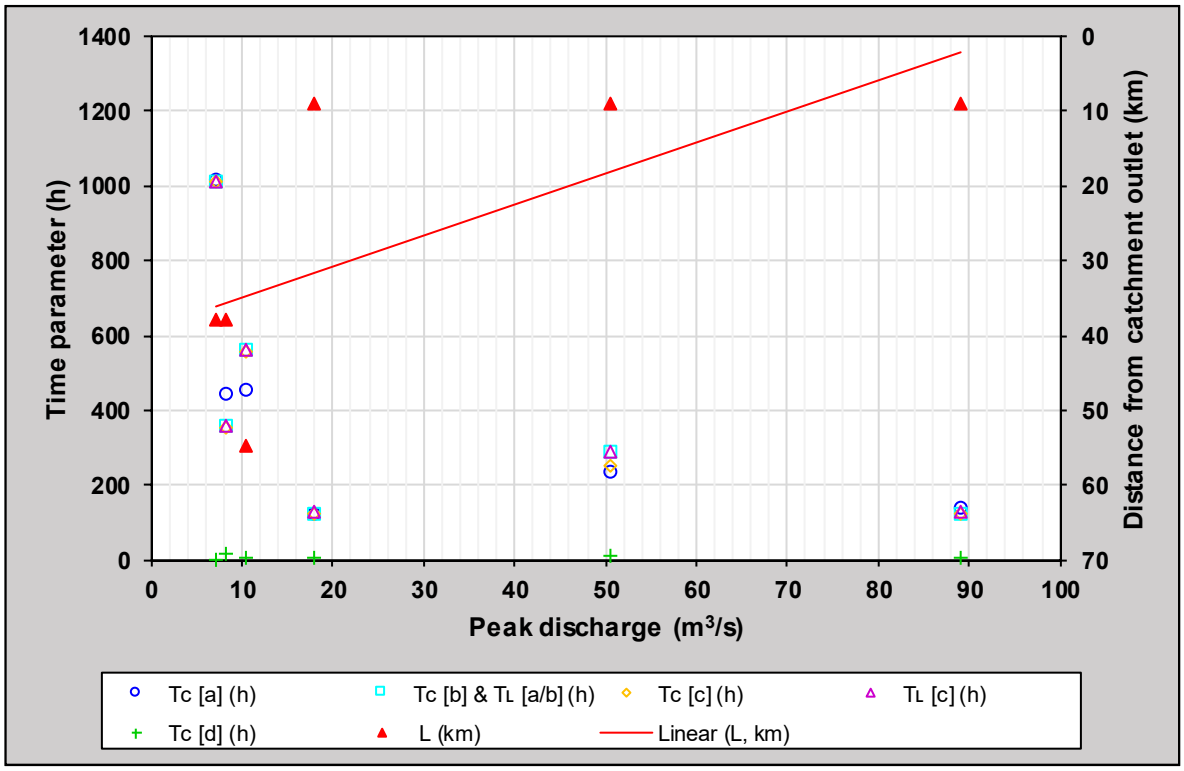

Figure B.49: Time parameters versus the distance (L) of a rainfall event from the catchment outlet in sub-catchment C5H012

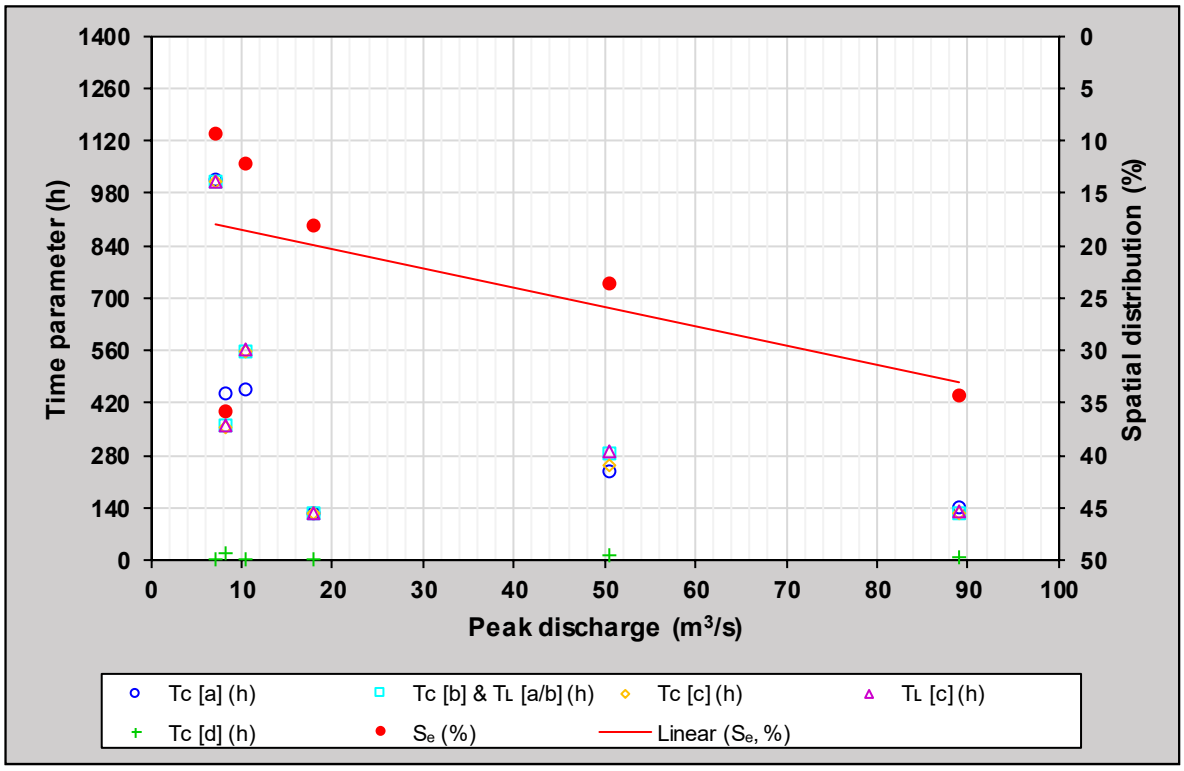

Figure B.50: Time parameters versus the spatial distribution of a rainfall event (S_e) in sub-catchment C5H012

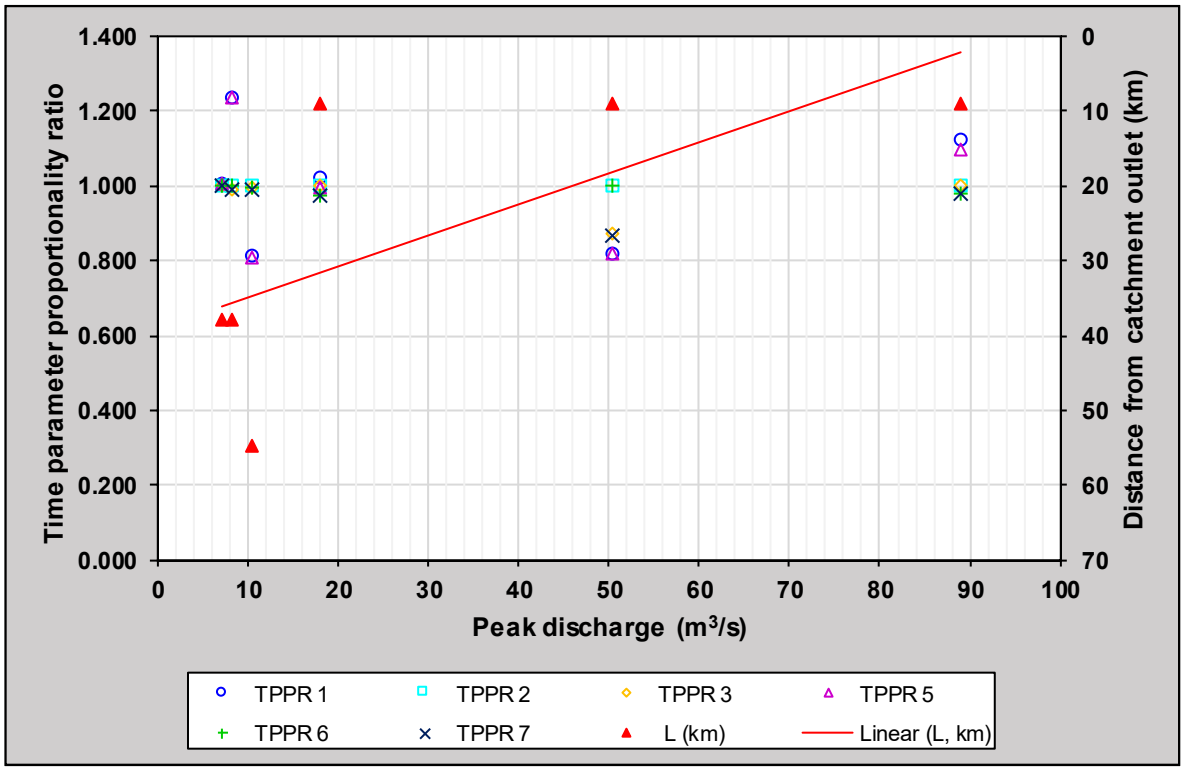

Figure B.51: Time parameter proportionality ratios versus the distance (L) of a rainfall event from the catchment outlet in sub-catchment C5H012

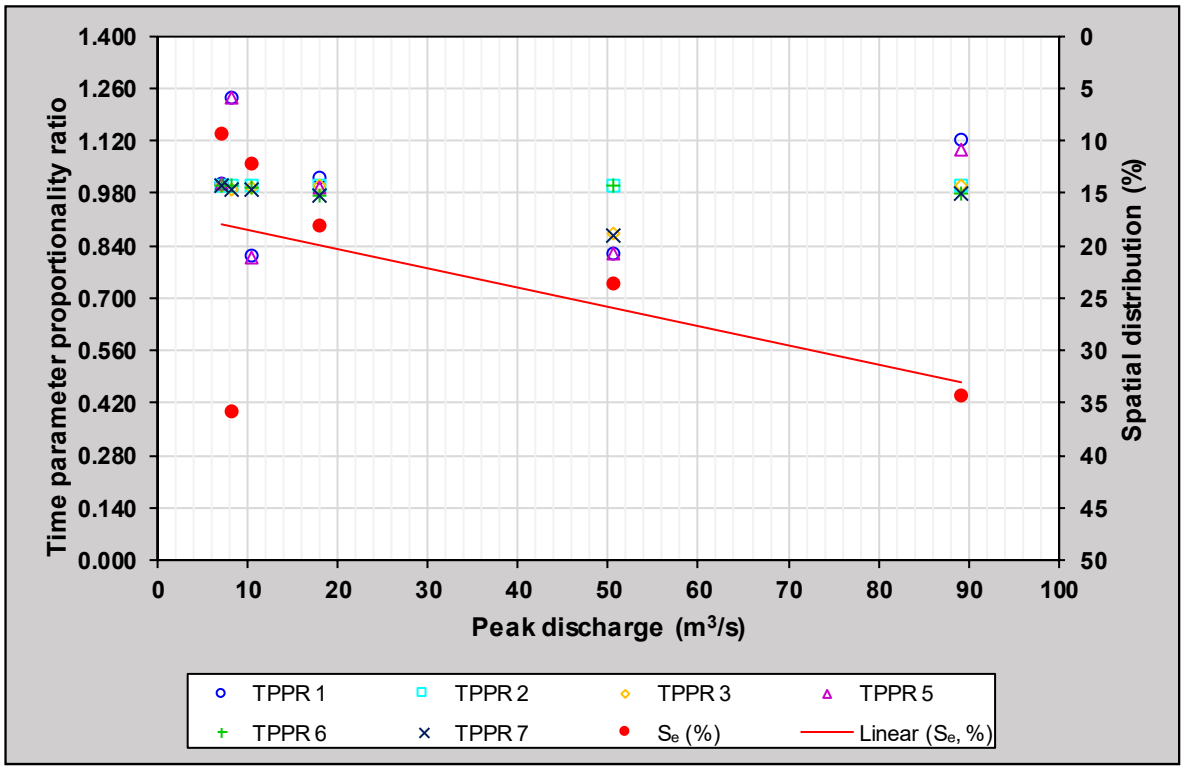

Figure B.52: Time parameter proportionality ratios versus the spatial distribution of a rainfall event (S_e) in sub-catchment C5H012

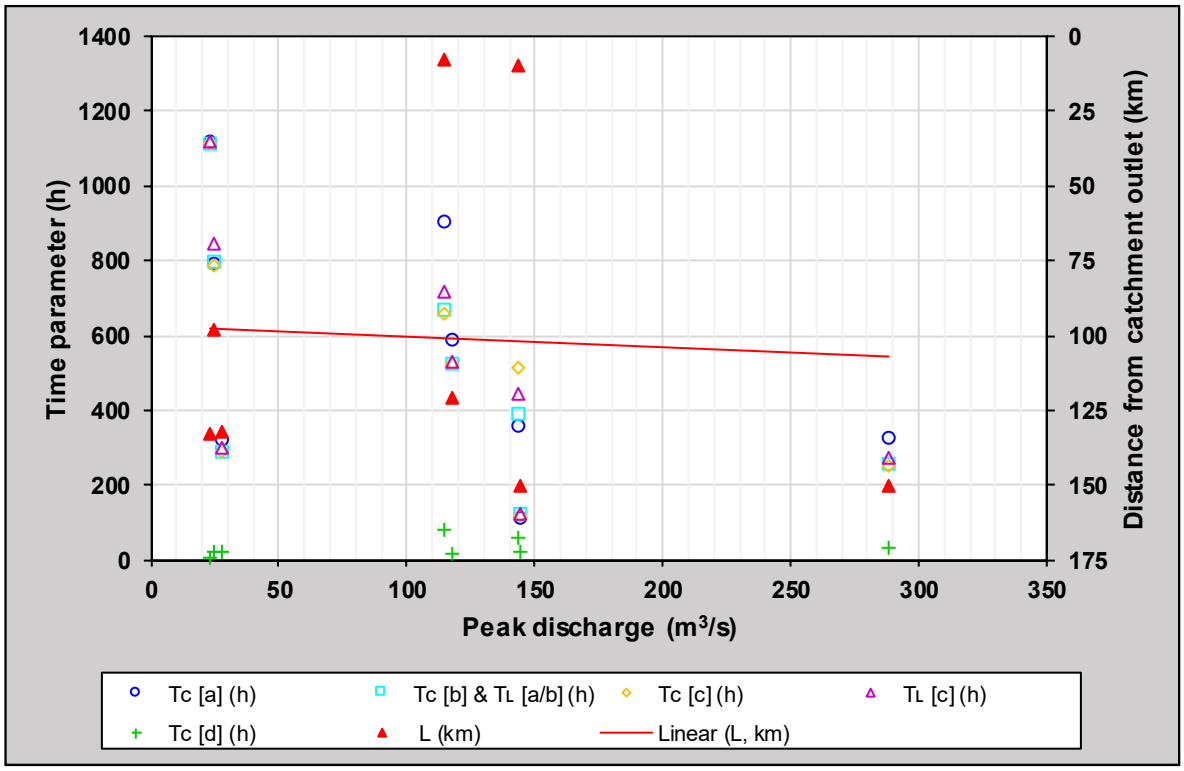

Figure B.53: Time parameters versus the distance (L) of a rainfall event from the catchment outlet in sub-catchment C5H014

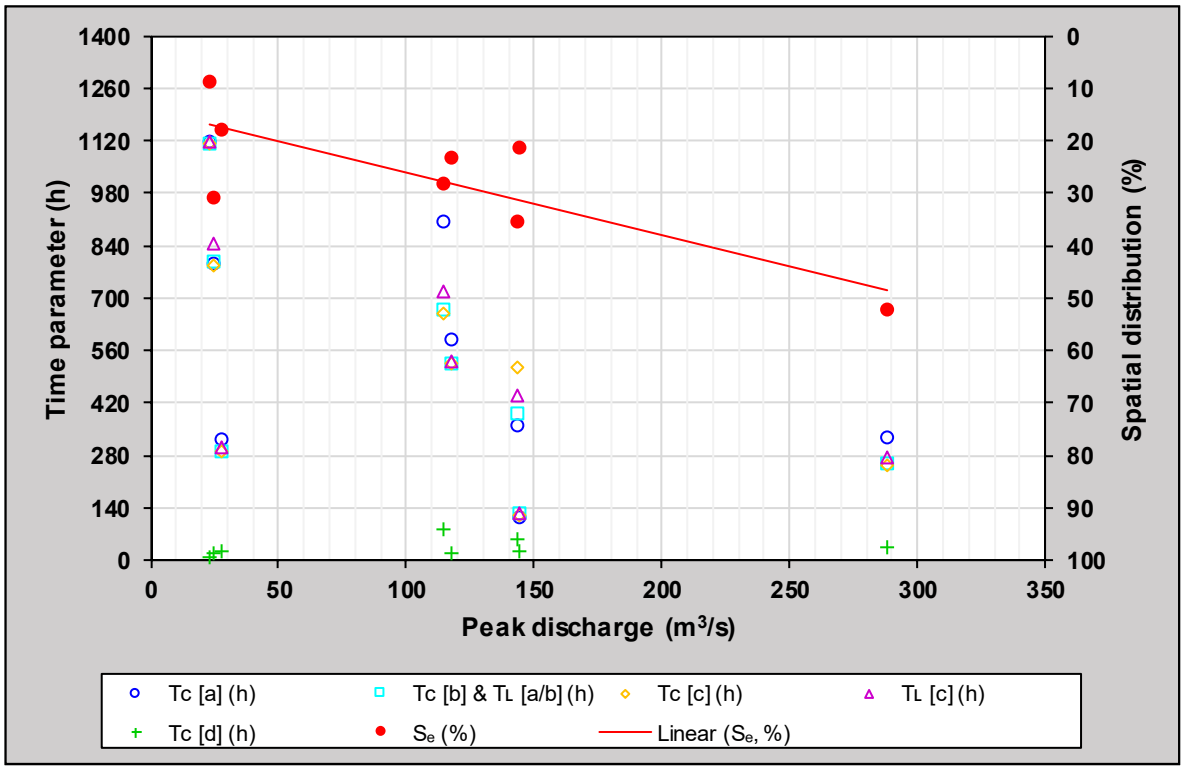

Figure B.54: Time parameters versus the spatial distribution of a rainfall event (S_e) in sub-catchment C5H014

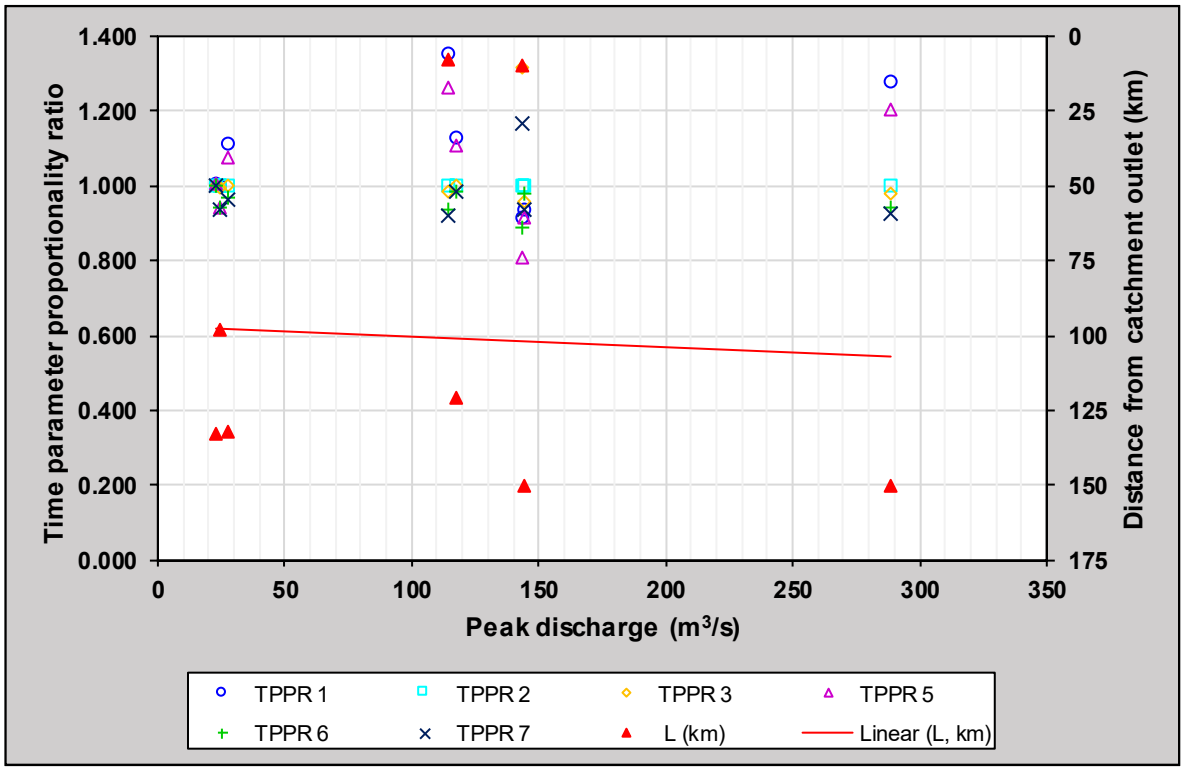

Figure B.55: Time parameter proportionality ratios versus the distance (*L*) of a rainfall event from the catchment outlet in sub-catchment C5H014

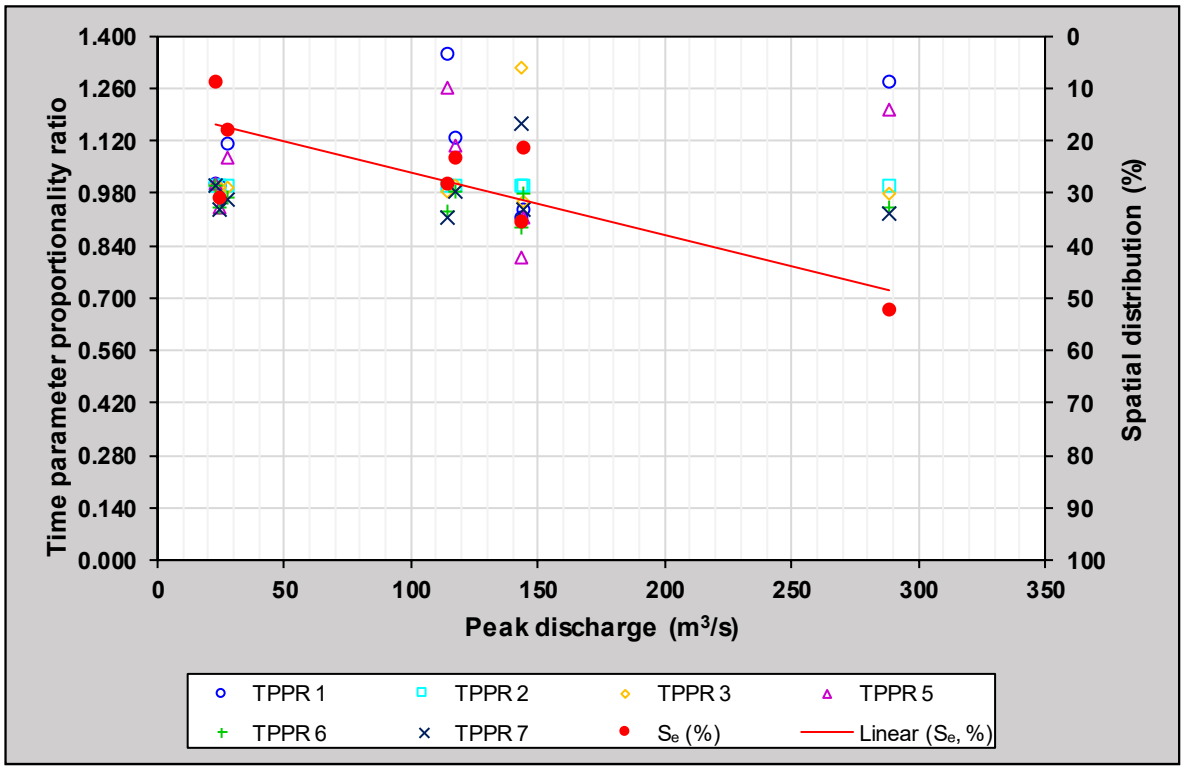

Figure B.56: Time parameter proportionality ratios versus the spatial distribution of a rainfall event (S_e) in sub-catchment C5H014

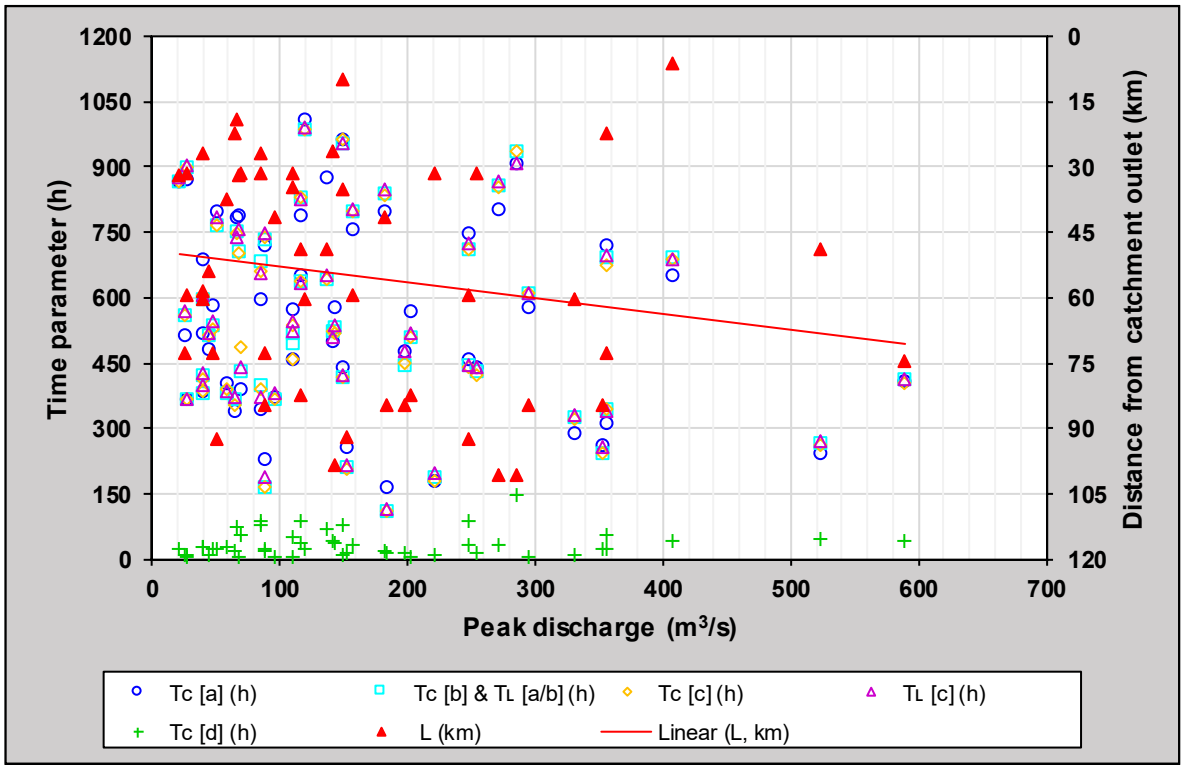

Figure B.57: Time parameters versus the distance (L) of a rainfall event from the catchment outlet in sub-catchment C5H015

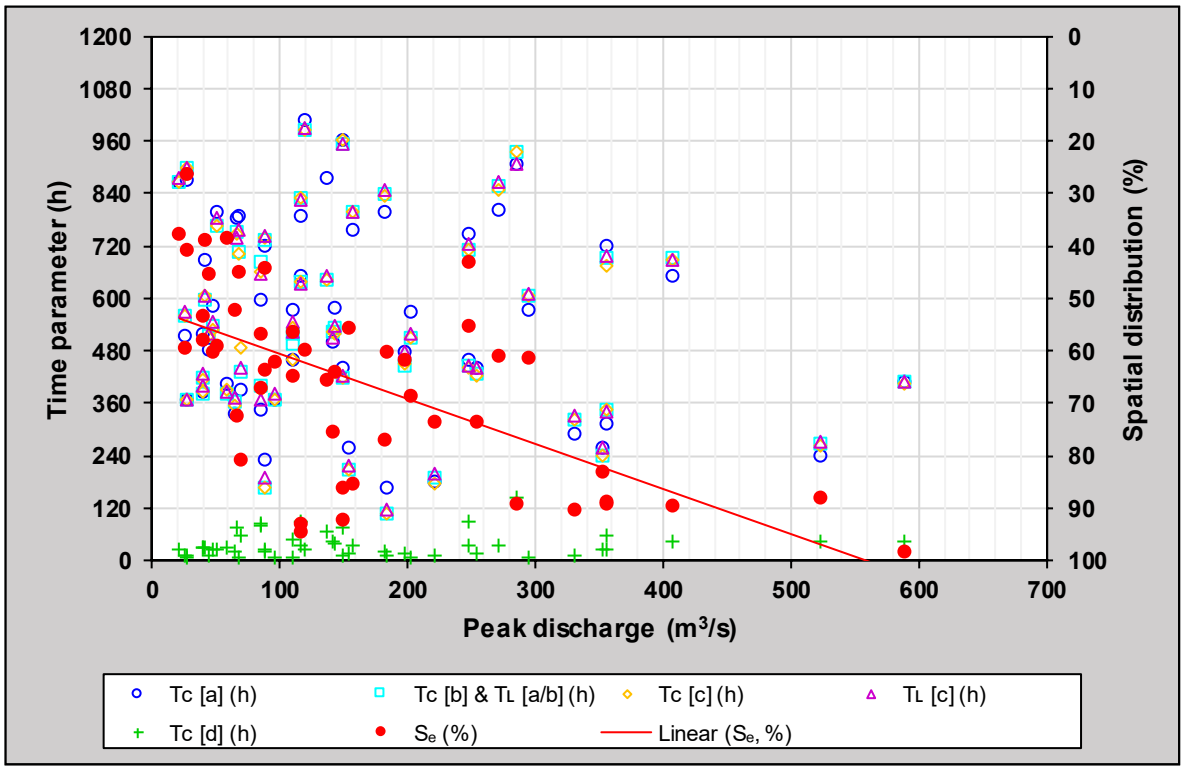

Figure B.58: Time parameters versus the spatial distribution of a rainfall event (S_e) in sub-catchment C5H015

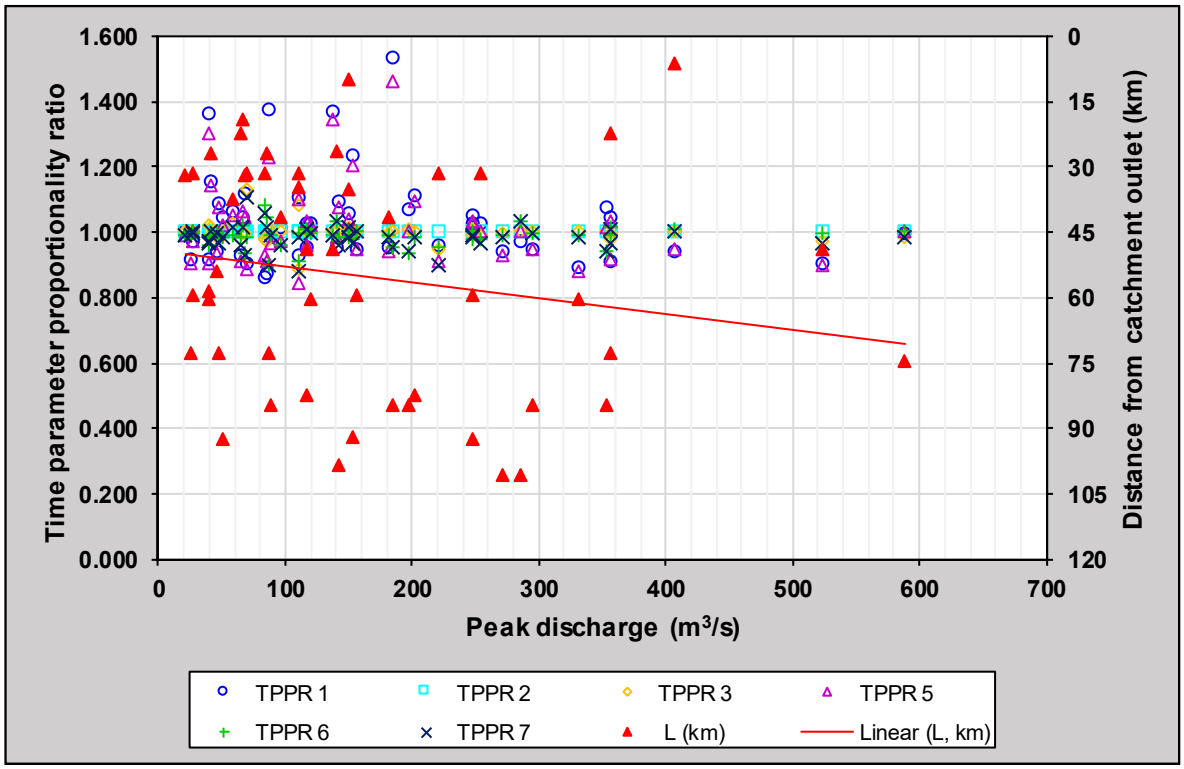

Figure B.59: Time parameter proportionality ratios versus the distance (L) of a rainfall event from the catchment outlet in sub-catchment C5H015

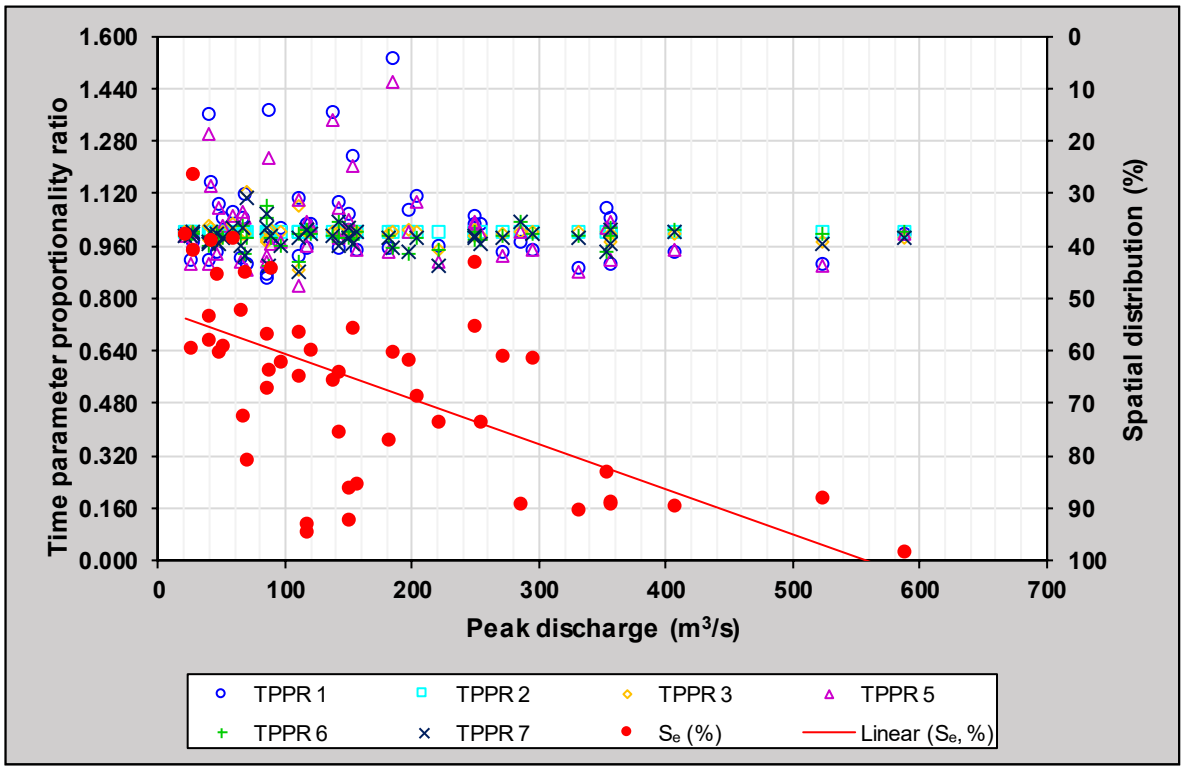

Figure B.60: Time parameter proportionality ratios versus the spatial distribution of a rainfall event (S_e) in sub-catchment C5H015

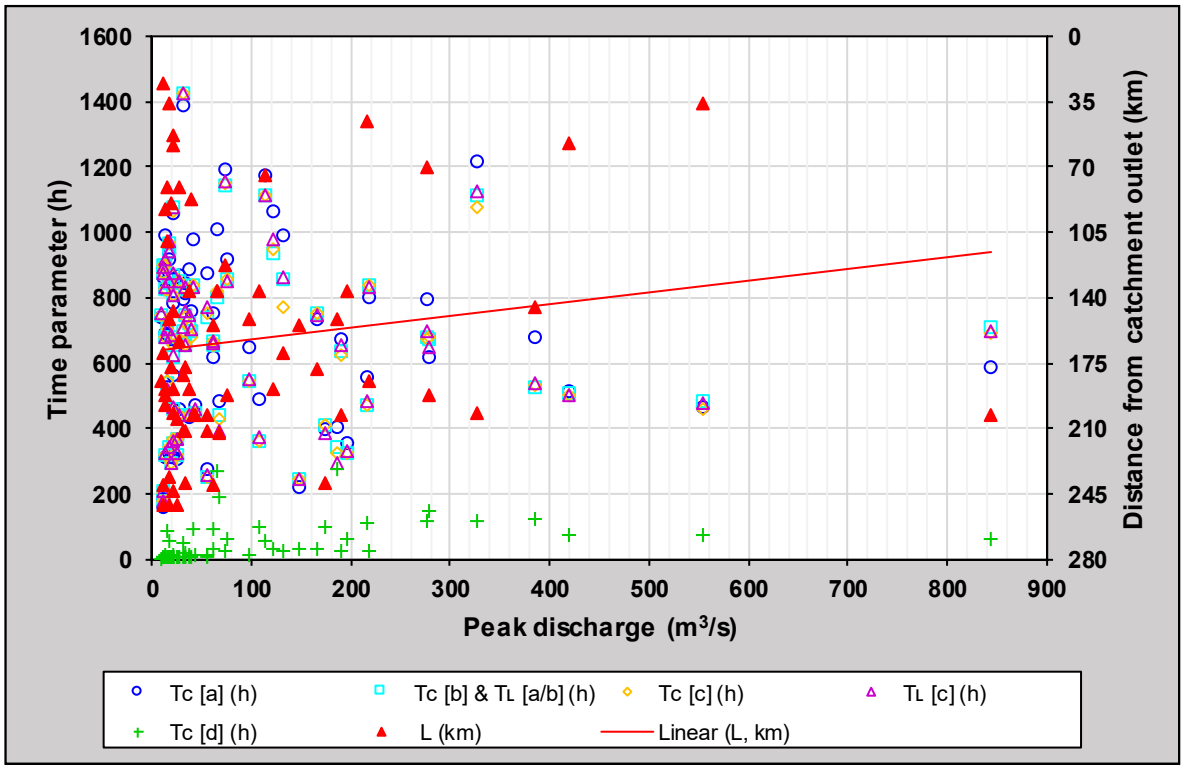

Figure B.61: Time parameters versus the distance (L) of a rainfall event from the catchment outlet in sub-catchment C5H016

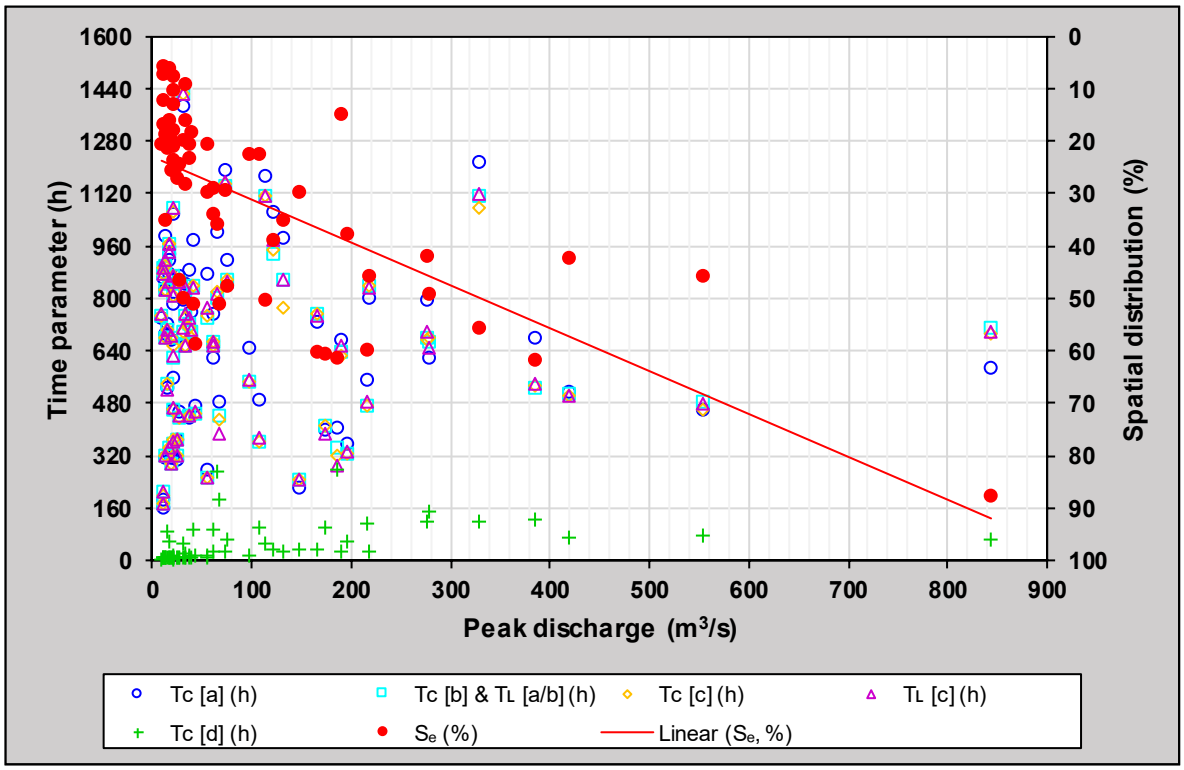

Figure B.62: Time parameters versus the spatial distribution of a rainfall event (S_e) in sub-catchment C5H016

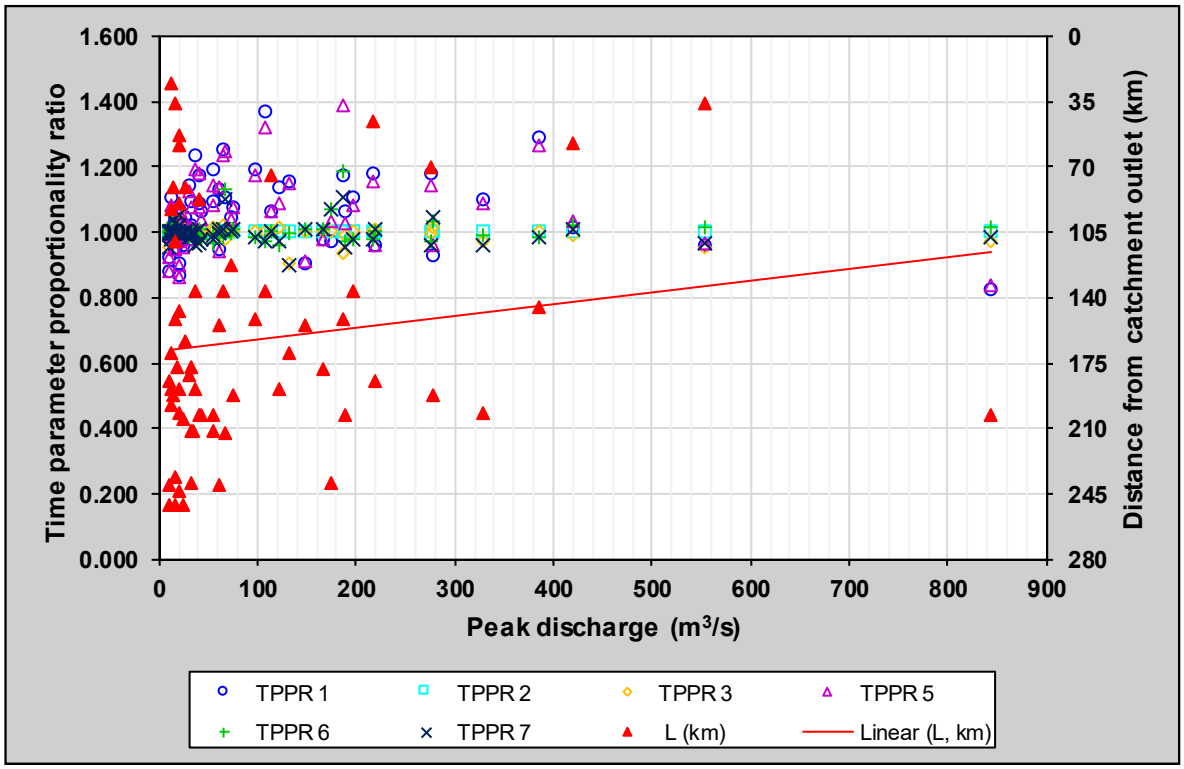

Figure B.63: Time parameter proportionality ratios versus the distance (L) of a rainfall event from the catchment outlet in sub-catchment C5H016

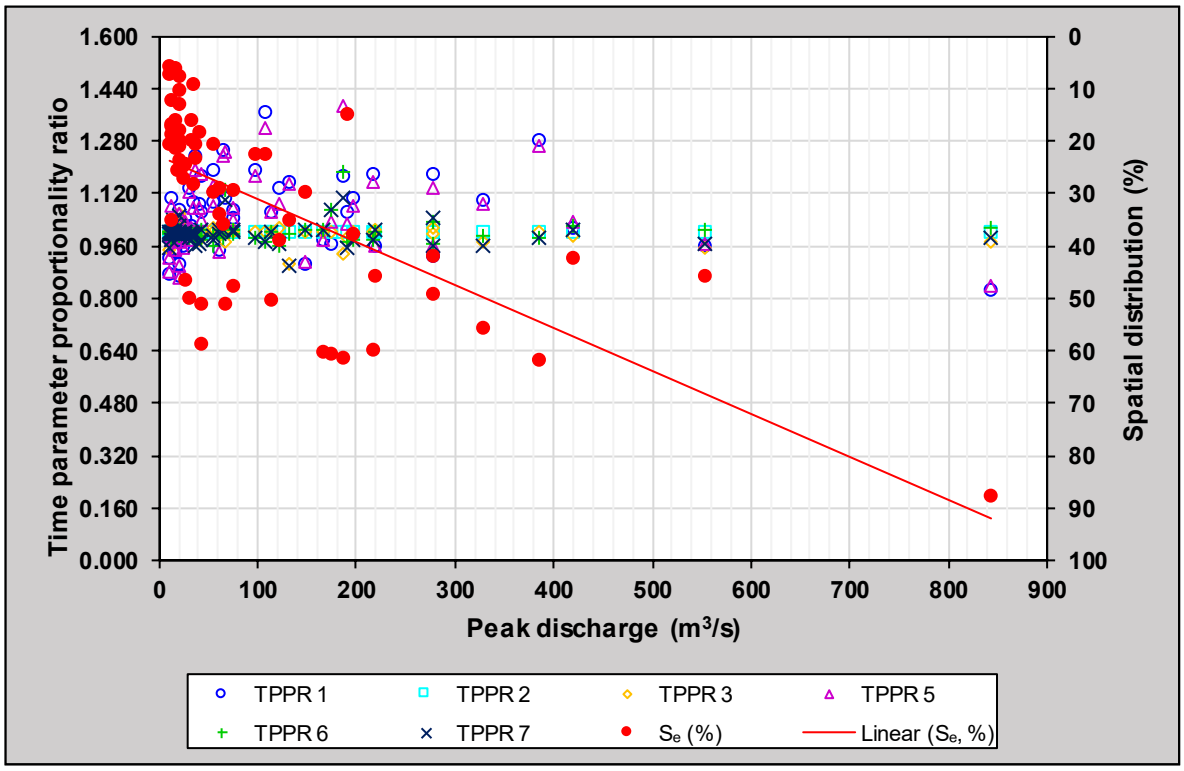

Figure B.64: Time parameter proportionality ratios versus the spatial distribution of a rainfall event (S_e) in sub-catchment C5H016

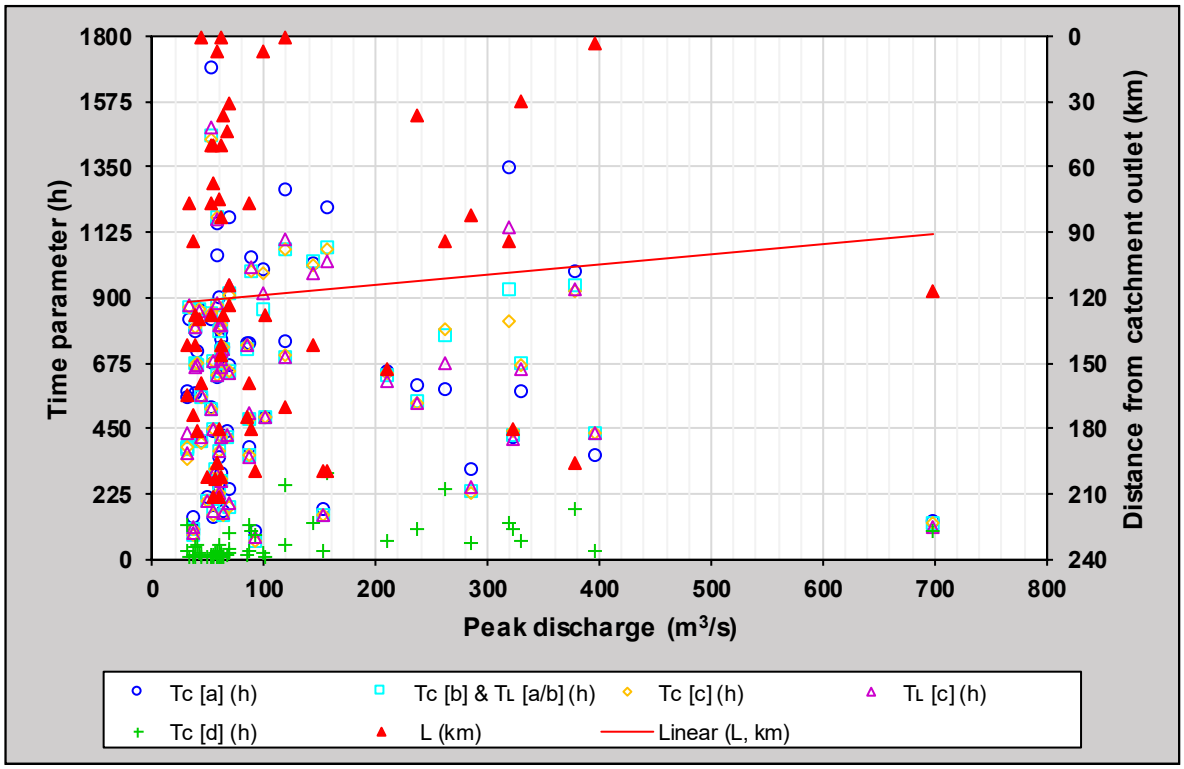

Figure B.65: Time parameters versus the distance (*L*) of a rainfall event from the catchment outlet in sub-catchment C5H018

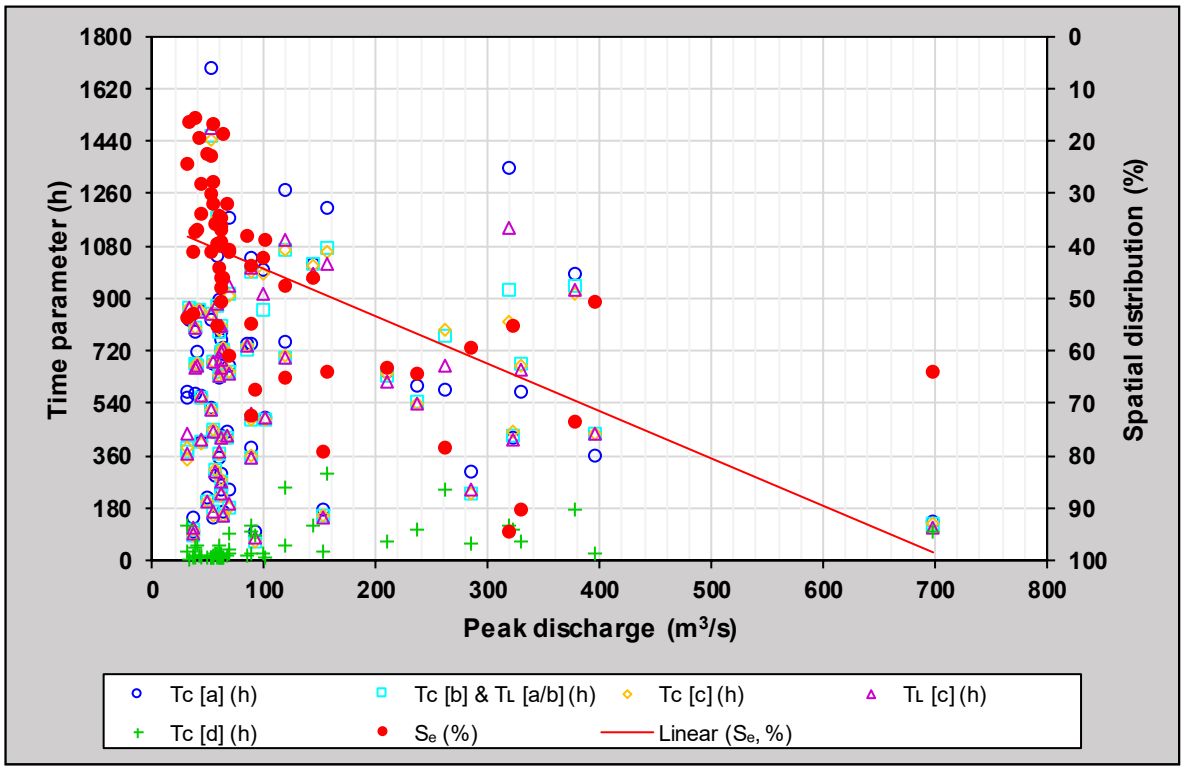

Figure B.66: Time parameters versus the spatial distribution of a rainfall event (S_e) in sub-catchment C5H018

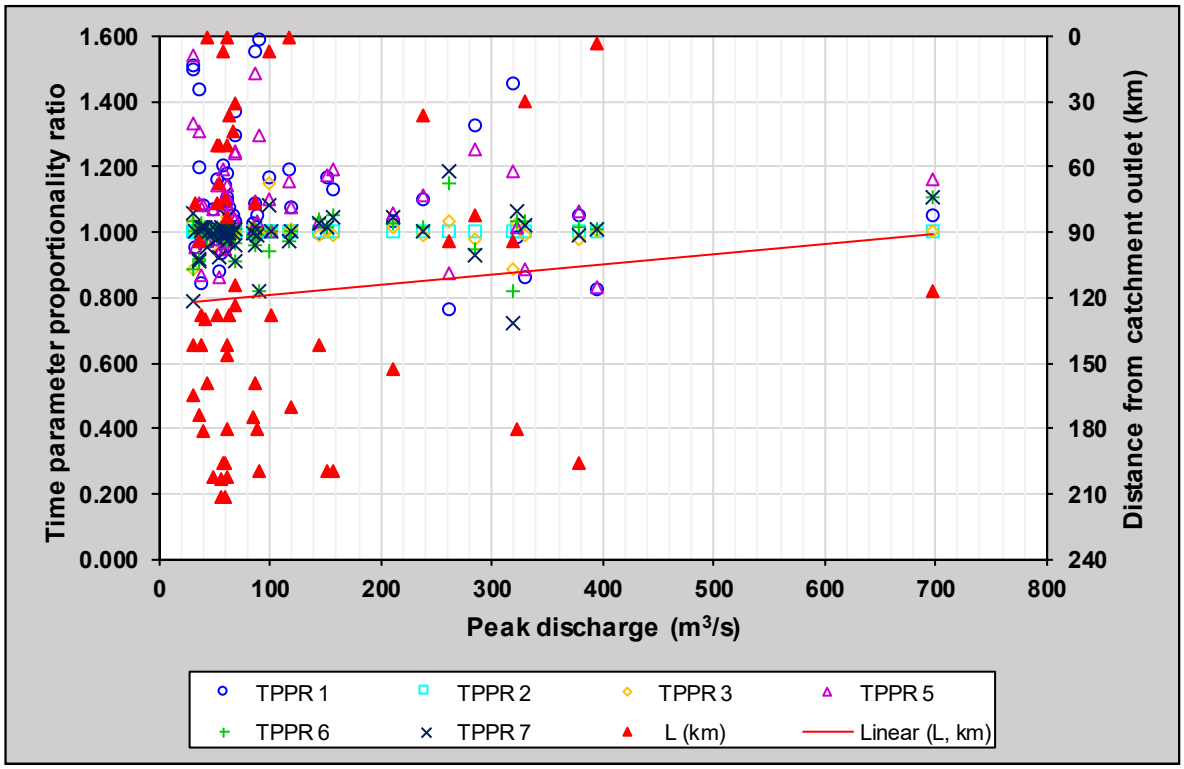

Figure B.67: Time parameter proportionality ratios versus the distance (L) of a rainfall event from the catchment outlet in sub-catchment C5H018

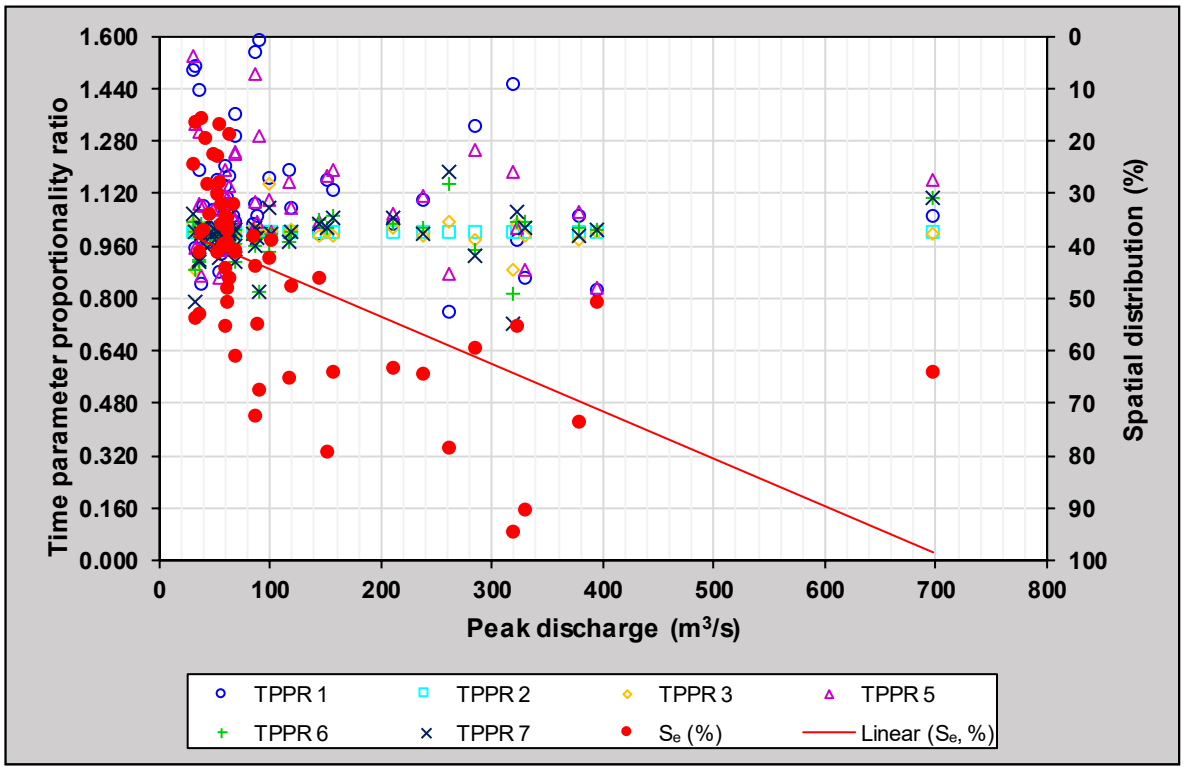

Figure B.68: Time parameter proportionality ratios versus the spatial distribution of a rainfall event (S_e) in sub-catchment C5H018

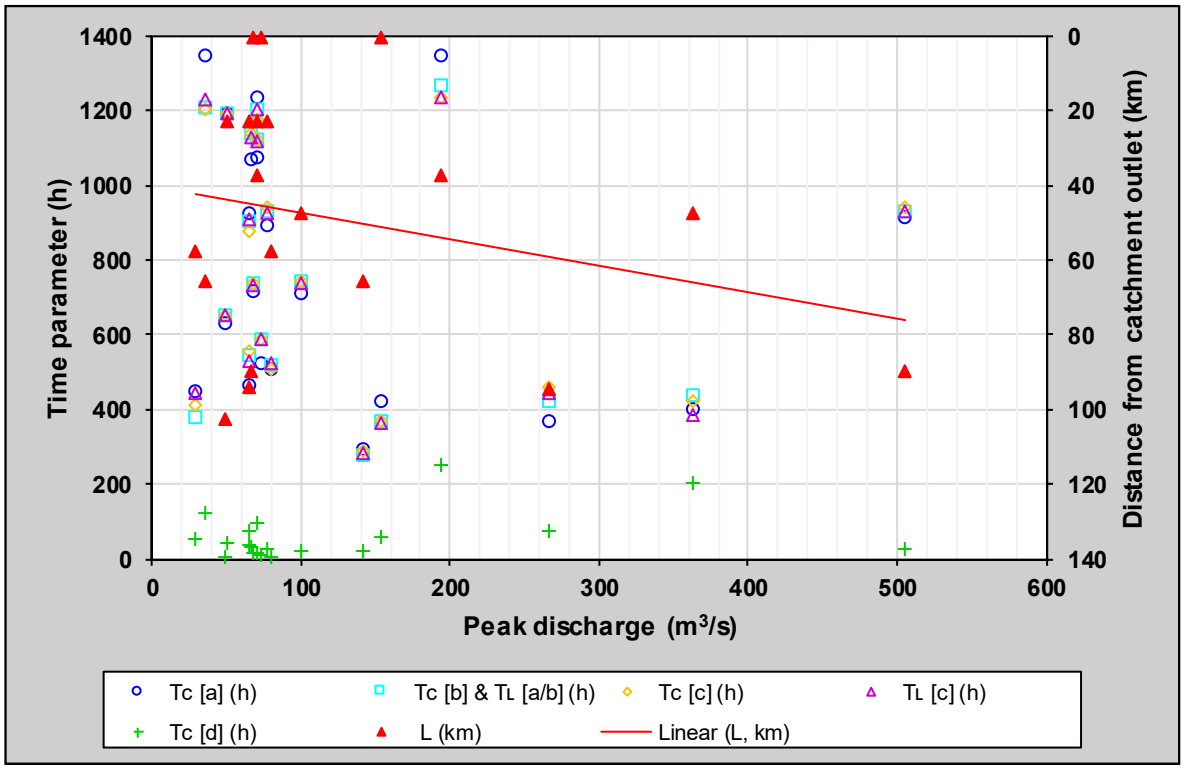

Figure B.69: Time parameters versus the distance (*L*) of a rainfall event from the catchment outlet in sub-catchment C5H039

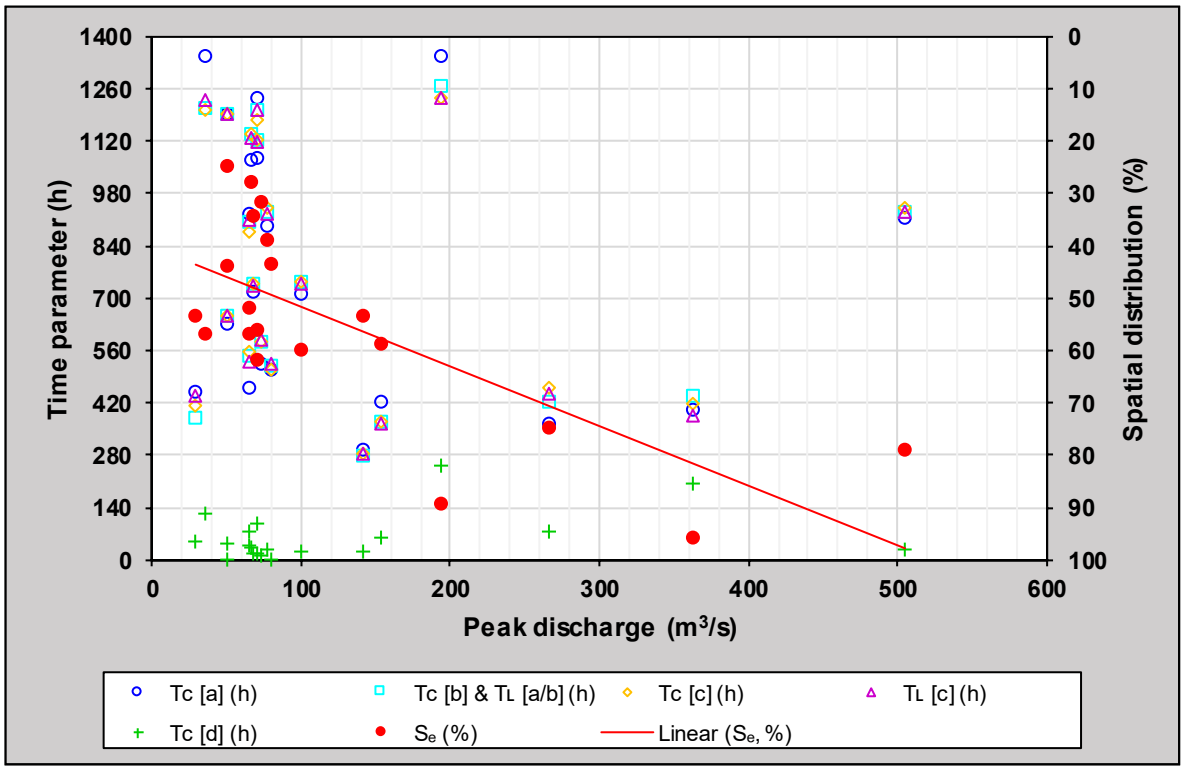

Figure B.70: Time parameters versus the spatial distribution of a rainfall event (S_e) in sub-catchment C5H039

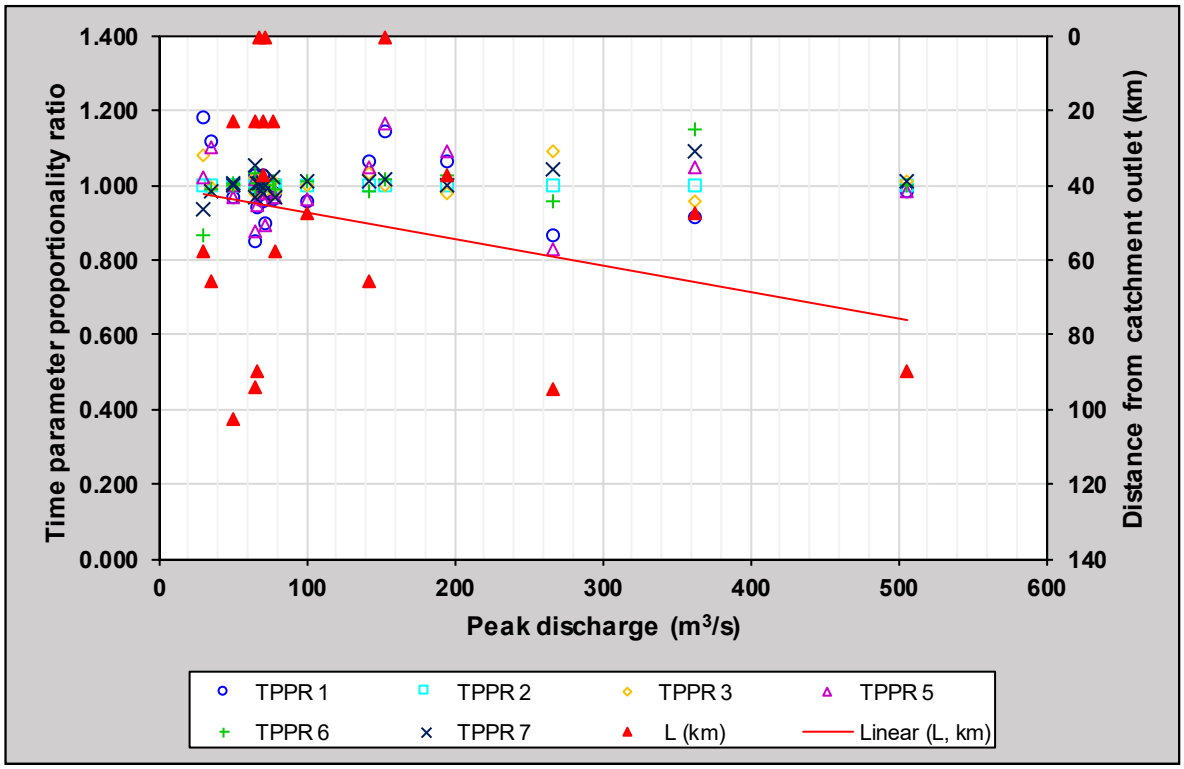

Figure B.71: Time parameter proportionality ratios versus the distance (L) of a rainfall event from the catchment outlet in sub-catchment C5H039

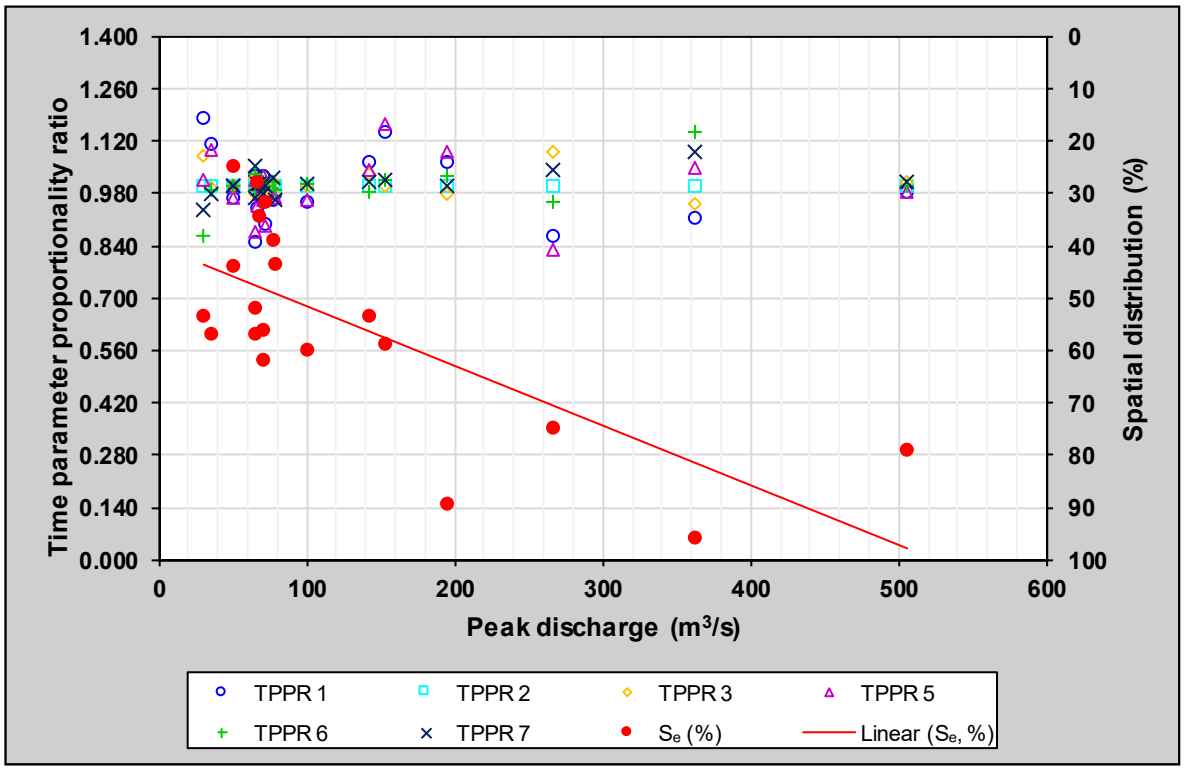

Figure B.72: Time parameter proportionality ratios versus the spatial distribution of a rainfall event (S_e) in sub-catchment C5H039

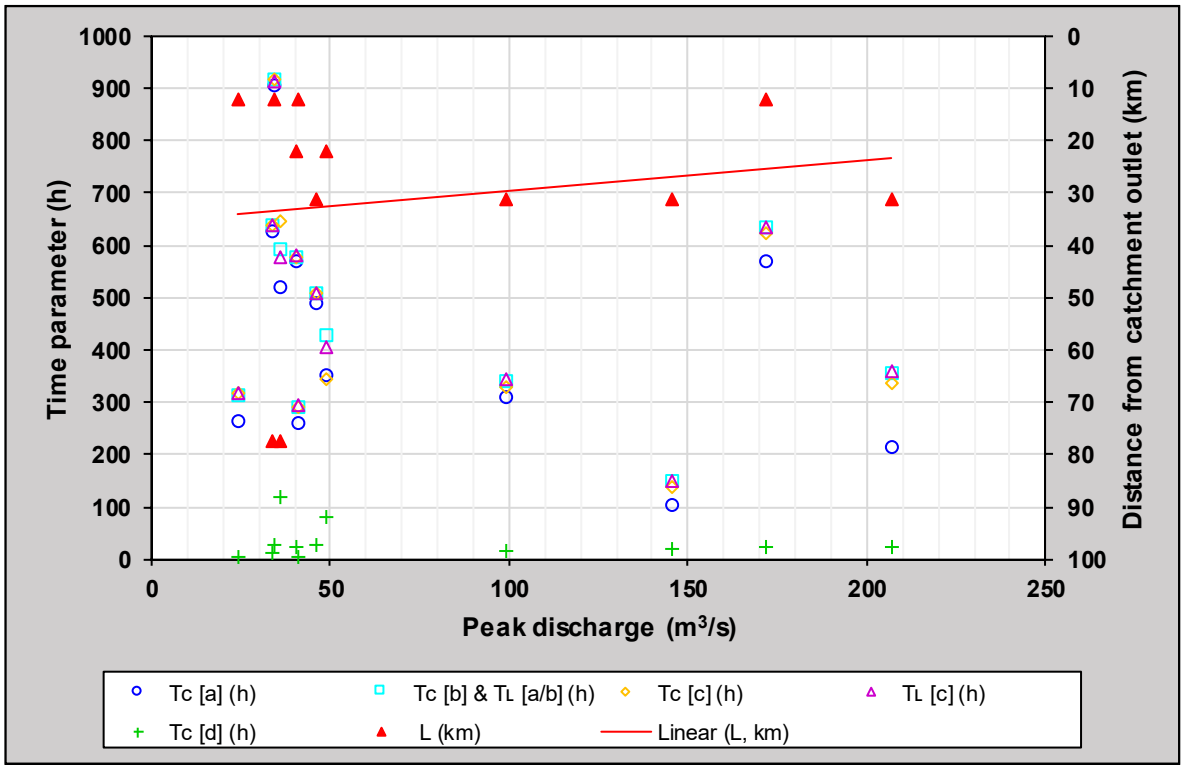

Figure B.73: Time parameters versus the distance (L) of a rainfall event from the catchment outlet in sub-catchment C5H053

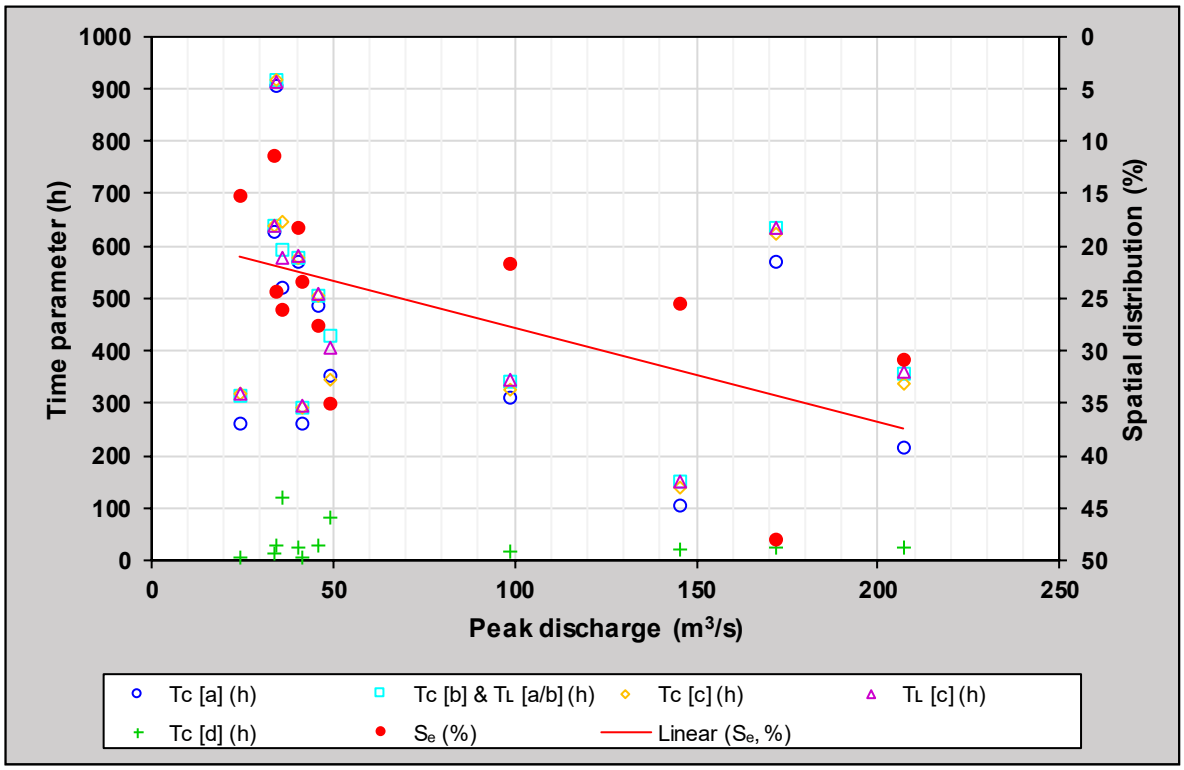

Figure B.74: Time parameters versus the spatial distribution of a rainfall event (S_e) in sub-catchment C5H053

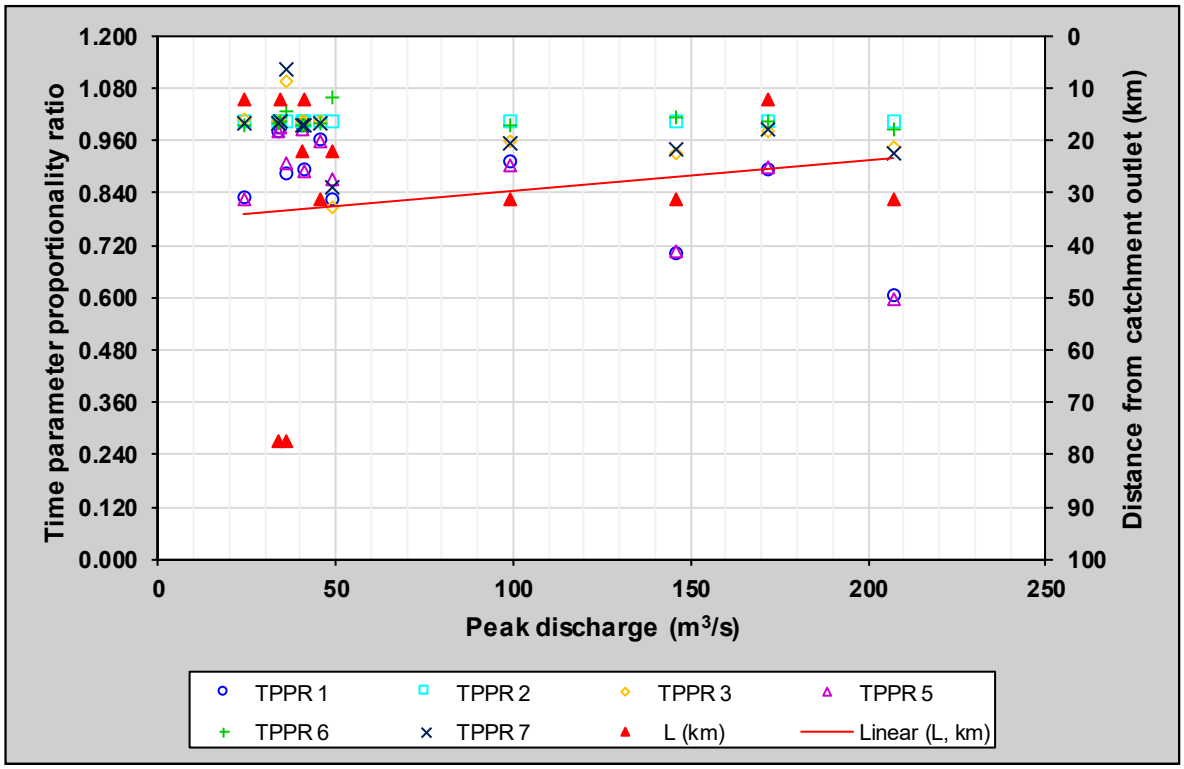

Figure B.75: Time parameter proportionality ratios versus the distance (L) of a rainfall event from the catchment outlet in sub-catchment C5H053

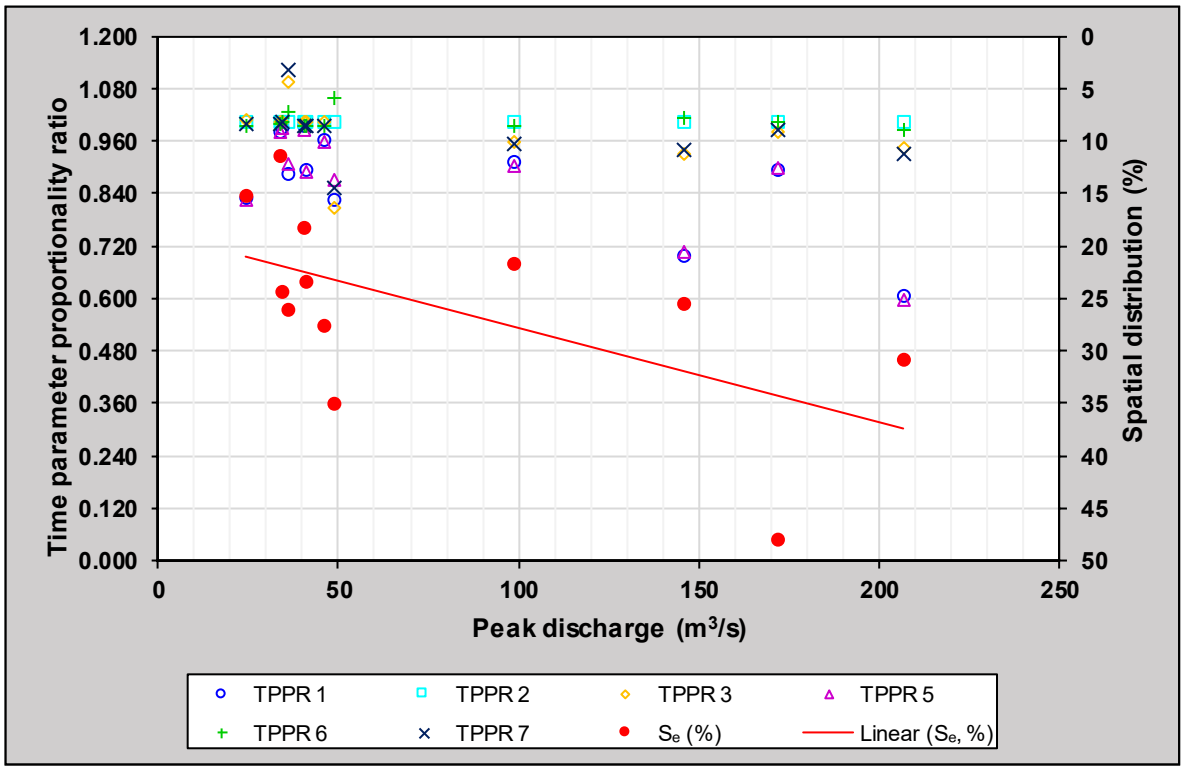

Figure B.76: Time parameter proportionality ratios versus the spatial distribution of a rainfall event (S_e) in sub-catchment C5H053

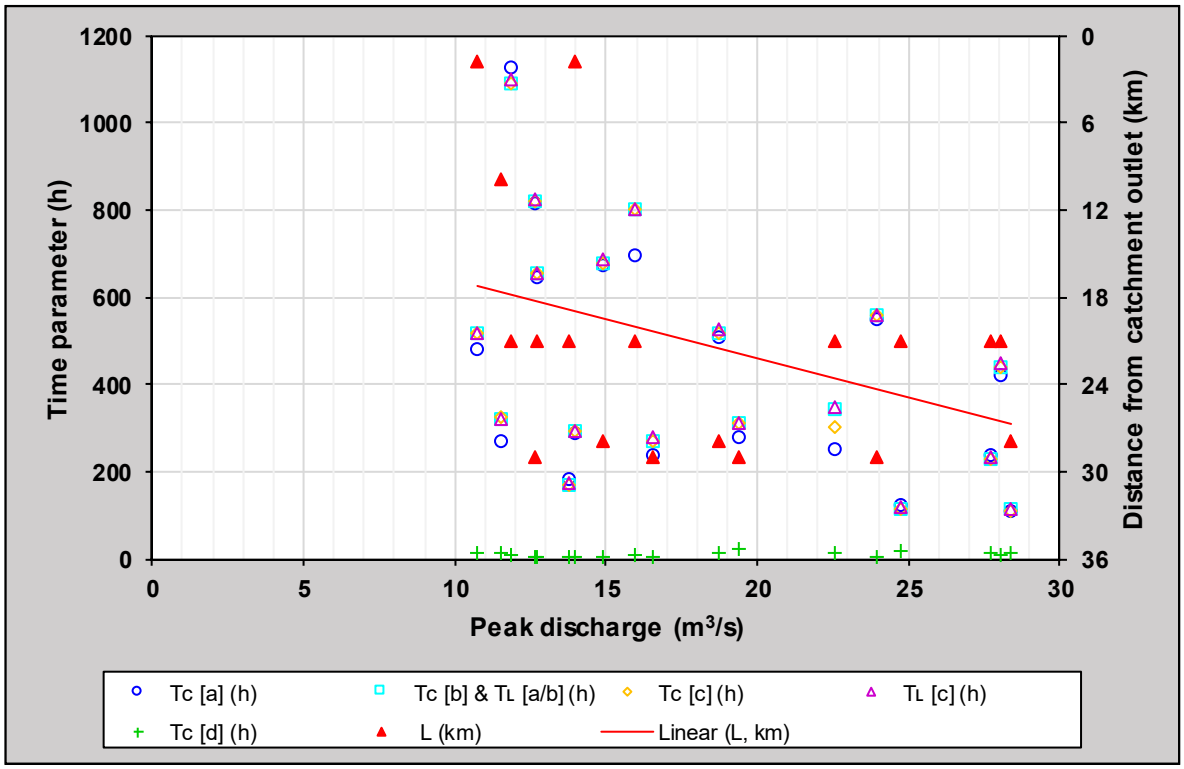

Figure B.77: Time parameters versus the distance (*L*) of a rainfall event from the catchment outlet in sub-catchment C5H054

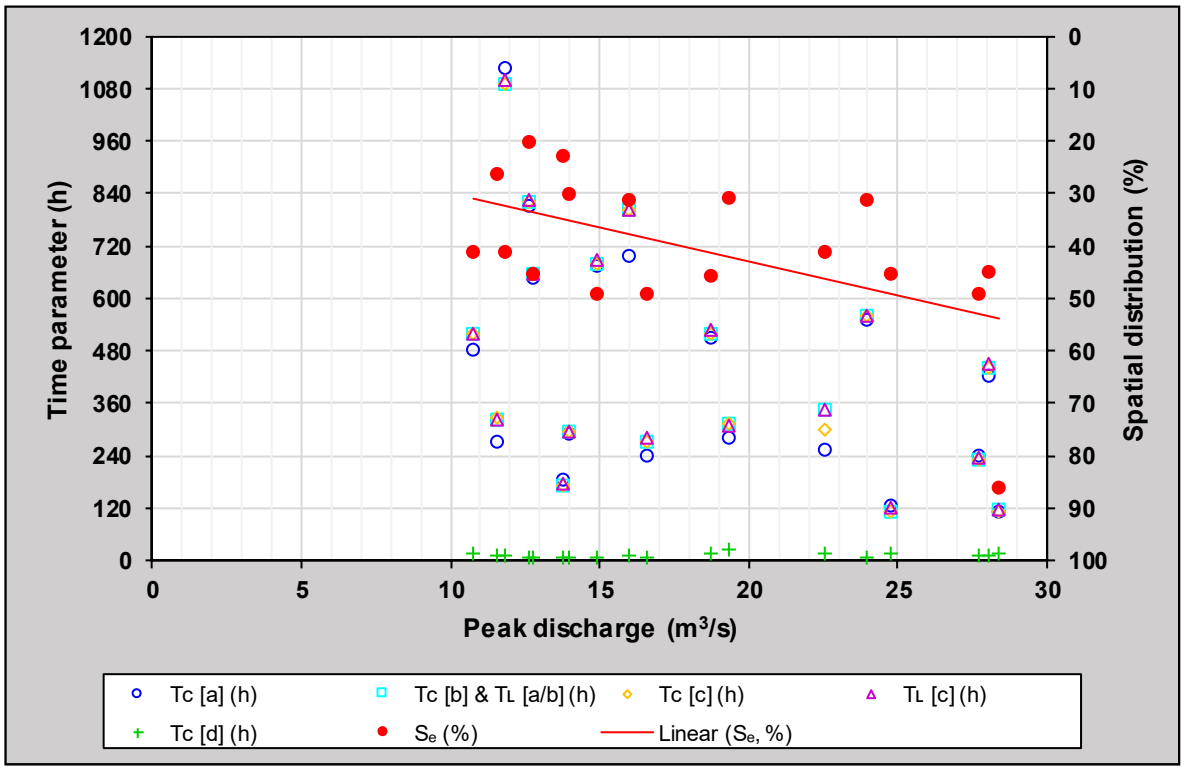

Figure B.78: Time parameters versus the spatial distribution of a rainfall event (S_e) in sub-catchment C5H054

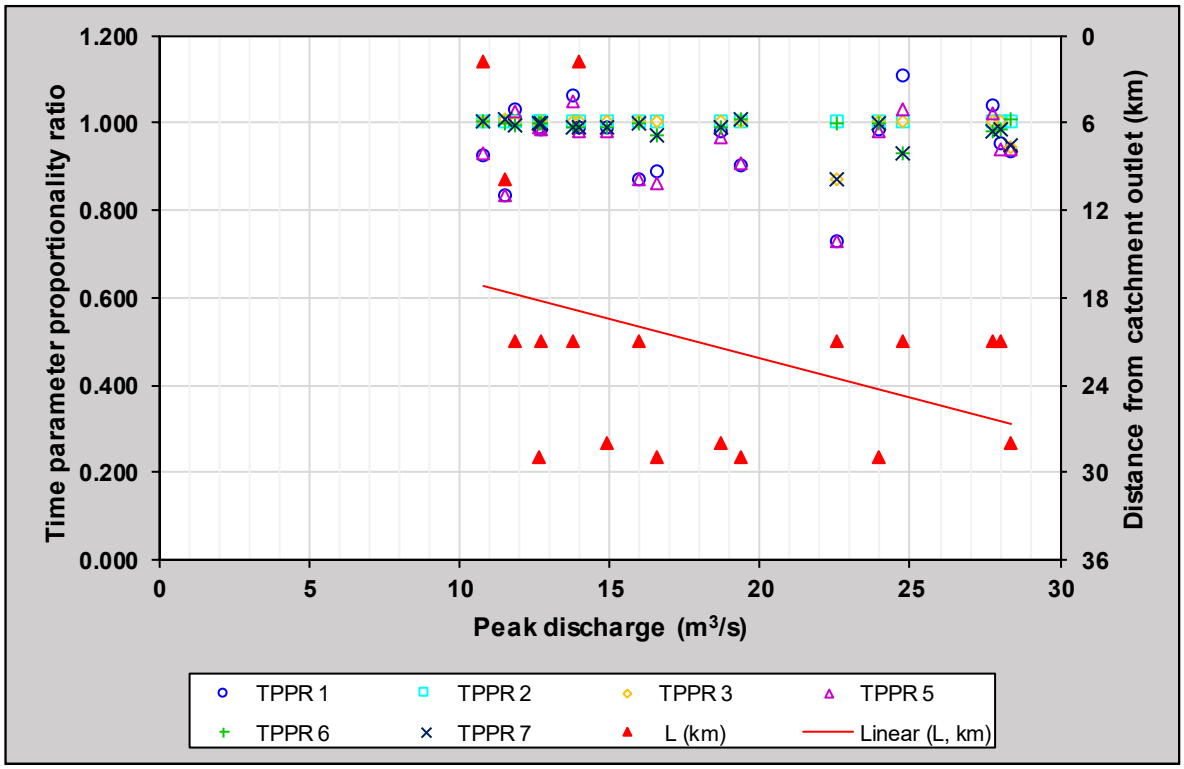

Figure B.79: Time parameter proportionality ratios versus the distance (L) of a rainfall event from the catchment outlet in sub-catchment C5H054

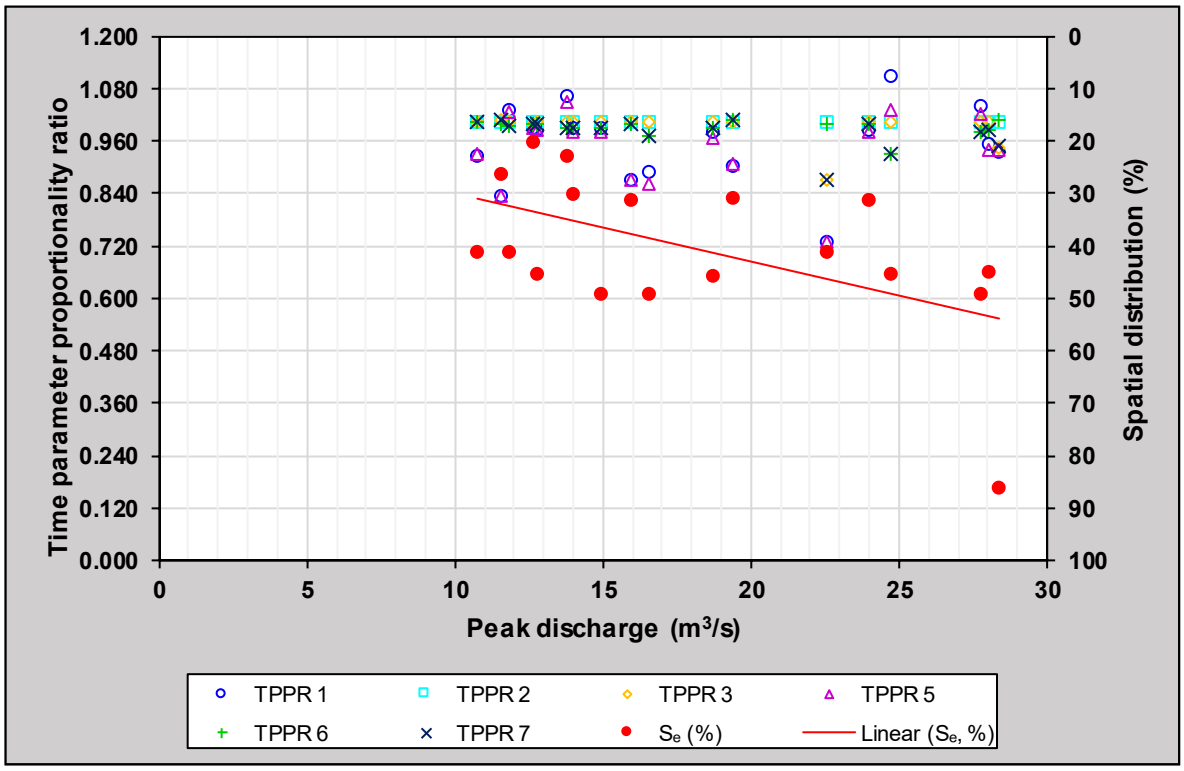

Figure B.80: Time parameter proportionality ratios versus the spatial distribution of a rainfall event (S_e) in sub-catchment C5H054